Water permeability of plant cells measured by pressure probes: effects of light and turgor, and the role of unstirred layers

Inaugural-Dissertation

zur Erlangung des Doktorgrades

der Fakultät Biologie, Chemie und Geowissenschaften

der Universität Bayreuth

von

Yangmin Kim

aus Incheon, Süd-Korea

Bayreuth, im Juli 2008

Die vorliegende Arbeit wurde am Lehrstuhl für Pflanzenökologie der Universität Bayreuth unter der Leitung von Prof. Dr. E. Steudle durchgeführt. Sie entstand im Zeitraum von Oktober 2004 bis Juli 2008, gefördert durch ein Stipendium des Deutschen Akademischen Austauschdienstes (DAAD).

1. Gutachter: Prof. Dr. E. Steudle
2. Gutachter: Prof. Dr. S. Clemens

Tag der Einreichung: 16.07.2008

Tag der mündlichen Prüfung: 01.12.2008

Prüfungsausschuss:

Prof. Dr. E. Komor (Vorsitz)

Prof. Dr. E. Steudle

Prof. Dr. S. Clemens

Prof. Dr. T. Fischer

Prof. Dr. G. Gebauer

Vollständiger Abdruck der von der Fakultät für Biologie, Chemie und Geowissenschaften der Universität Bayreuth genehmigten Dissertation zur Erlangung des Grades eines Doktors der Naturwissenschaften (Dr. rer. nat.)

To see… a heaven in a wild flower,

Hold… eternity in an hour.

William Blake

Sun light brings a *plant* not only energy but also thirst,

Unless the plant knows how to take care of *water*.

This dissertation is submitted as a "Cumulative Thesis" that covers four (4) publications; three (3) printed articles and one (1) article that is in press in Journal of Experimental Botany. In order to clarify the publications, they are listed below.

Printed articles:

1. **Ye Q., Kim Y., Steudle E.** 2006 A re-examination of the minor role of unstirred layers during the measurement of transport coefficients of *Chara corallina* internodes with the cell pressure probe. **Plant, Cell and Environment** 29, 964-980 (Chapter 2).

2. **Kim Y., Ye Q., Reinhardt H., Steudle E.** 2006 Further quantification of the role of internal unstirred layers during the measurement of transport coefficients in giant internodes of *Chara* by a new stop-flow technique. **Journal of Experimental Botany** 57, 4133-4144 (Chapter 3).

3. **Kim Y.X., Steudle E.** 2007 Light and turgor affect the water permeability (aquaporins) of parenchyma cells in the midrib of leaves of *Zea mays*. **Journal of Experimental Botany** 58, 4119-4129 (Chapter 4).

4. **Kim Y.X., Steudle E.** 2008 Gating of aquaporins by light and reactive oxygen species in leaf parenchyma cells of the midrib of *Zea mays*. **Journal of Experimental Botany** (in press) (Chapter 5).

Declaration of the self-contribution of research articles

The thesis is compiled with four research articles, which include different research work. Most of the research work in the thesis was carried out by myself independently at the Department of Plant Ecology, University of Bayreuth under guidance of Prof. Steudle.

In Chapter 2, I participated in experiments, and contributed to most of the theory parts applying analytical solutions. I did substantially contribute to the discussion and to the writing of the manuscript.

In Chapter 3, I participated in experiments, developed the computer analysis/simulations, and wrote most part of manuscripts. Other contributors were Dr. Qing Ye, a former Ph. D. student and Mr. Hagen Reinhardt, a Diplom student.

In Chapters 4 and 5, all the experiments were done by myself in addition to the writing of the manuscripts.

All published articles can be downloaded from the world wide web:
http://www.uni-bayreuth.de/departments/planta/research/steudle/index.html.

Acknowledgements

First of all, I would like to thank **Prof. Dr. E. Steudle**, Department of Plant Ecology, Bayreuth University, for his guidance during my Ph. D. His passion on the research that I felt at the moment I met him during his teaching in Korea in 2003 has influenced me during the whole period of my study. He showed me what a scientist could be. I thank him not only for introducing and teaching me the subject, plant water relations, but also for letting me realize the pleasure to study. Long and harsh discussions (which some people would think even derogatory) were what I have learned and will try to do through my career.

I thank **Burkhard Stumpf**, Department of Plant Ecology, Bayreuth University, for his expert technical supports and great help in many aspects. He is a magic person who can solve any technical problems that can happen in the lab. I appreciate all the cares he gave me for the pleasant stay in Bayreuth.

I am grateful to **Prof. Carol A Peterson**, Department of Biology, University of Waterloo, Canada, for her teaching of plant anatomy during various stays in the lab. Being brought as an engineer, this was quite new for me in which I had been totally ignorant before I met her. Her enthusiasm and knowledge on plant anatomy impressed me. It would be solely because of her that I became less ignorant of the plant anatomy.

I thank all the colleagues from various countries with whom I worked in Bayreuth. I learned many things from you: **Seonghee Lee, Kosala Ranathunge, Qing Ye, Lukasz Kotula, Ewa Przedpelska, Prof. Suiqi Zhang, Binbin Liu, Chris Meyer, Thorsten Knipfer, Hagen Reinhardt, Ola, Changxing, Lying, Debasish Das,** and **Ankur Joshi.**

Special thanks to **Jakob** for his corrections on German summary, to **Kosala** for English corrections, to **Moonyoung** for giving me an inspiration of the prologue, and to **Taeyoung** for uncountable endurance during my study.

Contents

I

Detailed Summary

1 General introduction

Water is a crucial component for plants to survive and grow. As water transport in plants has been investigated from early times, it was not found until 19th century that water is pulled up according to the 'cohesion-tension theory' of Böhm (1893) and Dixon and Joly (1894). Water is absorbed from soil by a root and transported through a stem, and exits from a leaf into atmosphere. This continuous system, where water is passing through a series arrangement of hydraulic resistors, is called soil-plant-air-continuum (SPAC; van den Honert, 1948). Evaporation of water from leaves causes water to transport from leaf tissue into atmosphere (lowering leaf water potential), and water molecules are pulled in a continuum ('tension' is produced) through stems and roots due to its 'cohesive' nature (Kramer and Boyer, 1995; Nobel, 1999; Steudle, 2001; Tyree and Zimmermann, 2002). The transport of water is analogous to the flow of electron in an electric circuit (Ohm's law). For water passing along a transpiring plant, roots and leaves play important roles in that their hydraulic conductances are variable and may be regulated by the plant within certain limits. The leaves of shoots play a major role within the SPAC, because their resistance to water flow is usually the biggest within the system, acting as a hydraulic bottleneck.

Despite the importance of leaf hydraulics in overall plant water relation, the hydraulic properties of leaves had received little attention. Mainly, stomatal regulations have been investigated in terms of gas exchange and water loss, and how this is regulating depending on water status (Schulze, 1986; Lösch, 2001). Other components of leaf hydraulics, besides of stomatal regulation, have only recently received greater attention. Decreases in those resistances can allow plants to adjust or even regulate the water supply from the root to provide a high water status (water potential) of the leaf, which is required to keep stomata open for maximal productivity (CO_2 assimilation; Sack and Holbrook, 2006). Changes in leaf hydraulics can occur in (i) xylem vessels (vascular part), which are pipe lines to transport bulk water at rather high rates, and in (ii) living cells (non-vascular part), which may play an important role for water storage and for fine regulation of water flow (Chapter 1.2). Although there have been studies to identify the hydraulic pathways in leaves, they are not yet

known, but, following the discovery of water channels or aquaporins in cell membranes in early 1990s, there has been a focus on the cell-to-cell rather than the apoplastic path.

Pathway of water movement *via* non-vascular parts may have a substantantial resistance compared to that by vascular component (Cochard *et al*., 2004; Nardini *et al*., 2005; Sack *et al*., 2005). The non-vascular part, namely, living cells have water channels (aquaporins) that can regulate water transport *via* changes in expression level or/and activity (Chapter 1.2). After the discovery of aquaporins in the early 1990s, for which Peter Agre was awarded for the 2003 Nobel Prize for Chemisty, it has been considered of great importance to see the functional role of them. The opening or closure (gating) of aquaporins must affect hydraulic conductance and water potential of leaves, which should be regulated to cope with environmental conditions that plants encounter. It is very plausible that there is an interplay of light and water for plants' growth and survival since both of them are components for photosynthesis. It is, therefore, timely to investigate effects of light on water management of a plant, namely, by measuring changes in leaf hydraulics by a gating of aquaporins, which has not been revealed as yet (Chapter 1.2).

Recently, doubts were raised as how the rapid movement of water (such as during transpiration) may cause problems in identifying the real forces that driving water flows. Although the problem is a general one, Tyree *et al*. (2005) raised the question whether or not the Bayreuth cell pressure probe would suffer from such problems, which are due to the fact, when causing rapid flows of water across cell membranes (or other hydraulic or osmotic barriers in a plant), this would tend modify the forces driving the flow of water and solutes. In the liquid phase, the problem is known in the transport literature as that of "unstirred layers" (Dainty, 1963; Barry & Diamond, 1984), and in gas phase as "boundary layers" (Nobel, 1999). In response to the criticism raised to measurements with the cell pressure probe, it was necessary to re-visit the problem in a rigorous quantitative manner to analyze the effects of unstirred layers residing in any kind of transport parameter measurements, where medium inside

or outside of a cell is not well or can not be stirred at all, such as during massive water flows or in the presence of rapidly permeating solutes (Chapter 1.3).

In this thesis, a cell pressure probe was applied to measure water permeability of leaf cells (cell *Lp*), which is one of component to determine leaf hydraulic conductance. I focused if cell *Lp* is a function of light. Effects of turgor or water availability in the leaf tissue, which changed in response to light, were also examined if they affected cell *Lp*. The scopes of the thesis are (1) quantification of the role of USLs in transport parameter measurements using the cell pressure probe (Chapter 2 and 3), (2) measuring changes in cell *Lp* in response to light and turgor (Chapter 4), and (3) providing evidence that changes in cell *Lp* are *via* a gating of aquaporins (Chapter 5).

1.1   Water and solute flows

Water and solute transport across cell membranes or more complex barriers was attemted to be explained using mathematical equations and it was possible by recruiting irreversible thermodynamics ('phenomenological equations'; Kedem and Katchalsky 1958; 1963 a, b; House, 1974; Dainty, 1963). This theoretical background, which is referred to as the "KK theory" can be applied to biological permeability data, and it can sucessfuly interpret water and solute flows measured by pressure probe techniques. In general terms, this theory considers flows (J_i) which are driven by corresponding forces (X_i), and the entropy production in the system ($\sum_i J_i \times X_i$). Separately considering water and solute flow across the membrane, they can be described by linear flow-force relationships, including couplings between flows, which extends the simple Ohm's law analogue, i.e., flow = conductance x force. For an ideal osmometer, it holds for the water (volume) flow (J_V in $m^3 \cdot m^{-2} \cdot s^{-1}$) that

$$J_V = Lp \cdot \Delta\Psi , \qquad\qquad\qquad (1)$$

where Lp is the hydraulic conductivity (in $m \cdot s^{-1} \cdot MPa^{-1}$); $\Delta\Psi$ (in MPa) is the difference of water potential in both sides of the membrane or barrier which is the force driving J_V. A passive diffusional solute flow (J_s in $mol \cdot m^{-2} \cdot s^{-1}$) is written analogously to Fick's first law:

$$J_s = P_s \cdot \Delta C_s , \qquad\qquad\qquad (2)$$

where P_s ($m \cdot s^{-1}$) is the permeability coefficient and ΔC_s the concentration difference, which is the driving force of J_s. However, Eqns (1) and (2) are not complete because they neglect interactions or couplings between different flows, i.e. interaction between water and solute flows. For example, when water moves across the membrane, solute can be driven (solvent drag).

The KK theory provides a correct and complete quantitative description of transports across a membrane (barrier). For the sake of simplicity, the theory is applied to a single cell in a medium to work out interactions between water and solute flows. If (i) the cell interior (superscript 'i') and the medium (superscript 'o') are treated as a

two-compartment system; (ii) only the volume flow (J_V; identified with the flow of water) and the flow of a single solute (J_s) are considered; (iii) flows out of the cell are defined as positive and flows in to the cell as negative, we get (Steudle 1993):

$$J_V = -\frac{1}{A}\frac{dV}{dt} = \underbrace{L_P \cdot P}_{\text{hydraulic flow}} - \underbrace{L_P\left[\sigma_s \cdot RT \cdot (C_s^i - C_s^o) + RT \cdot (C^i - C^o)\right]}_{\text{osmotic flow}} \qquad (3)$$

and

$$J_s = -\frac{1}{A}\cdot\frac{dn_s^i}{dt} = \underbrace{P_s(C_s^i - C_s^o)}_{\text{diffusion flow}} + \underbrace{(1-\sigma_s)\cdot\overline{C_s}\cdot J_v}_{\text{solvent drag}} + \underbrace{J_s^*}_{\text{active transport}}, \qquad (4)$$

respectively.

Here, J_V [m·s⁻¹]   water (volume) flow

      V [m³]   cell volume

      A [m²]   cell surface area

      t [s]   time

      Lp [m·(s·MPa)⁻¹]   hydraulic conductivity

      P [MPa]   hydrostatic pressure (turgor) of the cell as referred to the reference of atmospheric pressure

      σ_s [1]   reflection coefficient

      R [J·(mol·K)⁻¹]   gas constant (≈ 8.314)

      T [K]   absolute temperature

      C_s [mol·m⁻³]   osmotic concentration of a certain permeating solute with σ_s

      C [mol·m⁻³]   osmotic concentration of impermeable solutes

      J_s [mol·m⁻²·s⁻¹]   flow of a certain permeating solute

      n_s [mol]   number of a certain solute molecule in mol

      P_s [m·s⁻¹]   permeability coefficient of a certain permeating solute

      $\overline{C_s}$ [mol·m⁻³] mean concentration of a certain solute at both sides of the membrane

      J_s^* [mol·m⁻²·s⁻¹]   active transpot of a certain solute

In Eqn (3), volume flow J_V is shown as a change of cell volume with time, which is referred to unit area of cell surface (A). Hence, J_V has the dimensions of a velocity and

denotes the speed by which water molecules pass across the membrane. The water (volume) flow has two components: (i) a hydraulic flow ($Lp \cdot P$) driven by the hydrostatic pressure gradient, where Lp is the hydraulic conductivity of the cell membrane; and (ii) an osmotic water flow driven by the difference in osmotic pressure ($Lp \cdot \sigma_s \cdot \Delta\pi_s$; $\Delta\pi_s = RT \cdot (C_s^i - C_s^o)$, van't Hoff's law). The osmotic term is modified by another coefficient, the reflection coefficient σ_s. The physiological meaning of σ_s is that of a 'passive selectivity' of the membrane for a given solute. The reflection coefficient is a quantitative measure of the deviation of the osmotic cell from being ideally semipermeable. It denotes the interaction between water and solutes as they cross the membrane. In the case of an ideal osmometer, which has a semipermeable membrane, only solvent (water), but no solute can pass through ($P_s = 0$; $\sigma_s = 1$). In this case, the osmotic force driving the water will be identical with the water potential difference, i.e. $\Delta\Psi = - \Delta\pi_s = - RT \cdot (C^i - C^o)$:

$$J_v = -\frac{1}{A} \cdot \frac{dV}{dt} = Lp \cdot P - Lp \cdot RT(C^i - C^o) = Lp \cdot \Delta\Psi , \qquad (5)$$

which is identical with Eqn (1). On the other hand, when $\sigma_s = 0$, the membrane does not distinguish between the solute and water, i.e. both pass the membrane at the same rate. Usually, σ_s ranges between zero and unity. For the most of solutes naturally present in the cell sap of plant cells (ions, sugars, metabolites etc.), σ_s will be close to unity. There are also exotic cases, when $\sigma_s < 0$. This phenomenon could be observed in pressure probe experiments with plant cells and it is called anomalous or negative osmosis. Anomalous osmosis was shown to take place during the closure of water channels, when rapidly permeating solutes move across the membrane at a rate, which is higher than that of water (Steudle and Henzler, 1995; Henzler *et al.*, 2004; Ye and Steudle, 2006).

Eqn (4) contains three different components of the solute flow (J_s). A diffusional component, $P_s \cdot (C_s^i - C_s^o)$, relates concentration gradients to the solute flow according to Fick's first law. The second term is called 'solvent drag'. It quantifies the interactions between solute and water as they cross the membrane, i.e the amount of solute dragged along with the water flow. This term is zero, when the solutes are completely excluded

from the membrane, i.e. when $\sigma_s = 1$. The last term on the right side (J_s*) is the active component of the solute flow. It represents active pumping of solutes against the concentration gradients, for example, by recruiting the ATPase. This component is usually neglected during solute flow, but determines the absolute level of cell turgor which, for example, refers to the active pumping of ions (Steudle, 2001). There is no equivalent for a primary active pumping of water as in solute flows of Eqn (4), because there is no evidence for a direct coupling between water flow and metabolic energy (i.e., for an ATP-driven water pump; Steudle, 2001). The existence of H_2O-ATPases is highly unlikely, because the high water permeability (Lp) of cell membranes would cause a short circuit.

1.1.1 Elastic modulus

The elastic modulus (ε) characterizes elastic properties of the cell wall, i.e. its mechanical rigidity. The definition of ε is the change in cell turgor (dP) to produce a given change of the relative cell volume (dV/V):

$$\varepsilon = V \frac{dP}{dV} \approx V \frac{\Delta P}{\Delta V}. \tag{6}$$

High values of elastic moduli refer to a low extensibility or a rigid cell wall, i.e., big changes in pressure cause small changes of cell volume. On the other hand, low values of ε mean that the cell wall is extensible. Elastic properties refer to reversible changes in cell volume, which are typical for mature cells. The plastic (viscous) properties that refer to no complete reversibility, on the other hand, dominate extension growth (Cosgrove, 1998; Fricke, 2002). The elastic modulus can be directly measured with the aid of a pressure probe by producing defined changes in cell volume (ΔV) and measuring the responses in cell turgor. According to Eqn (6), ε has the dimension of a pressure (MPa). In Eqns (9) and (11), ε relates the volume change to the pressure change (see below). It is required when integrating Eqns. (5) and (6), to work out the cell hydraulic conductivity, Lp, indicating the speed of volume flow, from $P(t)$ curves (as measured with pressure probes). Typically, Lp is obtained from 'half times of pressure relaxations' (see below).

1.1.2 Hydrostatic pressure relaxations

In hydrostatic experiments, turgor pressure of a cell is rapidly increased or decreased in response to a step change in cell volume with the aid of a pressure probe (Fig. 1). The step change in turgor pressure, ΔP, causes water flow out of or into the cell and finally turgor pressure is 'relaxing' back to a value close to the original. This process is called 'hydrostatic relaxation' and can be described by a exponential $P(t)$ curve:

$$P(t) = P_E + (P_A - P_E) \cdot \exp(-k_w \cdot t). \qquad (7)$$

Here, P_A is the maximum value of P; P_E is the end value of P; k_w is the rate constant of the water flow, which is the inverse of time constant, τ.

$$k_w = \frac{1}{\tau} . \qquad (8)$$
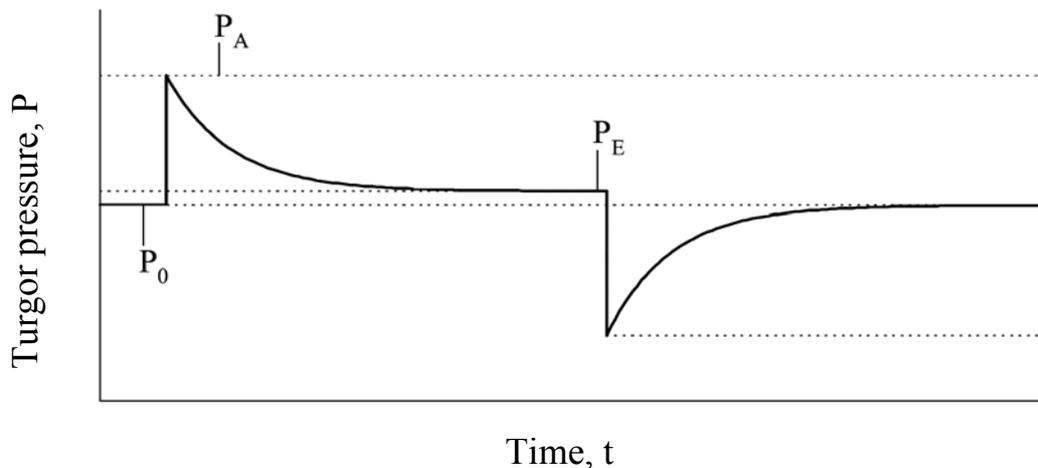
Figure 1. Schematic graph of ex- and endosmotic hydrostatic pressure relaxations. When the turgor pressure (P) is increased from original turgor, P_o to P_A, water flows out, and P exponentially relaxes back to P_E, which may slightly differ from P_o due to small changes in osmotic concentration of the cell sap.

Time constant for water flow (τ) is the time required for the step change in turgor pressure to reach approximately $1/e \approx 63\%$ of $(P_A - P_E)$. It is given by the product of hydraulic resistance and cell capacitance:

$$\tau = \frac{1}{Lp \cdot A} \cdot \frac{V}{(\varepsilon + \pi^i)} = R \cdot C. \tag{9}$$

Here, $1/(Lp \cdot A)$ is the hydraulic resistance (R), $V/(\varepsilon + \pi^i)$ is the storage capacity of a cell for water (C), and π^i = osmotic pressure of cell sap. Usually, half times ($T_{1/2}^w$) rather than time constant are given, which refer to the time required for a change in turgor or volume to reach a half (50%) of (P_A - P_E), i.e. when $P = [P_E + (P_A - P_E)/2]$. Half time, $T_{1/2}^w$ is related to time constants by:

$$T_{1/2}^w = \tau \cdot \ln(2). \tag{10}$$

By combining Eqns (9) and (10), we get the equation for calculating hydraulic conductivity (Lp), which is usually given in the unit of m·s^{-1}·MPa^{-1}:

$$Lp = \frac{V}{A} \cdot \frac{\ln(2)}{T_{1/2}^w (\varepsilon + \pi^i)}. \tag{11}$$

This equation is used to work out Lp from hydrostatic relaxations of turgor pressure by measuring $T_{1/2}^w$ and cell geometry (V and A) for a cylindrical internode of *Chara* or for leaf cells of corn (see Chapters 2 to 5). The osmotic pressure of the cell (π^i) is estimated from the steady cell turgor (P_o) and from π^o of the medium by $\pi^i = P_o + \pi^o$. In *Chara,* $\pi^i \approx P_o$ could be assumend in the presence of articifial pond water that has $\pi^o \approx 0$. In transpiring leaf cells, π^i could be underestimated when determining in this way.

1.1.3 Osmotic pressure relaxations in the presence of a permeating solute ($J_s \neq 0$; $\sigma_s < 1$; Steudle & Tyerman 1983)

In the presence of permeating solutes, osmotic response curves are biphasic as can be seen in Fig. 2. There is a first rapid phase during which turgor pressure rapidly decreases or increases due to an exosmotic/endosmotic water flow. It is called 'water phase' and it is rapid because of the high water permeability of the cell membrane. It is followed by a second phase called 'solute phase'. The second phase is due to the permeation of water into or out of the cell, following the solute transport, which tends

to equilibrate the concentration gradient across the cell membrane. Eventually, equilibrium is attained, when the concentration within the cell and in the medium become the same. It should be noted that the pressure changes measured during osmotic pressure relaxations are due to movements of water rather than solute. However, the latter causes the water flow, therefore, the rate constant ($k_s \propto P_s$) depends on the solute (P_s) rather than on the water permeability (Lp). Rates of solute phases strongly depend on the nature of solutes used. Solutes which are soluble in the lipid bilayer of the cell membrane have short half times ($T_{1/2}^s$); those which are polar (ions, hydrophilic solutes), have long half times (Henzler & Steudle 1995).
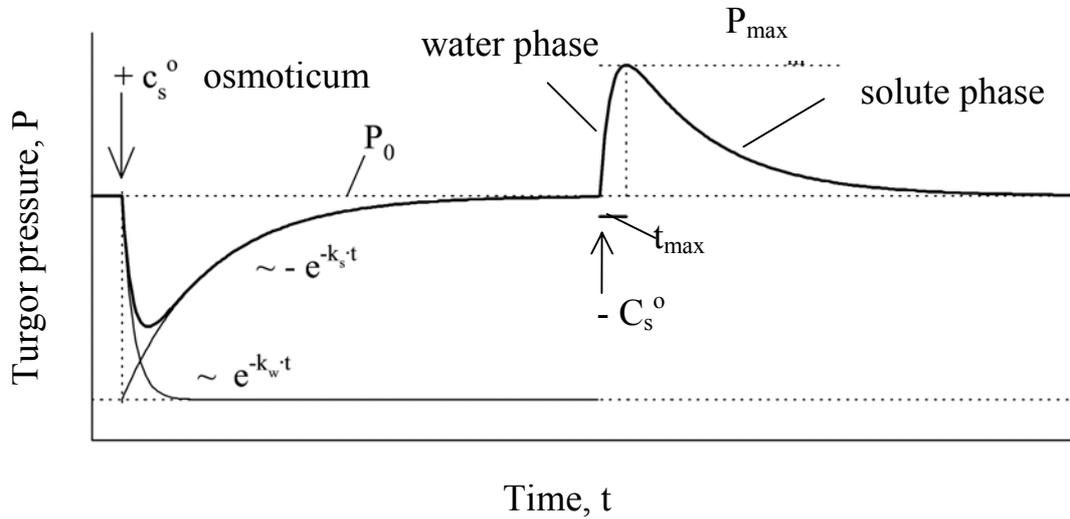
Figure 2. Schematic graph of biphasic osmotic pressure relaxations. When a permeating solute is added to the medium, water is sucked out of the cell in response to change in osmotic concentration and turgor pressure decreases. This first reponse is called water phase. In the following phase, turgor pressure increases back to the original value, because water follows the solute moving inside the cell and resulting in a new equilibrium (solute phase). Removal of the solute causes a symmetrical change in pressure, but to the opposite direction.

The solute permeability (P_s) is obtained from the rate constant of the solute phase (k_s):

$$k_s = \frac{\ln(2)}{T_{1/2}^s} = P_s \cdot \frac{A}{V} \quad \Rightarrow \quad P_s = \frac{V}{A} \cdot \frac{\ln(2)}{T_{1/2}^s}. \tag{12}$$

Here, $T^s_{1/2}$ is the half time of the solute phase; permeability coefficient (P_s) of the solute is determined by measuring $T^s_{1/2}$ and the geometry of the cell (volume, V; surface area, A). Permeability coefficient is a measure of the speed by which solutes move across the membrane with unit of m·s^{-1}.

The $P(t)$ or $V(t)$ curves of osmotic pressure relaxations can be described according to the Steudle/Tyerman theory (Steudle and Tyerman, 1983; Steudle and Henzler, 1995; Kim *et al*., 2006):

$$\frac{V(t) - V_0}{V_0} = \frac{P(t) - P_0}{\varepsilon} = \frac{\sigma_s \cdot \Delta\pi_s^o \cdot Lp}{(\varepsilon + \pi^i)Lp - P_s}\left[\exp(-k_w \cdot t) - \exp(-k_s \cdot t)\right]. \qquad (13)$$

Eqn (13) describes a biphasic pressure response as schematically depicted in Fig. 2. When the osmotic solute is added, there is a rapid decrease in turgor due to a rapid water efflux (mainly determined by the first exponential term in the brackets on the right side of Eqn (13)). Then, water is transported into the cell because of the equilibration of permeating solutes across the membrane (solute phase; see above). The theory assumes that both the internal and the external compartments are stirred, i.e., USLs can be either excluded or incorporated into k_w (Lp) or k_s (P_s) (see Ye *et al*., 2006 and Kim *et al*., 2006). The other assumption is that the permeability of the tonoplast for both water and solute is much bigger than that of the plasma membrane (Kiyosawa and Tazawa, 1977; Maurel *et al*., 1997).

The reflection coefficient (σ_s) is obtained from biphasic response curves at $J_V = 0$, i.e., by considering the minima or maxima of pressure in Fig. 2 (Steudle and Tyerman, 1983):

$$\sigma_s = \frac{P_0 - P_{\min(\max)}}{\Delta\pi_s^o} \cdot \frac{\varepsilon + \pi^i}{\varepsilon} \cdot \exp(k_s \cdot t_{\min(\max)}). \qquad (14)$$

It should be noted that the Steudle/Tyerman theory neglects the solvent drag (middle term on the right side of Eqn 4). However, it has been readily shown by numerical simulation that effects of solvent drag are usually small even in the presence of rapidly permeating solutes with a small σ_s (Rüdinger *et al*., 1992).

1.2 Role of living cells in overall leaf hydraulic conductance (K_{leaf})

Water relations and water transport across tissues are more complicated than that of an individual, isolated cell, where water crosses only the plasma membrane. At the tissue level, there are two parallel pathways involved for the water flow – apoplastic pathway and cell-to-cell pathway.

1.2.1   Water transport pathways in leaves

Overall leaf hydraulic conductance in kg H_2O s^{-1} m^{-2} MPa^{-1}, or its inverse, the resistance, has different components. Components are arranged either in series or in parallel such as the resistances of petioles, leaf lamina (consisting of living cells and vascular components), or stomata (Fig. 3). At steady state, resistances form a complicated network, and the regulation of individual conductances (resistances) of different components will result in overall changes of leaf hydraulics. In recent studies, it has been proposed that up to 90% of K_{leaf} may be attributed to living tissue (Cochard *et al.*, 2004; Nardini *et al.*, 2005; Sack *et al.*, 2005). As living cells can effectively regulate their water permeability by expression or by a gating of AQPs, living cells could substantially contribute to K_{leaf}. However, the problem with the figures from overall measurements is the reliable quantification of the components that eventually determine K_{leaf}. This conceptual work is still missing.

1.2.2 K_{leaf} regulation by light

The recent review by Sack and Holbrook (2006) summarized data on the effects of light on K_{leaf} of 14 different herbaceous and woody species. The overall result was that K_{leaf} strongly responded to light for many species. There is a lot of evidence that the overall hydraulic conductance of leaves (K_{leaf}) is substantially affected by light, but as yet the mechanisms of changes in K_{leaf} are poorly understood (Nardini *et al.*, 2005; Sack and Holbrook, 2006; Cochard *et al.*, 2007). For example, Lo Gullo *et al.* (2005) showed that leaf conductance was positively correlated with photosynthetically active radiation (PAR) in evergreen and deciduous trees. In lab experiments, Sack *et al.*

(2002) demonstrated that K_{leaf} of *Quercus* leaves measured by a high pressure flow meter (HPFM) was bigger under irradiance (> 1200 µmol m^{-2} s^{-1}) than that measured under ambient light condition. Also using the HPFM technique, Tyree *et al.* (2005) observed similar phenomena in six tree species. However, Brodribb and Holbrook (2004) showed midday depressions of K_{leaf} and stomatal conductance of a tropical tree, when the water status was unfavorable.

Copyright © Pearson Education, Inc., publishing as Benjamin Cummings.

Figure 3. Pathways for water movement in leaves. Water in leaf xylem vessels moves *via* cell-to-cell pathway and *via* apoplastic pathway (across cell walls), and finally escapes from leaf to atmosphere through stomata. Sack *et al.* (2005) estimated the hydraulic resistance of cell-to-cell pathway contributed 40-90% of total leaf hydraulic resistance. (Copyright © Pearson Education, Inc., publishing as Benjamin Cummings)

1.2.3 Change in cell water permeability (cell *Lp*) and gating of aquaporins in response to light

Although the mechanism(s) of responses of K_{leaf} to irradiance are not yet clear, Tyree *et al.* (2005) excluded a contribution of the stomatal conductance and suspected that the increase in K_{leaf} was due to either changes in the vascular component by hydrogel effects (Zwieniecki *et al.*, 2001), or due to changes in non-vascular components, probably related to water channels (aquaporins, AQPs). There is increasing evidence that AQPs play a key role in plant water relations (Steudle and Henzler, 1995; Maurel, 1997; Kjellbom *et al.*, 1999; Tyerman *et al.*, 1999; Steudle, 2000, 2001; Maurel and Chrispeels, 2001; Javot and Maurel, 2002). Cell water permeability may increase either by *de novo* expression of AQPs or by an opening of closed channels ("gating"). In roots of *Lotus japonicus* and in leaves of *Samanea saman*, the diurnal changes in hydraulic conductance have been attributed to changes in levels of mRNA encoding for AQPs (Henzler *et al.*, 1999; Moshelion *et al.*, 2002). In leaves of walnut, the increase in K_{leaf} by light was in accordance with the transcript abundance of two aquaporins and this effect occurred within 30 min (Cochard *et al.*, 2007). Aside from the regulation of transcript levels, 30-min-light treatments causing an increase of K_{leaf} are likely to involve the action of AQPs tending to open in response to light treatment (Nardini *et al.*, 2005; Tyree *et al.*, 2005). However, there have been as yet no direct measurements of changes of the cell hydraulic conductivity caused by irradiance (and possibly by a gating of AQPs by light). To do this, Kim and Steudle (2007; see Chapter 4) started to fill the gap by measuring changes in cell *Lp* in response to light. In leaf cell of corn, they found that turgor was also a factor that affected cell *Lp* and it was most likely by an effect on AQP activity. Therefore, they kept turgor constant to separate effects of light from those of turgor.

The oxidative gating of AQPs may be involved in response to light, when light intensity is high. As photosynthesis produces O_2, oxidative damages are anticipated by reactions involving the partial reduction of O_2 or production of reactive oxygen species (ROS such as superoxide, H_2O_2, hydroxyl radical; Foyer and Noctor, 2000). Oxidative gating of AQPs involving hydroxyl radicals has been known in *Chara* internode and

corn roots (Henzler *et al.*, 2004; Ye and Steudle, 2006). In those studies, AQPs could be reversibly closed by H_2O_2/OH^*. The treatment of 100 µM H_2O_2 decreased the root hydraulic conductance in a chilling sensitive maize genotype, but not in a chilling-tolerant (Aroca *et al.,* 2005). Oxidative gating may be a common response to different kinds of stresses (Pastori nd Foyer, 2002; Xiong *et al.*, 2002) and it may provide appropriate adjustments in water relations (Ye and Steudle, 2006). However, at present, there is much more experimental evidence about an oxidative gating in roots rather than in shoots. This is due to the fact that roots can be more easily handled experimentally and results obtained at the level of individual root cells can be combined with those at the root level (root cell *vs*. root hydraulic conductivity as obtained by pressure probes).

1.2.4   Implication of K_{leaf} regulation by light in whole plants

Sack and Holbrook (2006) expected diurnal changes of K_{leaf} in such a way that K_{leaf} should increase in response to increasing light and temperature. However, at high rates of transpiration K_{leaf} should decline as the water potential and turgidity decreases. Using a steady state evaporation technique, Brodribb and Holbrook (2006) reported that K_{leaf} decreased in proportion to decreasing cell turgor in 16 out of the 19 species investigated. The authors suggested that hydraulic conductivity of living cells were affected by decreasing turgor. There could be interaction between light and turgor pressure to affect $K_{leaf.}$ For example, high light intensity may tend to intensify the water flow across living tissue, but, as soon as the water status (turgor/water potential) declines, cell Lp is reduced, possibly by a closure of AQPs. This seems to be a reasonable response tending to minimize water losses and to keep cells turgid.

1.3   Unstirred layers (USLs)

At any permeation of water and solutes across a membrane or another osmotic barrier, there are, in principal, errors due to unstirred layers (USLs). This is so, since concentrations right at the membrane surfaces could be different from those in the bulk

external and internal medium, when the medium is not well mixed. Even in a well-mixed solutions, there should be an adhering layer left, which can not be stirred away even at high rates of mixing. The relative contribution of USLs to the overall measured permeability depends on the rate at which solutes or water move across the membrane as compared with the rate at which substances diffuse from the bulk solution to the membrane surface. Relative contributions of USLs increase with increasing permeability of solutes. Whenever the actual transport properties are to be known for a single membrane, rather than those of an entire barrier, the effects of USLs have to be quantified.

A USL is a region of slow laminar flow parallel to the membrane, in which the dominating transport mechanism is by diffusion (Dainty, 1963). When dealing with non-electrolytes, there are two different kinds of effects of USLs. For the first model, when a permeating solute diffuses across a membrane, depending on the diffusional supply from the bulk solution to the membrane, the actual concentration gradient driving the solution permeation across the membrane may be smaller than that measured in the bulk solution. This type of effect of USL has been termed the 'gradient-dissipation effect' (Barry and Diamond, 1984). In the second model, solutes are swept by convection with the water transport in the direction perpendicular to the membrane where they are concentrated on one side but depleted on the other. Concentration gradients built up in the solution and adjacent to the membrane will be opposed by a back-diffusion within USLs. This type of USL effect in the presence of water flow across the membrane has been termed 'sweep-away effect' ('convection *vs.* diffusion'; Dainty, 1963). Both types of effects of USLs result in overall permeabilities for water and solutes that are smaller than those of just the membrane.

The effect of external USLs could be minimized by measuring in fairly turbulent media to reduce the thickness of external. Therefore, the effect could be experimentally investigated. However, the cell interior could not be stirred, which could have caused the build up of substantial internal USLs. To investigate the effect of internal USLs, (i) a theoretical approach assuming the stagnant internal USL and (ii)

a new technique combining cell pressure probe experiments and numerical simulations were applied.

1.3.1 Sweep away effect

The 'sweep-away effect' refers to the action of a net water flow (J_V). At a steady J_V, there is a balance between convective and diffusive solute flow at the membrane. As a result, the solute concentration right at the membrane is increased on the side, to which bulk solution is swept. It is decreased on the other side from which solutes are swept away. Consequently, the osmotic component of the overall driving force for water is overestimated. An underestimation of the bulk water permeability (hydraulic conductivity; Lp) is caused.

The effect of changes of concentrations at the membrane surface (C_s^m) may be calculated as a function water flow (Dainty 1963; Steudle & Tyerman 1983):

$$C_s^m = C_s^b \cdot \exp\left(-\frac{J_V \cdot \delta}{D_s}\right), \tag{15}$$

for just one side of the membrane. Here, C_s^b is the concentration in the bulk solution, δ is the thickness of the USL, and D_s the diffusion coefficient of the solute. The effects on the two sides of the membrane would be additive, but both D_s and δ may be different. For example, the external solution may be stirred while the internal is stagnant and δ different. D_s may be smaller in the cell wall than in bulk medium or cytoplasm. According to Eqn (15), the effect increases with an increasing J_V as well as with an increasing thickness of the USL, but decreases with an increasing diffusional mobility of the solute. Often, thicknesses of USLs are hard to access experimentally. They are subject to external stirring, but this cannot completely remove them. During hydrostatic experiments with the probe, an upper limit of the thickness of USLs may be worked out for the hydrostatic type of experiment. In these experiments, cell volume is changed by a ΔV inducing a change of pressure (ΔP). According to the definition of the cell elasticity (elastic modulus; ε), we have from Eq.(6):

$$\varepsilon = V\frac{dP}{dV} \approx V\frac{\Delta P}{\Delta V}. \tag{6}$$

Here V is volume of the cell. Assuming that all of the water is extruded instantaneously during a relaxation building up an USL, the maximum value of the thickness (δ_{max}) can be worked out (Steudle *et al.*, 1980; Steudle and Tyerman, 1983). For a cylindrical cell such as a *Chara* internode, we have:

$$\delta_{max} = \frac{\Delta V}{A} = \frac{V \cdot \Delta P}{A \cdot \varepsilon} = \frac{R}{2} \cdot \frac{\Delta P}{\varepsilon}, \qquad (17)$$

where A is the cell surface area and R its radius. It can be seen that for typical experimental values of $R = 0.4$ mm, $\Delta P = 0.05$ MPa and $\varepsilon = 30$ MPa, the δ_{max} would be as small as 0.3 μm.
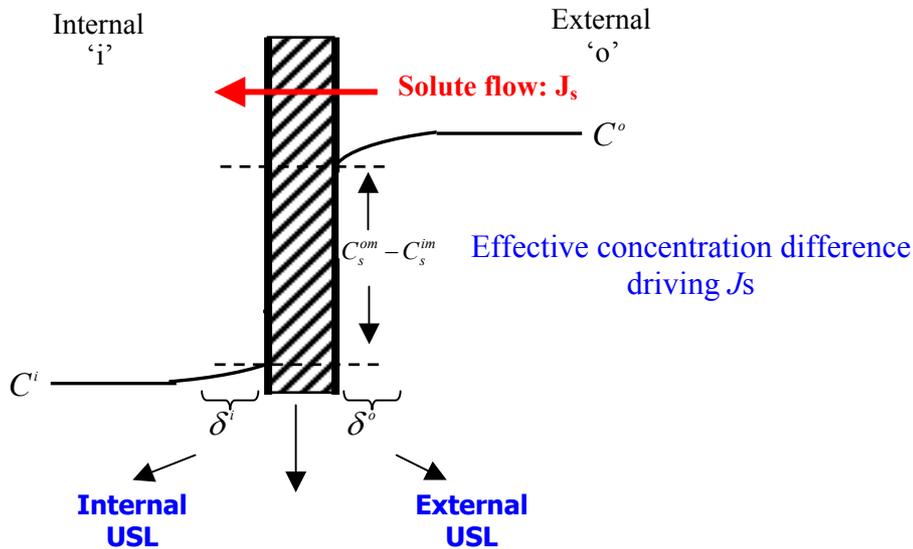
Figure 4. Concentration profile around the membrane, driving Js in the presence of unstirred layers. The effecrive concentration difference across the membrane is smaller than the concentration difference between external and internal medium, therefore, the force drivig the solute flow is overestimated, and the permeability coefficient underestimated when using the bulk concentrations to calculate Ps (gradient dissipation effect).

1.3.2   Gradient dissipation effect

The 'gradient-dissipation effect' refers to relative rates of diffusion of solutes across membranes and its supply from the bulk solution. When permeation is relatively rapid as compared with the supply, the latter could affect the overall solute transport

between compartments or may even dominate it. In this case, the actual concentration gradient driving permeation across the membrane is smaller than that between the bulk solutions (Fig. 4). There are three resistances in series, the permeation resistance of the membrane ($1/P_s$) and the two diffusional resistances related to USLs.

In the presence of rapidly permeating solutes such as heavy water (HDO), ethanol, or acetone, gradient dissipation should contribute to the absolute values of P_s and σ_s as measured with the pressure probe from biphasic pressure relaxations. Gradient dissipation tends to level off gradients of solute concentration across the membrane resulting in a local depletion of solutes on one side of the membrane and its enrichment on the other (Fig. 4). The overall measured 'permeation resistance' per unit area of the solute ($1/P_s^{meas}$) contains the true diffusional resistances for the membrane ($1/P_s$) and that of the two USLs on both side of the membrane δ^o/D_s^o and δ^i/D_s^i, respectively (δ^o and δ^i = equivalent thicknesses of USLs on the two sides of the membrane; D_s^o and D_s^i = diffusion coefficients of the solute which may be different on both sides):

$$\frac{1}{P_s^{meas}} = \frac{1}{P_s} + \frac{\delta^o}{D_s^o} + \frac{\delta^i}{D_s^i} \, . \tag{18}$$

Again, this assumes steady state, a planar, homogenous membrane, and linear concentration profiles within the layers. For the cylindrical *Chara* internodes, we may denote the radial distances from the center of the cell to the boundaries of USLs by 'a' (internal) and 'b' (external). Hence, the thicknesses of the external USL (δ^o) and of the internal USL (δ^i) would be $\delta^o = (b - R)$ and $\delta^i = (R - a)$, respectively. In the steady state, assuming $D_s^o = D_s^i = D_s$, the overall measured permeation resistance $1/P_s^{meas}$ can be written as:

$$\frac{1}{P_s^{meas}} = \frac{1}{P_s} + \frac{R}{D_s} \cdot \ln \frac{b}{a} \, . \tag{19}$$

Steudle and Frensch (1989) gave this equation, which they extensively discussed during solute permeation across roots with the endodermis being the main barrier ($R = E$). The cortex and stele acted as USLs, across which solutes had to diffuse,

preferentially in the apoplast. It should be noted that, as Eqn 18, Eqn 19 relates to linear concentration profiles within the USLs. In the presence of USLs at both sides of the plasma membrane of a *Chara* cell, for $D_s^o = D_s^i = D_s$, the measured value of reflection coefficient (σ_s^{meas}) would be given as (Steudle and Frensch, 1989):

$$\sigma_s^{meas} = \frac{1/P_s}{1/P_s + R/D_s \cdot (\ln(b/a))} \cdot \sigma_s. \tag{20}$$

By the first factor on the right side of Eqn 20, the measured coefficient would be smaller than the true one (σ_s). If D_s would be different in the medium/cell wall from that in the cytoplasm, a more extended expression may be used (Steudle and Frensch, 1989). Eqn 19 may be re-written to separate external from internal USLs, i.e.:

$$\underbrace{\frac{1}{P_s^{meas}}}_{\substack{\text{measured} \\ \text{resistance}}} = \underbrace{\frac{1}{P_s}}_{\substack{\text{true membrane} \\ \text{resistance}}} + \underbrace{\frac{R}{D_s} \cdot \ln\frac{b}{R}}_{\substack{\text{resistance of} \\ \text{external USL}}} + \underbrace{\frac{R}{D_s} \cdot \ln\frac{R}{a}}_{\substack{\text{resistance of} \\ \text{internal USL}}}. \tag{21}$$

In Eqns (19) to (21), the natural logs of ratios appear, because of the cylindrical geometry of cells. It is easily verified from the equations that, for $b \approx a$ or ($R-a$), (b-R) $<< R$, Eqn (21) reduces to the situation of the planar membrane (Eqn (18)).

1.3.3 Analytical solution assuming the stagnant internal USL

An analytical solution in the presence of a membrane surrounding a cylindrical *Chara* cell could be found when considering just internal and no external USLs. In this case (Crank 1975),

$$\frac{M_t}{M_\infty} = 1 - \sum_{n=1}^{\infty} \frac{4L^2}{\beta_n^2 \cdot (\beta_n^2 + L^2)} \cdot \exp\left[-\beta_n^2 \cdot \left(\frac{D_s \cdot t}{R^2}\right)\right] \tag{22}$$

is valid during the uptake of solute into the cylindrical cell, whereby M_t denotes the amount (not concentration) of solute in gram or mole in the cell at time t and M_∞ the amount when uptake is completed and $M_t/M_\infty = 1$. The β_n are the roots of $\beta \cdot J_1(\beta) - L \cdot J_0(\beta) = 0$, where J_1 and J_o are Bessel functions, and $L = P_s \cdot R/D_s$. (P_s = solute permeability across the membrane, D_s = diffusion coefficient of the solute). Re-

writing Eqn (22) in terms of the mean concentration in the cell, $<C_t>$, rather than amounts, one gets:

$$\frac{C_m - \langle C_t \rangle}{C_m} = \sum_{n=1}^{\infty} \frac{4L^2}{\beta_n^2 \cdot (\beta_n^2 + L^2)} \cdot \exp\left[-\beta_n^2 \cdot \left(\frac{D_s \cdot t}{R^2}\right)\right], \tag{23}$$

where C_m is the concentration of the medium. The equivalent relation describing the elution of solute from a cylindrical cell previously loaded with permeating solute, is given by:

$$\frac{M_t}{M_{or}} = \frac{C_t}{C_{or}} = \sum_{n=1}^{\infty} \frac{4L^2}{\beta_n^2 \cdot (\beta_n^2 + L^2)} \cdot \exp\left[-\beta_n^2 \cdot \left(\frac{D_s \cdot t}{R^2}\right)\right]. \tag{24}$$

M_{or} (C_{or}) denotes the original content (concentration) of the cell prior to elution by a medium which does not contain the solute. For given experimental values of L, the β_n of Eqn (23) are tabulated (see, for example, Table 5.2 of Crank 1975). The absolute amounts of the exponential terms in the series on the right sides of Eqns (23) and (24) rapidly decline with time. After a sufficiently long period of time, only the first term (β_1) has to be taken into account. The physical background for this is that for small t values, diffusion across the internal USL will be rapid. However, as this diffusive USL develops within the cylinder, the rate is slowing down. The USL tends to reach a certain quasi-steady thickness, and the overall permeability of the barrier (membrane plus internal USL) tends to become constant. In this case, we have ($\beta_1 = 1.68$ for a typical experimental value of $L = 2.36$; $P_s^{meas} = 4.2 \times 10^{-6}$ m·s^{-1}; $R = 0.4$ mm) and:

$$\frac{C_m - \langle C_t \rangle}{C_m} = \frac{4L^2}{\beta_1^2 \cdot (\beta_1^2 + L^2)} \cdot \exp\left[-\beta_1^2 \cdot \left(\frac{D_s \cdot t}{R^2}\right)\right], \tag{25}$$

during an uptake experiment. Under these conditions, Eqn (25) indicates an upper limit of around 40 % for the contribution of internal mixing for the rapidly permeating solute acetone (see Discussion of Chapter 2). This is in agreement with numerical solutions. When considering the uptake or loss of less permeating solutes such as 2-propanol or dimethyl-formamide (DMF), the contribution of internal mixing is smaller (see Fig. 8 of Chapter 2). This is a consequence of the series arrangement of permeation barriers (membrane and internal USL). In the absence of a membrane, i.e., when $P_s \rightarrow \infty$ and USLs dominate permeation (as claimed by Tyree et al. 2005), the equation corresponding to Eqn (22) is (Crank 1975):

$$\frac{M_t}{M_\infty} = 1 - \sum_{n=1}^{\infty} \frac{4}{\xi_n^2} \cdot \exp\left[-\xi_n^2 \cdot \left(\frac{D_s \cdot t}{R^2}\right)\right], \tag{26}$$

where the ξ_n are roots of a zeroth order Bessel function, and ξ_n = 2.405, 5.520, 8.654, 11.792, 14.931, 18.071, etc. (Jost 1960). Neglecting roots of higher order, we get:

$$\frac{M_t}{M_\infty} = 1 - \frac{4}{\xi_1^2} \cdot \exp\left[-\xi_1^2 \cdot \left(\frac{D_s \cdot t}{R^2}\right)\right], \tag{27}$$

analogous to Eqn (25). Permeability coefficients of the solutes used such as acetone (P_s = 4.2 × 10^{-6} m s^{-1}) would be still regarded as rather high when compared with those of nutrient ions, sugars or other metabolites in the cell sap (where values are ranging between 10^{-9} to 10^{-11} m s^{-1}; Nobel, 1999). Diffusional permeability coefficient for water is bigger than that of acetone by a factor of two (Henzler *et al.*, 2004; Ye *et al.*, 2006), but this effect may be cancelled by the bigger diffusion coefficient of heavy water as compared with acetone (Ye *et al.*, 2006). Hence, the P_s values derived for acetone are important for predicting the effects of internal USLs during the measurement of the permeability of isotopic water. On the other hand, in the case of endogenous solutes, the effects of USLs are negligible.

1.3.4 Stop flow technique

The role of diffusional USLs focusing on internal diffusional USLs had to be investigated. Ye *et al.* (2006) showed that vigorous external stirring minimized the effects of external USLs, but the role of the internal USLs could not yet be verified experimentally. To do this, a new stop-flow technique (SFT) was developed in the lab to work out the solute profile in the cell, which is otherwise difficult to access. Knowing the concentration right at the membrane surface is necessary to evaluate the 'true' membrane permeability of a solute, P_s. In the SFT, we intended to stop, by trial and error, the solute flow across the membrane by applying the same concentration in the external medium as that of the cell interior. In this way, the concentration right at the membrane was accessed or estimated, to get an idea of whether or not there was an USL inside the cell. Besides the SF measurements, a computer simulation of SF

experiments was performed, assuming either a well-stirred or a completely stagnant cell interior (minimum or maximum contribution of USLs). Results from simulations were compared with those of experiments to provide deeper insights to the effects of internal USLs. In both the experiments and simulations, we used solutes of different permeability. The P_s of the most rapid solute acetone was similar to that of isotopic water so that effects were tested in the presence of an extremely rapid permeant. Since water is an extremely rapidly permeating compound, the effect of USLs should be biggest and should provide the upper limit of the underestimation.

1.3.4.1   Simulation of diffusion inside the cell

To further quantify the role of internal diffusive transport in P_s measurement, we used classical numerical approaches for diffusion in a cylinder (see computational fluid dynamics text books such as that by Abbot and Basco, 1990). Internal USLs were modelled assuming that diffusion within *Chara* internodes was between concentric cylindrical shells of small thickness according to Fick's first law at a given time. Taking into account the cylindrical geometry, the differential equation for the diffusion of solute, 's' in a cylinder is (e.g. Steudle and Frensch, 1989):

$$J_s = -\frac{1}{A}\frac{dn_s^i}{dt} = -D_s \frac{1}{r}\frac{\partial}{\partial r}(r \cdot C_s^i).\tag{28}$$

The discrete analog of Eqn (28) is:

$$\frac{dC_s^i[i]}{dt} = \frac{2\pi L D_s (C_s^i[i-1] - C_s^i[i])}{\ln\left(\dfrac{r[i-1]}{r[i]}\right) \cdot V[i]} - \frac{2\pi L D_s (C_s^i[i] - C_s^i[i+1])}{\ln\left(\dfrac{r[i]}{r[i+1]}\right) \cdot V[i]},\tag{29}$$

assuming that

$$\frac{dC_s^i[i]}{dt} = \frac{n_s^i[i] - n_s^i[i+1]}{dt} \cdot \frac{1}{V[i]}\tag{30}$$

and

$$\frac{n_s^i[i]}{dt} = \frac{2\pi L D_s (C_s^i[i-1] - C_s^i[i])}{\ln\left(\dfrac{r[i-1]}{r[i]}\right)}.\tag{31}$$

Here, $C_s^i[i]$ is the concentration of solute in shell i at a given time, and radius $r[i]$ is the distance from the center of the cylinder to the center of the shell i; and L is the cell

length. In the simulations, time intervals of $dt = 0.01$ s and radius increments of the shells, $\Delta r = 5$ μm, were used (the radius of the cell, $R = 400$ or 500 μm). Further reduction of dt to 0.001 s and of Δr to 1 μm did not further refine the internal profiles of concentration (data not shown). Also, it was verified at given times, τ, and different distances from the membrane, Δx, that $\Delta x^2 / \tau$ was constant for a given concentration as predicted by basic diffusion kinetics (relation of Einstein and Smoluchowski, see textbooks on diffusion such as Jost, 1960).

1.3.4.2 Simulation of effects of internal USLs during stop flow

For membrane transport in a *Chara* internode, Eqns (3) and (4) were incorporated into simulations. During the simulations, solvent drag did not occur between shells, but instead was incorporated at the membrane. In Eqns (4) and Eqn (29), the transfer of solutes across the membrane and between adjacent shells is denoted, respectively. A standard computer program was used to numerically integrate Eqns (3), (4), and (28). This resulted in (i) concentration profiles within the cells and (ii) overall rates of uptake or losses by cells. Hence, it was tested in simulations whether or not the overall or mean concentration of solute 's' in the cell ('prospected concentration'; as assumed by Steudle and Tyerman, 1983; Eqn (13)) was a good estimate for the concentration adjacent to the membrane.

The Steudle/Tyerman theory assumes either that there are no effects of USLs or that these effects are incorporated into the value of P_s^{meas}. So far, the evidence that the contribution of internal USLs is relatively small is derived from the comparison of measured rates of solute flow (CPP) with rates expected from diffusion kinetics (Ye *et al.*, 2006). Hence, the evidence is indirect. The problem is twofold: (i) in contrast to the outer solution, the cell interior could not be stirred to test for the contribution of internal USLs; (ii) the concentration adjacent to the inner side of the PM could not be directly measured in order to determine how it would deviate from that used to calculate P_s, assuming that the cell interior was sufficiently stirred by mixing. To solve the problem, we compared results of simulations with those of experiments.

In the SFT, the concentration in the cell was first calculated using the Steudle/Tyerman theory (Eqn (13)) for a given time, i.e., a mean concentration was calculated and named the 'prospected concentration', C_{prosp}. The internal concentration could be calculated at each pressure (time) point of the solute phase by the difference between the extrapolated pressure to time zero and the original turgor, P_o (ΔP_{prosp}), because the solute phase and extrapolated curve of it represented the solute uptake or loss in the cell. In the endosmotic experiment (solute added outside and moving into the cell), once the cell's internal concentration was reached to C_{prosp}, the C_{prosp} was then applied to the outside medium, which tended to stop the solute flow across the membrane and bring the turgor pressure back to its original value, P_o. If there were no internal USLs, when C_{prosp} was added to external media, the C_{prosp} was the same as the concentration at the membrane, $C^{i}_{s\,mem}$, and no solute phase was observed in the simulation. However, assuming an internal USL, the solute flow did not stop when the C_{prosp} was added to the external media.

1.4   Aims of the research

First aim of the research was to respond to recent study of Tyree *et al.* (2005), who raised doubt that a pressure probe measures transport parameters that are underestimated due to the presence of unstirred layers.

(1) To quantify the role of unstirred layers during measurements of transport parameters using a cell pressure probe

Effects of USLs exist all the time in any kind of transport measurements, but the effects must be big especially in big-sized cells due to its diffusional nature. Therefore, a rigorous re-examination of effects of unstirred layers (USLs) during cell pressure probe (CPP) experiments with characean internodes has been performed to quantify their impact on measured values of hydraulic conductivity (Lp), and the permeability (P_s) and reflection (σ_s) coefficients. Both experiments and computer simulations were combined. A new stop-flow technique (SFT) was employed.

Second aim of the research was to test the change in water transport at cell level in response to light as recent studies indicated there could be light dependent gating of water channels (Nardini *et al.*, 2005; Tyree *et al.*, 2005). To do so, the CPP was applied to measure cell water permeability (cell Lp) in higher plants (*Zea mays* L.).

(2) To test the change in water permeability of leaf cells of corn in response to various light regimes

In response to light, water relation parameters (turgor and hydraulic conductivity, Lp) of individual cells of parenchyma sitting in the midrib of leaves of intact corn plants were investigated using the CPP. Light increased transpiration and it decreased cell turgor. To separate the effects by light and turgor, cell turgor (water potential) was kept constant during changes in light intensities either by applying gas pressure to the roots using a pressure chamber or by a perfusion technique in excised leaves. **Parenchyma cells were used as model cells for the leaf mesophyll, because they are (i) located in the vicinity of photosynthetically active cells, stomata and xylem**

vessels; (ii) easy to puncture due to their big size; (iii) suitable for long-term measurements since the midrib tissues could be well fixed.

(3) To check whether or not the change in cell water permeability could be attributed to a gating of water channels, aquaporins (AQPs)

Changes in cell Lp in response to light could happen most likely by a gating of AQPs. To support this, H_2O_2/Fe^{2+} treatments were used to reversibly close AQPs and light at a low level was treated to open AQPs. On the other hand, stress responses by high light were measured and those high light effects were also investigated in the presence of an antioxidant glutathione since an oxidative gating of AQPs in response to high light was suspected.

This research work can be divided into following sub-sections to investigate above aims:

I   A re-examination of the role of unstirred layers during the measurement of transport coefficients of *Chara corallina* internodes with the cell pressure probe (Ye, Kim and Steudle, 2006).

II   Further quantification of the role of internal unstirred layers during the measurement of transport coefficients in giant internodes of *Chara* by a new stop-flow technique (Kim, Ye, Reinhardt and Steudle, 2006).

III   Light and turgor affect the water permeability (aquaporins) of parenchyma cells in the midrib of leaves of *Zea mays* (Kim and Steudle, 2007).

IV   Gating of aquaporins by light and reactive oxygen species in leaf parenchyma cells of the midrib of *Zea mays* (Kim and Steudle, in press).

1.5 Materials and methods

1.5.1 Growth of corn plants

Corn (*Zea mays* L. cv. monitor and symphony) plants were grown in a greenhouse of Bayreuth University from caryopses in soil in plastic pots (1.7 L; diameter: 140 mm; depth: 110 mm). Plants were watered daily. Experiments were conducted on 4- to 8-week-old plants that were 0.8 to 1.2 m tall and contained about eight leaves. A maize plant was brought from the greenhouse, and the experimental set up was used as in Wei *et al.* (1999). Fourth or fifth leaves of the plants were used counting from the oldest. Leaf blades were 0.6 to 1 m long.

1.5.2 Growth of *Chara corallina*

Mature internodal cells of *Chara corallina* (50 to 120 mm long and 0.8 to 1.0 mm in diameter) were used in experiments. *Chara* had been grown in artificial pond water (APW) in tanks that contained layers of autoclaved mud from a natural pond. Composition of APW were 1.0 mM NaCl, 0.1 mM KCl, 0.1 mM $CaCl_2$ and 0.1 mM $MgCl_2$. Tanks were placed in the laboratory and illuminated for 24 h a day with a 15 W fluorescent lamp (Electronic, Germany) positioned 0.2 m over the water surface.

1.5.3 Pressure probe for *Chara* internodes

As shown in Fig. 5, a cell pressure probe (completely filled with silicone oil) was introduced through the protruding node adjacent to a *Chara* internode which had been placed in a glass tube with an inner diameter of 3 mm and fixed by a clamp. APW or test solutions were pumped through the other end of the glass tube along the cell (flow rates were $0.2 - 0.3$ m·s^{-1}), so that the solution around the cell was vigorously stirred. This minimized the thickness of external unstirred layers (USLs). Cell turgor pressure was measured by an electronic pressure transducer and was recorded by a computer connected to the output of the transducer. Two types of experiment can be performed with the aid of the probe. (i) In the hydrostatic experiments, the oil/cell sap meniscus

forming in the tip of the capillary was moved forward or backward by turning the micrometer and was then kept stable after each move until termination of a pressure relaxation; (ii) osmotic experiments were conducted by changing the osmotic pressure (concentration) of the medium while keeping the position of meniscus constant throughout.
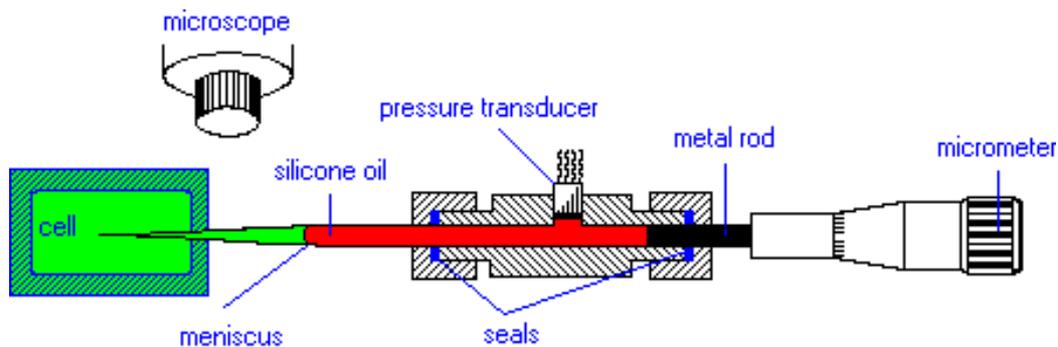
Figure 5. Schematic drawing of a cell pressure probe for giant single cells (*Chara corallina*). An oil/cell sap meniscus was forming in the tip of the capillary. The position of this meniscus was used as a point of reference during the measurements. Water flows were induced either by changing the pressure in the system using a metal rod (hydrostatic experiments) or by changing the osmotic pressure (concentration) of the medium (for a detailed explanation, see text).

1.5.4 Pressure probe for higher plant cells

The cell pressure probe was mounted on a Leitz manipulator (Wetzler, Germany) that was screwed on a thick iron plate and placed on a heavy stone table. Using magnetic bars, an intact leaf was mounted upside down on a metal sledge to securely expose the midrib for measurements of cell hydraulics. Cells in the midrib were punctured using the microcapillary of a CPP, which was filled with silicon oil up to the $\approx$ 8-μm tip (oil type AS4 from Wacker, Munich, Germany). When cells were punctured, a meniscus formed within the tip between cell sap and oil. With the aid of the probe, the meniscus was gently pushed back to close to the surface of the midrib to restore cell sap volume close to its original value. Compared with the equipment used for *Chara*, the volume

in the pressure chamber was small and the movement of meniscus was performed with the aid of a motor moving the metal rod of the probe.

As seen in Fig. 6, in order to separate effects of turgor from those of light, a pressure chamber encasing the root was used to keep turgor constant during illumination. The pot containing the root was sealed in a metal pressure chamber using rubber seals (Wei *et al*., 1999). Roots were pressurized with pressurized air from a gas tank. Measurements of relaxations (*Lp*) were continued during light phases.
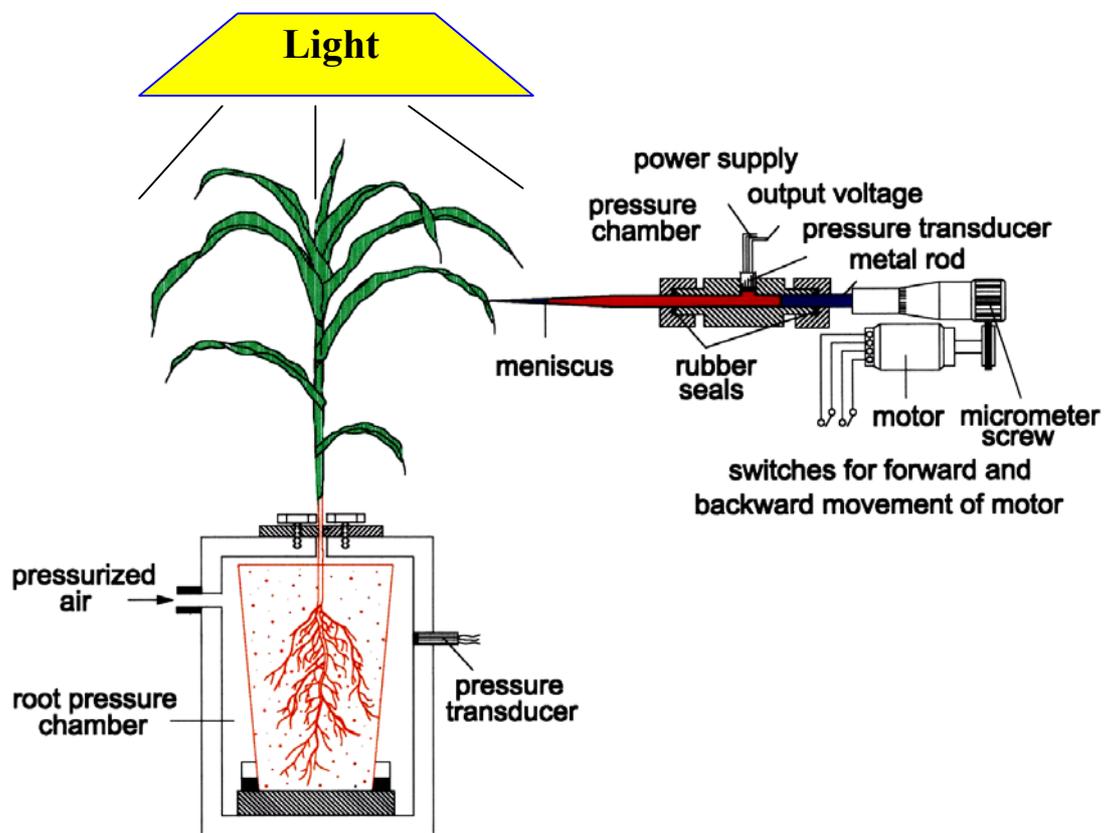
Figure 6. Schematic drawing of a cell pressure probe for higher plant tissue cells and a pressure chamber. The oil/cell sap meniscus in the tip of the glass capillary was used as a reference point. The meniscus was adjusted and water flows induced with a motor driving a metal rod into or out of the probe. The root of an intact corn plant was pressurized to keep turgor constant during illumination. The pot containing the root was sealed in a metal pressure chamber using rubber seals (modified after Wei *et al*., 1999).

1.5.5 Perfusion technique

The apoplastic environment of cells was varied during treatments, for example, by infiltration of AQP inhibitors. In order to perfuse a leaf tissue at constant turgor pressure during illumination and to provide certain ionic apoplastic environment, the pressure chamber (see Fig. 7) was provided with different solutions, which were infiltrated at a pressure of 0.1-0.2 MPa above atmospheric. The leaf tip was cut to enhance the transport through xylem vessels by perfusion. When pressurizing the basal cut end of the xylem, guttation droplets appeared at the leaf margin and at the cut surface outside of the pressure chamber.
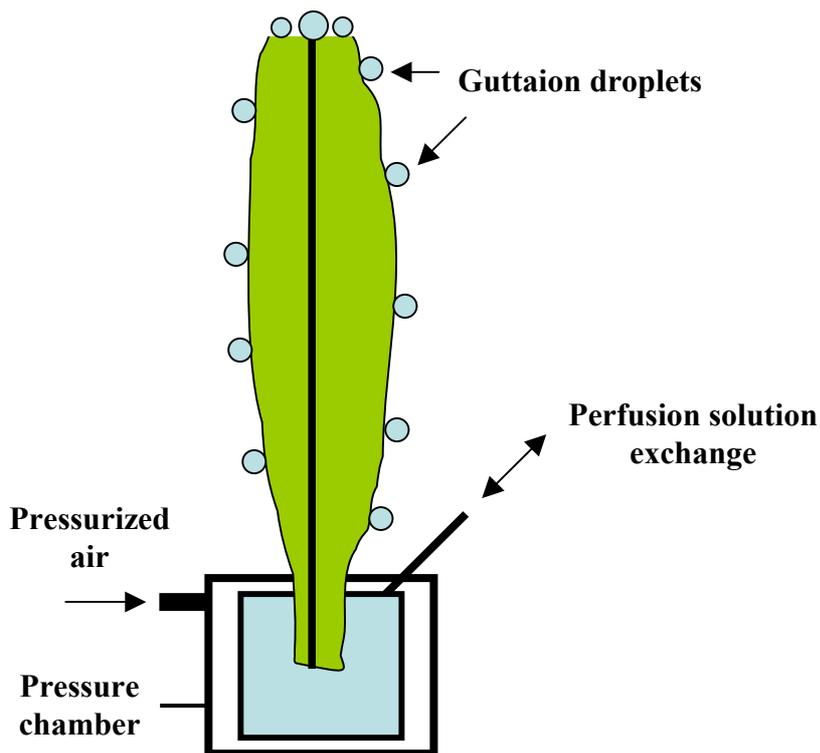
Figure 7. Schematic drawing of a perfusion system. Cut end of a leaf was encased in a pressure chamber to perfuse the solution *via* the cut end of the leaf immersed in a certain solution. The leaf was infiltrated with solutions and droplets were formed in the leaf margin. Perfusion could vary apoplastic condition around cells and turgor pressure was kept constant during illumination due to excessive water supply to a leaf.

1.6   Results and discussions

1.6.1   Quantification of the role of unstirred layers during measurements of transport parameters of water and solutes

The results show that the hydraulic conductivity measured in hydrostatic pressure-relaxation experiments (Lp_h) was not significantly affected by USLs ('sweep-away effect'), even when peak sizes of pressure pulses ($\pm \Delta P$) were increased by one order of magnitude above normal. In view of the constriction of water to aquaporins (AQPs) in the *Chara* membrane, the missing effect of a sweep-away (concentration polarization) is astonishing but may be explained by a rapid diffusional equilibration of solutes in arrays where water protruded across AQPs. During pressure clamp at $\pm$ ΔP, which was by an order of magnitude bigger than those usually used in relaxations, there was a reduction in Lp_h by 20 %, which was reversible within 20 s. Otherwise, it was hard to detect. As expected from theory, both external stirring and elevated concentration of the medium did not affect measurements of Lp_h. The hydraulic conductivity from the osmotic experiments (Lp_o) was measured as a function of the stirring of the medium at through flow rates (v_{med}) of between 0.02 and 0.55 m·s^{-1}. Lp_o tended to saturate at values close to Lp_h at rates of $v_{med} \approx 0.20$ m·s^{-1} (which are usually used in these experiments). Substantially smaller values of v_{med} were required to saturate P_s and σ_s ($v_{med} \approx 0.10$ m·s^{-1}). There was no further increase of Lp_o, P_s and σ_s, when the vigorous external stirring was furthermore increased by flushing air bubbles through the system at high rates (see http://www.uni-bayreuth.de/departments/planta/research/steudle/index.html). The stirring experiments allowed to estimate an upper limit of the thickness of external USLs of 30 μm (including the cell wall) at high rates of stirring. Comparison of calculated values for the diffusion into or out of a cylinder either lacking or containing an external membrane with experimental data of solute uptake or loss from cylindrical intact *Chara* internodes showed an upper limit of the equivalent thickness of diffusive internal USLs of between 100 to 120 μm (R = 0.4 mm). Different from the calculations according to classical diffusion kinetics, there was no early phase due to

the building up of diffusional USLs during the loading or elution experiments with intact cells. Results suggested an upper limit of the contribution internal USLs of between 15 and 29 % depending on the absolute value of measured overall solute permeability (P_s^{meas} = 1.6 × 10^{-6} m·s^{-1} or 4.2 × 10^{-6} m·s^{-1} for dimethylformamide (DMF) and acetone, respectively). Overall, the underestimation of P_s may be less than 25 ~ 30 % for these solutes. As discussed in some detail in Chapter 2, the data throw some doubt on recent claims by Tyree *et al*. (2005) of a dominating role of USLs in *Chara* experiments using the pressure probe. These authors claimed that the diffusional resistance across external and internal USLs would be larger by up to a factor of five than that across the plasma membrane. They were misled to this conclusion by several incorrect assumptions about pressure probe experiments as well as by some misunderstandings concerning the physics underlying USL concepts.

1.6.2 Quantification of the role of internal unstirred layers during the measurement of solute permeability coefficient (P_s)

Both the SF experiments and simulations provided quantitative data about internal concentration gradients and the contribution of USLs to overall measured values of P_s^{meas} for the three solutes. The SF experimental results agreed with SF simulations assuming that solutes diffused into a completely stagnant cell interior. The effects of internal USLs on the underestimation of membrane P_s declined with decreasing P_s. They were no bigger than 37% in the presence of the most rapidly permeating solute acetone (P_s^{meas} = 4.2 × 10^{-6} m s^{-1}), and 14% for the less rapidly permeating DMF (P_s^{meas} = 1.6 × 10^{-6} m s^{-1}). It is concluded that, even in the case of rapidly permeating solutes such as isotopic water and, even when making pessimistic assumptions about the internal mixing of solutes, an upper limit for the underestimation of P_s due to internal USLs was 37%. The current stop-flow data are in line with earlier estimations of the role of USLs in the literature on cell water relations (Steudle and Tyerman, 1983; Hertel and Steudle, 1997; Henzler and Steudle, 2000; Ye *et al*., 2005). Recent simulations on the effects of USLs in *Chara* by Tyree *et al*. (2005) are false because of erroneous assumptions and physical mistakes. They made a wrong assumption on the

sensitivity of the pressure, which can be measured by a pressure probe and neglected the turbulency, which existed in the external medium due to flow separation and entrance effects.

Since the ratio between the permeability of the plasma membrane of *Chara* and diffusion coefficient of acetone in the water is similar to that of heavy water, the data are of importance for the measurement of the diffusional permeability for water using isotopic water (P_d; HDO). As the ratio of P_f/P_d is equal to the number (N) of water molecules sitting in an aquaporin (AQP) pore (single-file pore; P_f = osmotic water permeability = $Lp \ V_w/RT$; V_w is the molar volume of liquid water), the comparison between P_d and P_f (Lp) has been used to estimate the volume of AQPs. This, however, requires values of P_d, which are corrected for USLs. Usually, data of Lp (P_f) are virtually free of effects of USLs (Ye *et al.*, 2006). When P_d values were underestimated, this would overestimate pore sizes.

1.6.3   Effects of low light (LL) and turgor on water permeability of leaf cells

Turgor pressures of cells in the midrib of corn leaves ranged from 0.2 to 1.0 MPa (2 to 10 bar) under laboratory light condition (40 µmol m^{-2} s^{-1} at the tissue level), and individual cells could be measured for up to six hours. By measuring effects of treatments on individual cells, this largely allowed to circumvent variability between cells. In accordance with earlier findings, there was a big variability in half times of hydrostatic relaxations, $T_{1/2}$s (inversely proportional to Lp) measured ranging from 0.5 s to 100 s, but the action of light on $T_{1/2}$s could be nevertheless figured out for cells having $T_{1/2}$s of bigger than 2 s, where AQPs were largely closed. Increasing light intensity ranging from 100 to 650 µmol m^{-2} s^{-1} decreased $T_{1/2}$ by a factor up to five within 10 min and increased Lp by the same factor. In the presence of light, turgor decreased due to an increase in transpiration, and this tended to compensate or even overcompensated for the effect of light on $T_{1/2}$. For example, during prolonged illumination, cell turgor dropped from 0.2 to 1.0 MPa to −0.03 to 0.4 MPa, and this drop caused an increase of $T_{1/2}$ and a reduction of cell Lp, i.e., there was an effect of

turgor on cell Lp besides that of light. To separate the two effects, cell turgor (water potential) was kept constant while changing light intensity by applying gas pressure to the roots using a pressure chamber. At a light intensity of 160 μmol m^{-2} s^{-1}, there was a reduction of $T_{1/2}$ by a factor of 2.5 after 10 to 30 min, when turgor was constant within ±0.05 MPa. Overall, the effects of light on $T_{1/2}$ (Lp) were overriding those of turgor only when decreases in turgor were less than about 0.2 MPa. Otherwise, turgor became the dominant factor. The results indicated that the hydraulic conductivity increased with increasing light intensity tending to improve the water status of the shoot. However, when transpiration induced by light tended to cause a low turgidity of the tissue, cell Lp was reduced. It was concluded that, when measuring the overall hydraulic conductivity of leaves, both the effects of light and turgor should be considered. Although the mechanism(s) of how light and turgor influence the cell Lp is still missing, it may involve the gating of aquaporins by both parameters.

1.6.4   Effects of high light (HL) and OH* on water permeability of leaf cells

High light (HL) at intensities of 800 and 1800 μmol m^{-2} s^{-1} increased $T_{1/2}$ in two third of cells by factors of 14 and 35, respectively. Effects of HL on $T_{1/2}$ were similar to those caused by H_2O_2 treatment in the presence of Fe^{2+}, which produced OH* (Fenton reaction; $H_2O_2 + Fe^{2+} = Fe^{3+} + OH^- + OH*$). An oxidative gating of AQPs, namely, by OH* have been found with *Chara* internodes and corn roots (Henzler *et al.*, 2004; Ye and Steudle, 2006). Treatments of 20 mM H_2O_2 following Fe^{2+} pre-treatments increased $T_{1/2}$ by a factor of 30. Those increased $T_{1/2}$ could be partly recovered, either when perfusion solution was changed back to the control solution or when LL of 200 μmol m^{-2} s^{-1} was applied. The antioxidant glutathione reversed HL effects as well. Cells pre-treated with 3 mM GSH + 0.5 mM $CaCl_2$ for 0.5-1.0 h, increased $T_{1/2}$ by HL as in the absence of GSH. In the presence of GSH, by contrast, there was a recovery within 15 min after light was switched off. Cells pre-treated by GSH for 24 h, did not increase $T_{1/2}$ by HL. These data suggest that HL could induce reactive oxygen species (ROS) such as OH*, and they affected water relations. It is known that, during light stress, ROS develop in leaves by the partial reduction of oxygen or from hydrogen

peroxide produced in many metabolic reactions (Foyer and Noctor, 2000). The results provide evidence that varying light climate adjusts water flow at cell level, i.e. water flow is maximized at a certain light intensity and then reduced again at HL. Possible mechanism(s) of how high light influence the cell Lp could be related to oxidative gating of AQPs. This may be important for the field, where plants experience light intensities of up to 2000 µmol m^{-2} s^{-1} on a bright day.

1.7 General conclusion

As aimed, changes in hydraulic conductivity at cell level in response to large ranges of light climate (100-1800 μmol m^{-2} s^{-1}) were investigated using a cell pressure probe. The results suggested that there could be an optimal light intensity, which would maximize water flow. However, at the high intensity of light, water flow was inhibited. This suggested that plants may increase hydraulic conductance in response to increasing light in a moderate level, since it would help leaf water potential favored (see General introduction). However, once water availability is disfavored, for example, in cases where turgor pressure decreases or plants are exposed to the high intensity of light, plants may need to change their strategy tending to save water by decreasing their hydraulic conductance. Although increasing hydraulic conductance of a leaf increases its water potential, thus keeping stomata open and maximizing the gas exchange and productivity, this would be acceptable only when water supply from soil is sufficient. Otherwise, increasing leaf hydraulic conductance may be harmful to plants when water supply is limiting. The present thesis was in line with this scenario, if one can assume the measured cells contributed to a certain part of hydraulic resistance of the whole leaf. Light and turgor separately affected cell hydraulics and high light (HL) affected cell hydraulics in the opposite direction to that by low light (LL). Changes in hydraulic conductivity of a cell in response to light were interpreted by a gating of water channels (aquaporins, AQPs). The response to HL intensity highlighted that there could be a connection between photosynthesis and water relations, recruiting reactive oxygen species as signalling species. Reactive oxygen species produced by HL, which is known to cause a photoinhibition by damage in a photosystem, are likely to inhibit water transport at a cell level by closing AQPs. Although there were clear effects of light on cell hydraulic conductivity, there was a large variability between cells. Further detailed studies are required to work out the different responses of cells and cell types. To scale up the results of cell hydraulics into overall leaf hydraulic conductance, hydraulic architecture of a leaf should be

found with identification of the major resistances that eventually determine overall leaf hydraulic conductance. This is still missing. Further open questions are:

- The exact mechanism(s) of how light acts on AQPs.
- Does negative turgor pressure of cells exist under conditions of high rates of transpiration causing substantial tensions in the xylem?

The existence of negative pressures, however, would require quite rigid cell walls, which are able to withstand tensions without 'imploding'. This may be thought to be unlikely (Tyree, 1976). On top of the above research, it was examined whether or not a cell pressure probe measured reliable transport parameters of a membrane, namely, in the context of unstirred layers, which exist in any kind of transport measurements. The rigorous experimental and theoretical investigation revealed a minor role of them, even in a big sized cell, which is most prone to be affected. On the other hand, recently, the role of unstirred layers in measurements of root hydraulics using a root pressure probe was rigorously investigated by Knipfer *et al*. (2007) and Knipfer and Steudle (2008). There were substantial effects of internal unstirred layers in the roots. The data suggested that initial water flows of root pressure relaxations should be used to overcome the difficulties. The problem is of some importance in the root, where the true root hydraulic conductivity should be used to compare hydraulic properties at the cell and root level, and to work out pathways for water movement in the root, e.g. to quantify the role of AQPs.

1.8   Short summary

- A rigorous re-examination of the role of **unstirred layers** (USLs) during pressure probe experiments with *Chara* internodes showed that USLs had **no measurable effect** on the **hydrostatic water permeability (Lp_h)**, even when considering an effect of a **flow constriction** due to the composite structure of the cell membrane, i.e., the existence of AQP arrays. In osmotic experiments, USLs should have resulted in **an underestimation of P_s and σ_s by at most 25 ~ 30 %** for the most rapidly permeating solutes like heavy water (HDO) and acetone, which is the **upper limit**. Results indicated that **cell membrane** acts as the **rate-limiting resistance for solutes** allowing sufficient time for an internal mixing by diffusion. The **real equivalent thicknesses** of internal USLs should be **smaller** than the estimated upper limits which were calculated by assuming a **completely stagnant and homogenous** internal compartment. It may be safe to estimate the **equivalent thickness of internal USLs of 50 μm.**

- The new **SFT** used to quantitatively elucidate the contribution of **internal USLs** on the measurement of solute permeability, P_s, in *Chara*, revealed that the **effects are lower** than previously estimated. Even in the presence of a rapidly permeating test solute (acetone) and assuming a completely stagnant cell interior, the upper limit of underestimation was **no bigger than 37%** in the presence of **most rapidly permeating** solutes. A similar figure may be obtained for heavy water, which represents the solute with the most rapid rate of permeation. Both the **simulation** and **experimental results** obtained by the new SFT agreed with earlier estimates of the contribution of USLs.

- **Hydraulics of parenchyma cells** of leaves of intact corn plants, which are close to xylem vessels and stomata, revealed **big ranges** of water permeability (and $T_{1/2}$) of the cells. **Long-term measurements** (up to **six hours** for an

individual cell) allowed investigating effects, despite some noise and variability in the hydraulics of cells.

- **Low light** intensity ranging from **100 to 650 μmol m^{-2} s^{-1} increased cell *Lp*** of parenchyma cells in the midrib of intact corn plants. **Turgor** had an ameliorative effect as well. Using a root-pressure chamber, **both effects could be separated** from each other. Illuminating the leaves while keeping turgor constant, cell *Lp* increased by a factor of three within 30 min at a light intensity of 160 μmol m^{-2} s^{-1}. Without keeping turgor constant, effects of light on cell *Lp* was compensated or even overcompensated by a decrease in turgor induced by an increase in transpiration. It is concluded that, without separating the effects of light and turgor, the results from measurements of overall leaf hydraulics (K_{leaf}) should be interpreted with caution.

- **High light** treatments of **800 and 1800** μmol m^{-2} s^{-1} decreased cell *Lp* of the excised corn leaves at constant turgor. It was a similar response to **H$_2$O$_2$/OH*** and could be reversed by an **antioxidant** glutathione. There could be an optimal light intensity to maximize water flow across leaf cells, but enhanced water flow could be inhibited at a certain light intensity. We may speculate that changes in **redox status** could have interplayed to **gate aquaporins** in response to high light.

1.9   References

Aroca R, Amodeo G, Fernandez-Illescas S, Herman EM, Chaumont F, Chrispeels MJ. 2005. The role of Aquaporins and membrane damage in chilling and hydrogen peroxide induced changes in the hydraulic conductance of maize roots. *Plant Physiology* **137**, 341-353.

Abbot MB, Basco DR. 1990. *Computational fluid dynamics, an introduction for engineers.* Harlow Essex, UK: Longman Scientific & Technical.

Alleva K, Niemietz CM, Sutka M, Maurel C, Parisi M, Tyerman SD, Amodeo G. 2006. Plasma membrane of *Beta vulgaris* storage root shows high water channel activity regulated by cytoplasmic pH and a dual range of calcium concentrations. *Journal of Experimental Botany* **57**, 609-621.

Barry PH, Diamond JM. 1984. Effects of unstirred layers on membrane phenomena. *Physiological reviews* **64**, 763–872.

Böhm J. 1893. Capillarität und Saftsteigen. *Berichte der Deutschen Botanischen Gesellschaft* **11**, 203–212.

Brodribb TJ, Holbrook NM. 2004. Diurnal depression of leaf hydraulic conductance in a tropical tree species. *Plant, Cell and Environment* **27**, 820-827.

Brodribb TJ, Holbrook NM. 2006. Declining hydraulic efficiency as transpiring leaves desiccate: two types of response. *Plant, Cell and Environment* **29**, 2205-2215.

Chaumont F, Barrieu F, Wojcik E, Chrispeels MJ, Jung R. 2001. Aquaporins constitute a large and highly divergent protein family in maize. *Plant Physiology* **125**, 1206–1215.

Cochard H, Nardini A, Coll L. 2004. Hydraulic architecture of leaf blades: where is the main resistance? *Plant, Cell and Environment* **27**, 1257-1267.

Cochard H, Venisse J-S, Barigah TS, Brunel N, Herbette S, Guilliot A, Tyree MT, Sakr S. 2007. Putative role of aquaporins in variable hydraulic conductance of leaves in response to light. *Plant Physiology* **143**, 122-133.

Cosgrove DJ. 1998. Cell wall loosening by expansins. *Plant Physiology* **118**, 333-339.

Crank J. 1975. *The mathematics of diffusion* (second edition of the original 1956 print). University Press Oxford, UK.

Dainty J. 1963. Water relations of plant cells. *Advances in Botanical Research* **1**, 279–326.

Dainty J, Ginzburg BZ. 1964a. The measurement of hydraulic conductivity (osmotic permeability to water) of internodal characean cells by means of transcellular osmosis. *Biochimica et Biophysica Acta* **79**, 102–111.

Dainty J, Ginzburg BZ. 1964b. The permeability of the protoplast of *Chara australis* and *Nitella translucens* to methanol, ethanol and iso-propanol. *Biochimica et Biophysica Acta* **79**, 122–128.

Dietz KJ. 2008. Redox signal integration: from stimulus to networks and genes. *Physiologia Plantarum* **133**, 459-468.

Dietz KJ, Jacob S, Oelze ML, Laxa M, Tognetti V, de Miranda SMN, Baier M, Finkemeier I. 2006. The function of peroxiredoxins in plant organelle redox metabolism. *Journal of Experimental Botany* **57**, 1697-1709.

Dixon HH, Joly J. 1894. On the ascent of sap. *Proceedings of Royal Society of London* **57,** 3–5.

Felle HH, Hanstein S. 2007. Probing apoplastic ion relations in *Vicia Faba* as influenced by nutrition and gas exchange. In: Sattelmacher B, Horst WJ, eds. *The apoplast of higher plants: compartment of storage, transport and reactions*. Dordrecht, the Netherlands: Springer, 295-306.

Finkelstein A. 1987. Water movement through lipid bilayers, pores and plasma membranes. Theory and reality. *Distinguished lecture series of the Society of General Physiologists*, Vol. 4 New York: Wiley.

Foyer CH, Noctor G. 2000. Tansley Review No. 112 Oxygen processing in photosynthesis: regulation and signalling. *New Phytologist* **146**, 359–388.

Franks PJ, Drake PL, Froend RH. 2007. Anisohydric but isohydrodynamic: seasonally constant plant water potential gradient explained by a stomatal control mechanism incorporating variable plant hydraulic conductance. *Plant, Cell and Environment* **30**, 19-30.

Frensch J, Schulze ED. 1988. The effect of humidity and light on cellular water relations and diffusion conductance of leaves of *Tradescantia virginiana* L. *Planta* **173**, 554-562.

Fricke W. 2002. Biophysical limitation of cell elongation in cereal leaves. *Annals of Botany* **90**, 157-167.

Fryer MJ, Oxborough K, Mullineaux PM, Baker NR. 2002. Imaging of photo-oxidative stress responses in leaves. *Journal of Experimental Botany* **53**, 1249-1254.

Gukasyan, HJ; Lee, VHL; Kim, KJ, Kannan R. 2002. Net glutathione secretion across primary cultured rabbit conjunctival epithelial cell layers. *Investigative Ophthalmology & Visual Science* **43**, 1154-1161.

Henzler T, Steudle E. 1995. Reversible closing of water channels in *Chara* internodes provides evidence for a composite transport model of the plasma membrane. *Journal of Experimental Botany* **46**, 199–209.

Henzler T, Waterhouse RN, Smyth AJ, Carvajal M, Cooke DT, Schäffner AR, Steudle E, Clarkson DT. 1999. Diurnal variations in hydraulic conductivity and root pressure can be correlated with the expression of putative aquaporins in the root of *Lotus japonicus*. *Planta* **210**, 50-60.

Henzler T, Steudle E. 2000. Transport and metabolic degradation of hydrogen peroxide: model calculations and measurements with the pressure probe suggest transport of H_2O_2 across water channels. *Journal of Experimental Botany* **51**, 2053–2066.

Henzler T, Ye Q, Steudle E. 2004. Oxidative gating of water channels (aquaporins) in *Chara* by hydroxyl radicals. *Plant Cell and Environment* **27**, 1184–1195.

Hertel A, Steudle E. 1997. The function of water channels in *Chara*: the temperature dependence of water and solute flows provides evidence for composite membrane transport and for a slippage of small organic solutes across water channels. *Planta* **202**, 324–335.

House CR. 1974. Water transport in cells and tissues. In: Davson H, Greenfield ADM, Whittam R, Brindley GS, eds. *Monographs of the physiological society*, London, UK: Edward Arnold (Publishers) LTD.

Javot H, Maurel C. 2002. The role of aquaporins in root water uptake. *Annals of Botany* **90**, 301-313.

Jiang MY, Zhang JH. 2001. Effect of abscisic acid on active oxygen species, antioxidative defence system and oxidative damage in leaves of maize seedlings. *Plant and Cell Physiology* **42**, 1265-1273.

Johansson I, Larsson C, Ek B, Kjellbom P. 1996. The major integral proteins of spinach leaf plasma membranes are putative aquaporins and are phoshorylated in response to Ca^{2+} and apoplastic water potential. *The Plant Cell* **8**, 1181-1191.

Johansson I, Karlsson M, Shukla VK, Chrispeels MJ, Larsson C, Kjellbom P. 1998. Water transport activity of the plasma membrane aquaporin PM28A is regulated by phosphorylation. *The Plant Cell* **10**, 451-459.

Jost W. 1960. Diffusion in solids, liquids, gases. In: Hutchinson E, van Rysselberghe P, eds. *Physical Chemistry a series of monographs*, New York, USA: Academic Press.

Kedem O, Katchalsky A. 1958. Thermodynamic analysis of the permeability of biological membranes to nonelectrolytes. *Biochimica et Biophysica Acta* **27,** 229-246.

Kim YX, Steudle E. 2007. Light and turgor affect the water permeability (aquaporins) of parenchyma cells in the midrib of leaves of *Zea mays*. *Journal of Experimental Botany* **58**, 4119-4129.

Kim Y., Ye Q., Reinhardt H., Steudle E. 2006 Further quantification of the role of internal unstirred layers during the measurement of transport coefficients in giant internodes of *Chara* by a new stop-flow technique. *Journal of Experimental Botany* **57**, 4133-4144.

Kiyosawa K, Tazawa M. 1972. Influence of intracellular and extracellular tonicities on water permeability in characean cells. *Protoplasma* **74**, 257–270.

Kiyosawa K, Tazawa M. 1977. Hydraulic conductivity of tonoplast free *Chara* cells *Journal of Membrane Biology* **37**, 157–166.

Kjellbom P, Larsson C, Johansson I, Karlsson M, Johanson U. 1999. Aquaporins and water homeostasis in plants. *Trends in Plant Science* **4**, 308-314.

Knipfer T, Das D, Steudle E. 2007. During measurements of root hydraulics with pressure probes, the contribution of unstirred layers is minimized in the

pressure relaxation mode: comparison with pressure clamp and high-pressure flowmeter. *Plant, Cell & Environment* **30**, 845-860.

Knipfer T, Steudle E. 2008. Root hydraulic conductivity measured by pressure clam is substantially affected by internal unstirred layers. *Journal of Experimental Botany* **59**, 2071-2084.

Kramer PJ, Boyer JS. 1995. *Water relations of plants and soils*. San Diego, California: Academic Press.

Lee SH, Chung GC, Steudle E. 2005. Low temperature and mechanical stresses differently gate aquaporins of root cortical cells of chilling-sensitive cucumber and chilling-resistant figleaf gourd. *Plant Cell and Environment* **28**,1191–1202.

Lee SH, Zwiazek JJ, Chung GC. 2008. Light-induced transpiration alters cell water relations in figleaf gourd (*Cucurbita ficifolia*) seedlings exposed to low root temperatures. *Physiologia Plantarum* **133**, 354-362.

Levitt DG. 1974. New theory of transport for cell-membrane pores. 1. general theory and application to red-cell. *Biochimica et Biophysica Acta* **373,** 115-131.

Lo Gullo MA, Nardini A, Trifilo P, Salleo S. 2005. Diurnal and seasonal variations in leaf hydraulic conductance in evergreen and deciduous trees. *Tree physiology* **25**, 505-512.

Lösch R. 2001 *Wasserhaushalt der Pflanzen*. Wiebelsheim: Quelle & Meyer Verlag.

Mathai JC, Mori S, Smith BL, Preston GM, Mohandas N, Collins M, van Zijl PC, Zeidel ML, Agre P. 1996. Functional analysis of aquaporin-1 deficient red cells. The Colton-null phenotype. *Journal of Biological Chemistry* **271,** 1309–1313.

Maurel C. 1997. Aquaporins and water permeability of plant membranes. *Annual Review of Plant Physiology and Plant Molecular Biology* **48**, 399-429.

Maurel C, Chrispeels MJ. 2001. Aquaporins. A molecular entry into plant water relations. *Plant Physiology* **125**, 135-138.

Maurel C, Tacnet F, Güclü J, Guern J, Ripoche P. 1997. Purified vesicles of tobacco cell vacuolar and plasma membranes exhibit dramatically different water permeability and water channel activity. *Proceedings of the National Academy of Sciences USA* **94**, 7103–7108.

Moshelion M, Becker D, Biela A, Uehlein N, Hedrich R, Otto B, Levi H, Moran N, Kaldenhoff R. 2002. Plasma membrane aquaporins in the motor cells of *Samanea saman*: diurnal and circadian regulation. *The Plant Cell* **14**, 727-739.

Nardini A, Salleo S, Andri S. 2005. Circadian regulation of leaf hydraulic conductance in sunflower (*Helianthus annuus* L. cv Margot). *Plant, Cell and Environment* **28**, 750-759.

Niemietz CM, Tyerman SD. 1997 Characterization of water channels in wheat root membrane vesicles. *Plant Physiology* **115,** 561–567.

Nobel PS. 1999. *Physicochemical and environmental plant physiology*. San Diego, USA: Academic Press.

Noctor G, Gomez L, Vanacker H, Foyer CH. 2002. Interactions between biosynthesis, compartmentation and transport in the control of glutathione homeostasis and signalling. *Journal of Experimental Botany* **53**, 1283-1304.

Nonami H, Boyer JS, Steudle E. 1987. Pressure probe and isopiestic psychrometer measure similar turgor. *Plant Physiology* **83**, 592-595.

Oertli JJ. 1986. The effect of cell size on cell collapse under negative turgor pressure. *Journal of Plant Physiology* **124**, 365-370.

Pastori G, Foyer CH. 2002. Common components, networks, and pathways of cross-tolerance to stress: the central role of "redox" and abscissic acid mediated controls. *Plant Physiology* **129**, 460-468.

Poling BE, Prausnitz JM, O'Connell JP. 2001. *The properties of gases and liquids* (fourth edition). New York, USA: McGraw-Hill.

Reid RC, Sherwood TK. 1966. *The properties of gases and liquids*. New York, USA: McGraw-Hill.

Rhizopoulou S. 1997. Is negative turgor fallacious? *Physiologia Plantarum* **99**, 505-510.

Rüdinger M, Hierling P, Steudle E. 1992. Osmotic biosensors. How to use a characean internode for measuring the alcohol content of beer. *Botanica Acta* **105**, 3–12.

Sack L, Holbrook NM. 2006. Leaf hydraulics. *Annual Review of Plant Biology* **57**, 361-381.

Sack L, Melcher PJ, Zwieniecki MA, Holbrook NM. 2002. The hydraulic conductance of the angiosperm leaf lamina: a comparison of three measurement methods. *Journal of Experimental Botany* **53**, 2177-2184.

Sack L, Tyree MT, Holbrook NM. 2005. Leaf hydraulic architecture correlates with regeneration irradiance in tropical rainforest trees. *New Phytologist* **167**, 403-413.

Schulze ED. 1986. Carbon-dioxide and water-vapor exchange in response to drought in the atmosphere and in the soil. *Annual Review of Plant Physiology and Plant Molecular Biology* **37**, 247-274.

Schütz K, Tyerman SD. 1997. Water channels in *Chara corallina*. *Journal of Experimental Botany* **48,** 1511-1518.

Sehy JV, Banks AA, Ackerman JJH, Neil JJ. 2002. Importance of intracellular water apparent diffusion to the measurement of membrane permeability. *Biophysical Journal* **83**, 2856–2863.

Shabala S, Newman I. 1999. Light-induced changes in hydrogen, calcium, potassium, and chloride ion fluxes and concentrations from the mesophyll and epidermal tissues of bean leaves. Understanding the ionic basis of light-induced bioelectrogenesis. *Plant Physiology* **119**, 1115-1124.

Slatyer, RO. 1967 *Plant-water relationships*. New York: Academic press.

Steudle E. 1993. Pressure probe techniques: basic principles and application to studies of water and solute relations at the cell, tissue, and organ level. In: Smith JAC, Griffith H, eds. *Water Deficits: Plant Responses from Cell to Community*, Oxford, UK: BIOS. Scientific Publishers, 5–36.

Steudle E, Brinckmann E. 1989. The osmometer model of the root: water and solute relations of *Phaseolus coccineus*. *Botanica Acta* **102**, 85–95.

Steudle E, Frensch J. 1989. Osmotic responses of maize roots. Water and solute relations. *Planta* **177**, 281–295.

Steudle E, Henzler T. 1995. Water channels in plants: do basic concepts of water transport change? *Journal of Experimental Botany* **46,** 1067-1076.

Steudle E, Tyerman SD. 1983. Determination of permeability coefficients, reflection coefficients and hydraulic conductivity of *Chara corallina* using the pressure probe: effects of solute concentrations. *Journal of Membrane Biology* **75**, 85–96.

Steudle E, Zimmermann U. 1974. Determination of the hydraulic conductivity and of reflection coefficients in *Nitella flexilis* by means of direct cell-turgor pressure measurements. *Biochimica et Biophysica Acta* **322**, 399–412.

Steudle E. 1993. Pressure probe techniques: basic principles and application to studies of water and solute relations at the cell, tissue and organ level. In: Smith JAC, Griffiths H, eds. *Water deficits: plant responses from cell to community*. Oxford, UK: BIOS Scientific Publishers, 5-36.

Steudle E. 2000. Water uptake by roots: effects of water deficit. *Journal of Experimental Botany* **51**, 1531-1542.

Steudle E. 2001. The cohesion-tension mechanism and the acquisition of water by plant roots. *Annual Review of Plant Physiology and Plant Molecular Biology* **52**, 847-875.

Steudle E, Smith JAC, Lüttge U. 1980. Water relation parameters of individual mesophyll cells of the crassulacean acid metabolism plant *Kalanchoe daigremontiana*. *Plant Physiology* **66**, 1155-1163.

Steudle E, Henzler T. 1995. Water channels in plants: do basic concepts of water transport change? *Journal of Experimental Botany* **46**, 1067-1076.

Steudle E, Peterson CA. 1998. How does water get through roots? *Journal of Experimental Botany* **49**, 775-788.

Stevenson J.F. 1974. Unsteady mass transfer in a long composite cylinder with interfacial resistances. *AIChE Journal* **20**, 461–466.

Stevenson JF, Von Deak MA, Weinberg M, Schuette RW. 1975. An unsteady state method for measuring the permeability of small tubular membranes. *AIChE Journal* **21**, 1192–1199.

Thürmer F, Zhu JJ, Gierlinger N, Schneider H, Benkert R, Geßner P, Herrmann B, Bentrup F-W, Zimmermann U. 1999. Diurnal changes in xylem pressure and mesophyll cell turgor pressure of the liana Tetrastigma voinierianum: the role of cell turgor in long-distance water transport. *Protoplasma* **206**, 152-162.

Tomos AD, Steudle E, Zimmermann U, Schulze ED. 1981. Water relations of leaf epidermal cells of Tradescantia virginiana. *Plant Physiology* **68**, 1135-1143.

Tournaire-Roux C, Sutka M, Javot H, Gout E, Gerbeau P, Luu DT, Bligny R, Maurel C. 2003. Cytosolic pH regulates root water transport during anoxic stress through gating of aquaporins. *Nature* **425**, 393-397.

Tyerman SD, Steudle E. 1984. Determination of solute permeability in *Chara* internodes by a turgor minimun method. Effect of external pH. *Plant Physiology* **74**, 464–468.

Tyerman SD, Bohnert HJ, Maurel C, Steudle E, Smith JAC. 1999. Plant aquaporins: their molecular biology, biophysics and significance for plant water relations. *Journal of Experimental Botany* **50**, 1055-1071.

Tyerman SD, Niemietz CM, Bramley H. 2002. Plant aquaporins: multifunctional water and solute channels with expanding roles. *Plant, Cell and Environment* **25**, 173-194.

Tyree MT. 1976. Negative turgor pressure in plant cells: fact or fallacy? *Canadian Journal of Botany* **54**, 2738-2746.

Tyree MT, Koh S, Sands P. 2005. The determination of membrane transport parameters with the cell pressure probe: theory suggests that unstirred layers have significant impact. *Plant Cell and Environment* **28,** 1475-1486.

Tyree MT, Nardini A, Salleo S, Sack L, Omari BE. 2005. The dependence of leaf hydraulic conductance on irradiance during HPFM measurements: any role for stomatal response? *Journal of Experimental Botany* **56**, 737-744.

Tyree MT, Zimmermann MH. 2002 *Xylem Structure and the Ascent of Sap* (second edition). Berlin: Springer.

van den Honert TH. 1948. Water transport in plants as a catenary process. *Discussions of the Faraday Society* **3,** 146–153.

Walz T, Smith BL, Zeidel ML, Engel A, Agre P. 1994. Biologically active two-dimensional crystals of aquaporin CHIP. *Journal of Biological Chemistry* **269**, 1583–1586.

Wan XC, Steudle E, Hartung W. 2004. Gating of water channels (aquaporins) in cortical cells of young corn roots by mechanical stimuli (pressure pulses): effects of ABA and of $HgCl_2$. *Journal of Experimental Botany* **55**, 411–422.

Wei C, Tyree MT, Steudle E. 1999. Direct measurement of xylem pressure in leaves of intact maize plants. A test of the cohesion-tension theory taking hydraulic architecture into consideration. *Plant Physiology* **121**, 1191-1205.

Westgate ME, Steudle E. 1985. Water transport in the midrib tissue of maize leaves. *Plant Physiology* **78**, 183-191.

White FM. 1999. *Fluid mechanics* (fourth edition). Boston, USA: McGraw-Hill.

Xiong LM, Schumaker KS, Zhu JK. 2002. Cell signaling during cold, drought and salt stress. *Plant Cell* **14 (suppl.)**, S165-S183.

Ye Q, Kim Y, Steudle E. 2006. A re-examination of the minor role of unstirred layers during the measurement of transport coefficients of Chara corallina internodes with the cell pressure probe. *Plant, Cell and Environment* **29,** 964-980.

Ye Q, Muhr J, Steudle E. 2005. A cohesion/tension model for the gating of aquaporins allows estimation of water channel pore volumes in *Chara*. *Plant Cell and Environment* **28**, 525–535.

Ye Q, Steudle E. 2006. Oxidative gating of water channels (aquaporins) in corn roots. *Plant Cell and Environment* **29,** 459-470.

Ye Q, Wiera B, Steudle E. 2004. A cohesion/tension mechanism explains the gating of water channels (aquaporins) in *Chara* internodes by high concentration. *Journal of Experimental Botany* **55,** 449–461.

Zeevalk GD, Manzino L, Sonsalla PK, Bernard LP. 2007. Characterization of intracellular elevation of glutathione (GSH) with glutathione monoethyl ester and GSH in brain and neuronal cultures: Relevance to Parkinson's disease. *Experimental Neurology* **203**, 512-520.

Zhang WH, Tyerman SD. 1999. Inhibition of water channels by $HgCl_2$ in intact wheat root cells. *Plant Physiology* **120**, 849-857.

Zhu GL, Steudle E. 1991. Water transport across maize roots − simultaneous measurement of flows at the cell and root level by double pressure probe technique. *Plant Physiology* **95**, 305-315.

Zwieniecki MA, Melcher PJ, Holbrook NM. 2001. Hydrogel control of xylem hydraulic resistance in plants. *Science* **291**, 1059-1062.

II

Publications

2   A re-examination of the minor role of unstirred layers during the measurement of transport coefficients of *Chara corallina* internodes with the cell pressure probe

Qing Ye, Yangmin Kim, and Ernst Steudle

Department of Plant Ecology, Bayreuth University, D-95440 Bayreuth, Germany

Corresponding author: E. Steudle
E-mail: ernst.steudle@uni-bayreuth.de
Fax: +49-921-552564

Number of Figures: 8
Number of Tables: 2

Abstract

The impact of unstirred layers (USLs) during cell pressure probe experiments with *Chara corallina* internodes has been quantified. The results show that the hydraulic conductivity (Lp) measured in hydrostatic relaxations was not significantly affected by USLs even in the presence of high water flow intensities ('sweep-away effect'). During pressure clamp, there was a reversible reduction in Lp by 20%, which was explained by the constriction of water to aquaporins (AQPs) in the *C. corallina* membrane and a rapid diffusional equilibration of solutes in arrays where water protruded across AQPs. In osmotic experiments, Lp, and permeability (P_s) and reflection (σ_s) coefficients increased as external flow rate of medium increased, indicating some effects of external USLs. However, the effect was levelling off at 'usual' flow rates of 0.20-0.30 m·s^{-1} and in the presence of vigorous stirring by air bubbles, suggesting a maximum thickness of external USLs around 30 μm including the cell wall. Because the diameter of internodes were around 1 mm, internal USLs could have played a significant or even a dominating role, at least in the presence of the rapidly permeating solutes used [acetone, 2-propanol, and dimethylformamide (DMF)]. A comparison of calculated (diffusion kinetics) and of measured permeabilities indicated an upper limit of the contribution of USLs for the rapidly moving solute acetone of 29%, and of 15% for the less rapidly permeating DMF. The results throw some doubt that in *C. corallina*, USLs rather than the cell membrane dominate solute uptake, at least for the most rapidly moving solute acetone.

Key-words: *Chara corallina;* aquaporin; hydraulic conductivity; permeability coefficient; reflection coefficient; water channel.

Introduction

The solute concentrations that govern the permeation of solutes and water across cell membranes are the concentrations adjacent to the membrane/solution interfaces, which are usually not measurable. Due to 'unstirred layers (USLs)', these concentrations differ from the concentration in the bulk solutions which are usually measured. When bulk concentrations are used to quantify the driving forces such as an osmotic pressure difference driving a water flow (J_V) or a concentration difference driving a solute flow (J_s), the 'real' forces may be overestimated due to the existence of USLs. As a consequence, transport parameters such as the hydraulic conductivity (Lp), the permeability (P_s) and reflection (σ_s) coefficient are underestimated.

Concentration changes at the membrane surface may be either caused by a volume flow (induced by either hydrostatic or osmotic gradients) or they are caused by solute transfer. The first type of a diffusion *vs.* convection is referred to as a 'sweep-away effect' (Dainty 1963). The second type in the presence of purely diffusional USLs, has been denoted as a 'gradient-dissipation effect' tending to increase as solute permeability increases (Barry & Diamond 1984). For tissue cells, sweep-away can be studied using the cell pressure probe (Steudle, Smith & Lüttge 1980), but the evaluation of gradient-dissipation is difficult, as the entire tissue around a cell will act as an USL. Rather than the plasma membrane, the latter should usually dominate the exchange of water and solutes (Steudle & Frensch 1989; Ye & Steudle 2005). Isolated, giant cells of algae have been used in the past and recently to study USLs using different techniques such as isotopic exchange of solutes, transcellular osmosis, or the cell pressure probe (Dainty & Ginzburg 1964a; Steudle & Tyerman 1983; Steudle 1993; Hertel & Steudle 1997; Henzler & Steudle 2000; Ye, Wiera & Steudle 2004). Most of these data refer to internodes of *Chara corallina*. USLs of isolated cells can be treated as additional permeation resistances in series to the cell membrane. They add to the overall transport resistance. It has been shown that the contribution of sweep-away is usually small and that of gradient-dissipation more significant although not dominating, even in the presence of rapidly permeating solutes such as monohydric alcohols, acetone, formamide, dimethylformamide or isotopic water (heavy water;

HDO). For the most rapidly permeating solute HDO, a value of 25 % of underestimation was recently given (Ye, Muhr & Steudle 2005). In isolated giant cells or suspensions of small cells or vesicles, the thickness of external USLs can be efficiently reduced by stirring. However, the cell interior can not be stirred. For small cells, dimensions of a few μm provide a small upper limit of USLs (Finkelstein 1987; Niemietz & Tyerman 1997), but for giant cells this is not the case. For example, for the cylindrical internodes of *Chara* with a diameter of around 1.0 mm, the thickness of internal USL could, in principle, be identical with the radius, i.e. the thickness could be 500 μm in the worst case. However, it has been shown that it is substantially smaller than the radius (Hertel & Steudle 1997; Henzler & Steudle 2000). Hence, transport coefficients (Lp, P_s (P_d), and σ_s) measured with the probe are usually dominated by the membrane rather than by internal USLs. At least for isotopic water and the most rapidly permeating test solutes used so far, the system behaves like two compartments. This is in agreement with older findings that removal of the tonoplast did not affect cell Lp in *Chara* (Kiyosawa & Tazawa 1977), and with more recent data that indicate a much higher Lp of the tonoplast than of the plasmalemma (Maurel *et al*. 1997). Recent measurements demonstrated that there are different AQPs in the plasma membrane of *Chara,* which, in part, transport small organic solutes besides the water (Hertel & Steudle 1997; Henzler & Steudle 2000; Henzler, Ye & Steudle 2004; Ye & Steudle 2005). The comparison of the osmotic ($P_f = Lp \cdot RT/V_w$; V_w is the molar volume of liquid water) with the diffusional water permeability (P_d) allowed conclusions about the amounts of water molecules aligned in AQPs which relate to P_f/P_d ratios. However, when P_d was underestimated due to a substantial contribution of USLs, ratios would be overestimated. Hence, it is important to know the contribution of USLs, namely, when discussing basic mechanisms of water and solute flow across membranes (Hertel & Steudle 1997; Henzler *et al*. 2004; Ye *et al*. 2005).

Recently, Tyree, Koh & Sands (2005) argued that transport coefficients measured with the probe in *Chara* are subject to substantial or even dominating effects of USLs. In part, this should be due to the experimental arrangement of characean internodes fixed in tubes which are perfused with solution at a certain rate to minimize thicknesses of external USLs (Steudle & Zimmermann 1974; Steudle & Tyerman

1983). Tyree *et al*. (2005) used results from a simulation model to support their view. They assumed thicknesses of external and internal USLs of as big as 100 and 350 μm, respectively. They concluded that the permeation resistance of external and internal USLs may be larger by a factor of five than that of the plasma membrane and should, therefore, dominate the overall rate of permeation. According to Tyree *et al*. (2005), no conclusions can be drawn from the pressure probe experiments with *Chara* about the true permeation properties of membranes in the presence of rapidly permeating solutes.

In this paper, we present a rigorous re-examination of the role of external and internal USLs using rapidly permeating solutes (as in Tyree *et al*. 2005). We consider the roles of sweep-away and of gradient-dissipation on measurements of cell Lp, P_s, and σ_s. We provide quantitative evidence that (i) the thicknesses of USLs claimed by Tyree *et al*. (2005) have no basis from the literature. (ii) We show that Tyree *et al*. (2005) are wrong in their conclusions about the vigorous stirring in the experimental set-up used so far in experiments with *Chara*. (iii) We demonstrate that the analysis of pressure relaxations by Tyree *et al*. (2005) is based on false assumptions about the resolution of the pressure probe. (iv) Our data strongly support the view that the conventional sweep-away does not play a role during pressure relaxations. (v) New evidence is presented that during pressure clamp, there is a reversible reduction of cell Lp by 20 %. This is explained by a combined action of a constriction of water flow in the membrane to arrays containing AQPs and a local effect of elevated concentration on the open/closed state AQPs. (vi) When there is an efficient stirring of the medium, the upper limit of the thickness of external USLs was estimated as 30 μm. (vii) The theoretical comparison of the rates of uptake (loss) into a cell cylinder either lacking a plasma membrane or containing it with measured rates revealed an upper limit of 50 μm for the thickness of internal USLs. Hence, for rapidly permeating solutes, this may cause an underestimation of P_s and σ_s by 25 ~ 30 %. (viii) It was concluded that most of the points raised by Tyree *et al*. (2005) lack a sound physical basis or are based on wrong assumptions, largely, because no original experimental data were presented to support the conclusions.

Theory

At any permeation of water and solutes, there are, in principal, errors due to unstirred layers (USLs) caused by the fact that concentrations right at the membrane surfaces change. A lack or surplus of solutes has to be levelled off by an equilibration with the bulk media on both sides of the membrane. Equilibration may be rapid or slow compared to membrane permeation tending to make the effect of USLs either small or substantial. The *sweep-away effect* refers to the action of a net water flow (J_V). At a steady J_V, there is a balance between convective and diffusive solute flow at the membrane. As a result, the solute concentration right at the membrane is increased on the side, to which bulk solution is swept. It is decreased on the other side from which solutes are swept away (Fig. 1B). Consequently, the osmotic component of the overall driving force for water is overestimated. An underestimation of the bulk water permeability (hydraulic conductivity; Lp) is caused. The *gradient-dissipation effect* refers to relative rates of diffusion of solutes across membranes and its supply from the bulk solution. When permeation is relatively rapid as compared with the supply, the latter could affect the overall solute transport between compartments or may even dominate it. In this case, the actual concentration gradient driving permeation across the membrane is smaller than that between the bulk solutions. There are three resistances in series, the permeation resistance of the membrane ($1/P_s$) and the two diffusional resistances related to USLs.

In the presence of a steady water flow, the amount of solutes moved to the membrane or moved away from it by convection would be equilibrated by a diffusional counter flow of the solutes. The effect of changes of concentrations at the membrane surface (C_s^m) may be calculated as a function water flow (Dainty 1963; Steudle & Tyerman 1983):

$$C_s^m = C_s^b \cdot \exp\left(-\frac{J_V \cdot \delta}{D_s}\right), \tag{1}$$

for just one side of the membrane. Here, C_s^b is the concentration in the bulk solution; δ is the thickness of the USL, and D_s the diffusion coefficient of the solute. The effects on the two sides of the membrane would be additive, but both D_s and δ may

be different. For example, the external solution may be stirred while the internal is stagnant and δ different. D_s may be smaller in the cell wall than in bulk medium or cytoplasm. According to Eqn 1, the effect increases with an increasing J_V as well as with an increasing thickness of the USL, but decreases with an increasing diffusional mobility of the solute. Often, thicknesses of USLs are hard to access experimentally. They are subject to external stirring, but this cannot completely remove them. During hydrostatic experiments with the probe, an upper limit of the thickness of USLs may be worked out for the hydrostatic type of experiment. In these experiments, cell volume is changed by a ΔV inducing a change of pressure (ΔP). According to the definition of the cell elasticity (elastic modulus; ε), we have:

$$\varepsilon = V \frac{dP}{dV} \approx V \frac{\Delta P}{\Delta V}. \tag{2}$$

Here V is volume of the cell. Assuming that all of the water is extruded instantaneously during a relaxation building up an USL, the maximum value of the thickness (δ_{max}) can be worked out (Steudle *et al.* 1980; Steudle & Tyerman 1983). For a cylindrical cell such as a *Chara* internode, we have:

$$\delta_{max} = \frac{\Delta V}{A} = \frac{V \cdot \Delta P}{A \cdot \varepsilon} = \frac{R}{2} \cdot \frac{\Delta P}{\varepsilon}, \tag{3}$$

where A is the cell surface area and R its radius. It can be seen that for typical experimental values of R = 0.4 mm, ΔP = 0.05 MPa and ε = 30 MPa, the δ_{max} would be as small as 0.3 μm. Using realistic values of J_V and D_s (Eqn 1), this results in a rather small sweep-away, even in the presence high external solute concentrations, C_s^b (see Results section). However, the above treatment may underestimate the role of sweep-away. It assumes that water flow is even throughout the entire cell surface. This may not be true. Water flow should be largely constricted to certain arrays in the membrane such as aquaporins (AQPs). In the literature, constrictions of water flow have been discussed on the tissue scale such as for epithelia (Barry & Diamond 1984), but not yet for membranes in the presence of AQPs, where the concept should apply as well. When water flow across a membrane is largely across AQPs, the water flow density in these arrays should be higher than in the rest of the membrane tending to increase sweep-away in these arrays. In order to correct for the channelling of water, a flow-constriction factor, ϕ, has been used, which denotes the fraction of the
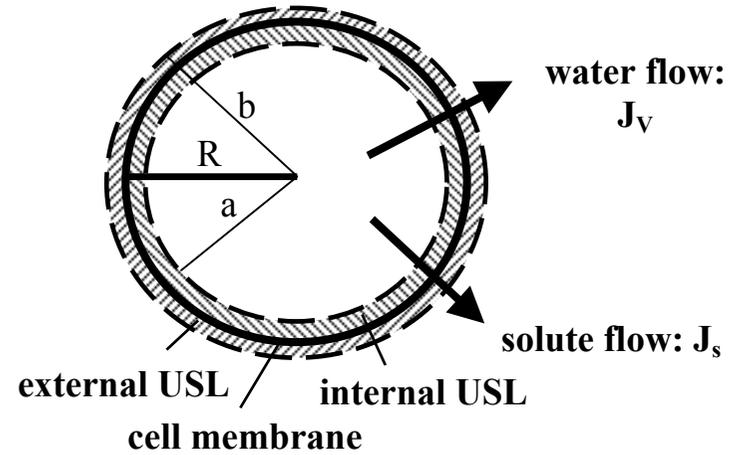
conducting area to the overall area ($\phi < 1$; Barry & Diamond 1984). The actual flow density across the conducting array would be then J_V/ϕ. There should be also an effect of flow constriction on the actual thickness of USLs in the arrays where AQPs are located tending to increase the δ. However, effects of flow constriction are, perhaps, substantially smaller than expected, because the water layers built up on parts of the cell surface should rapidly even out (see Discussion).

In the presence of rapidly permeating solutes such as HDO or acetone, gradient dissipation should contribute to the absolute values of P_s and σ_s as measured with the pressure probe from biphasic pressure relaxations. As outlined in the Introduction, gradient dissipation tends to level off gradients of solute concentration across the membrane resulting in a local depletion of solutes on one side of the membrane and its enrichment on the other (Fig. 1). The overall measured 'permeation resistance' per unit area of the solute ($1/P_s^{meas}$) contains the true diffusional resistances for the membrane ($1/P_s$) and that of the two USLs on both side of the membrane δ^o/D_s^o and δ^i/D_s^i, respectively (δ^o and δ^i = equivalent thicknesses of USLs on the two sides of the membrane; D_s^o and D_s^i = diffusion coefficients of the solute which may be different on both sides):
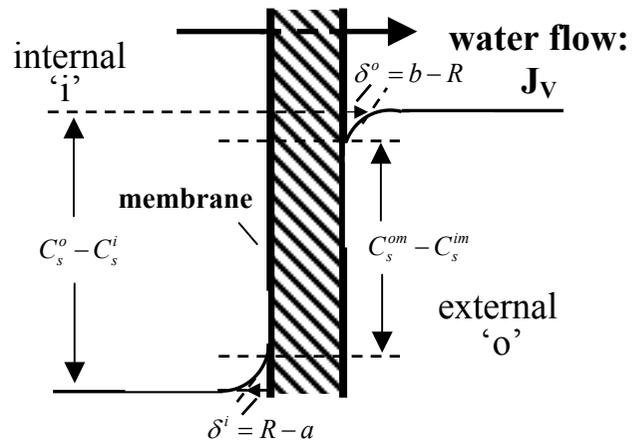
$$\frac{1}{P_s^{meas}} = \frac{1}{P_s} + \frac{\delta^o}{D_s^o} + \frac{\delta^i}{D_s^i}. \tag{4}$$

Again, this assumes steady state, a <u>planar</u>, homogenous membrane, and linear concentration profiles within the layers. For the <u>cylindrical</u> *Chara* internodes used in this paper, we may denote the radial distances from the center of the cell to the boundaries of USLs by 'a' (internal) and 'b' (external) (Fig 1A).

A: USLs in a cylindrical cell (schematic)

water flow:
$\mathbf{J_V}$

b

R

a

solute flow: $\mathbf{J_s}$

external USL

internal USL

cell membrane

B: Sweep away (planar membrane)

internal
'i'

water flow:
$\mathbf{J_V}$

$\delta^o = b - R$

membrane

$C_s^o - C_s^i$

$C_s^{om} - C_s^{im}$

external
'o'

$\delta^i = R - a$

C: Gradient dissipation (planar membrane)

internal
'i'

solute flow:
$\mathbf{J_s}$

$\delta^o = b - R$

membrane

$C_s^o - C_s^i$

$C_s^{om} - C_s^{im}$

external
'o'

$\delta^i = R - a$
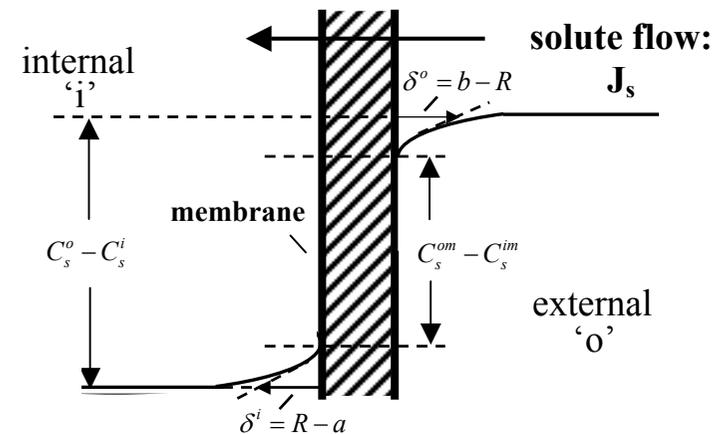
Figure 1. (A) Schematic picture of external and internal USLs in a cylindrical cell. (B, C) Concentration profiles of a solute 's' at a planar membrane separating two compartments with different concentrations (schematic; 'o' = external and 'i' = internal, respectively). δ^o and δ^i are the thicknesses of USLs on the two sides of the membrane. In (B), a net volume (water) flow (J_V) caused a sweep away of solutes right at the membrane surface (concentration, C_s^m), i.e., an increase on one side and a decrease on the other. In (C), decreases of the actual concentration of permeating solutes on one side of the membrane and increases on the other are caused by rapid membrane permeation (solute flow, J_s). In both cases, the forces driving the flows are reduced. When the hydraulic conductivity (Lp) is calculated assuming the osmotic pressure gradient between the bulk media (RT·($C_s^i - C_s^o$)) or the permeability coefficient assuming the concentration difference between them ($C_s^i - C_s^o$), values of Lp and P_s are underestimated. Usually, δ^o and δ^i should be larger during gradient dissipation than during sweep away (for further explanations, see text).

Hence, the thicknesses of the external USL (δ^o) and of the internal USL (δ^i) would be δ^o = (b − R) and δ^i = (R − a), respectively (Fig 1B and C). In the steady state, assuming $D_s^o = D_s^i = D_s$, the overall measured permeation resistance $1/P_s^{meas}$ can be written as:

$$\frac{1}{P_s^{meas}} = \frac{1}{P_s} + \frac{R}{D_s} \cdot \ln \frac{b}{a} \, .$$ (5)

Steudle & Frensch (1989) gave this equation, which they extensively discussed during solute permeation across roots with the endodermis being the main barrier (R = E). The cortex and stele acted as USLs, across which solutes had to diffuse, preferentially in the apoplast. It should be noted that, as Eqn 4, Eqn 5 relates to linear concentration profiles within the USLs. In the presence of USLs at both sides of the plasma membrane of a *Chara* cell, for $D_s^o = D_s^i = D_s$, the measured value of reflection coefficient (σ_s^{meas}) would be given as (Steudle & Frensch 1989):

$$\sigma_s^{meas} = \frac{1/P_s}{1/P_s + R/D_s \cdot (\ln(b/a))} \cdot \sigma_s \, .$$ (6)

By the first factor on the right side of Eqn 6, the measured coefficient would be smaller than the true one (σ_s). If D_s would be different in the medium/cell wall from that in the cytoplasm, a more extended expression may be used (Steudle & Frensch 1989). Eqn 5 may be re-written to separate external from internal USLs, i.e.:

$$\underbrace{\frac{1}{P_s^{meas}}}_{\substack{\text{measured} \\ \text{resistance}}} = \underbrace{\frac{1}{P_s}}_{\substack{\text{true membrane} \\ \text{resistance}}} + \underbrace{\frac{R}{D_s} \cdot \ln \frac{b}{R}}_{\substack{\text{resistance of} \\ \text{external USL}}} + \underbrace{\frac{R}{D_s} \cdot \ln \frac{R}{a}}_{\substack{\text{resistance of} \\ \text{internal USL}}}. \qquad (7)$$

In Eqns 5 to 7, the natural logs of ratios appear because of the cylindrical geometry of cells. It is easily verified from the equations that, for b ≈ a or (R-a), (b-R) << R, Eqn 7 reduces to the situation of the planar membrane (Eqn 4).

In a typical permeation experiment, solutes are added to the stirred medium and pass the membrane. Within the cell, mixing is largely by diffusion, which may take some time. Depending on the relative rate of the internal mixing as compared with that required for solute transfer across the membrane, internal diffusion may rate-limit the overall process as suggested by Tyree *et al*. (2005) for the rapidly permeating solute acetone. An analytical solution in the presence of a membrane surrounding a cylindrical *Chara* cell may be found when considering just internal and no external USLs. In this case (Crank 1975),

$$\frac{M_t}{M_\infty} = 1 - \sum_{n=1}^{\infty} \frac{4L^2}{\beta_n^2 \cdot (\beta_n^2 + L^2)} \cdot \exp\left[-\beta_n^2 \cdot \left(\frac{D_s \cdot t}{R^2}\right)\right] \qquad (8)$$

is valid during the uptake of solute into the cylindrical cell, whereby M_t denotes the amount of solute in gram or mole in the cell at time t and M_∞ the amount when uptake is completed and M_t/M_∞ = 1. The β_n are the roots of $\beta \cdot J_1(\beta) - L \cdot J_0(\beta) = 0$, where J_1 and J_o are Bessel functions and $L = P_s \cdot R / D_s$. Re-writing Eqn 8 in terms of the mean concentration in the cell, $<C_t>$, rather than amounts, one gets:

$$\frac{C_m - \langle C_t \rangle}{C_m} = \sum_{n=1}^{\infty} \frac{4L^2}{\beta_n^2 \cdot (\beta_n^2 + L^2)} \cdot \exp\left[-\beta_n^2 \cdot \left(\frac{D_s \cdot t}{R^2}\right)\right], \qquad (9)$$

where C_m is the concentration of the medium. The equivalent relation describing the elution of solute from a cylindrical cell previously loaded with solute, is given by:

$$\frac{M_t}{M_{or}} = \frac{C_t}{C_{or}} = \sum_{n=1}^{\infty} \frac{4L^2}{\beta_n^2 \cdot (\beta_n^2 + L^2)} \cdot \exp\left[-\beta_n^2 \cdot \left(\frac{D_s \cdot t}{R^2}\right)\right]. \qquad (10)$$

M_{or} (C_{or}) denotes the original content (concentration) of the cell prior to elution by a medium which does not contain the solute. For given experimental values of L, the β_n of Eqn 9 are tabulated (see, for example, Table 5.2 of Crank 1975). The absolute amounts of the exponential terms in the series on the right sides of Eqns 9 and 10 rapidly decline with time. After a sufficiently long period of time, only the first term (β_1) has to be taken into account. The physical background for this is that for small t values diffusion across the internal USL will be rapid. However, as this diffusive USL develops within the cylinder, the rate is slowing down. The USL tends to reach a certain quasi-steady thickness, and the overall permeability of the barrier (membrane plus internal USL) tends to become constant. In this case, we have ($\beta_1 = 1.68$ for a typical experimental value of $L = 2.36$; $P_s^{meas} = 4.2 \times 10^{-6}$ m·s^{-1}; $R = 0.4$ mm) and:

$$\frac{C_m - \langle C_t \rangle}{C_m} = \frac{4L^2}{\beta_1^2 \cdot (\beta_1^2 + L^2)} \cdot \exp\left[-\beta_1^2 \cdot \left(\frac{D_s \cdot t}{R^2}\right)\right], \qquad (11)$$

during an uptake experiment. Under these conditions, Eqn 11 indicates an upper limit of around 40 % for the contribution of internal mixing for the rapidly permeating solute acetone (see Discussion). This is in agreement with numerical solutions (data not shown). When considering the uptake or loss of less permeating solutes such as 2-propanol or DMF, the contribution of internal mixing is less (Fig. 8). This is a consequence of the series arrangement of permeation barriers (membrane and internal USL; see Discussion). In the absence of a membrane, i.e., when Ps $\rightarrow \infty$ and USLs dominate permeation (as claimed by Tyree *et al*. 2005), the equation corresponding to Eqn 8 is (Crank 1975):

$$\frac{M_t}{M_\infty} = 1 - \sum_{n=1}^{\infty} \frac{4}{\xi_n^2} \cdot \exp\left[-\xi_n^2 \cdot \left(\frac{D_s \cdot t}{R^2}\right)\right], \qquad (12)$$

where the ξ_n are roots of a zeroth order Bessel function, and $\xi_n = 2.405, 5.520, 8.654, 11.792, 14.931, 18.071$, etc. (Jost 1960). Neglecting roots of higher order, we get:

$$\frac{M_t}{M_\infty} = 1 - \frac{4}{\xi_1^2} \cdot \exp\left[-\xi_1^2 \cdot \left(\frac{D_s \cdot t}{R^2}\right)\right],$$ (13)

analogous to Eqn 11.

Materials and methods

Plant material

Chara corallina was grown in artificial pond water (APW; composition in mM: 1.0 NaCl, 0.1 KCl, 0.1 $CaCl_2$ and 0.1 $MgCl_2$) as described in earlier publications such as Henzler *et al.* (2004) and Ye *et al.* (2005). *Chara* internodes used in experiments were 40 to 100 mm long and 0.7 to 1.0 mm in diameter.

Determination of cell wall elasticity (ε) and transport parameters (Lp, P_s and σ_s)

Using a cell pressure probe, three transport parameters were measured (Steudle 1993): (i) the hydraulic conductivity (Lp) is a measure of water permeability across the cell membrane; (ii) the permeability coefficient (P_s) denotes the passive permeability of the cell membrane for a given solute; (iii) the reflection coefficient (σ_s) is a quantitative measure of the 'passive selectivity' of the cell membrane for a solute as compared to that for the water. Cell Lp was evaluated from both hydrostatic ($\rightarrow Lp_h$) and osmotic ($\rightarrow Lp_o$) pressure relaxations and calculated from half times (rate constants) of such relaxations and cell geometry (V = volume, A = surface area) and the elastic modulus (ε) of the cell which was determined separately (Eqn 2):

$$L_P = \frac{V}{A} \times \frac{\ln(2)}{T_{1/2}^w (\varepsilon + \pi^i)} .$$ (14)

In the osmotic experiments with rapidly permeating solutes (acetone), the permeation of the solute contributed to the water phase of relaxations, namely close to the minima (maxima) of biphasic curves (Steudle & Tyerman 1983; Tyerman & Steudle 1984; Ye & Steudle 2005). Using semi-log plots, these ranges were omitted when determining $T_{1/2}^w$, as well as the short period in the beginning of curves which was due to the time required for the exchange of solutions in the tube which contained the *Chara* internodes. Pressure signals coming from the pressure transducer (Honeywell;

26PCGFA6D) were continuously recorded, amplified and digitized using the sensor interface from Burster, D-96593 Gernsbach, Germany (types 92101 & 92101-Z001; RS232/RS485), which also contained the starter set with the software. Relaxations (water & solutes) were analyzed using exponential fits which also allowed semi-log plots and statistics.

Permeability (P_s) and reflection (σ_s) coefficients, were determined from the biphasic pressure (volume) relaxations according to the theory of Steudle & Tyerman (1983):

$$\frac{V(t)-V_0}{V_0} = \frac{P(t)-P_0}{\varepsilon} = \frac{\sigma_s \cdot \Delta\pi_s^o \cdot Lp}{(\varepsilon+\pi^i)Lp - P_s}\left[\exp(-k_w \cdot t) - \exp(-k_s \cdot t)\right]. \qquad (15)$$

From the half time (rate constant) of the solute phase, $T_{1/2}^s$ ($\propto 1/k_s$), P_s was given by:

$$P_s = \frac{V}{A} \times \frac{\ln(2)}{T_{1/2}^s} = \frac{V}{A}k_s . \qquad (16)$$

As for the water, ranges around extrema in pressure were not included in the analysis. From the minimum (maximum) changes in pressure ($P_{min(max)}$), σ_s was derived according to (Steudle & Tyerman 1983):

$$\sigma_s = \frac{P_o - P_{min(max)}}{RT \cdot \Delta C_s^o} \times \frac{\varepsilon+\pi^i}{\varepsilon}\exp(k_s \cdot t_{min(max)}) . \qquad (17)$$

Here $t_{min(max)}$ is the time required to reach $P_{min(max)}$. Values of osmotic Lp_o, P_s and σ_s may contain contributions of USLs which would tend to underestimate the real coefficients as discussed in the Theory section (see also Steudle & Tyerman 1983; Steudle & Frensch 1989; Henzler & Steudle 2000; Ye et al. 2005; Ye & Steudle 2005). USLs may develop during experiments in which transient flows of water and solutes are induced to measure transport coefficients. One would expect effects of external stirring on the measurement of coefficients (see Results). However, Eqns 15 to 17 either hold only in the absence of USLs or in a steady state, when thicknesses of USLs are constant.

Hydrostatic experiments with small or big pressure pulses and pressure 'clamp'

Pressure pulses (ΔP) of different sizes were used to induce transient water flows across the membrane (J_V) of different intensity ($\Delta P \propto J_V$). With the aid of the probe, the

oil/cell sap meniscus was moved forward or backward and was kept in a constant position after each move. This resulted in pressure relaxations. According to Eqn 14, hydrostatic Lp_h was calculated from half times ($T_{1/2}^w$) of pressure relaxations. In control experiments, conventional small peak sizes of pressure pulse ($\Delta P \approx \pm 0.04$ MPa) and big peak size of pressure pulse ($\Delta P \approx \pm 0.4$ MPa) were performed to measure $T_{1/2}^w$ of water flows across the cell membrane. According to Eqn 3, different ΔP (J_V) should result in different δ_{max}, i.e. the effects of sweep-away were varied. Experiments were repeated in the presence of high concentrations of osmotic solute presented at both sides of the membrane (1.0 M acetone and 1.0 M 2-propanol). This should have increased the effect which was expected to be bigger at high ΔP than at lower one (Eqn 3). The biggest sweep-way effects may be expected during pressure clamp, when turgor pressure was clamped at a reasonable $\Delta P \approx \pm 0.2$ MPa for about 5 seconds to move larger amounts of water across the membrane tending to build up an USL. The ΔP was limited to about 0.2 MPa in these experiments, due to the rather small diameter of the capillary in the tip region. Following pressure clamps, $T_{1/2}^w$ of water flows were measured from pressure relaxations by fixing the meniscus right at the end of the clamp. When the original turgor was re-attained, pressure relaxations were repeated at a time of between 10 and 20 s after the termination of the clamp. These experiments should show how USLs built up during the clamp affected $T_{1/2}^w$ (Lp_h) and of how rapid USLs would dissipate away by diffusion following its build-up.

Effects of external flow rate (v_{med}) on P_s, σ_s, and Lp_o

In order to induce turbulent water flow within the glass tube that contained the cells (internal diameter: 3 mm; length: 250 mm), solutions were injected across a stopcock and a constriction (Ye & Steudle 2005). To vary the intensity of turbulent flow within the pipe, the average flow of solution (v_{med}) was varied between 0.02 m·s^{-1} (nearly stagnant) and 0.55 m·s^{-1} by opening or closing the stopcock in the experimental set-up (see Fig. 1 of Hertel & Steudle 1997). Average flow rates were calculated by dividing the volume passing through the tube in a given time by the cross-sectional area of the tube containing the *Chara* internode. Depending on the flow rate, it took 2.0 to 0.1 s to completely replace the solution around the shortest (40 mm long) and 5.0 to 0.2 s to

replace it around the longest (100 mm) internodes used. At high rates, the turbulent water flow should have minimized the thickness of USLs attached to the cell surface. To test whether or not the stirring by the speed of the external solution was sufficient to minimize the thickness of USLs, an additional stirring was provided in some experiments by injecting air bubbles into the pipe which were flushing across the tube at a frequency of 160 to 200 bubbles per minute. Effects of stirring of the turbulent solution around the internodes were measured for the osmotic hydraulic conductivity (Lp_o), and permeability (P_s) and reflection (σ_s) coefficients. Three different osmolytes of different permeability were employed at different concentrations: acetone (300 mM), 2-propanol (120 mM), and dimethylformamide (DMF; 60 mM). Values of osmotic Lp_o, P_s and σ_s were derived from biphasic pressure (volume)/time curves (Eqn 15).

Results

Figure 2. Effects of pressure pulses of different peak sizes on $T_{1/2}^w$ during hydrostatic pressure relaxations induced in a *Chara* internode. Rates of water flow across the membrane (J_V) were increased by increasing the size of pulses by about an order of magnitude. This, however, did not increase $T_{1/2}^w$ (decrease Lp_h). (a) It is concluded that USLs due to sweep away do not play a significant role during relaxations ($Lp_h \propto 1/T_{1/2}^w$). (b) There was also no effect of increases in peak size on $T_{1/2}^w$ in the presence of a solute such as 1.0 M acetone on both sides of the membrane, although high concentration should have increased sweep away according to Eqn 3. However, due to the gating of AQPs in the presence of high concentration, $T_{1/2}^w$ increased (Lp_h decreased) by a factor of about 1.5, when cells were treated with 1.0 M acetone (Ye *et al*. 2004). (c) Effects of the cell elastic modulus (ε) around the steady state turgor (0.65 MPa) were too small in the presence of the small pulses ($\Delta P \approx \pm$ 0.04 MPa) and had no effect in the presence of big positive pulses ($\Delta P \approx +$ 0.4 MPa). They may have caused a tendency in $T_{1/2}^w$ to increase in the presence of the negative pulses ($\Delta P \approx -$ 0.4 MPa). The latter effect, however, was not caused by a change in Lp_h (see text).
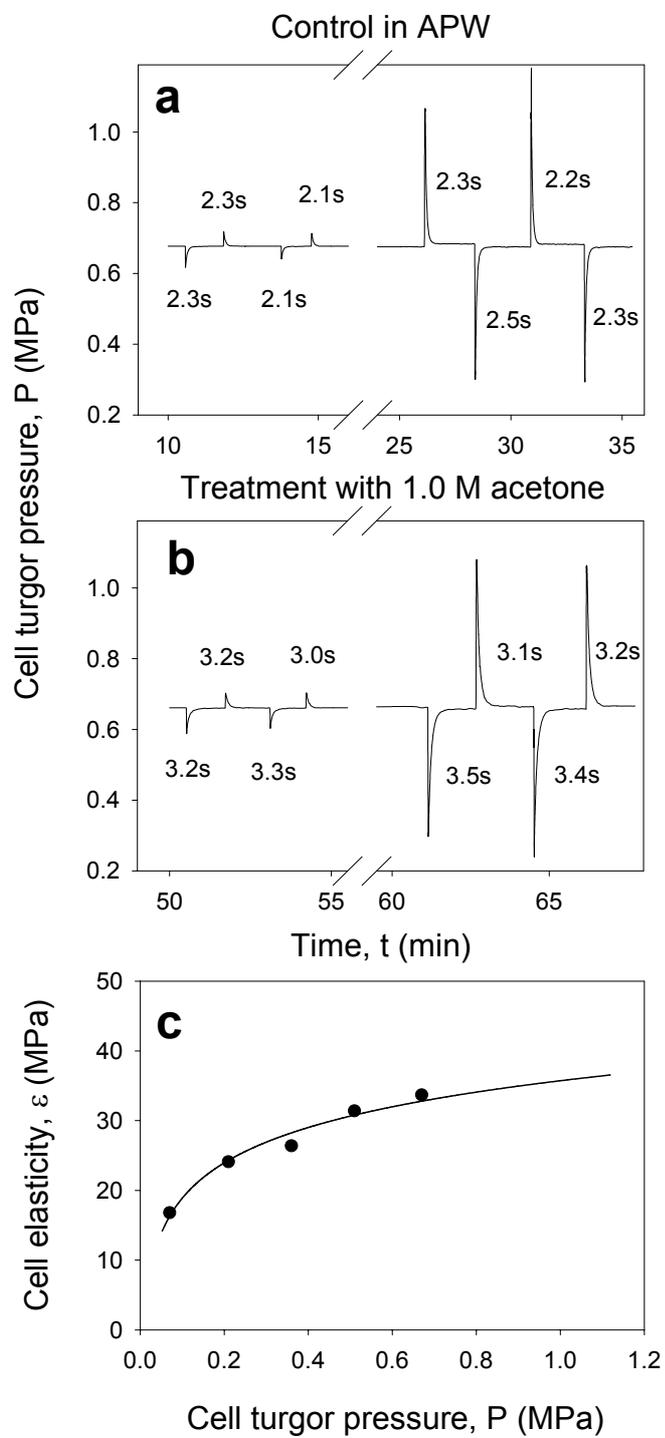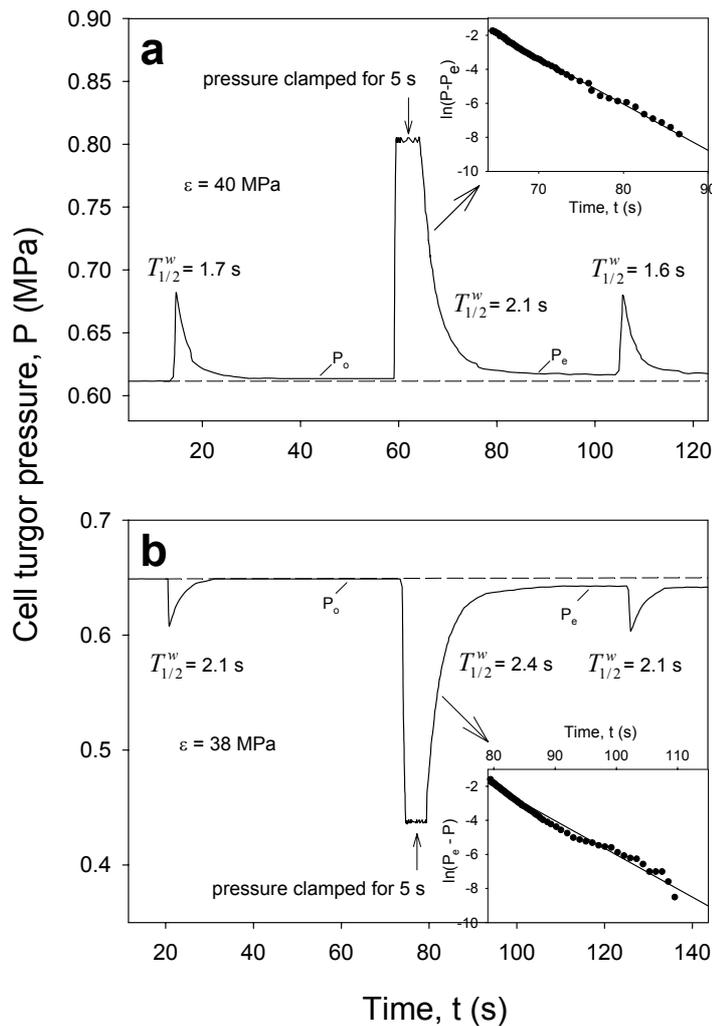
Figure 2 shows typical pressure relaxations obtained during hydrostatic experiments with an individual *Chara* internode. To test for effects of USLs due to 'sweep-away', half times of water flow across the cell membrane ($T_{1/2}^w$) were measured with small ($\Delta P \approx \pm 0.04$ MPa) or big ($\Delta P \approx \pm 0.4$ MPa) peak size of pressure pulses. Since the intensities of water flow across the cell membrane were proportional to the size of pulses (Eqn 3), the J_V induced by big pulses should have been larger by an order of magnitude than that in the presence of small pulses. The thickness of USLs built up by sweep-away during big pulses should have had a bigger effect on $T_{1/2}^w$ than during the small ones. However, there was no significant difference in $T_{1/2}^w$ when comparing the results both in the presence of just APW (Fig. 2a) or of 1.0 M acetone (Fig. 2b). The reason is that in either case thicknesses of USLs were too small to cause significant effects, even in the presence of a flow constriction (Table 1). For the cell used in Fig. 2, $\varepsilon = 34$ MPa, R = 0.4 mm, and δ_{max} was calculated to be 0.24 and 2.4 µm for small and big pulses, respectively (Eqn 3; without considering flow constriction of AQPs). It may be argued that cell elasticity (ε) could have changed with cell turgor pressure during the peaks and this could have compensated for the effect, at least for positive ΔP (Eqn 3). However, it can be seen from Fig. 2c that changes of ε around the steady state turgor of 0.65 MPa were too small both in the presence of small ($\Delta P \approx \pm 0.04$ MPa) or big positive pulses ($\Delta P \approx + 0.4$ MPa). It may have caused the slight increase of $T_{1/2}^w$ in the presence of the big negative pulses ($\Delta P \approx - 0.4$ MPa), but the Lp_h should have remained constant due to the compensating decrease of ε with decrease of cell turgor pressure (Eqn 14). Results suggested that hydraulic conductivity ($Lp_h \propto 1/T_{1/2}^w$) as measured by pressure relaxations should be rather free of effects of USLs (see Discussion). There was no difference, when cells were subjected to 1.0 M acetone or 2-propanol. This treatment should have increased absolute values of ($C_s^b - C_s^m$) and, therefore reduced J_V and Lp_h. It should be noted that in Fig. 2b, $T_{1/2}^w$ increased (Lp_h decreased) by a factor of about 1.5, when cells were treated with 1.0 M acetone. This was due to a gating of AQPs in the presence of high concentration (Ye *et al.* 2004; 2005).

Table 1. Half-times ($T_{1/2}^{w}$) of hydrostatic water flows across cell membranes of *Chara* were measured in APW and in the presence of 1.0 M acetone or 1.0 M 2-proponal. $T_{1/2}^{w}$ increased due to the gating of AQPs by high concentration. $T_{1/2}^{w}$ measured with small pressure pulses ($\Delta P \approx \pm 0.04$ MPa) were not significantly different from those measured in the presence of big pressure pulses ($\Delta P \approx \pm 0.4$ MPa) both in APW and at high concentration. Relative changes of the mean of $T_{1/2}^{w}$ are given as mean $\pm$ SD (n = 6 cells).

| cell No. | Half-times (s) of hydrostatic water flows across cell membranes of *Chara* | | | | | |
| | experiments in APW | | | treatment with 1.0 M acetone (cell 1 to 3) or 1.0 M 2-proponal (cell 4 to 6) | | |
	$\Delta P \approx \pm$ 0.04 MPa	$\Delta P \approx \pm$ 0.4 MPa	relative change of the mean (%)	$\Delta P \approx \pm$ 0.04 MPa	$\Delta P \approx \pm$ 0.4 MPa	relative change of the mean (%)
1	2.4 ± 0.2	2.5 ± 0.2	4	3.3 ± 0.3	3.7 ± 0.2	12
2	2.2 ± 0.1	2.3 ± 0.1	5	3.2 ± 0.1	3.3 ± 0.2	3
3	1.7 ± 0.1	2.0 ± 0.2	18	3.6 ± 0.2	4.1 ± 0.4	14
4	2.5 ± 0.2	2.6 ± 0.1	4	5.1 ± 0.4	5.2 ± 0.9	2
5	2.8 ± 0.3	3.0 ± 0.4	7	5.0 ± 0.3	5.5 ± 0.6	10
6	2.5 ± 0.2	2.6 ± 0.1	4	4.3 ± 0.2	4.4 ± 0.4	2
mean			7			7
SD			5			5

Figure 3. Effects of 'sweep-away' during a pressure-clamp experiment. In order to increase amounts of water moving across the membrane, a steady-state pressure clamp was used, where the pressure was clamped at a ΔP of $\pm$ 0.2 MPa for 5 s. Immediately following this treatment, half times ($T_{1/2}^w$) increased by 24 % at a $\Delta P \approx$ + 0.2 MPa (ε = 40 MPa) and by 14 % at a $\Delta P \approx$ - 0.2 MPa (ε = 38 MPa). The insets in (a) and (b) provide semilog plots of either (P- P_e) or (P_e - P) *vs*. time showing that, during the hydrostatic pressure relaxations, there were no significant changes in the USLs, i.e., a tendency of $T_{1/2}^w$ to decrease as J_V decreased during the relaxations. $T_{1/2}^w$ reached the original values after about 20 s after termination of relaxations indicating that the USLs or other polarization effects were rapidly dissipated away by diffusion after that time. There were slight differences between the original values of cell turgor pressure (P_o) and the steady pressure following the pressure clamp which was due to either a concentration (exosmotic water flow; a) or to a dilution of cell sap (endosmotic water flow; b). For further explanation, see text.

Table 2. Half-times ($T_{1/2}^w$) of water flows across cell membranes of *Chara* as measured during hydrostatic pressure relaxation and following a pressure clamp for 5 seconds at $\Delta P \approx \pm 0.2$ Mpa. It can be seen that the clamp increased $T_{1/2}^w$ by 20 % as compared with the control ($\Delta P \approx \pm 0.04$ MPa). Relative changes of the mean of $T_{1/2}^w$ are given as mean $\pm$ SD (n = 6 cells).

| cell No. | Half-time (s) of hydrostatic water flows across cell membranes of *Chara* | | |
	Control ($\Delta P \approx \pm 0.04$ MPa)	pressure clamp for 5 sec ($\Delta P \approx \pm 0.2$ MPa)	relative change of the mean (%)
1	2.5 ± 0.2	3.1 ± 0.2	24
2	1.7 ± 0.1	2.0 ± 0.2	18
3	2.2 ± 0.2	2.4 ± 0.1	9
4	4.8 ± 0.3	5.7 ± 0.4	19
5	2.7 ± 0.1	3.3 ± 0.2	22
6	2.9 ± 0.2	3.4 ± 0.3	17
mean			18
SD			5

To increase the amounts of water flowing across the cell membrane ($J_V \times$ t), a pressure-clamp was used to produce a steady water flow or nearly so. In Fig. 3, the pressure was clamped for 5 s at a ΔP of ± 0.2 MPa causing an amount of water flowing across the membrane larger than that in the relaxation experiments of Fig. 2 in the presence of small pulses. Effects of sweep away during pressure-clamp experiments were tested by directly going from the clamp to the relaxation mode. It can be seen that clamping resulted in an increase of $T_{1/2}^w$ by about 20 % as compared with the control (for statistics, see Table 2). The effect vanished rapidly (within less than 20 s). When the original turgor pressure was re-attained, subsequent pressure relaxations following the clamp showed $T_{1/2}^w$ values which were not different from the original (Fig. 2a and b). The slight increase of steady turgor during pressure clamp was caused by the displacement of water from the cell during exosmotic water flow resulting in an increase of its osmotic concentration. There was a slight decrease of turgor, when water was taken up by the cell. These changes remained during subsequent relaxations.

Relative changes of steady turgor of $\pm$ 2 % agreed with the estimated relative changes of cell volume. The changes in the overall thickness of USLs during pressure clamp were 2.4 – 3.2 μm in the absence of flow constriction of AQPs (see Theory and Discussion sections). The relaxation back to steady-state pressure could be fitted by a single exponential (see insets of Fig. 2). The results indicate that 'sweep-away-effects' in the presence of a pressure clamp may have caused transient increases of $T_{1/2}^{w}$ (decreases of Lp_h) which could have been affected by flow constriction or concentration polarization effects (see Discussion).

Fig. 4 indicates that Lp_o increased with increasing external stirring (mean external flow rates) tending to reach saturation at rates of between 0.20 and 0.30 m·s^{-1} (depending on solute used). This is similar to results of Steudle & Tyerman (1983), who used mannitol as the osmolyte. At saturation, Lp_o values were identical with the Lp_h values measured in the presence of the same solutes at the given concentrations. Changing the direction of water flows (endosmotic; en (closed symbols) *vs*. exosmotic; ex (open symbols)) did not change the dependence of Lp_o on v_{med}.

In Fig. 5, typical effects of external stirring on permeability (P_s) and reflection (σ_s) coefficients are shown as worked out from biphasic osmotic relaxation curves for three different osmolytes and cells. It can be seen that in a nearly stagnant solution, where replacement of the solution around the internodes should have been rate limiting, P_s and σ_s were rather small. Both P_s (a) and σ_s (b) increased as v_{med} increased. Saturation values were attained at smaller rates ($v_{med} \approx 0.10$ m·s^{-1}) than during the measurement of Lp_o ($v_{med} \approx 0.20$ m·s^{-1}). This would be expected considering the different half times of water and solute transport across the membrane (see Discussion).

Figure 4. Effects of external stirring on $T_{1/2}^{w}$ (Lp_o) in osmotic experiments. In order to vary the thicknesses of external USLs and solution exchange along *Chara* internodes during osmotic experiments, external stirring was varied by changing mean flow rates across tubes (v_{med} in m·s^{-1}). Three different concentrations and osmolytes of different permeability (P_s) and reflection (σ_s) coefficients: (a) 300 mM acetone, $\sigma_s = 0.12$; (b) 120 mM 2-propanol, $\sigma_s = 0.34$; and (c) 60 mM dimethylformamide (DMF), $\sigma_s = 0.57$ were used. It can be seen that Lp_o ($T_{1/2}^{w}$) was quite low in nearly

stagnant solution tending to increase with increasing flow rates. Depending on the solutes used, saturation of Lp_o was reached at flow rates between 0.20 and 0.30 m·s^{-1}, the latter range being the standard flow rate usually used in earlier experiments. The data in the figure refer to three different internodes (a to c). Horizontal lines denote values of hydrostatic Lp_h determined in the absence of the solute (i.e. in APW ·---·) or in its presence (----). It can be seen that, at saturation, Lp_o values were identical with the Lp_h values measured in the presence of solute. It should be noted that the response of Lp_o to v_{med} should incorporate (i) the reduction of the thickness of USLs as turbulences increase, (ii) effects of progressed coverage of cells during the exchange of solution around the cells, and (iii) effects of the concentration dependence of Lp_o as coverage proceeds. The latter two points may dominate at low flow rates. The data show that changing the direction of water flows (endosmotic (closed symbols) *vs.* exosmotic (open symbols)) did not change the dependence of Lp_o on v_{med}.
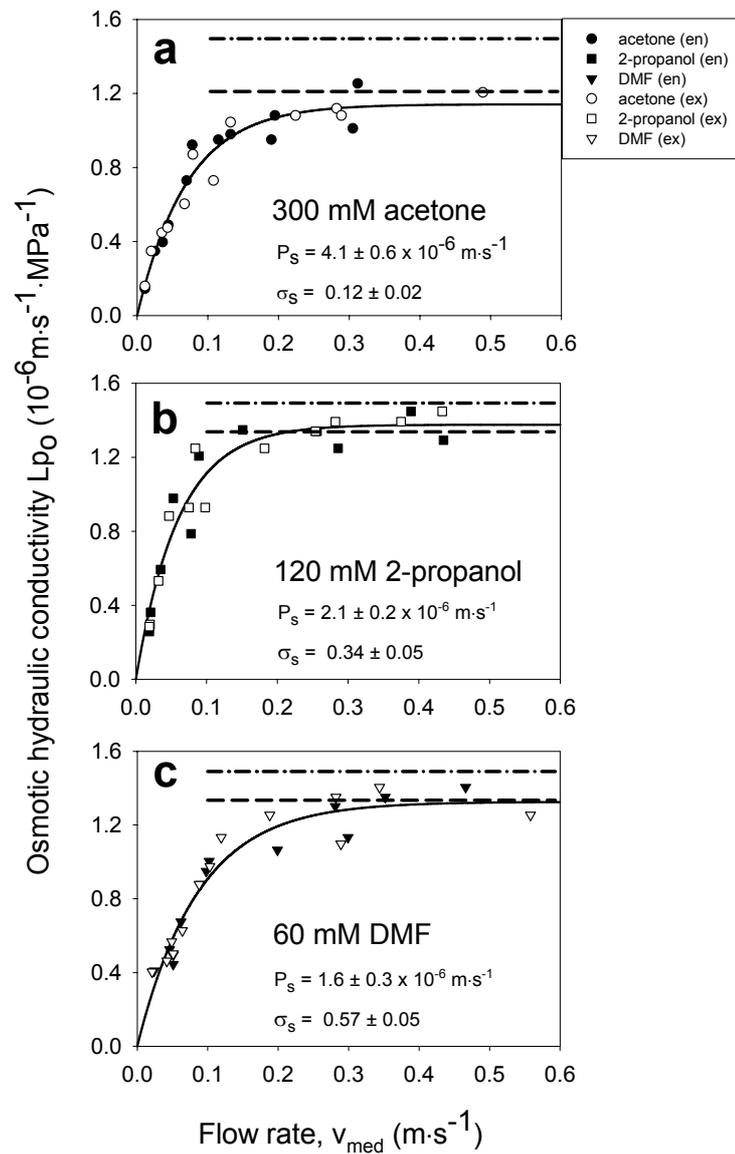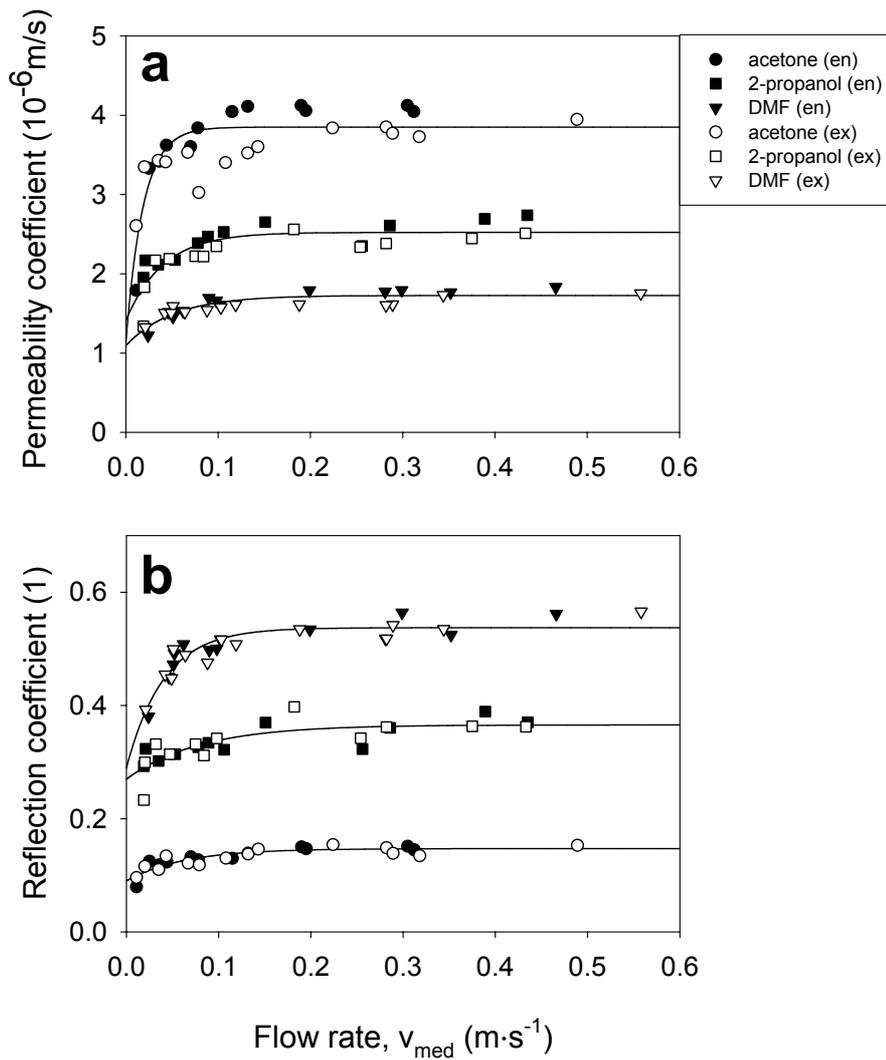
Figure 5. Effects of external stirring (flow rates) on (a) permeability coefficient (P_s) and (b) reflection coefficient (σ_s) of *Chara* internodes for the three osmolytes and cells of Fig. 4 (300 mM acetone, circles; 120 mM 2-propanol, squares; 60 mM DMF, triangles). Both P_s and σ_s were reduced in nearly stagnant solution ($v_{med} < 0.02$ m·s^{-1}). Saturation was reached at a $v_{med} \geq 0.1$ m·s^{-1}, which was smaller than the rates required for reaching a saturation value of osmotic Lp_o (Fig. 4). This indicated that external stirring had less effect on both P_s and σ_s than on osmotic Lp_o.

In some experiments, the stirring at high rates of v_{med} was enhanced by injecting air bubbles into the water flow along the pipe. This caused a tremendous sweeping away of the solution along the internodes as can be seen in Fig. 6 and on a video provided at http://www.uni-bayreuth.de/departments/planta/research/steudle/index.html. However, the additional stirring by air bubbles did not further increase the Lp_o (data not shown).
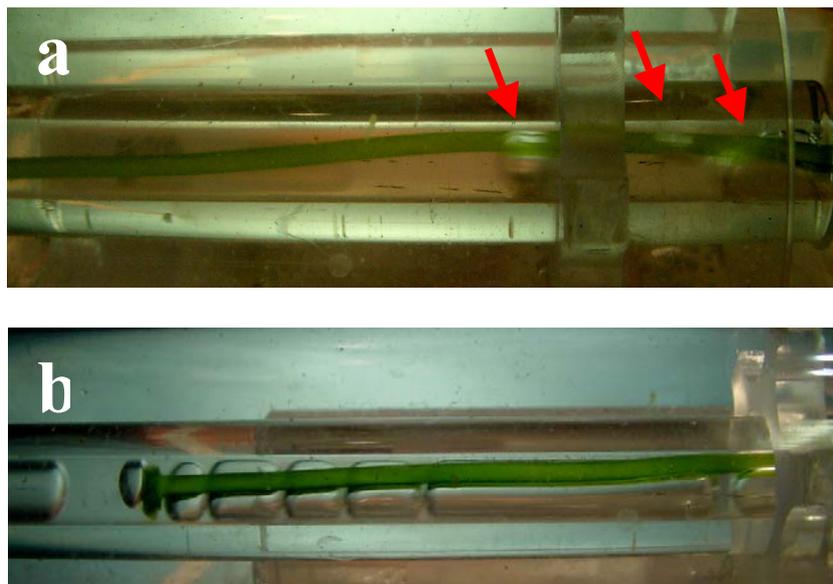
Figure 6. (a) Vigorous stirring of external solution by injecting air bubbles into the water stream along the pipe. Air bubbles (red arrows) were rapidly flushed through at frequencies of between 160 and 200 air bubbles per minute, which caused a tremendous stirring by sweeping away the solution around the *Chara* internodes. For the sake of a clearer view on the air bubbles, (b) was taken under conditions of a slow motion of air bubbles.

Usually, the hydrostatic relaxations measured with the pressure probe could be nicely fitted by a single exponential. The same was true for the solute phases of biphasic responses in the presence of permeating solutes, provided that analyses are not made just around the minima or maxima of P(t) curves (Tyerman & Steudle 1984). However, when relaxations approached the final value of turgor pressure (P_e), semi-log plots of the differences of ($P - P_e$) *vs*. time tended to become scattered, when ($P - P_e$) got close to the resolution of the probe (around 0.002 MPa; Steudle & Tyerman 1983). When the fitted P_e value slightly differed from the real one, there could be either a bending up or down in the plots (Fig. 7). As discussed by Steudle & Tyerman (1983) and others, this is due to a systematic error, which results from the facts that, under these conditions, (P-Pe) represents a small difference of two rather big figures, as $P \rightarrow P_e$ errors get fairly large. Data from this part of relaxations should not be used for analysis. Bending of semi-long plots in one way or the other in this range of relaxations are artefacts. In Fig. 7, the effect is demonstrated by varying the P_e in steps of ± 0.001 MPa which is close to the resolution of the transducer in the probe.
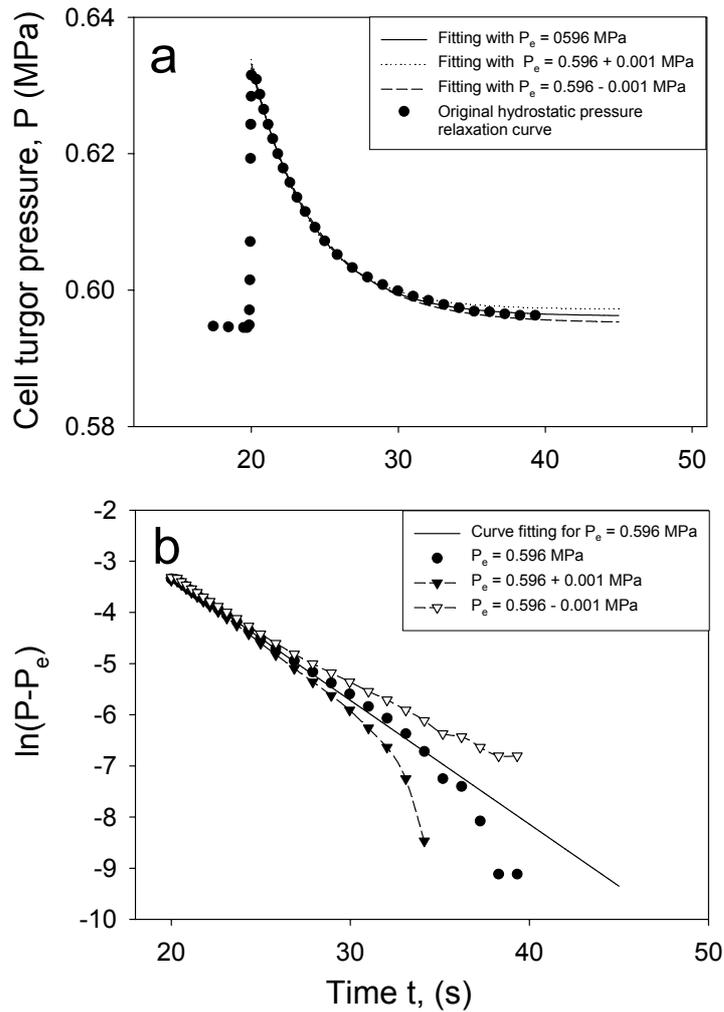
Figure 7. Analysis of a typical hydrostatic relaxation of cell turgor pressure as measured by a cell pressure probe. Lines (a) are fits of the data using $P = P_e + \Delta P \cdot \exp(-\ln(2) \cdot t / T_{1/2}^w)$. The solid line is the best fit with the P_e value of 0.596 MPa. Dashed lines are fits with P_e values fixed either at 0.596 + 0.001 MPa or at 0.596 - 0.001 MPa. Closed circles are the original data of hydrostatic relaxation. (b) Natural logarithm of (P- P_e) versus time for the pressure relaxation data from (a). The circles and triangles represent the logarithm of (P- P_e), when P equals the original data and P_e is 0.596 MPa (closed circles), 0.596 + 0.001 MPa (closed triangles), and 0.596 - 0.001 MPa (open triangles). The solid line is the fit of natural logarithm of (P- P_e) with P_e = 0.596 MPa. The results show that small variations of P_e of an order similar to the resolution of the pressure probe ($\pm$ 1 kPa) caused a bending of the log plots upward or downward. Hence, a wrong choice of P_e within the limits of accuracy may suggest that pressure relaxations have more than one exponential phase. This type of systematic errors should be avoided by cutting off the pressure range where P-P_e gets close to the resolution of the probe.

To work out upper limits of USLs during experiments with permeating solutes, both ordinary steady state diffusion (Eqns 4 to 7) and unsteady state diffusion kinetics in the presence of a membrane were employed (Eqns 8 to 11). During steady state, the maximum thickness of an internal USL was estimated assuming that the measured P_s^{meas} just reflects the permeation across internal USLs rather than across the membrane, i.e., USLs dominated permeation. Neglecting the external USL, we then get for acetone ($P_s^{meas} = 4.2 \times 10^{-6}$ m·s^{-1}; $D_s = 1.2 \times 10^{-9}$ m^2·s^{-1}; R = 0.4 mm) a $\delta_{max}^i =$ 204 µm. In the presence of an additional external USL of 30 µm, this value is reduced to 189 µm. In terms of unsteady state diffusion, we first made the approach that the membrane was not rate limiting at all ($P_s \rightarrow \infty$), i.e., there was free diffusion across the boundary of a cylinder having the same diameter as a cell (R = 0.4 mm; Eqn 13; in the absence of an external USL). This result was then compared with the uptake into a cylinder bounded by a membrane (Eqn 11). Eventually, results were compared with data measured with an intact *Chara* internode using the probe. Fig. 8 provides typical results for the rapidly permeating acetone and the less permeating DMF ($D_s = 1.0 \times 10^{-9}$ m^2·s^{-1}; Poling, Prausnitz & O'Connell 2001). Natural logs for solute uptake into a cylinder bounded by a membrane and free diffusion inside a cylinder are plotted against time according to Eqn 9 and 12, respectively. It can be seen from the figure that during free diffusion, uptake was rather rapid during the first 10 s as already discussed in the Theory section. During later stages, the process could be described by a single exponential, when the internal USLs formed rate-limited further uptake. Hence, a straight line was obtained in the semi-log plot of the relative uptake/loss versus time. From the rate constant (slope k_D) during this phase, an equivalent thickness of the USL could be obtained which was 117 µm (R = 0.40 mm) and 108 µm (R = 0.37 mm), respectively. In the presence of a membrane with measured $P_s^{meas} = 4.2$ x 10^{-6} m·s^{-1} containing resistance of membrane and USL (R = 0.40 mm in the example), the maximum thickness of the internal USL was reduced to 97 µm, calculated by Eqn 5 & 11. These values of 117 and 97 µm are substantially smaller than the steady state value of 204 µm given above. Results indicate that for the most rapidly permeating acetone ($P_s^{meas} = 4.2$ x 10^{-6} m·s^{-1}), the contribution of internal USLs was maximally 40 %.
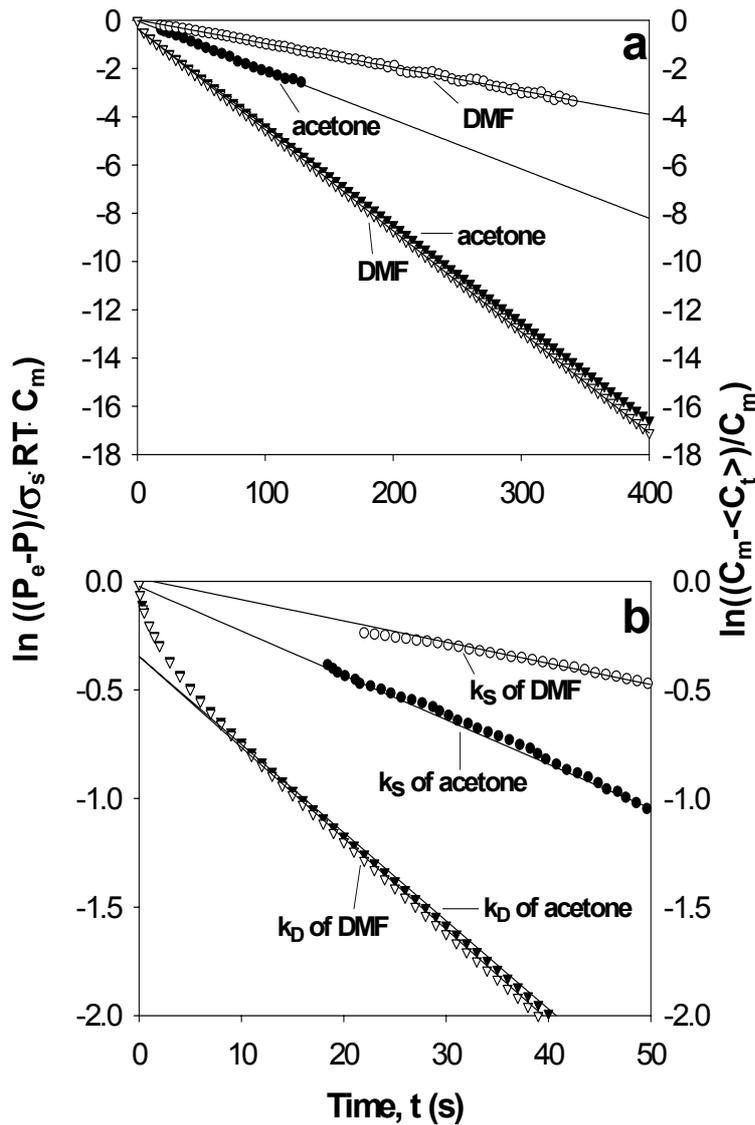
Figure 8. (a) Kinetics of solute uptake into two typical *Chara* internodes measured with the pressure probe as compared with the calculated diffusion into cylinders with the same diameter lacking a plasma membrane for two permeating solutes (acetone and DMF). Natural logs of relative amounts of solute taken up by the cell are given as a function of time. Relative amounts of solute taken up by the cell at time t were $(P_e - P(t))/(\sigma_s \cdot RT \cdot C_m)$ (P_e = final value of cell turgor pressure; C_m = concentration of solute in the medium). For diffusion into cylinders, relative amounts were given by $(C_m - \langle C_t \rangle)/C_m$, where $\langle C_t \rangle$ denotes the average concentration in the cylinder (Eqn 9). Diffusion kinetics of acetone uptake (closed triangles; $D_s = 1.2 \times 10^{-9}$ m$^2 \cdot$s^{-1}) is given for a cylinder of the same diameter of 0.81 mm as the cell. The diffusion kinetics of DMF uptake (open triangles; $D_s = 1.0 \times 10^{-9}$ m$^2 \cdot$s^{-1}; diameter: 0.74 mm) is very similar to that of acetone. (b) Extended part of curves (a) for small time intervals. The data show that the measured curves differ from those of calculated in the absence of a membrane in that the bended part close to t = 0 is missing or can not be resolved in the presence of the membrane. The bended part during diffusion kinetics relates to the building up of a diffusional USL in

the outer part of the cylinders. When this layer is quasi-steady, the process can be described by a single exponential, i.e. the layer acts like a membrane. In the given examples, maximum equivalent thickness of USLs of acetone and DMF were 120 µm (diameter: 0.80 mm, see Theory section). In the presence of a membrane these should have been substantially smaller as indicated by intercepts with the ordinate close to zero. Analogous curves have been obtained for the loss from cells previously loaded with permeating solutes (data not shown). For further discussion, see text.

The equivalent calculation for the less permeating DMF (P_s^{meas} = 1.8 x 10^{-6} m·s^{-1}) resulted in a steady state equivalent thickness of 124 µm and maximum thicknesses of 108 and 95 µm, respectively (R = 0.37 mm), and the contribution of internal USLs was maximally 18 %. This means that the effect caused by internal USLs substantially decreased as P_s decreased (see Discussion). Accordingly, internal USLs contributed to 40 % (acetone) or 18 % (DMF) of the measured permeability.

The semi-log plots of Fig. 8 demonstrate the effects of USLs in terms of slopes which represent rates of uptake. Slopes were biggest in the absence of membranes (slope: k_D) followed by slopes in just the presence of the membrane without any USL (slope: k_s^{memb}). The combined effect of USLs and membrane resistances resulted in the smallest slopes (slope: k_s^{total}). Using calculations based on measured data, the figure shows that, in this case, calculated curves (slope: k_s^{total}) and measured values (slope: k_s^{meas}) were nearly identical. However, measured values resulted in intercepts which were often > 0, which was, of course, not the case for calculated data. It should be noted that all calculation were based on the assumption of a completely stagnant and homogenous internal compartment which may be questioned (see Discussion).

Discussion

Present results

During hydrostatic relaxations, Lp_h was not significantly affected by sweep-away, even in the presence of water flows across the membrane (J_V), which were bigger than usual by a factor of ten. Sweep-away did not play a role because maximum thicknesses of USLs (δ_{max}) remained as small as fractions of a micrometer, i.e., they were substantially smaller than the thickness of the cell wall (5 to 10 μm) or of the cytoplasmic layer (a few μm). Calculations assumed a maximum (peak) J_V during the entire relaxation and are, therefore, pessimistic with respect to the effects of USLs. Sweep-away also remained small in the presence of high external concentration which should have increased the effect. However, all these estimates did not incorporate the constriction of water flow across AQPs, which could have been crucial. The effect should refer to both J_V and δ. The estimation of flow constriction would require the knowledge of the density of AQPs and of the hydraulic conductivity of individual subunits (lp). At present, there are no data of the density of AQPs of *Chara* and of their lp. However, there are data for the water channels of red blood cells (AQP1). The lp of a single water channel subunit of AQP1 is lp $= 4.0 \times 10^{-22}$ m^3 H$_2$O·s^{-1}·MPa^{-1}·(AQP subunit)$^{-1}$ (Walz *et al*. 1994; see also Wan, Steudle & Hartung 2004). This may be used for a rough estimate of the effect of flow constriction neglecting the contribution of the bilayer which is only 5 to 10 % of the overall Lp (Henzler *et al*. 2004). A typical value of cell Lp of *Chara* is 1.6×10^{-6} m^3·m^{-2}·s^{-1}·MPa^{-1}. Hence, we get an AQP density of Lp/lp $= 4.0 \times 10^{15}$ (AQP subunits)·m^{-2}. Given a cross section of about 10 nm^2 for an AQP subunit (Walz *et al*. 1994), this results in a value for ϕ of 0.04. Hence, J_V and δ should be each corrected by a factor of as large as 25. However, the measured effect was much smaller if any. One reason could be that as the water protrudes out of AQPs, it may be rapidly evened out by creeping along the hydrophilic membrane surface surrounding the pores. It is, perhaps, more likely that, as columns of distilled water protrude either into the cytoplasm or wall space, they are rapidly evened out by lateral diffusion of solutes into them. According to Eqn 12, the time constant required for this diffusional equilibration should be as short as 4 ns (using a radius of

1.8 nm of the columns (equivalent to a cross sectional area of AQP subunits of 10 nm^2, see above); and a diffusion coefficient of 1.0×10^{-10} m$^2 \cdot$s^{-1} of the solutes). This time constant is much shorter than that of water flow equilibration. As a consequence, changes of the local concentration by sweep-away or concentration polarization should be substantially smaller than expected from the overall enhancement by constriction by a factor of 625 (25×25). Accordingly, there was no effect of sweep away during hydrostatic relaxations, even in the presence of big peak sizes. Only during pressure clamp, when rather large amounts of water were continuously moved across AQPs, the effect was measurable, i.e. there was a significant dilution/concentrating effect around the vestibules of AQPs. In addition, we may think that there could have been effects of concentration polarization and dilution within the non-selective mouth parts (vestibules) of channels. There is evidence that at least some of the AQPs of *Chara* have a rather large internal volume suggesting that volumes of vestibules may be substantial (Ye *et al*. 2004, 2005). It is also known that *Chara* exhibits a reversible inhibition of AQP activity in response to elevated concentration (Kiyosawa & Tazawa 1972; Steudle & Tyerman 1983). The latter has been interpreted in terms of a cohesion/tension mechanism (Ye *et al*. 2004, 2005). Hence, high concentrations created on one side of the membrane could result in a channel closure. Experiments are underway to test the different hypotheses by varying both the size of osmolytes and its chemical nature (electrolytes *vs*. non-electrolytes; polar *vs*. non-polar). For these experiments, pressure probes have been modified in order to extend the range of water flow intensity and of its duration. The AQP activity of *Chara* did not change in response to considerable water flow densities, i.e., substantial inputs of kinetic energy into AQPs do not seem cause conformational changes of AQPs as found in other systems (Wan *et al*. 2004; Lee, Chung & Steudle 2005). Therefore, *Chara* is a suitable object to test the idea of concentration polarization effects close to or within the vestibules of AQPs during extreme rates of J_V.

Different from Lp_h, the osmotic Lp_o depended on external stirring in accordance with earlier findings of Steudle & Tyerman (1983). This has been referred to the existence of external USLs. For low v_{med} and nearly stagnant conditions, the effect was rather big, and Lp_o small. However, it would be premature to assume that, in this case,

it was just the diffusion of solute from bulk solution to the membrane surface across an extended external USL which was rate limiting. As already mentioned in the Results, there are two other factors, which should be even more important at low flow rates. One is the fact that, during a slow exchange of solution, there will be no 'instantaneous' replacement of solution around the internodes. At low rates of stirring and relatively long lengths of internodes, complete exchange of solution will require up to 5 s (see MM section), which is longer than the $T_{1/2}^w$. The other factor is the fact that the Lp of *Chara* decreases with increasing external concentration, which may also happen with a certain delay and proceed as solution is exchanged along the cell. Hence, at low flow rates, values of low osmotic Lp_o can not be directly referred to increases in the thickness of external USLs.

The fact that Lp_h and Lp_o were close at high rates of stirring, enabled Steudle & Tyerman (1983) to estimate the thickness of external USLs (as measured in a set-up similar to the present and at high stirring) to be less than 50 μm. The present data support this view, that due to vigorous stirring, external layer thickness was minimized. This view was strongly supported by the experiments in which air bubbles were introduced into the system at high frequency that efficiently swept away solution from around the cylindrical cells except for a thin boundary layer at their surface. This vigorous external stirring did not furthermore increase Lp_o. Overall, the results show that the conclusions of Tyree *et al*. (2005) about the stirring and in earlier experiments with the probe are premature. Because of possible complications by external USLs and by the effect of elevated concentration, the Lp of *Chara* was usually measured in the past hydrostatically such as in the paper by Henzler *et al*. (2004). Tyree *et al*. (2005) ignored this important point.

Rebuttal to Tyree et al. (2005)

Tyree *et al*. (2005) stressed that hydrostatic relaxations could not entirely be described by a single exponential and were bending off at their very ends in semi-log plots. They criticized the 'usual procedure' of Steudle & Tyerman (1983) and others for not analyzing this part and just cutting it off. However, Tyree *et al*. (2005) overlooked that the reason for the cut off is that in a range where measured pressure differences (P(t) –

P_e) get close to the sensitivity of the pressure measurement. Hence, errors in the differences are quite big in these ranges. Systematic errors may be produced which may result in either a bending upwards and downwards of semi-log plots. In the pressure probe literature, the point has been stressed several times (e.g., Steudle & Tyerman 1983; Henzler & Steudle 2000). The literature also provides the reason for the cut off. It is touching to realize that Tyree *et al*. (2005), rather than accepting the physical limit of the resolution of the probe, think that the output from the transducer given as accurate as 0.1 kPa (0.0001 MPa) can be taken as the resolution of the pressure measurement. As a consequence, curves were bending for Tyree *et al*. (2005) as $P(t)$ approached P_e. The authors interpreted their artifact as an effect of a 'membrane movement' which is strange.

Tyree *et al*. (2005) claim that during the osmotic experiments of Henzler *et al*. (2004), stirring was not sufficient. They think that the flow of solution around the internodes fixed in a glass tube of an inner diameter of 3 mm was not turbulent and stirring not vigorous. On p. 3, para 4, of their paper, Tyree *et al*. (2005) state that the flow in the tube was laminar at all rates used. Hence, there should have been USLs of substantial thickness. These claims of Tyree *et al*. (2005) have no physical basis. In the experiments of Henzler *et al*. (2004) (and of others), cylindrical *Chara* internodes (lengths of 40 to 150 mm; thickness of around 1 mm) were centered in a tube of an inner diameter of 3 mm and of a length of 250 mm and fixed at one end in a slid (see, for example, Fig. 1 of Hertel & Steudle 1997). From the other end of the tube, solutions were applied *via* a tube across a stopcock which reduced the speed from a few m·s^{-1} to a speed that would be tolerated during the experiments without causing leakages of the cell due to an intense trembling of the internode (Ye & Steudle 2005). There was also a constriction (teflon tube of an inner diameter of 2 mm that was fitted into the entrance of the glass tube over a length of 80 mm). Flow was turbulent at the entrance because of the stopcock, and it was furthermore stirred when it left the constriction to reach the internode after a passage of 70 to 130 mm. According to basic fluid dynamics, this path is not sufficient to make the turbulent flow laminar. This length (l_e) would be (see textbooks of fluid dynamics, e.g. White 1999):

$$l_e = 0.06 \times \mathrm{Re} \cdot d . \qquad\qquad (18)$$

Here, d is the diameter of the tube and Re the Reynolds number, which is around 750 for a cylindrical pipe having a d = 3 mm (viscosity of water $\eta = 1.002 \times 10^{-3}$ Pa·s at 20 ^{o}C and flow rate of 0.25 m·s^{-1}). Hence, we may estimate a distance of $l_e = 135$ mm for a laminar flow to develop which was not available. Even if basic fluid dynamics would not apply for Tyree *et al*. (2005) and there were a laminar Poiseuillian flow profile arriving at the internode, the existence of the latter would tend to disturb the parabolic flow pattern making it turbulent again. After a sufficiently long distance along the annulus of solution around the *Chara* internode, flow would tend to become laminar again. The maximum flow rate should establish close to the center of the annulus, whereby the velocity profile should be that of a parabola wrapped around the *Chara* like a doughnut. However, this will not happen over distances of as short as 40 to 150 mm, and flow should remain turbulent. The question is just how thick the remaining laminar boundary layer adjacent to the cell is, which is not affected by turbulence. This question is difficult to address theoretically. Therefore, we used two different approaches to test it, i.e., we varied v_{med} and we were flushing air bubbles around the cell at high frequency, which displaced most of the solution tending to even enhance the vigorous stirring (see video). The result of both procedures was that we could not further reduce thicknesses of USLs, which adhered as thin films close to the cell surface. Hence, we may conservatively estimate the thickness of external USLs to be around 30 μm (including the cell wall) at sufficient rates of stirring. The value of Tyree *et al*. (2005) of 100 μm in the experiments of Henzler et al. (2004) clearly overestimated δ^o. It would have been adequate for Tyree *et al*. (2005) to provide some own data and experience on the subject prior to judging about the experiments of Henzler *et al*. (2004).

On p. 3 (left column), para 3 and on p. 4 (left column), para 5, of the Online Early of Plant Cell and Environment (electronic file), Tyree *et al*. (2005) state that in their simulations the system of two USLs and a membrane soon assumed conditions of steady state, where the Steudle/Tyerman theory applied (which they seem to accept; Eqn 15). According to Tyree *et al* (2005), this happened at times of substantially smaller than the time required to reach the extrema of pressure during biphasic responses (around 10 s for acetone). This finding is not new. Tyerman & Steudle

(1984) used a turgor-minimum technique to analyze the k_s (P_s) obtained around the maxima (minima) for different solutes. The result was that the k_s (P_s) measured around the minimum was similar to that obtained from solute phases. Because the solute flow is buried within the water phase at time periods of close to zero, it is not possible to use the pressure probe to directly measure k_s (P_s) at times close to zero. However, there are P_s values from isotopic measurements where P_s was worked out from the initial uptake for some of the solutes studied (Dainty & Ginzburg 1964b). These data are rather free of USLs and agree with those measured with the pressure probe. We do agree with Tyree *et al*. (2005) that the system very soon becomes steady with constant thicknesses of USLs. However, this just indicates that USLs developed fast and that their thickness should have been relatively small.

Tyree *et al*. (2005) did not realize that their simulations contained the solvent drag which was neglected in the Steudle/Tyerman theory (1983). In simulations of biphasic responses, Rüdinger, Hierling & Steudle (1992) showed that the solvent drag had no significant effect on the shape of curves. From their simulations, these latter authors concluded that Eqn 15 could be used to describe the entire course of P(t) during biphasic pressure relaxations. In principal, there could be another type of interaction between solutes and water which was not considered by Rüdinger *et al*. (1992) and is not incorporated in Eqn 15. This is active solute (ion) transport which may change during osmotic treatments. However, this effect should be quite small for *Chara*, but should be considered during biphasic responses of roots measured with the root pressure probe, as shown in the simulations of Steudle & Brinckmann (1989).

Unlike osmotic Lp_o, values of both P_s and σ_s were only slightly smaller at low flow rates and tended to saturate earlier. This is expected because of the longer half-times of solute exchange which would reduce effects of external USLs. Assuming an external USL of a thickness of ≈ 30 μm, a half time of 0.2 s would be required for the filling of this layer with solute (acetone; $D_s = 1.2 \times 10^{-9}$ m²·s⁻¹; Jost 1960; Ye & Steudle 2005). This can be neglected at values of $T_{1/2}^s \geq 30$ s (Ye & Steudle 2005). Nevertheless, effects of USLs on permeability coefficient (P_s) and reflection coefficient (σ_s) were very much dependent on the property of solutes. USLs could more likely act as rate-

limiting diffusion barriers for rapidly than for slowly permeating solutes (Barry & Diamond 1984). This was found in the present paper. Three different solutes were used with a sequence of the P_s as $P_{s(acetone)} > P_{s(2-propanol)} > P_{s(DMF)}$. A tendency sequence of USLs effects on P_s and σ_s was (acetone) > (2-propanol) > (DMF) as shown in Fig. 5.

Tyree *et al*. (2005) argue that values of P_s and σ_s of acetone measured with a CPP were considerably underestimated. Assuming external and internal USLs of as large as 100 μm and 350 μm, respectively, they arrived at the conclusion that true values of P_s and σ_s of acetone of Henzler *et al*. (2004) could have been underestimated by a factor of as large as five (see p. 4, right column of the cited Online Early of PC&E). This meant that USLs instead of the cell membrane represent the rate-limiting resistance of acetone permeation through *Chara* internodes. The argument of Tyree *et al*. (2005) fails. They assumed steady state diffusion during most of the biphasic responses measured with the pressure probe. Hence, there will be a series arrangement of permeation resistances (2 USLs plus membrane) according to Eqn 7 of the Theory section. Since this is true and agrees with Tyree *et al*. (2005), Eqn 5 may be used to evaluate maximum thicknesses of USLs, when $1/P_s$ can be neglected as compared to the diffusional resistances, i.e. when $P_s \rightarrow \infty$. In the example used in Table 1 of Tyree *et al*. (2005) ($P_s^{meas} = 4.2 \times 10^{-6}$ m·s^{-1}; $D_s = 1.2 \times 10^{-9}$ m^2·s^{-1}; R = 0.40 mm), one gets a limiting ratio of b/a of 2.1 from Eqn 5. For 6 out of 9 combinations of the table the b/a ratio was bigger indicating a negative P_s, which is not possible. Hence, there is either something wrong with the values given in Table 1 of Tyree *et al*. (2005) or the table does not refer to steady state as does the rest of their paper.

The conclusions of Tyree *et al*. (2005) are contradictive in view of the comparison between free unsteady state diffusion into a cylinder and the values measured with the probe (Fig. 8). If Tyree *et al*. (2005) were right, the uptake kinetics measured with the probe should be similar to the type of kinetics obtained in the absence of a membrane which shows two distinct phases. However, this was not observed in the experiments. No building up of an internal USL was observed. When uptake curves were extrapolated back to t = 0 in the semi-log plots of Fig.8, their intercepts with the

ordinate were close to zero. Hence, these layers should have had a rather small impact on the measurement of transport coefficients.

According to Tyree *et al.* (2005), changes in membrane properties such as the closure of AQPs should have had little if any effect on the P_s^{meas} of rapidly permeating solutes such as acetone (P_s = 4.2 × 10^{-6} m·s^{-1}) or HDO (P_d = 7.0 × 10^{-6} m·s^{-1}) as demonstrated by Henzler *et al.* (2004). This is so because membrane treatment should not affect USLs. However, this was not the case in the experiments of Henzler *et al.* (2004) and others. For example, when using hydroxyl radicals (*OH) to inhibit AQP activity, there was a substantial decrease of the P_d of HDO by a factor of 3 and of the P_s of acetone (in part, also using AQPs to cross the membrane) by a factor of 2. When Tyree *et al.* (2005) were right and USLs had permeation resistances of larger by a factor of five than those of membranes, this would result in a decline of the real membrane P_s (P_d) by factors of 6 and 11 for acetone and HDO, respectively. This would mean that there were a tremendous permeability of acetone across water channels. Absolute values are unlikely to be true in view of other findings of changes in P_s and P_d upon channel closure (Henzler & Steudle 1995; Mathai *et al.* 1996). Similarly, the re-examination of reflection coefficients (negative for acetone upon channel closure) would result in extreme values. Tyree *et al.* (2005) avoid to discuss these consequences although the effects of a closure of AQPs on permeability and reflection coefficients are dealt with in the paper of Henzler *et al.* (2004).

Tyree *et al.* (2005) claim that they obtained the estimated thicknesses of USLs of up to 350 μm (Henzler *et al.* 2004; see also Henzler & Steudle 2000). This is a misquote. Henzler *et al.* (2004) discuss the possibility that internal USLs of the solute HDO may, in principle, be as large as the radius of the cells, which sets a geometric upper limit. However, they conclude that the idea that USLs extend across the entire cell has to be rejected for different reasons. The most important, perhaps, is that a rate-limitation by internal USL could not explain that the experiments clearly showed a rate limitation by membrane transport (see Discussion on p. 333 of Hertel *et al.* 1997). Henzler & Steudle (2000) conclude that, 'although there may be some influence of internal USLs, on the absolute values of the P_s and $σ_s$ of H_2O_2 (D = 1.3 × 10^{-9} m^2·s^{-1}), membrane

permeation and the subsequent degradation of the substrate in the cell should have dominated the process measured'. For the rapidly permeating solute HDO, Ye *et al.* (2005) estimate the contribution of internal USLs in P_d as 25 %. These earlier statements have been overlooked by Tyree *et al.* (2005).

In the present paper, we show that, under conditions of vigorous external stirring, external USL may have a thickness of 30 μm, at maximum (including the reduction of D_s in wall pores and the tortuosity during the passage of solutes within wall pores). The contribution of internal USLs was estimated by the data presented in Fig. 8 (see last para of Results). According to these data, the overall measured permeability of a *Chara* cell for acetone was equivalent to a thickness of an internal USL of 204 μm. In the presence of membrane plus an internal USL, the thickness of the latter is reduced to 97 μm (at maximum), which was equivalent to 40 % of the entire permeation resistance. It should be noted this estimation refers to a completely stagnant and homogenous internal compartment. However, this was not the case. There is some internal mixing by cytoplasmic streaming and by the shaking of the cell during the experiments (see discussion in Stevenson *et al.* 1975). Hence, the underestimation by 40 % has to be taken as an upper limit. Preliminary experiments in which the concentration of solute right at the surface of the inner side of the plasma membrane was followed during permeation experiments, indicated an actual underestimation of around 20 % for acetone and of around 2 % for DMF, which may turn out to be more realistic (Ye, Kim & Steudle, unpublished results). Hence, we may and up with an internal USL of a thickness of around 50 μm. It has to be stressed that the effects of USLs that have been worked out here for acetone should be similar to those for HDO. This solute has permeability that is bigger by a factor of two than that of acetone, but this should be compensated for by a bigger diffusion coefficient ($D_s = 2.4 \times 10^{-9}$ m^2·s^{-1}; Reid & Sherwood 1966). Values of the diffusional permeability of isotopic water have been often compared with those of the bulk permeability ($Lp \propto P_f$) to work out the internal size of aquaporins (see Introduction; Ye *et al.* 2005). In an analysis similar to the present, Sehy *et al.* (2002) provide evidence that the contribution of internal mixing by diffusion to the overall rate of uptake of HDO by spherical oocytes of *Xenopus* laevis (R = 0.6 mm) was 30 % (39 % were actually reported in the paper for

the ratio of P_s^{memb} / P_s^{meas}, i.e., 2.7×10^{-6} m·s^{-1}/1.9×10^{-6} m·s^{-1} = 1.39). This percentage is smaller than that given here for acetone in *Chara*. However, the oocytes used by Sehy *et al*. (2002) had a spherical geometry so that the contribution of internal mixing should have been smaller. Stevenson *et al*. (1975) used cylindrical tubes of collagen and cellulose acetate (as used during the purification of blood; R = 0.14 to 0.35 mm) to work out the contribution of unsteady experimental condition to the overall permeability. Using an equation identical with Eqn 11, they calculated a membrane permeability of urea of $P_s = 6.0 \times 10^{-6}$ m·s^{-1}. They then compared this value with a known permeability coefficient obtained from a steady state experiment. When the external solution was vigorously stirred, the difference was found to be less than 20 % for urea which is similar to the result obtained here for acetone at a similar P_s. Stevenson *et al*. (1975) concluded that unsteady experimental conditions do not significantly affect the measurement of membrane permeability.

In conclusion, the re-examination of the role of USLs during pressure probe experiments with isolated internodes of *Chara* showed that effects of internal and external USLs don't play a significant role when hydrostatic pressure pulses are applied to induce monophasic pressure relaxations. Careful consideration of the limitations of the pressure probe to resolve relaxations indicated that the claim of Tyree *et al*. (2005) of an additional phase in relaxations is due to an artifact. Tyree *et al*. (2005) overlooked limitations in the resolution of the probe. During hydrostatically driven water flow, an effect of high flow rates was only observed in the present paper during pressure clamp when using substantial step changes in turgor pressure. Effects could not completely be explained by conventional sweep away where the water flow density is evenly distributed within the cell membrane, but may be due to a sweep away in the presence of a considerable constriction of water flow through AQPs including a concentration polarization of solutes within the vestibules of AQPs. A rigorous examination of the stirring of the solution surrounding the internodes during osmotic experiments indicated that external USLs had a small thickness of less than 30 μm. The conclusions drawn by Tyree *et al*. (2005) that, in standard pressure probe experiments, water flow around the internodes is laminar, lacks a physical basis. The earlier conclusion that flow is turbulent and the medium vigorously stirred was

strongly supported by experiments in which air bubbles were flushed through the tubes containing *Chara* internodes. The additional stirring caused complete replacements of solution around the cells which did not result in a further increase of measured transport coefficient in osmotic experiments. By applying unsteady-state diffusion kinetics, upper limits of equivalent thickness of internal USLs were provided for cylindrical compartments lacking a membrane. For acetone, the upper limit was 117 µm (R = 0.4 mm), which is smaller than the maximum figure of 350 µm erroneously assumed by Tyree *et al.* (2005). The real equivalent thickness of USLs was estimated to be smaller by at least a factor of 2 to 3 than the upper limit of 120 µm. This in turn would provide an upper limit of around 50 µm for the most rapidly permeating solutes (acetone, HDO). It should be smaller for other solutes having a more favourable ratio of D_s/P_s. (e.g. monohydric alcohols, H_2O_2, or DMF). The quantitative estimates are in line with earlier findings, which showed that closure of water channels massively affected overall Lp, P_s, and σ_s. These results are hard to explain in the presence of a dominating effect of USLs.

Acknowledgements

References

Barry P.H. & Diamond J.M. (1984) Effects of unstirred layers on membrane phenomena. *Physiological reviews* **64**, 763–872.

Crank J. (1975) The mathematics of diffusion (second edition of the original 1956 print). University Press Oxford, UK.

Dainty J. (1963) Water relations of plant cells. *Advances in Botanical Research* **1**, 279–326.

Dainty J. & Ginzburg B.Z. (1964a) The measurement of hydraulic conductivity (osmotic permeability to water) of internodal characean cells by means of transcellular osmosis. *Biochimica et Biophysica Acta* **79**, 102–111.

Dainty J. & Ginzburg B.Z. (1964b) The permeability of the protoplast of *Chara australis* and *Nitella translucens* to methanol, ethanol and iso-propanol. *Biochimica et Biophysica Acta* **79**, 122–128.

Finkelstein A. (1987) Water movement through lipid bilayers, pores and plasma membranes. Theory and reality. Distinguished lecture series of the Society of General Physiologists, vol. 4. Wiley, New York.

Henzler T. & Steudle E. (1995) Reversible closing of water channels in *Chara* internodes provides evidence for a composite transport model of the plasma membrane. *Journal of Experimental Botany* **46**, 199–209.

Henzler T. & Steudle E. (2000) Transport and metabolic degradation of hydrogen peroxide: model calculations and measurements with the pressure probe suggest transport of H_2O_2 across water channels. *Journal of Experimental Botany* **51**, 2053–2066.

Henzler T., Ye Q. & Steudle E. (2004) Oxidative gating of water channels (aquaporins) in *Chara* by hydroxyl radicals. *Plant Cell and Environment* **27**, 1184–1195.

Hertel A. & Steudle E. (1997) The function of water channels in *Chara*: the temperature dependence of water and solute flows provides evidence for composite membrane transport and for a slippage of small organic solutes across water channels. *Planta* **202**, 324–335.

Jost W. (1960) Diffusion in solids, liquids, gases. In *Physical Chemistry a series of monographs* (eds E. Hutchinson & van P. Rysselberghe), Academic Press, New York, USA.

Kiyosawa K. & Tazawa M. (1972) Influence of intracellular and extracellular tonicities on water permeability in characean cells. *Protoplasma* **74**, 257–270.

Kiyosawa K. & Tazawa M. (1977) Hydraulic conductivity of tonoplast free *Chara* cells *Journal of Membrane Biology* **37**, 157–166.

Lee S.H., Chung G.C. & Steudle E. (2005) Low temperature and mechanical stresses differently gate aquaporins of root cortical cells of chilling-sensitive cucumber and chilling-resistant figleaf gourd. *Plant Cell and Environment* **28**,1191–1202.

Mathai J.C., Mori S., Smith B.L., Preston G.M., Mohandas N., Collins M., van Zijl P.C., Zeidel M.L. & Agre P. (1996) Functional analysis of aquaporin-1 deficient red cells. The Colton-null phenotype. *Journal of Biological Chemistry* **271,** 1309–1313.

Maurel C., Tacnet F., Güclü J., Guern J. & Ripoche P. (1997) Purified vesicles of tobacco cell vacuolar and plasma membranes exhibit dramatically different water permeability and water channel activity. *Proceedings of the National Academy of Sciences USA* **94**, 7103–7108

Niemietz C.M. & Tyerman S.D. (1997) Characterization of water channels in wheat root membrane vesicles. *Plant Physiology* **115,** 561–567.

Poling B.E., Prausnitz J.M. & O'Connell J.P. (2001) The properties of gases and liquids (fourth edition). McGraw-Hill, New York, USA.

Reid R.C. & Sherwood T.K. (1966) The properties of gases and liquids. McGraw-Hill, New York, USA.

Rüdinger M., Hierling P. & Steudle E. (1992) Osmotic biosensors. How to use a characean internode for measuring the alcohol content of beer. Botanica Acta **105**, 3–12.

Sehy J.V., Banks A.A., Ackerman J.J.H. & Neil J.J. (2002) Importance of intracellular water apparent diffusion to the measurement of membrane permeability. *Biophysical Journal* **83**, 2856–2863.

Steudle E. (1993) Pressure probe techniques: basic principles and application to studies of water and solute relations at the cell, tissue, and organ level. In *Water*

Deficits: Plant Responses from Cell to Community (eds J.A.C. Smith & H. Griffith), pp. 5–36. BIOS. Scientific Publishers, Oxford, UK.

Steudle E. & Brinckmann E. (1989) The osmometer model of the root: water and solute relations of *Phaseolus coccineus*. *Botanica Acta* **102**, 85–95.

Steudle E. & Frensch J. (1989) Osmotic responses of maize roots. Water and solute relations. *Planta* **177**, 281–295.

Steudle E. & Tyerman S.D. (1983) Determination of permeability coefficients, reflection coefficients and hydraulic conductivity of *Chara corallina* using the pressure probe: effects of solute concentrations. *Journal of Membrane Biology* **75**, 85–96.

Steudle E. & Zimmermann U. (1974) Determination of the hydraulic conductivity and of reflection coefficients in *Nitella flexilis* by means of direct cell-turgor pressure measurements. *Biochimica et Biophysica Acta* **322**, 399–412.

Steudle E., Smith J.A.C. & Lüttge U. (1980) Water relation parameters of individual mesophyll cells of the crassulacean acid metabolism plant *Kalanchoe daigremontiana*. *Plant Physiology* **66**, 1155-1163.

Stevenson J.F. (1974) Unsteady mass transfer in a long composite cylinder with interfacial resistances. *AIChE Journal* **20**, 461–466.

Stevenson J.F., Von Deak M.A., Weinberg M. & Schuette R.W. (1975) An unsteady state method for measuring the permeability of small tubular membranes. *AIChE Journal* **21**, 1192–1199.

Tyerman S.D. & Steudle E. (1984) Determination of solute permeability in *Chara* internodes by a turgor minimun method. Effect of external pH. *Plant Physiology* **74**, 464–468.

Tyree M.T., Koh S. & Sands P. (2005) The determination of membrane transport parameters with the cell pressure probe: theory suggests that unstirred layers have significant impact. *Plant Cell and Environment* **28**, (in press). doi: 10.1111/j.1365-3040.2005.01384.x

Walz T., Smith B.L., Zeidel M.L., Engel A. & Agre P. (1994) Biologically active two-dimensional crystals of aquaporin CHIP. *Journal of Biological Chemistry* **269**, 1583–1586.

Wan X.C., Steudle E. & Hartung W. (2004) Gating of water channels (aquaporins) in cortical cells of young corn roots by mechanical stimuli (pressure pulses): effects of ABA and of $HgCl_2$. *Journal of Experimental Botany* **55**, 411–422.

White F.M. (1999) Fluid mechanics (fourth edition). McGraw-Hill, Boston, USA.

Ye Q., & Steudle E. (2005) Oxidative gating of water channels (aquaporins) in corn roots. *Plant Cell and Environment* **28**, (in press). doi: 10.1111/j.1365-3040.2005.01423.x

Ye Q., Muhr J. & Steudle E. (2005) A cohesion/tension model for the gating of aquaporins allows estimation of water channel pore volumes in *Chara*. *Plant Cell and Environment* **28**, 525–535.

Ye Q., Wiera B. & Steudle E. (2004) A cohesion/tension mechanism explains the gating of water channels (aquaporins) in *Chara* internodes by high concentration. *Journal of Experimental Botany* **55**, 449–461.

3   Further quantification of the role of internal unstirred layers during the measurement of transport coefficients in giant internodes of *Chara* by a new stop-flow technique

Yangmin Kim, Qing Ye, Hagen Reinhardt and Ernst Steudle

Department of Plant Ecology, Bayreuth University, D-95440 Bayreuth, Germany

Corresponding author: E. Steudle
E-mail: ernst.steudle@uni-bayreuth.de
Fax: +49 921 552564

Number of Figures: 7
Number of Tables: 0

Abstract

A new stop-flow technique (SFT) was employed to quantify the impact of internal unstirred layers (USLs) on the measurement of the solute permeability coefficient (P_s) across the plasma membrane of internodes of the giant-celled alga *Chara corallina* using a cell pressure probe (CPP). During permeation experiments with rapidly permeating solutes (acetone, 2-propanol, and dimethylformamide, DMF), the solute concentration inside the cell was estimated and the external medium was adjusted in order to stop the solute transport across the membrane, after which responses in turgor were measured. This allowed estimation of the solute concentration right at the membrane. SF experiments were also simulated with a computer. Both the SF experiments and simulations provided quantitative data about internal concentration gradients and the contribution of USLs to overall measured values of P_s^{meas} for the three solutes. The SF experimental results agreed with SF simulations assuming that solutes diffused into a completely stagnant cell interior. The effects of internal USLs on the underestimation of membrane P_s declined with decreasing P_s. They were no bigger than 37% in the presence of the most rapidly permeating solute acetone ($P_s^{meas} = 4.2 \times 10^{-6}$ m s^{-1}), and 14% for the less rapidly permeating DMF ($P_s^{meas} = 1.6 \times 10^{-6}$ m s^{-1}). It is concluded that, even in the case of rapidly permeating solutes such as isotopic water and, even when making pessimistic assumptions about the internal mixing of solutes, an upper limit for the underestimation of P_s due to internal USLs was 37%. The data are discussed in terms of recent theoretical estimates of the effect of internal USLs by Ye *et al*. (2006) and in terms of some recent criticism of CPP measurements of water and solute transport coefficients. The current stop-flow data are in line with earlier estimations of the role of USLs in the literature on cell water relations.

Key-words: Cell pressure probe, *Chara corallina,* internal unstirred layers, solute permeability coefficient, stop-flow technique.

Abbreviations: CPP, cell pressure probe; C_{prosp}, prospected concentration; C_{SF}, internal concentration suggested by SF; δ^i, thickness of internal USLs; D_s, diffusion

coefficient of a solute in water; Lp, hydraulic conductivity; P_d, diffusional water permeability; P_f, osmotic water permeability; P_s, true membrane permeability for a solute; P_s^{meas}, measured overall permeability including USLs for a solute; RDC, relative difference between C_{prosp} and C_{SF}; $C_{s\,mem}^i$, concentration inside of the cell at the membrane; σ_s, reflection coefficient; SFT, stop-flow technique; USL, unstirred layer.

Introduction

Whenever transport across membranes or other types of permeation barriers is measured and quantified in terms of certain coefficients, such as the permeabilities of water and solutes, unstirred layers (USLs) may affect the measurement and should be accounted for. This is so, because the permeation of substances across the membrane (or barrier) should cause a depletion of the permeant on one side of the membrane while increasing its concentration on the other. The relative contribution of USLs to the overall measured permeability depends on the rate at which solutes or water move across the membrane as compared with the rate at which substances diffuse from the bulk solution to the membrane surface or *vice versa*. Stirring of the media separated by the membrane can substantially reduce the thickness of USLs but can never completely eliminate them (Ye *et al.*, 2006). Relative contributions of USLs increase with increasing permeability of solutes. Whenever the actual transport properties are to be known for a single membrane, rather than those of an entire barrier, the effects of USLs have to be quantified.

A USL is a region of slow laminar flow parallel to the membrane in which the only mechanism of transport is by diffusion (Dainty, 1963). When dealing with non-electrolytes, there are two different kinds of effects of USLs. These depend on (i) whether transport across the complex barrier consisting of USLs and membrane is just diffusional in nature, or (ii) is both diffusional and convective in nature. For the first model, when a permeating solute diffuses across a membrane, depending on the diffusional supply from the bulk solution to the membrane, the actual concentration gradient driving the solution permeation across the membrane may be smaller than that measured in the bulk solution. This type of effect of USL has been termed the

'gradient-dissipation effect' (Barry and Diamond, 1984). In the second model, solutes are swept by convection with the water transport in the perpendicular direction to the membrane where they are concentrated on one side but depleted on the other side. Concentration gradients built up in the solution and adjacent to the membrane will be opposed by a back-diffusion within USLs. This type of USL effect in the presence of water flow across the membrane has been termed 'sweep-away effect' ('convection versus diffusion'; Dainty, 1963). Both types of effects of USLs result in overall permeabilities for water and solutes that are smaller than those of just the membrane.

In a previous paper, Ye *et al.* (2006) examined how USLs contributed to the measurement of transport coefficients such as the hydraulic conductivity (Lp, water permeability), permeability coefficient (P_s, solute permeability), and reflection coefficients of solutes (σ_s) in giant cylindrical internodes of *Chara corallina*. The big, isolated cells (diameter: $\approx$1 mm; length: 40 to 120 mm) could be measured in fairly turbulent media to reduce the thickness of external USLs, thus minimizing their effects. However, the cell interior could not be stirred, which could have caused the build up of substantial internal USLs. The results of Ye *et al.* (2006) showed that sweep-away effects are usually negligibly small, but gradient-dissipation effects could be significant in the presence of rapidly permeating solutes (the typical solute used was acetone with a high membrane P_s). In the latter case, the diffusional resistances of internal USLs (δ^i / D_s; δ^i = thickness of internal USL; D_s = diffusion coefficient) were not negligible. For example, Tyree *et al.* (2005) claimed that, for the rapidly permeating test solute acetone, the real membrane permeability could be as big as 5 times the measured permeability suggesting a rate-limitation by USLs. The authors assumed fairly big thicknesses of internal and external USLs that dominated the overall solute transport. On the other hand, Ye *et al.* (2006) applied non-steady state diffusion kinetics to *Chara* internodes that were taking up or losing a rapidly permeating solute (e.g. the test solute acetone as measured with the CPP). The upper limit of the equivalent δ^i of internal USLs was 97 μm in this case, which referred to an upper limit of 40% of the contribution of internal USLs to the overall measured permeability coefficient (P_s^{meas}). The authors stress that this referred to a completely stagnant cell interior with no mixing by cytoplasmic streaming, local differences in

density, or shaking and bending of cells during the experiments. Ye *et al.* (2006) estimated the real equivalent δ^i to be around 50 μm. Using δ^i values of 50 and 100 μm for acetone and a P_s^{meas} of 4.2×10^{-6} m s^{-1}, the actual P_s of the membrane equalled 5.2×10^{-6} m s^{-1} or 7.0×10^{-6} m s^{-1}, respectively ($D_s = 1.2 \times 10^{-9}$ m^2 s^{-1}; $R = 0.4$ mm). This means that the contribution of internal USLs could have been as large as 19 or 40%, respectively.

The problem is important in cell water relations whenever comparisons are made between the osmotic water permeability, P_f ($P_f =$ Lp V_w/RT; V_w is the molar volume of liquid water), and the diffusional water permeability, P_d, measured with isotopic water (Steudle and Henzler, 1995; Sehy *et al.*, 2002; Henzler *et al.*, 2004). It has been readily shown that the ratio of P_f/P_d is equal to the number (N) of water molecules sitting in an aquaporin (AQP) pore, provided that effects of USLs (namely in P_d) can be neglected (Levitt, 1974; Finkelstein, 1987; Ye *et al.*, 2005). This is always the case when cells or vesicles are small, but may present a problem for big cells such as *Chara* internodes or *Xenopus* oocytes (Sehy *et al.*, 2002).

In the present paper, we continue to quantify the role of diffusional USLs focusing on internal diffusional USLs. Ye *et al.* (2006) showed that vigorous external stirring minimized the effects of external USLs, but the role of the internal USLs could not yet be verified experimentally. To do this, a new stop-flow technique (SFT) was developed to work out the solute profile in the cell, which is otherwise difficult to measure. Knowing the concentration right at the membrane surface is necessary to evaluate the 'true' membrane permeability of a solute, P_s. In the SFT, we intended to stop the solute flow across the membrane by applying the same concentration in the external medium as that of the cell interior by trial and error. In this way, the concentration right at the membrane was accessed or estimated to get an idea of whether or not there was an USL inside the cell. Besides the SF measurements, a computer simulation of SF experiments was performed, assuming either a well-stirred or a completely stagnant cell interior (minimum or maximum contribution of USLs). Results from simulations were compared with those of experiments to provide deeper insights to the effects of internal USLs. In both the experiments and simulations, we

used solutes of different permeability. The P_s of the most rapid solute acetone was similar to that of isotopic water so that effects were tested in the presence of an extremely rapid permeant.

The results of the present paper were in line with recent findings of Ye *et al.* (2006) who showed that (i) during sweep-away, effects of USLs on Lp measurements were negligibly small and that (ii) the effects on permeability coefficients were up to 40% in the case of the most rapid solute acetone. The latter conclusion was drawn from a theoretical consideration of the diffusion within the cylindrical internodes. Additionally, the current results agreed with conclusions from other workers in the field (e.g. Steudle and Tyerman, 1983; Hertel and Steudle, 1997; Henzler and Steudle, 2000; Ye *et al.*, 2005). In contrast, they disagreed with recent estimates of Tyree *et al.* (2005), who claimed that USLs may dominate the measurement of transport coefficients with cell pressure probes, at least in the presence of rapidly permeating substances (such as the test solute acetone; see discussion in Ye *et al.*, 2006).

Theory and results from computer simulations

When a permeating solute is added to an isolated cell sitting in a well-stirred medium, the water (J_V) and solute flow (J_s) are calculated by two coupled differential equations derived from irreversible thermodynamics ('phenomenological equations'; Kedem and Katchalsky, 1958; Dainty, 1963; Steudle and Tyerman, 1983; Steudle, 1993; Steudle and Henzler, 1995):

$$J_V = -\frac{1}{A}\frac{dV}{dt} = L_P\left[P - \sigma_s \cdot RT \cdot (C_s^i - C_s^o) - RT \cdot (C^i - C^o)\right], \text{ and} \qquad (1)$$

$$J_s = -\frac{1}{A}\frac{dn_s^i}{dt} = P_s(C_s^i - C_s^o) + (1 - \sigma_s) \cdot \overline{C_s} \cdot J_V + J_s^*. \qquad (2)$$

Here, V is the actual cell volume, A, the cell surface area, and n_s^i, the number of moles of permeating solute, s, in the cell; P denotes the actual turgor pressure; Lp is the hydraulic conductivity; P_s, the permeability coefficient of the membrane for a given solute; σ_s is the reflection coefficient of solute 's', which denotes the passive selectivity of the membrane for a given solute; C_s^i is the concentration of 's' inside of

the membrane; C_s^o is the concentration outside of the membrane, and $\overline{C_s}$, the mean concentration in the membrane ($=(C_s^i + C_s^o)/2$). The C^i and C^o are concentrations of impermeable solutes inside and outside of the membrane. On the right side of Eqn (1), it is indicated that there are two components of water flow, a hydrostatic and an osmotic. The solute flow in Eqn (2) has three components, a diffusional ($P_s(C_s^i - C_s^o)$), a solvent-drag component ($(1-\sigma_s)\cdot\overline{C_s}\cdot J_V$), as well as an active flow of solute 's' (J_s^*). Active transport was neglected for the test solutes used in the current work. Usually, the solvent drag does not contribute much to the overall solute flow and may be neglected as well as shown in earlier comparisons with experimental findings and computer simulations (Rüdinger *et al.*, 1992; see below). Using these assumptions, Steudle and Tyerman (1983) provided an analytical solution of Eqns (1) and (2) that represents the time course of biphasic pressure relaxations in the presence of permeating solutes, added at $t = 0$:

$$\frac{V(t)-V_o}{V_o} = \frac{P(t)-P_o}{\varepsilon} = \frac{\sigma_s\cdot\Delta\pi_s^o\cdot Lp}{(\varepsilon+\pi^i)\cdot Lp - P_s}\left[\exp(-k_w\cdot t) - \exp(-k_s\cdot t)\right] . \qquad (3)$$

In Eqn (3), V_o is the original cell volume, and P_o, the original turgor pressure; ε is the cell elastic modulus; $\Delta\pi_s^o$ is the change in the external osmotic pressure of permeating solute added at $t = 0$ to produce the osmotic response; π^i is osmotic pressure of the cell; and k_w and k_s are the rate constants for water and solute exchange, respectively, whereby $k_w >> k_s$ usually holds.

Equation (3) states that, following a rapid water phase, solute flow will be following first order kinetics, i.e., the solute phase should be exponential after sufficiently long time intervals, when the term $\exp(-k_w\cdot t)$ vanishes. In the Steudle/Tyerman theory, USLs either play no role or are quickly constant and contribute to the overall measured value of solute permeability (P_s^{meas}), which depends on the solute permeability of the membrane (P_s), the thickness of internal USLs (δ^i), and the diffusion coefficient of the solute in the cell (D_s; see above), i.e.:

$$\frac{1}{P_s^{meas}} = \frac{1}{P_s} + \frac{\delta^i}{D_s^i} . \qquad (4)$$

This refers to the steady state and to a planar membrane. For a cylindrical cell, we have, again in the steady state, an equivalent relation (Steudle and Frensch, 1989; Ye *et al.*, 2006):

$$\frac{1}{P_s^{meas}} = \frac{1}{P_s} + \frac{R}{D_s} \ln \frac{R}{r} . \tag{5}$$

Here, r denotes the radial distance from the center of the cell to the boundaries of internal USLs and *R*, the radius of the cell. Hence, the thickness of the internal USL would be $\delta^i = R\text{-}r$. In the presence of an external USL, Eqn (5) may be extended (Ye *et al*., 2006). Different from Eqns (4) and (5), real diffusive USLs do not have well-defined edges, and the term 'thickness' is used somewhat vaguely. There are two definitions: (i) USLs with a sharp physical boundary to the rest of the cell that is vigorously stirred, and (ii) USLs created during non-steady state diffusion, when the contribution of the USL becomes virtually constant ('equivalent unstirred layer thickness'). Definition (i) is a useful hypothetical situation because it assumes that the interior of a compartment, such as a *Chara* internode, can be well stirred except for a layer of δ^i thickness. Provided that δ^i is small compared to the radius, the concentration gradient within the USL should be linear to a good approximation, following a rather short time interval after adding the solute to the medium. In definition (ii), solutes cross the plasma membrane (PM) and then diffuse into a completely stagnant cell interior. During this non-steady process, the actual thickness will continuously grow until, at a certain thickness of the diffusive layer, it will tend to become quasi-steady. During this state, an "equivalent USL thickness" may be defined (Ye *et al.*, 2006). This case appears to be more realistic than case (i). In the present paper, we used the concept of equivalent USL thickness. Despite the difficulties in defining equivalent thicknesses of USLs, the USL concept is useful. It provides figures to judge about the contribution of boundary layers close to membranes to overall measured permeabilities, namely in the presence of rapidly permeating solutes. Other concepts, such as the use of time constants, result in similar difficulties (Sehy *et al.*, 2002) that are due to the complex nature of diffusion kinetics in the non-steady case.

When we assume a steady internal thickness of USLs and hence a steady P_s^{meas}, Eqn (3) should hold, as indicated by numerous earlier results from pressure probe

measurements using a suite of test solutes of different permeability (Steudle and Tyerman, 1983; Tyerman and Steudle, 1984; Rüdinger *et al.*, 1992; Steudle and Henzler, 1995; Henzler and Steudle, 1995; Schütz and Tyerman, 1997; Hertel and Steudle, 1997). However, measurements with most rapidly permeating solutes, including heavy water (HDO) and acetone, may cause a problem (Ye *et al.*, 2004; Tyree *et al.*, 2005; Ye *et al.*, 2006). For these solutes, an estimated upper limit for the contribution of internal USLs was between 25 to 40% (Ye *et al.*, 2005, 2006).

Simulations of diffusion inside the cell

To further quantify the role of internal diffusive transport in P_s measurement, we used classical numerical approaches for diffusion in a cylinder (see computational fluid dynamics text books such as that by Abbot and Basco, 1990). Internal USLs were modelled assuming that diffusion within *Chara* internodes was between concentric cylindrical shells of small thickness according to Fick's first law at a given time. Taking into account the cylindrical geometry (Eqn (5)), the differential equation for the diffusion of solute, 's' in a cylinder is (e.g. Steudle and Frensch, 1989):

$$J_s = -\frac{1}{A}\frac{dn_s^i}{dt} = -D_s \frac{1}{r}\frac{\partial}{\partial r}(r \cdot C_s^i). \tag{6}$$

The discrete analog of Eqn (6) is:

$$\frac{dC_s^i[i]}{dt} = \frac{2\pi L D_s (C_s^i[i-1]-C_s^i[i])}{\ln\left(\frac{r[i-1]}{r[i]}\right)\cdot V[i]} - \frac{2\pi L D_s (C_s^i[i]-C_s^i[i+1])}{\ln\left(\frac{r[i]}{r[i+1]}\right)\cdot V[i]}, \tag{7}$$

assuming that

$$\frac{dC_s^i[i]}{dt} = \frac{n_s^i[i]-n_s^i[i+1]}{dt}\cdot\frac{1}{V[i]} \text{ and} \tag{8}$$

$$\frac{n_s^i[i]}{dt} = \frac{2\pi L D_s (C_s^i[i-1]-C_s^i[i])}{\ln\left(\frac{r[i-1]}{r[i]}\right)}. \tag{9}$$

Here, $C_s^i[i]$ is the concentration of solute in shell i at a given time, and radius $r[i]$ is the distance from the center of the cylinder to the center of the shell i; and L is the cell length. In the simulations, time intervals of $dt = 0.01$ s and radius increments of the shells, $\Delta r = 5$ μm, were used (the radius of the cell, $R = 400$ or 500 μm). Further reduction of dt to 0.001 s and of Δr to 1 μm did not further refine the internal profiles

of concentration (data not shown). Also, it was verified at given times, τ, and different distances from the membrane, Δx, that $\Delta x^2/\tau$ was constant for a given concentration as predicted by basic diffusion kinetics (relation of Einstein and Smoluchowski, see textbooks on diffusion such as Jost, 1960).

Simulation of effects of internal USLs during stop flow

For membrane transport in a *Chara* internode, Eqns (1) and (2) were incorporated into simulations. During the simulations, solvent drag did not occur between shells, but instead was incorporated at the membrane. In Eqns (2) and Eqn (7), the transfer of solutes across the membrane and between adjacent shells is denoted, respectively. A standard computer program was used to numerically integrate Eqns (1), (2), and (6). This resulted in (i) concentration profiles within the cells and (ii) overall rates of uptake or losses by cells. Hence, it was tested in simulations whether or not the overall or mean concentration of solute 's' in the cell ('prospected concentration'; as assumed by Steudle and Tyerman, 1983; Eqn (3)) was a good estimate for the concentration adjacent to the membrane.

The Steudle/Tyerman theory assumes either that there are no effects of USLs or that these effects are incorporated into the value of P_s^{meas}. So far, the evidence that the contribution of internal USLs is relatively small is derived from the comparison of measured rates of solute flow (CPP) with rates expected from diffusion kinetics (Ye *et al.*, 2006). Hence, the evidence is indirect. The problem is twofold: (i) in contrast to the outer solution, the cell interior could not be stirred to test for the contribution of internal USLs; (ii) the concentration adjacent to the inner side of the PM could not be directly measured in order to determine how it would deviate from that used to calculate P_s, assuming that the cell interior was sufficiently stirred by mixing. In the following, we present results of simulations (Figs. 1 to 4), which are later compared with those of experiments (Figs. 5 to 7).

In the SFT, the concentration in the cell was first calculated using the Steudle/Tyerman theory (Eqn (3)) for a given time, i.e., a mean concentration was calculated and named the 'prospected concentration', C_{prosp}. The internal concentration

could be calculated at each pressure (time) point of the solute phase by the difference between the extrapolated pressure to time zero and the original turgor, P_o (ΔP_{prosp}), because the solute phase and extrapolated curve of it represented the solute uptake or loss in the cell (Fig. 1). In the endosmotic experiment (solute added outside and moving into the cell), once the cell's internal concentration was reached to C_{prosp}, the C_{prosp} was then applied to the outside medium, which tended to stop the solute flow across the membrane and bring the turgor pressure back to its original value, P_o. If there were no internal USLs, when C_{prosp} was added to external media, the C_{prosp} was the same as the concentration at the membrane, $C^i_{s\,mem}$, and no solute phase was observed in the simulation (Fig. 2b, black line). However, assuming an internal USL, the solute flow did not stop when the C_{prosp} was added to the external media (Fig. 2b, red line). This was due to the concentration gradient developed in the cell by the diffusion process. Concentrations that were higher and lower than C_{prosp} were selected and applied to external media to find the appropriate value at which solute flow would stop. Depending on whether the selected concentration was smaller or bigger, this resulted in either an overshoot (Fig. 2a) or undershoot (Fig. 2c) of the turgor pressure, respectively. After solution exchange, pressure responses showed another 'water phase' as in Fig. 1. Some water had to be transferred to adjust the pressure, when the solution was changed. The true stop-flow pressure, P_{stop}, could be obtained by extrapolating to the time when the solution was changed as shown in Fig. 2.

Simulated values of $\Delta P = P_{stop} - P_e$ were plotted against the concentration applied to stop the solute flow where P_{stop} was the turgor pressure extrapolated to the time, and P_e, the final steady-state turgor. The internal mean concentration at the point at which the solution was changed, as suggested by SF (C_{SF}), was determined by the intercept with the abscissa (Fig. 3).
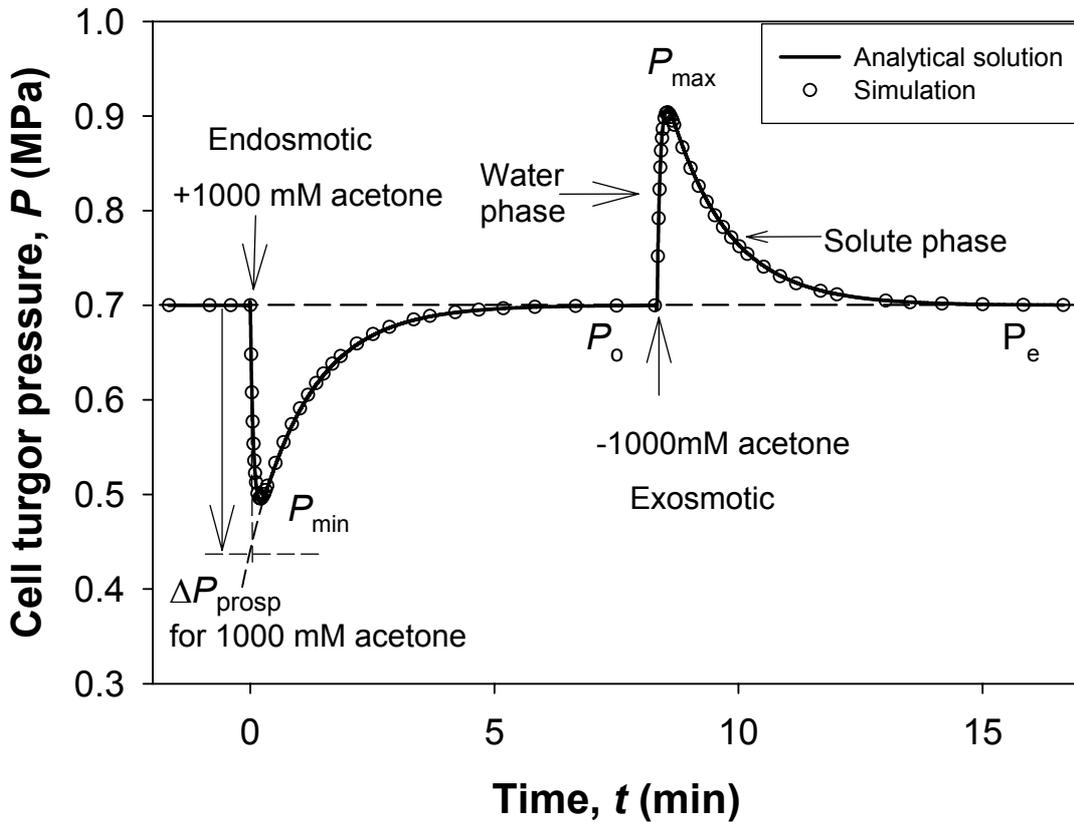
Figure 1. Computer simulation of the osmotic experiment in the absence of USLs was compared to the analytical solution of the osmotic response. At time zero, the cell was exposed to 1000 mM of acetone solution and a biphasic endosmotic response was observed (solute uptake). Once the pressure returned to the final steady-state turgor, the acetone was removed and a biphasic exosmotic curve was produced (solute loss). The simulated curve (circles) fitted nicely to the analytical solution (drawn line; Eqn (3)). The osmotic response consisted of a water phase and a solute phase with a rate constant of k_w and k_s, respectively. The solute phase curve from the endosmotic response was fitted exponentially and extrapolated back to time zero. The solute phase and extrapolated curve provided the overall solute uptake by the cell. The difference between the extrapolated pressure and P_o (ΔP_{prosp}) corresponded to the pressure drop by addition of 1000 mM acetone when we eliminated the water phase assuming very rapid water transport. Based on this, the internal concentration was calculated at each pressure point of the solute phase. The parameters used were $L_p = 1.3 \times 10^{-6}$ m s^{-1} MPa^{-1}, $\sigma_s = 0.10$, $P_s = 3.5 \times 10^{-6}$ m s^{-1}, $\varepsilon = 44.5$ MPa, $\pi^i = 0.70$ MPa, cell diameter $= 0.001$ m, and time step $dt = 0.01$ s.
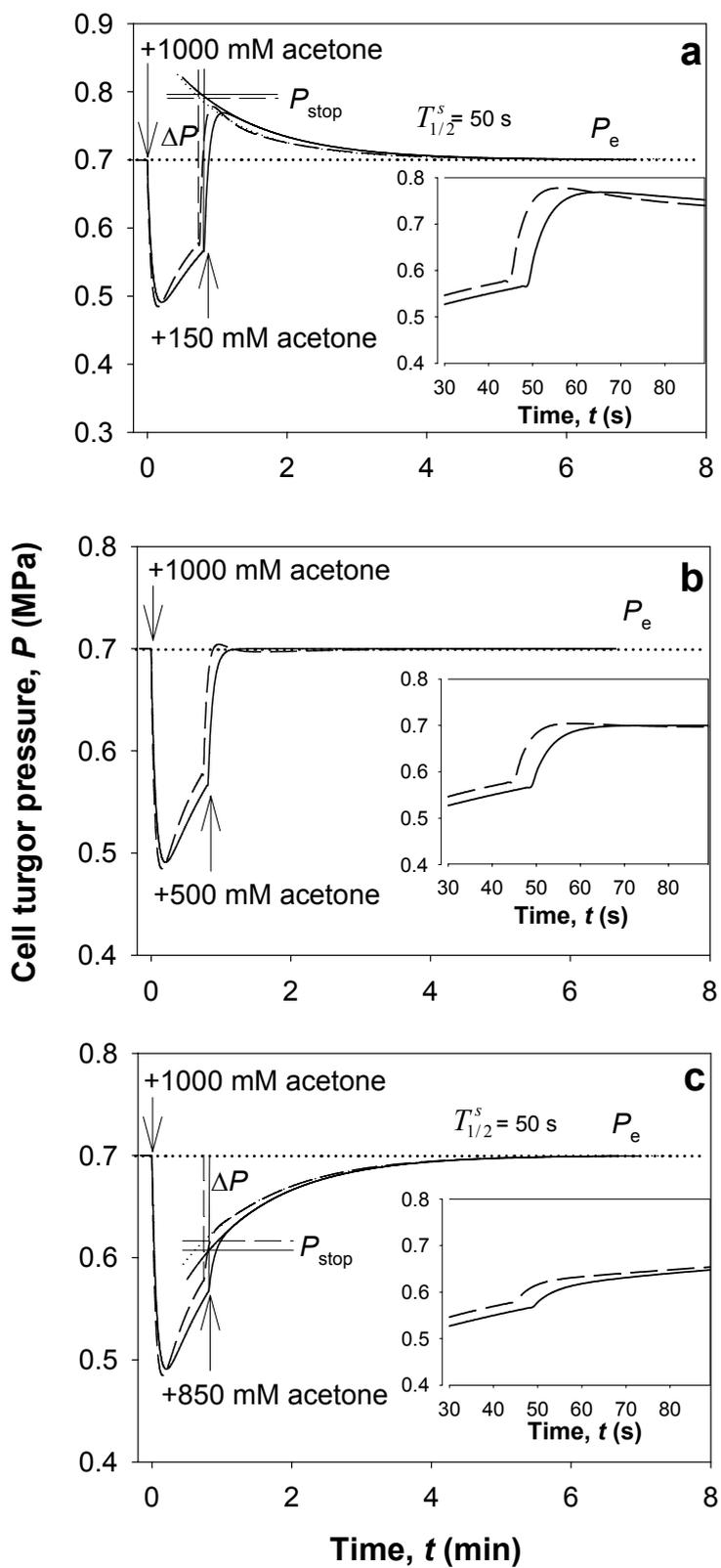
Figure 2. Simulation of a 'stop-flow experiment' according to SFT in the absence (solid lines) and presence (dashed lines) of internal USLs as they develop in a completely stagnant interior of a *Chara* internode ($R = 500$ μm). SF simulations were conducted on endosmotic curves. Effects of external USLs were excluded. The hydrostatic Lp in the absence of solutes was assumed. At $t = 0$, the external solution was changed from artificial pond water (APW) to APW plus 1000 mM acetone to produce a biphasic pressure response as in Fig. 1. When the prospected concentration in the cell, C_{prosp}, was 500 mM, the external concentration of acetone was changed to different values in order to find the concentration that stopped the solute flow (150, 300, 500, 700, 850 mM; data not shown for 300 and 700 mM) and the real P_{stop} was extrapolated to the time when the solution was changed. (a) When the 1000 mM external acetone solution was exchanged with a 150 mM acetone solution, overshoots of the pressure ($P_{stop} > P_e$) occurred in both the presence and absence of USLs. (b) An exchange with 500 mM could not completely stop the solute flow in the presence of USLs (red line). However, solute flow was stopped in the absence of USLs (black line). (c) The exchange with 850 mM resulted in undershoots of the pressure ($P_{stop} < P_e$) in the presence and absence of USLs. Each inset in a to c is the part of the curve where the external solution was exchanged.

Figure 3 shows that in the absence of USLs, the simulation produced the C_{SF} value identical to C_{prosp}, which was the internal mean concentration when the solution was changed (500 mM in the example shown in the figure). However, in the presence of internal, diffusive USLs, the intercept occurred at a concentration of 477 mM of C_{SF}, which is smaller than 500 mM by 5% (Fig. 3). This was observed because at the solution changing point, the concentration inside of the cell at the membrane ($C_{s\,mem}^{i}$) was bigger than C_{prosp}, and solutes moved out of the cell when the external concentration of C_{prosp} was added. This first outward solute movement was buried in the water phase. After a certain amount of solutes were moving out of the cell, the direction of solute movement was reversed to go into the cell and this was observed in a solute phase. Because we used the solute phase showing the solutes going into the cell, C_{SF} value was estimated to be smaller than C_{prosp}. At the solution changing point, the $C_{s\,mem}^{i}$ was obtained as 703 mM by the computer simulation of the internal concentration profile (data not shown). We identified $C_{s\,mem}^{i}$ only by simulations and not by experiment. By contrast, C_{SF} was measured using both experiments and simulations. C_{SF} is an internal mean concentration calculated from SF curves and a good indicator of whether or not there is an USL inside the cell. In the corresponding exosmotic experiment (such as in Fig. 1; solutes moving out of the cell), C_{SF} was 5%

greater than the prospected 500 mM. This means that the effects were symmetrical and independent of the direction of solute flow, as one would expect (data not shown).
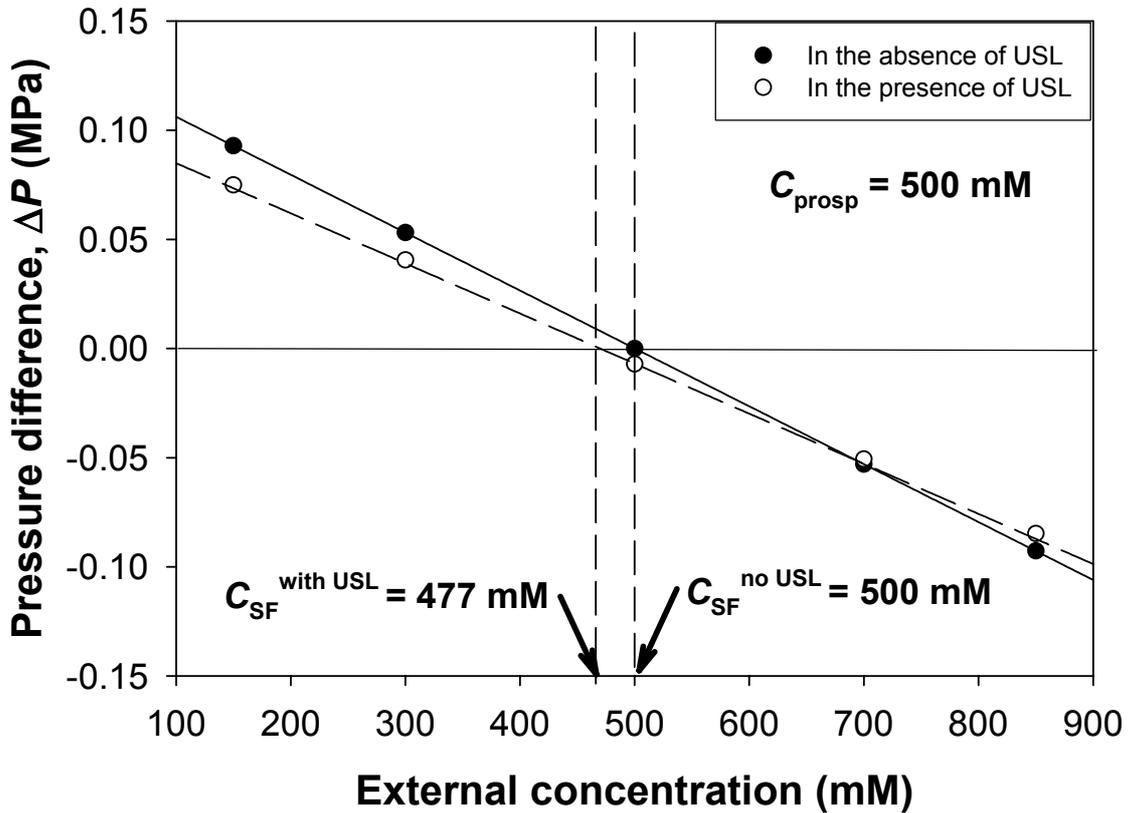
Figure 3. Plots of pressure differences ($\Delta P = P_{stop} - P_e$) measured from SF simulations versus the concentrations of interrupting solution applied in the solute phase in Fig. 2. From the intercept with the abscissa, C_{SF} was obtained. In the absence of USLs, C_{SF} was the same as C_{prosp} (500 mM), which was the internal mean concentration when the solution was changed. On the other hand, in the presence of USLs, C_{SF} provided a smaller concentration of 477 mM. In the exosmotic experiment when USLs were present, C_{SF} was greater than 500 mM (data not given). Open and closed circles represented data in the presence and absence of USLs, respectively.
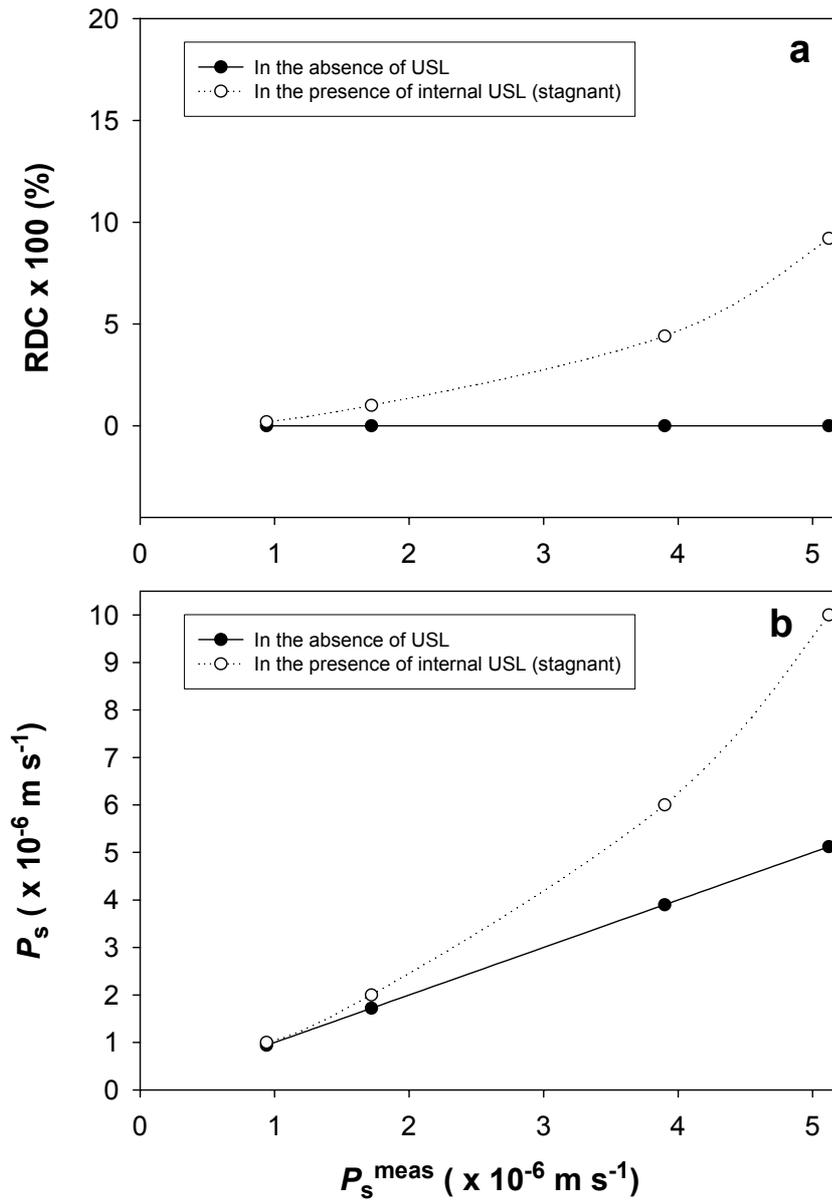
Figure 4. The effects of membrane permeabilities on the relative difference of concentrations (RDC) and underestimation of P_s. The permeability coefficient, P_s^{meas} was varied and other parameters were constant. (a) In the absence of USLs, RDCs were zero for every P_s^{meas}. If there were USLs, RDCs were greater for bigger P_s^{meas}. (b) In the absence of USLs, the measured permeabilities were the same as the real membrane permeabilities. However, in the presence of USLs, P_s^{meas} values were underestimated compared to the true membrane P_s. Lp = 1.0×10^{-6} m s^{-1} MPa^{-1}, $\sigma_s = 0.20$, $\varepsilon = 44.5$ MPa, $\pi^i = 0.7$ MPa, cell diameter = 0.0008 m, and time step $dt = 0.01$ s.

When the measured permeability coefficient, P_s^{meas}, was varied during simulations, but the other parameters left constant, the relative contribution of internal USLs increased as P_s^{meas} increased, as one would expect (Fig. 4). We introduced a new parameter, the relative difference of concentrations (RDC = $(C_{SF} - C_{prosp})/ C_{prosp}$) between C_{SF} and C_{prosp}. The RDC was a direct measure that could quantify the effects of internal USLs. In their absence, RDCs were zero for every P_s, and measured permeabilities were identical with the true membrane P_s (Figs. 4a, b). However, in presence of USLs, RDCs increased for bigger P_s tending to increase the underestimation of solute permeability (Figs. 4a, b). The relative contribution of USLs was bigger in the values of P_s^{meas} than in those of RDC, because the calculation of P_s accounted for the concentration profile in the cell (Fig. 4b).

In simulations based on the measured permeability coefficient for acetone ($P_s^{meas} = 4.2 \times 10^{-6}$ m s^{-1}), the RDC was $\pm$ 6% in endosmotic and exosmotic experiments, respectively (data not shown). The corresponding underestimation of P_s (accounting for the concentration profile in the cell) was 37% in both cases (data not shown). For the less rapidly permeating DMF ($P_s^{meas} = 1.6 \times 10^{-6}$ m s^{-1}) simulations resulted in an underestimation of RDC by only 1%, and the underestimation in P_s was 14% (data not shown; see comparison with experiments in the Results section).

Materials and methods

Algal material

Chara corallina was grown in artificial pond water (APW; composition in mM: 1.0 NaCl, 0.1 KCl, 0.1 CaCl$_2$ and 0.1 MgCl$_2$ at a pH $\approx$ 5.5). For detailed information of the growing conditions, the reader is referred to Henzler *et al*. (2004), and Ye *et al*. (2005). *Chara* internodes were 40 to 120 mm long and 0.8 to 1.0 mm in diameter and could be treated as cylinders to a good approximation.

Determination of transport parameters (Lp, P_s and σ_s) and cell wall elasticity (ε)

Using the cell pressure probe, three transport parameters were measured (Steudle 1993): (i) hydraulic conductivity (Lp) is a measure of water permeability across the cell membrane; (ii) permeability coefficient (P_s) denotes the passive permeability of the cell membrane for a given solute; (iii) reflection coefficient (σ_s) is a quantitative measure of the 'passive selectivity' of the cell membrane for a solute as compared to that of water. The elastic coefficient of the cell wall was measured as well (elastic modulus; ε). This parameter is required to relate the pressure/time curves measured with the probe to volume/time curves to determine water flow and cell Lp. Hydraulic conductivity was calculated from half times of hydrostatic pressure relaxations ($T_{1/2}^{w}$). In the presence of permeating solutes, $P(t)$ curves were biphasic with a water and solute phase. From the latter phase, P_s values were calculated from the half times ($T_{1/2}^{s}$). Reflection coefficients were obtained from maximum changes in pressure following step changes in the concentration of permeating solutes. Equations used for calculating ε, Lp, P_s and σ_s were:

$$\varepsilon = V\frac{dP}{dV} \approx V\frac{\Delta P}{\Delta V} \quad , \tag{10}$$

$$L_P = \frac{V}{A} \times \frac{\ln(2)}{T_{1/2}^{w}(\varepsilon + \pi^{i})} \quad , \tag{11}$$

$$P_s = \frac{V}{A} \times \frac{\ln(2)}{T_{1/2}^{s}} = \frac{V}{A}k_s \quad , \text{ and} \tag{12}$$

$$\sigma_s = \frac{P_o - P_{\min(\max)}}{RT \cdot \Delta C_s^{o}} \times \frac{\varepsilon + \pi^{i}}{\varepsilon} \exp(k_s \cdot t_{\min(\max)}) \quad . \tag{13}$$

Here, V = cell volume; A = cell surface area; π^{i} = osmotic pressure of cell sap; k_s is the rate constant of solute exchange; $P_o - P_{\min(\max)}$ is the maximum change in cell turgor pressure (Fig. 1); $RT \cdot \Delta C_s^{o}$ is the given change of osmotic pressure of the medium; and $t_{\min(\max)}$ is the time spent to reach the minimum (maximum) change in cell turgor pressure during the first phase (water phase) of the osmotic experiments.

'Stop-flow technique (SFT)' in osmotic experiments with permeating solutes

Stop-flow experiments were performed with three different solutes that varied in their rates of membrane permeation. Differences between prospected and measured concentrations (C_{prosp} and C_{SF}, respectively) were expected to be largest for the most rapidly permeating solute acetone (P_s^{meas} = 4.2 x 10^{-6} m s^{-1}; D_s = 1.2 x 10^{-9} m^2 s^{-1}). These differences were expected to decrease for 2-propanol (P_s^{meas} = 2.1 x 10^{-6} m s^{-1} and D_s = 1.0 x 10^{-9} m^2 s^{-1}) and DMF (P_s^{meas} = 1.6 x 10^{-6} m s^{-1} and D_s = 1.0 x 10^{-9} m^2 s^{-1}). In the experiments, 1000 mM of acetone, 600 mM of 2-propanol and 300 mM of DMF were used and the concentrations of these solutes in the cell changed with time as they permeated into or out of the cell. Prospected concentrations of these solutes inside of the cell at certain times (pressures) during biphasic pressure/time courses (Fig. 1) were chosen to be around 500 mM, 300 mM and 150 mM for acetone, 2-propanol and DMF, respectively (C_{prosp}). First, a cell was exposed to either acetone (500 mM), 2-propanol (300 mM) or DMF (150 mM) and biphasic curves were observed. The solute phase was fitted exponentially, and pressure differences (ΔP_{prosp}) were measured after extrapolating the solute phase back to the exact point where the solute was added, namely, at time zero to consider the solute movement during the water phase (Fig. 1). Next, a higher concentration of acetone (1000 mM), 2-propanol (600 mM) or DMF (300 mM) was added to the external solution. At that time (pressure) point calculated from ΔP_{prosp}, the solute phase was interrupted when the internal cell concentration was expected to be 500 mM (acetone), 300 mM (2-propanol) or 150 mM (DMF). Depending on the internal concentration chosen, the concentration series for the exchange solution were 150, 300, 500, 700, 850 mM for acetone; 100, 200, 300, 400, 500 mM for 2-propanol; and 50, 100, 150, 200, 250 mM for DMF. For each SF pressure/time curve produced, the true stop-flow pressure, Pstop, was found by extrapolation to the time when the solution was changed and the pressure differences ($\Delta P = P_{stop} - P_e$) were measured. Internal concentration at the solution changing point, suggested by SF (C_{SF}), was obtained from the intercept with the abscissa ($\Delta P = 0$) by plotting ΔP versus the concentration added during the solute phase.

Results
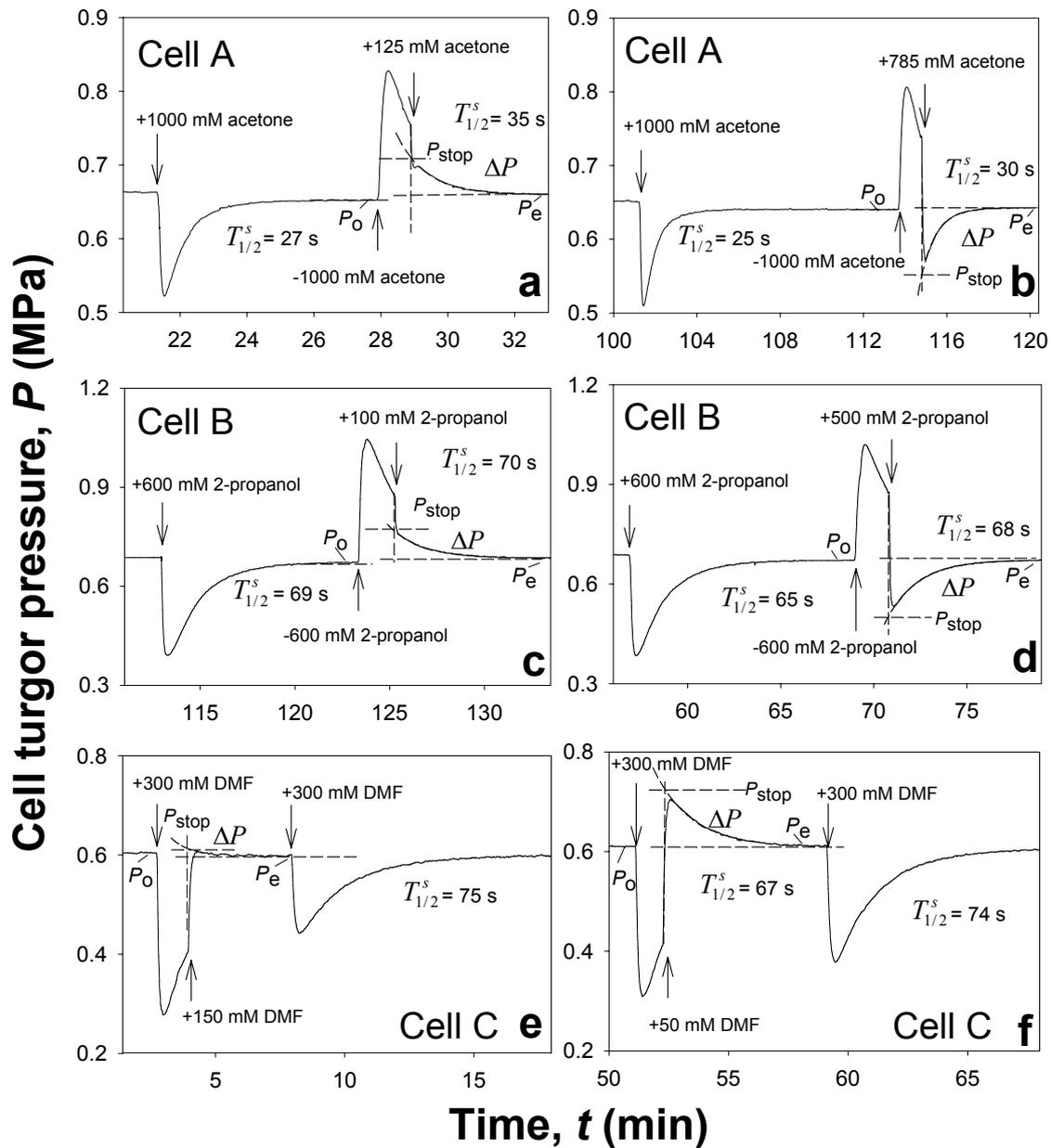
Figure 5. Typical experimental curves of the SFT, when the solute diffuses into or out of *Chara* internodes. (a, b) Cell A was first treated with 1000 mM acetone. After cell turgor reached a new equilibrium (the same concentration of acetone on both sides of the PM), acetone was replaced by normal medium (APW; i.e. removal of 1000 mM acetone from the medium). At a certain point of the solute phase in the exosmotic curve, where the concentration of acetone was expected to be 490 mM,

acetone solutions with different concentrations (a: 125 mM; b: 785 mM) were added to the medium to interrupt the solute phase. (c, d) Cell B was first treated with 600 mM 2-propanol. After cell turgor reached a new equilibrium (the same concentration of 2-propanol on both sides of the cell), the 2-propanol solution was replaced by APW. At a certain point of the $P(t)$ curve where the concentration of 2-propanol was expected to be 278 mM, 2-propanol solutions with different concentrations (c: 100 mM; d: 500 mM) were added to the medium to interrupt the solute phase. (e, f) Cell C was first treated with 300 mM DMF. Solute phase of DMF diffusing into the cell was interrupted by adding a DMF solution with a concentration of 150 mM (e), or 50 mM (f), when concentration of DMF in the cell was expected to be 154 mM. There was virtually no difference in $T_{1/2}^{s}$ for all the solute permeabilities measured from the solute phases. The pressure difference ($\Delta P = P_{\text{stop}} - P_{\text{e}}$) was measured after extrapolation (dashed lines) of the solute phase to the time when the interrupting solution was added to calculate P_{stop}.

Typical curves from SF experiments are shown in Fig. 5. In the first example, Cell A was initially treated with 1000 mM acetone, causing an endosmotic response in pressure (solute uptake). After reaching solute flow equilibrium, there was the same concentration of acetone at all points within the cell (1000 mM). When the acetone solution was replaced by APW free of acetone, the acetone permeated out of the cell due to the concentration difference between the cell interior and the medium (C_{s}^{o} was kept at zero). Consequently, an exosmotic pressure curve was produced. During the solute phase, when acetone diffused out of the cell, the internal acetone concentration decreased from 1000 mM. Solute efflux was interrupted at the point where the internal acetone concentration was expected to be $C_{\text{prosp}} = 490$ mM by adding acetone solutions with concentrations of between 125 mM and 785 mM (see Material and Methods section). In Figs. 5a and b, the lowest and highest concentrations in the series are given as examples. Addition of 125 mM produced an undershoot (Fig. 5a) and 785 mM an overshoot (Fig. 5b) in pressure relative to the baseline (P_{o}). Since the pressure/time curve during the solute phase was exponential, the pressure difference ($\Delta P = P_{\text{stop}} - P_{\text{e}}$) was measured after extrapolation of the solute phase to the time when the solution was changed. The values of ΔP were used to determine C_{SF} as the intercept with the abscissa (Fig. 6), as was also done in the simulations (Fig. 3). It should be noted that

during SF experiments, the solute phases following the water exchange had similar $T_{1/2}^s$ as those measured in unchanged biphasic responses (Figs. 5a, b).

In the second example, Cell B was first treated with 600 mM of the less permeating 2-propanol. After replacing the 2-propanol solution with APW, the solute phase was interrupted by the addition of 100 mM (Fig. 5c) or 500 mM (Fig. 5d) of 2-propanol, at $C_{prosp} = 278$ mM. Again, ΔP values were worked out after extrapolation to the point of solution exchange (Figs. 5c, d).

In the last example, Cell C was treated with DMF but the results were presented for an endosmotic SF experiment (solute uptake; Figs. 5e, f). First, 300 mM of DMF was added to the medium, and after it began to diffuse into the cell, the movement was interrupted by adding 150 mM (Fig. 5e) or 50 mM (Fig. 5f) of DMF at a time when $C_{prosp} = 154$ mM. Again, ΔP values were measured after extrapolation to the point of solution exchange (Figs. 5e, f).

Data from the SF experiments were used to plot ΔP versus the external concentration, allowing for the calculation of C_{SF} (Fig. 6). Representative examples of endosmotic SF experiments show the deviation between C_{SF} and C_{prosp} for the three solutes: C_{SF} and C_{prosp} were (i) for acetone, 464 and 490 mM, respectively (Fig. 6a), (ii) for 2-propanol, 272 and 278 mM (Fig. 6b), and (iii) for DMF, 152 and 154 mM (Fig. 6c). Hence, deviations from the prospected values were biggest for the most rapidly permeating solute (acetone), and lowest for the slowly permeating DMF.
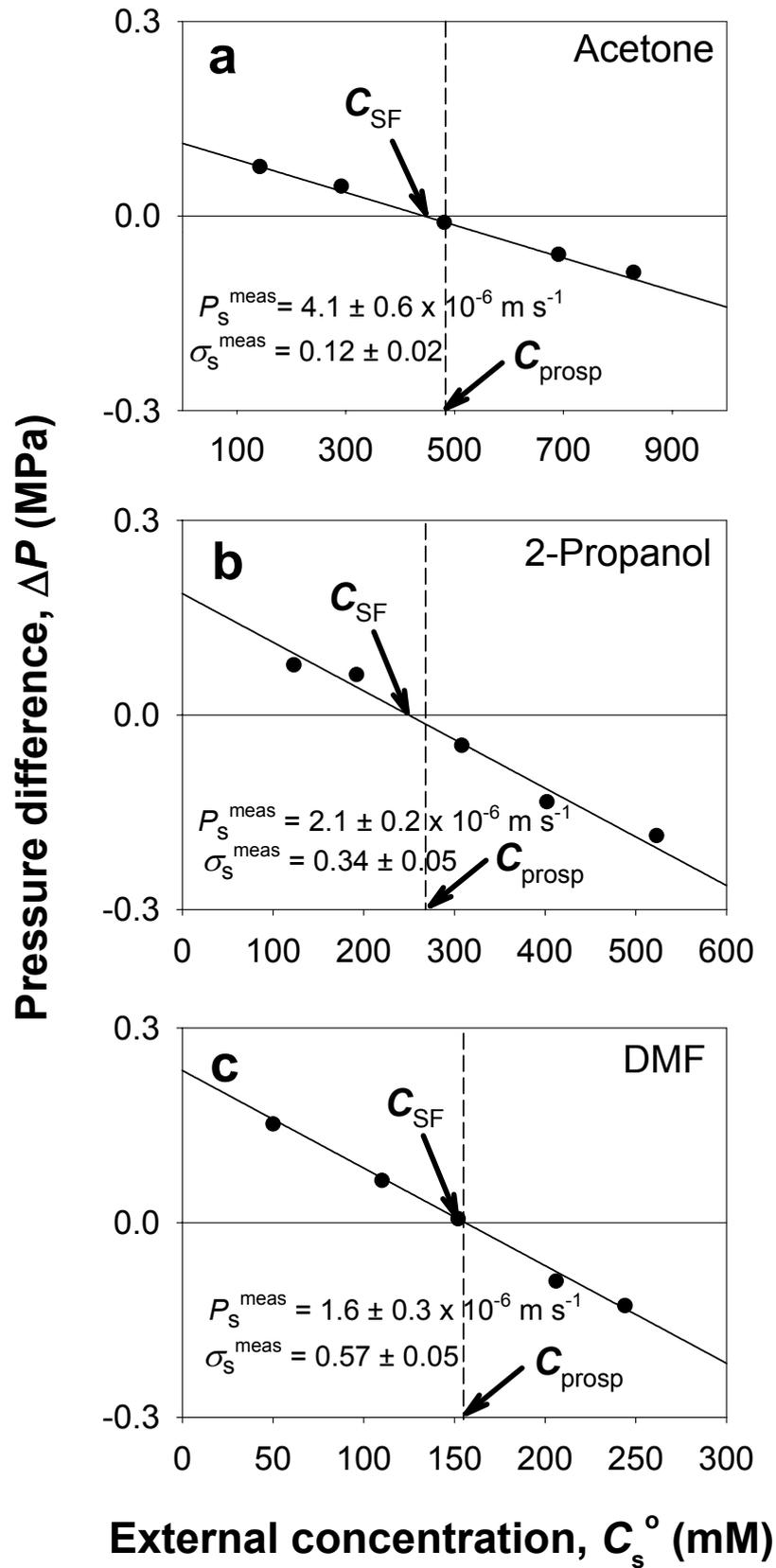
Figure 6. Experimental plots of pressure difference ($\Delta P = P_{stop} - P_e$) measured from SF experiments versus the concentrations of interrupting solution applied (as in Fig. 5). These are representative examples from endosmotic SF experiments. From the intercept with the abscissa, C_{SF} was obtained.

C_{SF} and C_{prosp} were (a) for acetone, 469 and 482 mM, respectively, (b) for 2-propanol, 272 and 278 mM, and (c) for DMF, 152 and 154 mM. The permeability coefficient (P_s^{meas}) and reflection coefficient (σ_s^{meas}) of the three solutes were given as mean ± SD (n = 7 to 12 cells).

To avoid variability between cells, RDCs were measured from SF experiments in repetition. Results are summarized in Fig. 7 (mean ± SD; n = 2 to 3 cells). The values of C_{prosp} were around 500 mM, 300 mM, and 150 mM for acetone, 2-propanol and DMF, respectively. The mean values of RDC decreased for acetone (-13/+11%: endo/exo), 2-propanol (-3/+1%), and DMF (-2/+1%) with a decreasing permeability coefficient of solutes (P_s). This was in agreement with the results obtained during the simulation (± 6% for acetone; ± 2% for 2-propanol; ± 1% for DMF; see results from computer simulations). This indicated that effects of internal USLs differed depending on the P_s of the solute used (see Discussion). Effects were biggest for acetone and smallest for DMF due to the relative importance of USLs (δ^i/D_s) as compared with $1/P_s$ (see the Theory and results from computer simulations section).
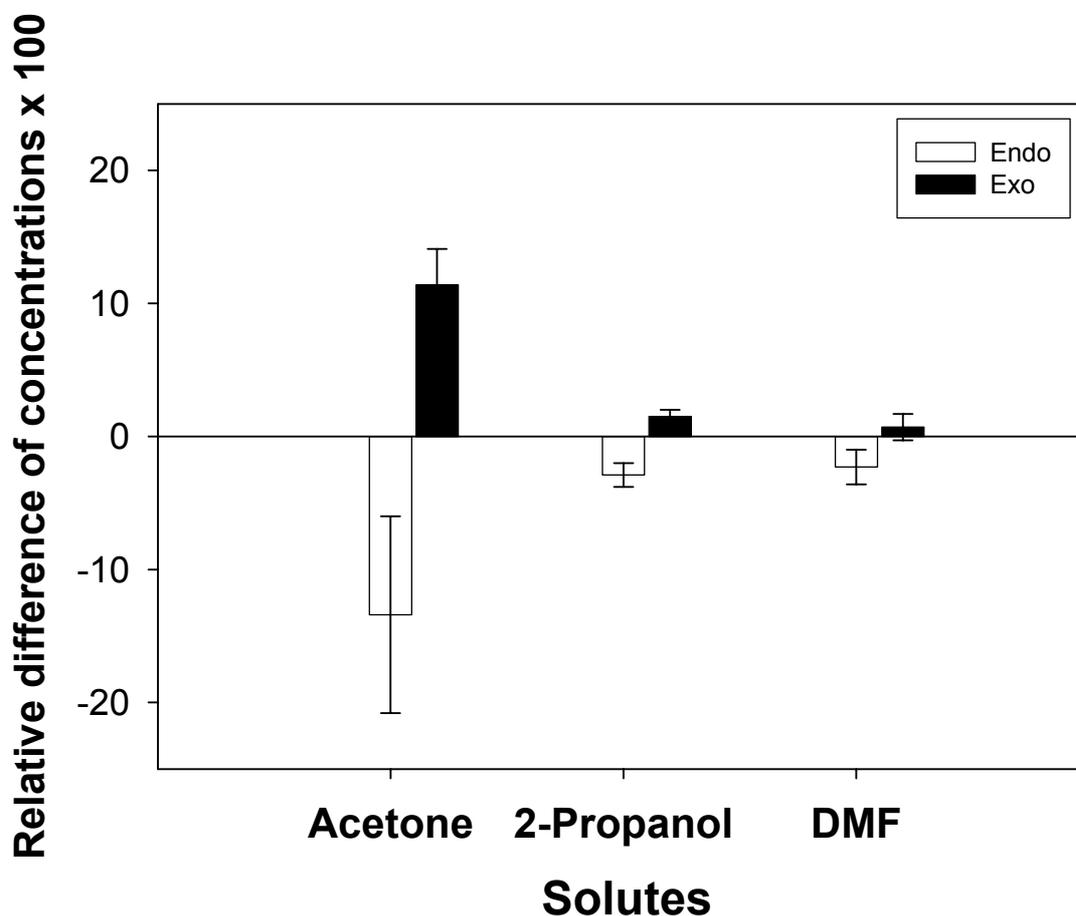
Figure 7. Summary of the relative difference of concentrations (RDC) from the experiments. The mean values of RDC declined with decreasing solute permeability coefficients (P_s). Acetone: -13/+11% (endo/exo); 2-propanol: -3/+1%; DMF: -2/+1%. This data corresponded with the simulation results assuming the stagnant cell interior (mean ± SD; n = 2 to 3 cells).

Discussion

Both the experimental data obtained from stop-flow experiments and the simulations indicated a similar pattern of effects of internal USLs. As the solute permeability of the membrane decreased, the role of internal USLs also decreased. Effects due to internal USLs were only substantial for the most rapidly permeating solute acetone, where the underestimation of P_s was found to be up to 37% according to the results from simulations which refer to a completely stagnant cell interior. When P_s was decreased by a factor of two (2-propanol) or more (DMF), the effects were as small as 19 or 14%, respectively. Permeability coefficients of the solutes used (4.2 to 1.6×10^{-6} m s^{-1}) would be still regarded as rather high when compared with those of nutrient ions, sugars or other metabolites in the cell sap (where values are ranging between 10^{-9} to 10^{-11} m s^{-1}; Nobel, 1999). It is concluded that, in the case of endogenous solutes, the effects of USLs are negligible. However, absolute values of solute permeability play a role during the measurement of the permeability of heavy water (P_d). A comparison between the 'diffusional water permeability, P_d' and the osmotic or hydraulic water permeability (P_f, Lp) is often made to calculate the number of water molecules sitting in AQP pores (N = P_f/P_d; Levitt, 1974; Finkelstein, 1987; Henzler *et al.*, 2004; Ye *et al.*, 2005; Ye *et al.*, 2006; see Introduction). When P_d is underestimated due to the existence of internal USLs, N may be overestimated. The P_d for water is bigger than that of acetone by a factor of two (Henzler *et al.*, 2004; Ye *et al.*, 2006), but this effect may be cancelled by the bigger diffusion coefficient of heavy water as compared with acetone (Ye *et al.*, 2006). Hence, the P_s values derived for acetone are important for predicting the effects of internal USLs during the measurement of the permeability of isotopic water. Overall, the data presented indicate an underestimation of up to 37%

for the most rapidly permeating solutes; a result that coincides with the earlier estimates of Ye *et al*. (2006).

It should be noted that our estimates of the role of internal USLs were based on the most pessimistic assumption, i.e. that the cell interior was completely stagnant. Of course this condition is not true because there would have been some stirring in the cytoplasm due to cyclosis. There would also be some stirring caused by local differences in density (e.g., when concentration gradients of solutes with a density lower than that of cell sap develop in the cell) and the shaking of the internodes while they sit in a turbulent medium during the experiments. Plus, we referred to the permeability of just the PM, but the tonoplast membrane may have also influenced USL formation. However, for *Chara* and other plant cells, the tonoplast is known to be rather permeable for water and solutes and may be incorporated into the PM or internal USLs (Kiyosawa and Tazawa, 1977; Maurel *et al*., 1997). Overall, the idea of a relatively small contribution by internal USLs agrees with the finding of first order kinetics for both the water and solute permeation throughout the pressure/time course of biphasic pressure relaxations as expected from the Steudle/Tyerman theory (Eqn 3). Hence, the present data confirm this older view for the contribution of internal USLs as a function of solute permeability (Fig. 4).

During stop-flow simulations, the assumption of a stagnant cell interior corresponded with experimental findings suggesting that the model was close to reality. The majority of cells behaved as predicted by the model. Results from the present work indicated that the recent estimates of Ye *et al*. (2006) provided an upper limit for the contribution of internal USLs. Clearly, the present data show that the claims made by Tyree *et al*. (2005) that USLs may dominate the permeability of rapidly permeating solutes as measured with the pressure probe, are wrong. These authors claimed that the diffusional resistance across external and internal USLs would be larger by up to a factor of five than that across the PM. As already discussed extensively by Ye *et al*. (2006), Tyree *et al*. (2005) were misled to this conclusion by several incorrect assumptions about pressure probe experiments as well as by some misunderstandings concerning the physics underlying USL concepts.

The stop-flow technique produced a parameter, RDC that was used to quantify the effect of internal USLs on the solute permeability measurements. Comparisons of RDC values obtained by simulation with those obtained in experiments suggested that the inside of the cell was nearly stagnant. Both SF simulations (assuming stagnant conditions) and experiments revealed similar differences in the prospected internal concentration and the concentration right at the membrane as simulated/measured at the RDC (Figs. 4 and 7). This means that the model used during simulations was fairly realistic, assuming stagnant conditions. This may indicate that the mixing by cytoplasmic streaming was smaller than one may assume. However, cytoplasmic streaming should affect the solute concentration close to the PM, which is important during osmotic water flow and can, in turn, determine the turgor pressure measured by the CPP. Hence, the inclusion of cytoplasmic streaming into the simulation models is, perhaps, necessary in a future refinement of simulation models. Since stagnant conditions appeared to be a realistic approach, effects of local changes in density, and the shaking cells within the turbulent external solution may be smaller than expected (Stevenson *et al*. 1975).

The simple comparison of shapes of measured biphasic pressure/time curves (Fig. 1) with simulations, as done by Tyree *et al*. (2005), cannot be used to elucidate the effects of USLs. It has limitations because there are too many unknown factors to be considered in order to obtain a perfect fit between the measured biphasic curve and simulated one. The water phase of the osmotic curve was the critical zone necessary for a good fit. In the experiment, the Lp should have decreased as the concentration applied to the cell increased (Ye *et al*., 2004). However, the exact function of Lp with regards to the concentration is not clear yet, therefore it is hard to be incorporated. In addition, the instantaneous solution exchange in the external media was not possible experimentally and it has to be considered if one intends to get perfect fitting curves. In the simulation, choosing the correct Lp and considering a non-instantaneous media exchange would greatly change the shape of the water phase in the biphasic osmotic curve. This was overlooked by Tyree *et al*. (2005). In contrast to their curve fitting

approach, the SFT has the advantage that it is free from these problems. The resulting solute concentration profile in the cell is virtually free from the changes in Lp.

In the past, effects of internal USLs, such as those investigated here for *Chara* internodes, have also been discussed for plant tissues such as roots (Steudle and Frensch, 1989; Ye and Steudle, 2006). In roots, the endodermis should be the main osmotic barrier where both diffusional USLs and concentration polarization effects may play a role (sweep away; Dainty, 1963; Steudle and Frensch, 1989). Different from the *Chara* internode, effects of USLs in roots may be more pronounced because the diffusive mobility of solutes such as nutrient ions in the root apoplast may be substantially smaller than in bulk solution. Furthermore, the thickness of USLs may be bigger than in *Chara*, and even as big as the entire thickness of the cortex or the radius of the stele (Steudle and Frensch, 1989). Experiments are underway to experimentally determine the effects of USLs in young corn roots using the root pressure probe. In parallel to this, the effects are simulated in analogy to the SF experiments of this paper.

In conclusion, the new SFT used in the current study to quantitatively elucidate the contribution of internal USLs on the measurement of solute permeability in *Chara*, revealed that the effects are lower than previously estimated. Even in the presence of a rapidly permeating test solute (acetone) and assuming a completely stagnant cell interior, the underestimation was no bigger than 37%. A similar figure may be obtained for heavy water. Both the simulation and experimental results obtained by the new SFT indicated estimates of the contribution of USLs similar to those predicted earlier by Ye *et al.* (2006). Recent simulations on the effects of USLs in *Chara* by Tyree *et al.* (2005) are false because of erroneous assumptions and physical mistakes. Since the ratio between the permeability of the PM of *Chara* and diffusion coefficient of acetone in the water is similar to that of heavy water, the data are of importance for the measurement of diffusional permeability (P_d; isotopic water), which is used to estimate the volume of AQPs by comparison of P_d with bulk flow permeability (P_f, Lp).

Acknowledgements

References

Abbot MB, Basco DR. 1990. Computational fluid dynamics, an introduction for engineers. Harlow Essex, UK: Longman Scientific & Technical.

Barry PH, Diamond JM. 1984. Effects of unstirred layers on membrane phenomena. *Physiological reviews* **64,** 763–872.

Dainty J. 1963. Water relations of plant cells. *Advances in Botanical Research* **1,** 279–326.

Finkelstein A. 1987. Water movement through lipid bilayers, pores and plasma membranes. Theory and reality. *Distinguished lecture series of the Society of General Physiologists*, Vol. 4. New York, USA: Wiley.

Henzler T, Steudle E. 1995. Reversible closing of water channels in *Chara* internodes provides evidence for a composite transport model of the plasma membrane. *Journal of Experimental Botany* **46,** 199–209.

Henzler T, Steudle E. 2000. Transport and metabolic degradation of hydrogen peroxide: model calculations and measurements with the pressure probe suggest transport of H_2O_2 across water channels. *Journal of Experimental Botany* **51,** 2053–2066.

Henzler T, Ye Q, Steudle E. 2004. Oxidative gating of water channels (aquaporins) in *Chara* by hydroxyl radicals. *Plant Cell and Environment* **27,** 1184–1195.

Hertel A, Steudle E. 1997. The function of water channels in *Chara*: the temperature dependence of water and solute flows provides evidence for composite membrane transport and for a slippage of small organic solutes across water channels. *Planta* **202,** 324–335.

Jost W. 1960. Diffusion in solids, liquids, gases. In: Hutchinson E, Van Rysselberghe P, eds. *Physical Chemistry a series of monographs,* New York, USA: Academic Press.

Kedem O, Katchalsky A. 1958. Thermodynamic analysis of the permeability of biological membranes to nonelectrolytes. *Biochimica et Biophysica Acta* **27,** 229-246.

Kiyosawa K, Tazawa M. 1977. Hydraulic conductivity of tonoplast free *Chara* cells *Journal of Membrane Biology* **37,** 157–166.

Levitt DG. 1974. New theory of transport for cell-membrane pores. 1. general theory and application to red-cell. *Biochimica et Biophysica Acta* **373,** 115-131.

Maurel C, Tacnet F, Güclü J, Guern J, Ripoche P. 1997. Purified vesicles of tobacco cell vacuolar and plasma membranes exhibit dramatically different water permeability and water channel activity. *Proceedings of the National Academy of Sciences USA* **94,** 7103–7108.

Nobel PS. 1999. *Physicochemical and environmental plant physiology*. San Diego, USA: Academic Press.

Rüdinger M, Hierling P, Steudle E. 1992. Osmotic biosensors. How to use a characean internode for measuring the alcohol content of beer. *Botanica Acta* **105,** 3–12.

Schütz K, Tyerman SD. 1997. Water channels in *Chara corallina*. *Journal of Experimental Botany* **48,** 1511-1518.

Sehy JV, Banks AA, Ackerman JJH, Neil JJ. 2002. Importance of intracellular water apparent diffusion to the measurement of membrane permeability. *Biophysical Journal* **83,** 2856–2863.

Steudle E. 1993. Pressure probe techniques: basic principles and application to studies of water and solute relations at the cell, tissue, and organ level. In: Smith JAC, Griffith H, eds. *Water Deficits: Plant Responses from Cell to Community*, Oxford, UK: BIOS. Scientific Publishers, 5–36.

Steudle E, Frensch J. 1989. Osmotic responses of maize roots. Water and solute relations. *Planta* **177,** 281–295.

Steudle E, Henzler T. 1995. Water channels in plants: do basic concepts of water transport change? *Journal of Experimental Botany* **46,** 1067-1076.

Steudle E, Tyerman SD. 1983. Determination of permeability coefficients, reflection coefficients and hydraulic conductivity of *Chara corallina* using the pressure probe: effects of solute concentrations. *Journal of Membrane Biology* **75,** 85–96.

Stevenson JF, Von Deak MA, Weinberg M, Schuette RW. 1975. An unsteady state method for measuring the permeability of small tubular membranes. *AIChE Journal* **21,** 1192–1199.

Tyerman SD, Steudle E. 1984. Determination of solute permeability in *Chara* internodes by a turgor minimun method. Effect of external pH. *Plant Physiology* **74,** 464–468.

Tyree MT, Koh S, Sands P. 2005. The determination of membrane transport parameters with the cell pressure probe: theory suggests that unstirred layers have significant impact. *Plant Cell and Environment* **28,** 1475-1486.

Ye Q, Kim Y, Steudle E. 2006. A re-examination of the minor role of unstirred layers during the measurement of transport coefficients of Chara corallina internodes with the cell pressure probe. *Plant, Cell and Environment* **29,** 964-980.

Ye Q, Muhr J, Steudle E. 2005. A cohesion/tension model for the gating of aquaporins allows estimation of water channel pore volumes in *Chara. Plant, Cell and Environment* **28,** 525–535.

Ye Q, Steudle E. 2006. Oxidative gating of water channels (aquaporins) in corn roots. *Plant Cell and Environment* **29,** 459-470.

Ye Q, Wiera B, Steudle E. 2004. A cohesion/tension mechanism explains the gating of water channels (aquaporins) in *Chara* internodes by high concentration. *Journal of Experimental Botany* **55,** 449–461.

4   Light and turgor affect the water permeability (aquaporins) of parenchyma cells in the midrib of leaves of *Zea mays*

Yangmin X. Kim and Ernst Steudle

Department of Plant Ecology, Bayreuth University, D-95440 Bayreuth, Germany

Corresponding author: E. Steudle

E-mail: ernst.steudle@uni-bayreuth.de

Fax: +49 921 552564

Abstract

In response to light, water relation parameters (turgor, half time of water exchange, $T_{1/2}$, and hydraulic conductivity, Lp; $T_{1/2} \propto 1/Lp$) of individual cells of parenchyma sitting in the midrib of leaves of intact corn (*Zea mays* L.) plants were investigated using a cell pressure probe. Parenchyma cells were used as model cells for the leaf mesophyll, because they are close to photosynthetically active cells at the abaxial surface, and there are stomata at both the adaxial and abaxial sides. Turgor ranged from 0.2 to 1.0 MPa under laboratory light condition (40 µmol m^{-2} s^{-1} at the tissue level), and individual cells could be measured for up to six hours avoiding the variability between cells. In accordance with earlier findings, there was a big variability in $T_{1/2}$ s measured ranging from 0.5 s to 100 s, but the action of light on $T_{1/2}$ s could be nevertheless figured out for cells having $T_{1/2}$ s of bigger than 2 s. Increasing light intensity ranging from 100 to 650 µmol m^{-2} s^{-1} decreased $T_{1/2}$ by a factor up to five within 10 min and increased Lp by the same factor. In the presence of light, turgor decreased due to an increase in transpiration, and this tended to compensate or even overcompensated for the effect of light on $T_{1/2}$. For example, during prolonged illumination, cell turgor dropped from 0.2 to 1.0 MPa to –0.03 to 0.4 MPa, and this drop caused an increase of $T_{1/2}$ and a reduction of cell Lp, i.e., there was an effect of turgor on cell Lp besides that of light. To separate the two effects, cell turgor (water potential) was kept constant while changing light intensity by applying gas pressure to the roots using a pressure chamber. At a light intensity of 160 µmol m^{-2} s^{-1}, there was a reduction of $T_{1/2}$ by a factor of 2.5 after 10 to 30 min, when turgor was constant within ±0.05 MPa. Overall, the effects of light on $T_{1/2}$ (Lp) were overriding those of turgor only when decreases in turgor were less than about 0.2 MPa. Otherwise, turgor became the dominant factor. The results indicate that the hydraulic conductivity increased with increasing light intensity tending to improve the water status of the shoot. However, when transpiration induced by light tends to cause a low turgidity of the tissue, cell Lp was reduced. It is concluded that, when measuring the overall hydraulic conductivity

of leaves, both the effects of light and turgor should be considered. Although the mechanism(s) of how light and turgor influence the cell Lp is still missing, it may involve the gating of aquaporins by both parameters.

Key-words: Aquaporins, cell pressure probe, hydraulic conductivity, leaf, light, parenchyma cells, turgor, *Zea mays.*

Introduction

There is a lot of evidence that the overall hydraulic conductance of leaves (K_{leaf}) is substantially affected by light, but as yet the mechanisms of changes in K_{leaf} are poorly understood (Nardini *et al.*, 2005; Sack and Holbrook, 2006; Cochard *et al.*, 2007). For example, Lo Gullo *et al.* (2005) showed that leaf conductance was positively correlated with photosynthetically active radiation (PAR) in evergreen and deciduous trees. In lab experiments, Sack *et al.* (2002) demonstrated that K_{leaf} of *Quercus* leaves measured by a high pressure flow meter (HPFM) was bigger under irradiance (> 1200 μmol m^{-2} s^{-1}) than that measured under ambient light condition. Also using the HPFM technique, Tyree *et al.* (2005) observed similar phenomena in six tree species. However, Brodribb and Holbrook (2004) showed midday depressions of K_{leaf} and stomatal conductance of a tropical tree, when the water status was unfavorable.

Although the mechanism(s) of responses of K_{leaf} to irradiance are not yet clear, Tyree *et al.* (2005) used the HPFM to find out why K_{leaf} increased during short-term illumination of 30 min. They excluded a contribution of the stomatal conductance and suspected that the increase in K_{leaf} was due to either changes in the vascular component by hydrogel effects (Zwieniecki *et al.*, 2001), or due to changes in non-vascular components, probably related to water channels (aquaporins, AQPs). There is increasing evidence that AQPs play a key role in plant water relations (Steudle and Henzler, 1995; Maurel, 1997; Kjellbom *et al.*, 1999; Tyerman *et al.*, 1999; Steudle, 2000, 2001; Maurel and Chrispeels, 2001; Javot and Maurel, 2002). Cell water permeability may increase either by *de novo* expression of AQPs or by an opening of

closed channels ("gating"). In roots of *Lotus japonicus* and in leaves of *Samanea saman*, the diurnal changes in hydraulic conductance have been attributed to changes in levels of mRNA encoding for AQPs (Henzler *et al*., 1999; Moshelion *et al*., 2002). In leaves of walnut, the increase in K_{leaf} by light was in accordance with the transcript abundance of two aquaporins and this effect occurred within 30 min (Cochard *et al*., 2007). Aside from the regulation of transcript levels, 30-min-light treatments causing an increase of K_{leaf} are likely to involve the action of AQPs tending to open in response to light treatment (Nardini *et al*., 2005; Tyree *et al*., 2005). However, there have been as yet no direct measurements of changes of the cell hydraulic conductivity caused by irradiance (and possibly by a gating of AQPs by light).

Using overall measurements, there are difficulties in confining the components affected by light. Overall leaf hydraulic conductance in kg H_2O s^{-1} m^{-2} MPa^{-1}, or its inverse, the resistance, has different components. Components are arranged either in series or in parallel such as the resistances of petioles, leaf lamina (consisting of living cells and vascular components), or stomata. At steady state, resistances form a complicated network, and the regulation of individual conductances (resistances) of different components will result in overall changes of leaf hydraulics. In recent studies, it has been proposed that up to 90% of K_{leaf} may be attributed to living tissue (Cochard *et al*., 2004; Nardini *et al*., 2005; Sack *et al*., 2005). As living cells can effectively regulate their water permeability by expression or by a gating of AQPs, living cells could substantially contribute to K_{leaf}. However, the problem with the figures from overall measurements is the reliable quantification of the components that eventually determine K_{leaf}. This conceptual work is still missing. Another item that should be considered in the overall measurements is whether or not experimental conditions are similar to the real. Principal doubts have been raised whether or not leaf conductances measured with the HPFM technique relate to the real situation (Nardini *et al*., 2005). With the HPFM, leaf tissue is usually infiltrated with pressurized water *via* the xylem, filling intercellular spaces so that liquid water is eventually dropping out of stomata or hydathodes. This is not the situation in a transpiring leaf. However, people using the HPFM tended to convince themselves and others that what they measured was meaningful, namely, by comparing their data with those obtained by other techniques

(Sack *et al.*, 2002; Nardini *et al.*, 2005). Brodribb and Holbrook (2006) showed that K_{leaf} would be different, when measured either in the steady state (evaporation technique) or by following transient water uptake (capacitive recharge, relaxation of water potential upon rehydration through the petiole) and discussed that the former method would be a more realistic measure than the latter. These authors discussed the discrepancy in terms of decreases of turgor pressure, which were substantial and immediate, when the evaporation technique was used to measure K_{leaf}. This may indicate an effect of turgor on K_{leaf}.

In the present study, we intended to fill the gap between overall measurements of leaf hydraulics and the molecular level, i.e. direct action of AQPs. We used a cell pressure probe (CPP) to do so. At present, the CPP is the most sensitive technique used for measurements of water permeability with intact cells (half time of water exchange, $T_{1/2}$ and hydraulic conductivity, Lp; $T_{1/2} \propto 1/Lp$). It should be emphasized that in this first study we did intend to identify neither the gating of AQPs in leaves in response to light nor its mechanisms. Rather, using a CPP we examined how the permeability of individual cells in the leaves of intact corn plants changed in response to light and discussed whether or not these changes would correlate to what was found at the whole leaf level. The leaf tissue used for the measurements was the midrib of 4- to 8-week-old corn plants, where cells close to vascular bundles could be investigated in response to increasing light intensity (ambient light intensity = 40 μmol m^{-2} s^{-1}, light treatments = 100, 160, or 650 μmol m^{-2} s^{-1}). In the past, the parenchyma cells in the midrib tissue have been shown to be an excellent object for measuring turgor and hydraulics of individual cells over periods of time of up to six hours. This is a pre-requisite for the studies, because it is known that cells from higher plant tissue may substantially vary in their $T_{1/2}$ (Lp) or turgor (Tomos *et al.*, 1981; Westgate and Steudle, 1985; Nonami *et al.*, 1987; Zhu and Steudle, 1991). Measuring effects on individual cells eliminates the variability between cells. Due to their big size, cells were easy to puncture. As they were located in the vicinity of photosynthetically active cells, stomata, and xylem vessels, parenchyma cells from the midrib may be considered as a good model for mesophyll cells from the leaf blade, which are much more difficult to measure over long terms (Frensch and Schulze, 1988).

During the studies, it turned out that, besides light, cell turgor was a variable as well, which may affect cell Lp. Hence, the effects of the two variables had to be separated using a root-pressure chamber to keep the turgor pressure of individual cells constant while varying light intensity. This could not be done in the overall studies mentioned above. The results clearly showed that there were separate effects of light and turgor on $T_{1/2}$ (Lp).

Materials and methods

Plant material

Corn (*Zea mays* L. cv. monitor) plants were grown in a greenhouse of Bayreuth University from caryopses in soil in plastic pots (1.7 L; diameter: 140 mm; depth: 110 mm). Plants were watered daily. Experiments were conducted on 4- to 8-week-old plants that were 0.8 to 1.2 m tall and contained about eight leaves. A maize plant was brought from the greenhouse, and the experimental set up was used as in Wei *et al*. (1999). Fourth or fifth leaves of the plants were used counting from the oldest. Leaf blades were 0.6 to 1 m long. All measurements were made on cells in the midrib region located 100 to 200 mm behind the tip of leaves. At this point, the midrib looked like a half cylinder with a diameter of about 1 mm (Figs. 1A,B). At its convex surface, it contained several parallel vascular bundles, one rather big located in the center of the periphery and five bundles at both sides. Within the centered big bundle, there were two metaxylem vessels, each about 50 μm in diameter (v). There was a group of small tracheary elements between them, and protoxylem elements or protoxylem lacuna in the direction to the adaxial surface. Within the smaller bundles, vessel diameters were around 20 μm. Between bundles, there were stomata at the abaxial side (about 100 per mm^2; Fig.1C). There were also stomata on the adaxial side of midribs (about 45 per mm^2; Fig. 1D). The bulk of the midrib tissue consisted of about five layers of parenchyma cells containing no chlorophyll. These cells were used in experiments.
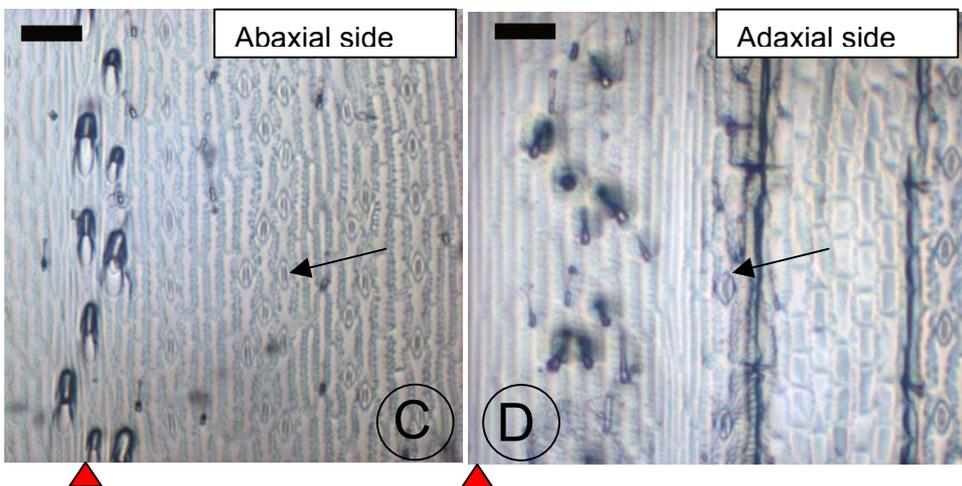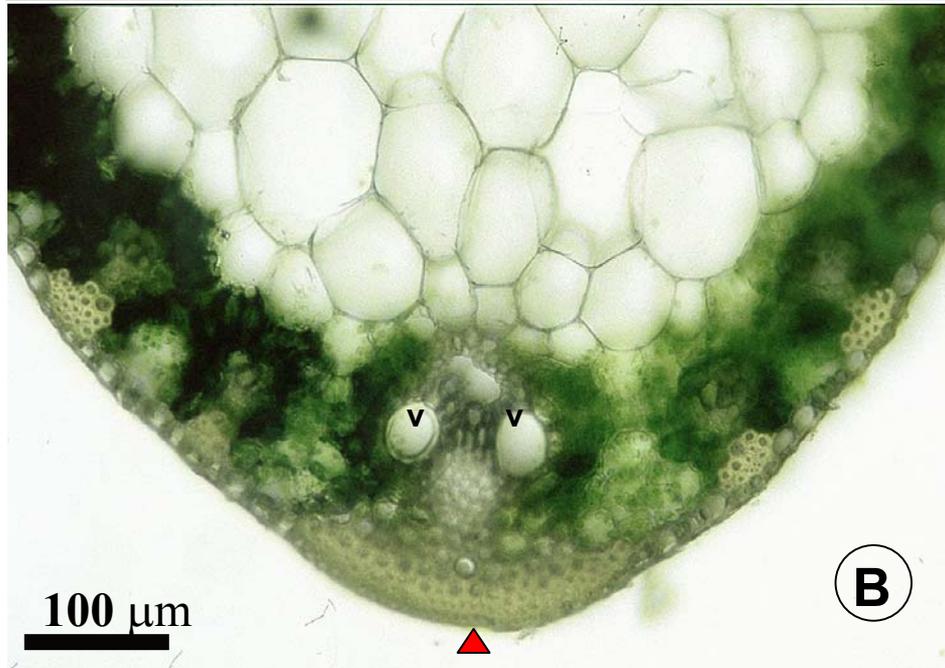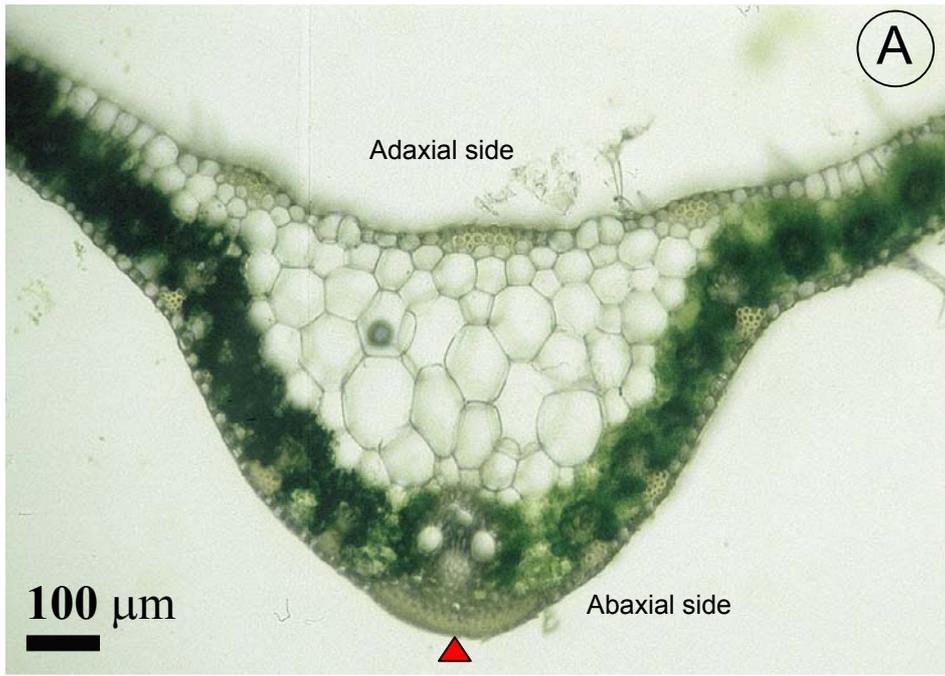
Figure 1. Cross sections and surface patterns of the midrib of a corn leaf. Red triangles indicate the center of the midrib. (A) Section was taken 150 mm from the tip of leaf number four of an 8-week-old plant (counting from the oldest one). The midrib looked like a half cylinder having a diameter of 1 mm. The bulk of the midrib tissue consisted of about 5 layers of achlorophyllous parenchyma cells and in the periphery were one big vein in the center and several smaller veins. Bar = 100 μm. (B) Part of (A) showing that the big vein has two large metaxylem vessels (v). Water relation parameters were determined using a CPP for cells, which were usually in the second layer of parenchyma cells, counting from the abaxial surface. It be can seen from the figure that there was some variability in the diameters of cells (see Table 1). (C) Imprint (obtained with nailpolish) of the abaxial side of the leaf. The abaxial side had about 100 stomata per mm^2 leaf surface. Bar = 100 μm. (D) The surface replica of adaxial side showed about 45 stomata per mm^2 leaf surface. Bar = 100 μm. Arrows indicate guard cells.

The position of parenchyma cells used was estimated from the depth of microcapillary tip inside the midrib tissue. The depth was 100 to 250 μm from the abaxial surface of the midrib (and stomata). The cells used were usually of the second layer of parenchyma cells, when counting from the abaxial surface. They were about 100 μm away from the vessels and 50 μm away from photosynthetically active tissue.

Experimental setup using a CPP

The cell pressure probe was mounted on a Leitz manipulator (Wetzler, Germany) that was screwed on a thick iron plate and placed on a heavy stone table. Using magnetic bars, an intact leaf was mounted upside down on a metal sledge to securely expose the midrib for measurements of cell hydraulics. Cells in the midrib were punctured using the microcapillary of a CPP, which was filled with silicon oil up to the ≈ 8-μm tip (oil type AS4 from Wacker, Munich, Germany). When cells were punctured, a meniscus formed within the tip between cell sap and oil. With the aid of the probe, the meniscus was gently pushed back to close to the surface of the midrib to restore cell sap volume close to its original value. Turgor pressure (P) was measured by a pressure transducer and recorded by a computer. The function of the CPP has been described in many earlier papers (e.g. Steudle, 1993; Henzler and Steudle, 1995). To investigate the hydraulic conductivity of cell membranes (Lp), hydrostatic relaxations of turgor were induced with pressure differences being less than 0.1 MPa to avoid possible effects by

big pressure pulses ('energy-injection'; Wan *et al.*, 2004). From half times of hydrostatic relaxation ($T_{1/2}$), *Lp* was calculated by:

$$Lp = \frac{V}{A} \times \frac{\ln(2)}{T_{1/2}(\varepsilon + \pi^i)} .$$ (1)

Here, the cell geometry (*V* = volume, *A* = surface area) was measured from cross (Fig. 1) and longitudinal sections (not shown) to work out mean values of *V* and *A*, and π^i is the osmotic pressure of a cell and could be approximated by the turgor pressure measured when transpiration was low under laboratory light condition. The volumetric elastic modulus of the cell (ε) was determined by the change in pressure (*dP*) according to the relative volume change (*dV/V*) by:

$$\varepsilon = V \frac{dP}{dV} \approx V \frac{\Delta P}{\Delta V} .$$ (2)

As summarized in Table 1, the mean ε was calculated as 3.8±3.4 MPa (range: 0.4 to 13 MPa), incorporating the cell volume. Volumes of cells were calculated assuming that they were cylindrical. The average cell volume was 2.4×10^{-13} m^3 (240 pl) with a standard deviation of $\pm 1.2 \times 10^{-13}$ m^3 (±120 pl or ± 50%; Table 1, error propagation considered). Anatomical data and elastic moduli were similar to those given by Westgate and Steudle (1985), who used the same tissue of younger plants of an age of 13 to 17 d. Usually, ε was much bigger than π^i. In most of the cases, $T_{1/2}$ was used as a direct measure of change in cell *Lp*, as ε did not change significantly during measurements with individual cells.

Illumination experiment

In the lab, where the experiments were performed, the light intensity was 5 μmol m^{-2} s^{-1} (temperature = 20-30ºC; RH = 30-60%). In order to run the CPP, an Osram halogen lamp (150 W, Xenophot HLX, Munich, Germany) was used through glass fiber optics (Schott, Mainz, Germany) to illuminate the microcapillary and tissue near the cell punctured at a light intensity of about 40 μmol m^{-2} s^{-1}. After a cell was punctured, half times from hydrostatic relaxations, $T_{1/2}$s, were continuously measured. When for 10 minutes cells had stable $T_{1/2}$s, light was switched on. Using a 400 W mercury vapour lamp (Siemens AG, Frankfurt, Germany), the light intensity at the leaf level was then

changed to different levels by changing the height of the lamp. Following light treatments, measurements of relaxations (Lp) were continued for up to 1.5 hours. During illumination, the lamp was set up above a plant and the plant experienced a gradient of light intensity. The upper part of the plant experienced a somewhat higher light intensity, and light intensity was measured at the point of CPP measurements. Light intensities at the level of a given leaf were varied at stages of 100, 160, or 650 μmol m^{-2} s^{-1} PAR.

Illumination experiments at constant turgor with an employment of a pressure chamber

In order to separate effects of turgor from those of light, a pressure chamber encasing the root was used to keep turgor constant during illumination of 160 μmol m^{-2} s^{-1}. The pot containing the root was sealed in a metal pressure chamber using rubber seals (Wei *et al.*, 1999). Roots were pressurized with pressurized air from a gas tank. Measurements of relaxations (Lp) were continued during light phases.

Measurement of rates of transpiration by a porometer

Following CPP measurements, a steady-state porometer (LI-1600 from LI-COR, Lincoln, Nebraska, USA) was used to measure transpiration (E in mmol m^{-2} s^{-1}), relative humidity (RH in %), and air temperature near the area where CPP measurements were performed. After one hour from the CPP measurements, porometer measurements were conducted using the same time of exposure to light as during the CPP measurements.

Table 1. Dimensions, turgor pressure (P), volumetric elastic modulus (ε), half times ($T_{1/2}$), and hydraulic conductivity (Lp) of leaf parenchyma cells of the second layer counting from the abaxial surface at a distance of 100-200 mm from the leaf tip (means ±SD). Lp values were calculated for the smallest and largest half times measured.

| Measurements	
Cell dimensions	
Diameter (µm)	63±19 (n=59 cells, 3 plants)
Length (µm)	76±20 (n=56 cells, 3 plants)
Volume (10^{-13} m^3)	2.4±1.2
Water relation parameters	
Stationary turgor pressure (P; MPa)	0.2–1.0, 0.5±0.2 (n=74 cells)
Volumetric elastic modulus (ε, MPa)	0.4-13, 3.8±3.4 (n=41 cells)
(ε/V; 10^{13} MPa m^{-3})	(1.6±1.2)
Half-time of water exchange ($T_{1/2}$; s)	0.5-95 (n=74 cells)
Hydraulic conductivity (Lp; 10^{-6} m s^{-1}MPa^{-1})	5.1-0.026

Results

Cell turgor pressure of parenchyma cells and its response to light regimes

After introducing the tip of the microcapillary of a CPP into a midrib parenchyma cell, turgor pressure was either getting stable within a few minutes, or there was a transient overshoot in turgor due to the fact that the meniscus had to be pushed close to the surface of the leaf to restore cell volume close to original. In any case, turgor pressure stabilized within 30 min and was measured stable for six hours at maximum. When cells were leaky, turgor continuously dropped, and these cells were disregarded. In

Table 1, turgor pressure values are given for 74 non-leaky cells, which ranged between 0.2 and 1.0 MPa under laboratory light conditions (40 μmol m^{-2} s^{-1} at the tissue level). It can be seen from Table 1 that there was some scatter in the absolute values of turgor, half time, elastic modulus, and cell Lp, which has been known from earlier studies of plant tissues such as the root cortex and leaf epidermis and mesophyll (Tomos et $al.$, 1981; Westgate and Steudle, 1985; Nonami et $al.$, 1987; Zhu and Steudle, 1991).

Following an increase in irradiance, turgor pressure decreased in response to an increased transpiration. A representative response in turgor of a midrib cell to short-term (18 min) illumination is shown in Fig. 2A (light intensity of 100 μmol m^{-2} s^{-1}). According to the figure, there was a delay of about five minutes in the response of turgor, which was due to the time required for opening stomata. When light was switched off, both turgor and transpiration required a time delay of about 10 min to assume their previous values. For the cell given in Fig. 2A, the half time of recovery of turgor ($t_{1/2}$ = 400 s, when fitted exponentially) was similar to that of the decrease in transpiration ($t_{1/2}$ = 390 s) suggesting that transpirational water losses rate-limited changes in turgor. The original turgor pressure was re-attained after about 20 min. During the period of illumination, the surroundings of the measured tissue experienced an increase in temperature of 1.2 ºC and a decrease of RH of 5 %, respectively. The increase in temperature at the leaf surface was 1.4 ºC.

Fig. 2B shows a typical response of a midrib cell, which reduced turgor to a steady value, following an illumination with a duration of 30 min at a light intensity of 160 μmol m^{-2} s^{-1}. Turgor declined to a steady value of close to zero ($t_{1/2}$ = 240 s). During light off, there was a somewhat slower recovery of turgor ($t_{1/2}$ = 440 s). Usually, the time required for recovery was bigger than that for turgor loss during illumination. As seen in Fig. 2B, the minimum steady values of turgor were often close to zero (atmospheric pressure). The same type of recovery was found, even when turgor dropped to pressures of -0.03 MPa (below atmospheric).
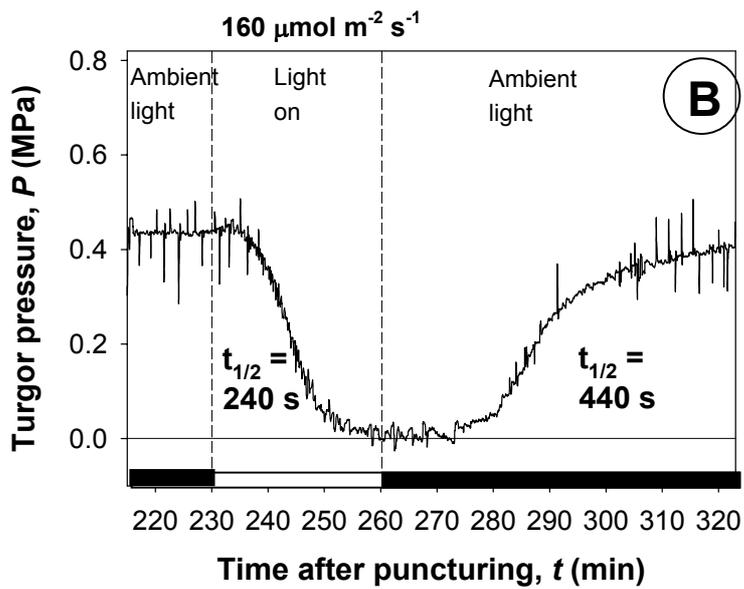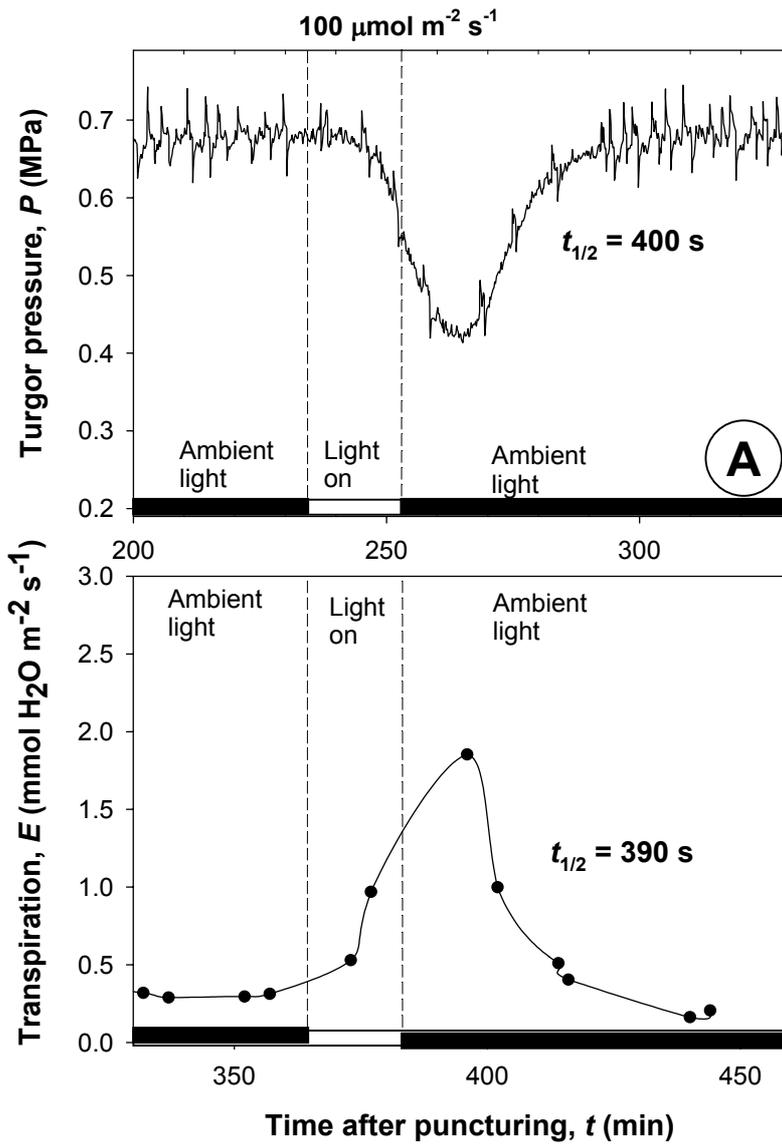
Figure 2. Time course of turgor of two cells measured by a CPP in response to an illumination (vertical dashed lines). The rate of transpiration of the same leaf in (A) was measured at the position of 40 cm from the leaf tip and of 25 cm from the cell punctured. Time zero was the time when cells were punctured. The peaks in the turgor curve are hydrostatic relaxations. (A) During illumination of 100 μmol m^{-2} s^{-1} at the level of a punctured cell, turgor pressure decreased as transpiration increased. When light was again switched off, both turgor and transpiration required a time delay of about 10 min to assume their previous values, probably due to the time needed for a closure of stomata. Half time of recovery of turgor ($t_{1/2}$ = 400 s, when fitted exponentially) was similar to that of the decrease in transpiration ($t_{1/2}$ = 390 s). (B) At a light intensity of 160 μmol m^{-2} s^{-1}, turgor declined to a steady minimum value of close to zero (atmospheric pressure).

Half times of water exchange ($T_{1/2}$*) of parenchyma cells as measured by CPP*

After introducing the tip of the microcapillary of the CPP into a midrib parenchyma cell, half times of hydrostatic relaxations of turgor pressure ($T_{1/2}$) were measured for up to six hours (on average, for three hours). The measured $T_{1/2}$ in 74 cells showed a big range of values of between 0.5 s and 95 s (Table. 1, corresponding Lp values for the smallest and largest half times were 5.1 $\times$ 10^{-6} and 2.6 $\times$ 10^{-8} m s^{-1} MPa^{-1}, respectively). Different from earlier studies on cortical cells of roots of young corn plants (Wan *et al*., 2004), there was no transient increase in $T_{1/2}$ after puncturing, which may have indicated a transient closure of AQPs. Rather, the $T_{1/2}$s of leaf cells varied somewhat with time even in the absence of any treatment, but were stable during periods of 10 to 20 min as verified from the long-term measurements with individual cells (see Discussion). Hence, when measuring effects of light and turgor, we concentrated on these time periods. In this way, we could get rid of the "noise" in $T_{1/2}$. In order to get rid of variations between cells, for statistics changes in $T_{1/2}$ were given as relative rather than absolute values. The half time before illumination was taken as the control half time, $T_{1/2}^{c}$.
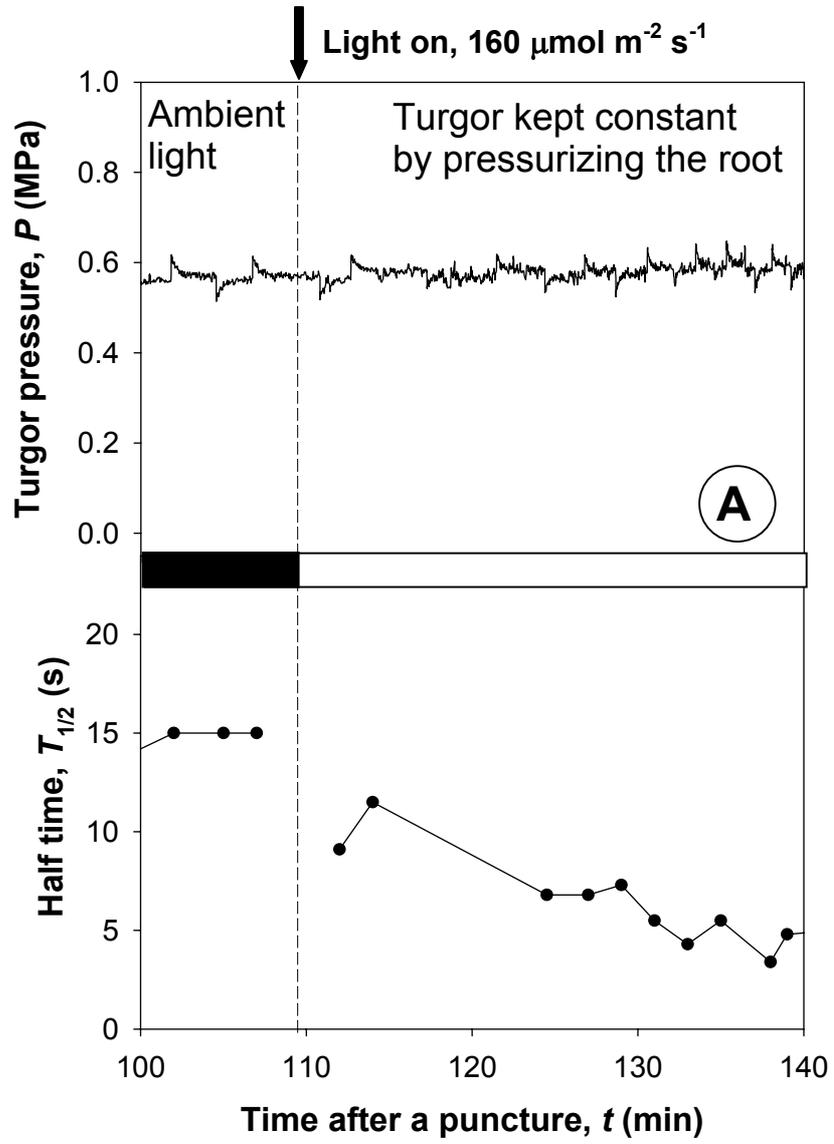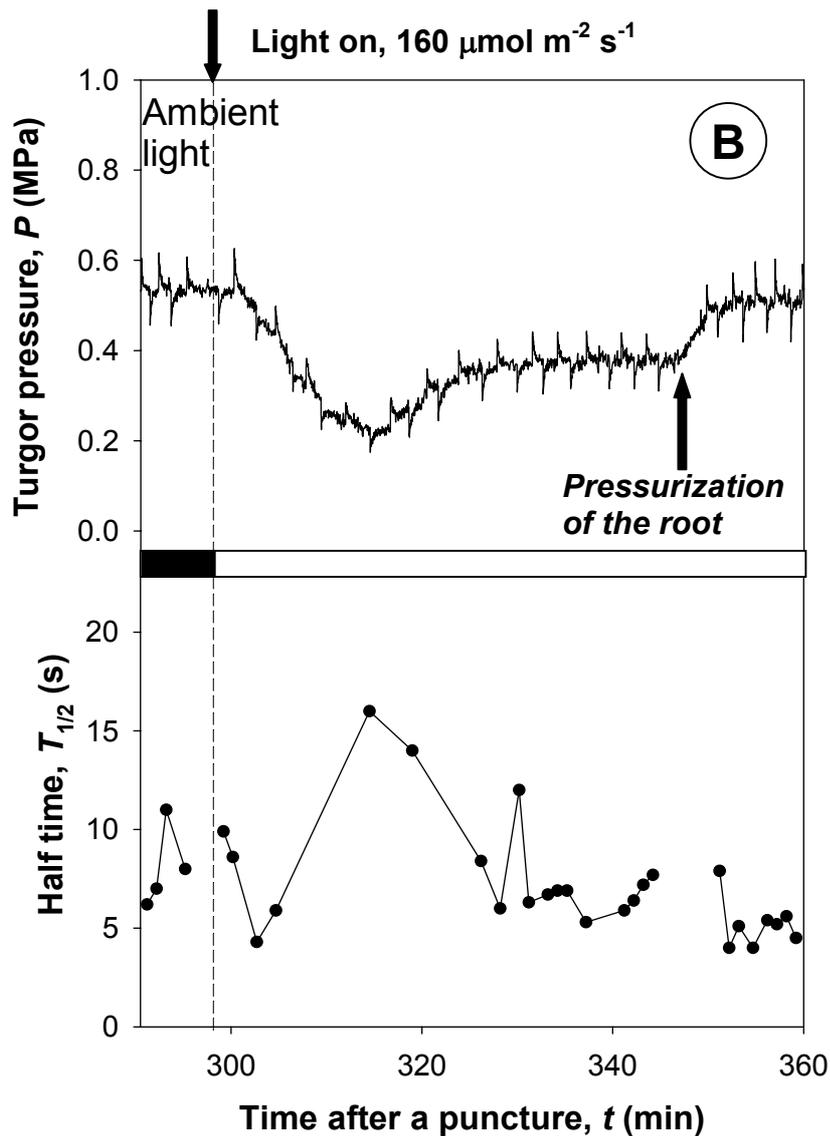
Figure 3. Illumination reduced half time of water exchange, $T_{1/2}$, at constant turgor, but increased $T_{1/2}$ when turgor declined. (A) While turgor was kept constant at 0.55 MPa using a root-pressure chamber, a light intensity of 160 μmol m^{-2} s^{-1} caused a decrease in $T_{1/2}$ by a factor of about three in 30 min and Lp increased by the same factor. (B) During illumination of 160 μmol m^{-2} s^{-1}, $T_{1/2}$ first decreased but increased again as turgor pressure decreased to a low value of 0.2 MPa. There was an increase in turgor during illumination and it caused an ameliorative effect on $T_{1/2}$. When turgor pressure was increased back to the original using the root-pressure chamber during a light phase, there was the same effect on $T_{1/2}$. Time zero was the time when cells were punctured. The peaks appearing in the turgor curve are hydrostatic relaxations.

Effects of light on $T_{1/2}$ *of parenchyma cells*

(1) Effects of light on $T_{1/2}$ at constant turgor

During illumination, the effect of light could have been masked by the effect of turgor, which may have resulted in an increase of $T_{1/2}$ as turgor decreased. Therefore, turgor was kept constant using a root-pressure chamber to solely refer to effects of light. As seen in Fig. 3A, there was an effect of light, which was independent of that of turgor. When keeping turgor constant, $T_{1/2}$ decreased by a factor of 3 within 30 min at a light intensity of 160 μmol m^{-2} s^{-1} (increase of cell *Lp*; Eqn. 1). The results of this type of experiment are summarized in Fig. 4 (see below).
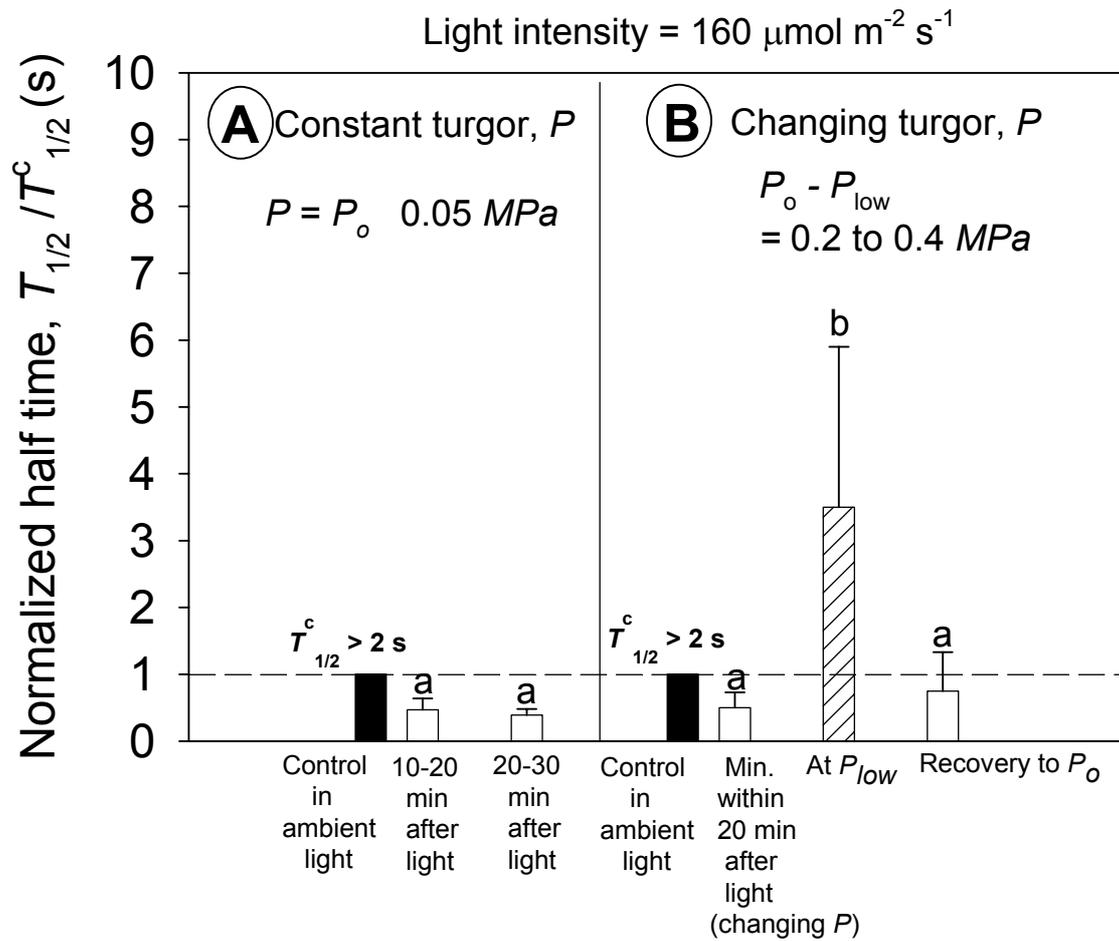
(2) Effects of changes in turgor on $T_{1/2}$

According to Fig. 2, light of 100 and 160 μmol m^{-2} s^{-1} caused substantial decreases in turgor of bigger than 0.2 MPa. The latter could have affected $T_{1/2}$, in addition to the light. As seen in Fig. 3B, during longer periods of illumination at a light intensity of 160 μmol m^{-2} s^{-1}, $T_{1/2}$ first decreased. However, at the low turgor, $T_{1/2}$ increased in spite of illumination, i.e., the effect of turgor was overriding that of light. The turgor increased again without pressurizing the root, and this sometimes happened, perhaps, by an improved water supply from the root in response to a demand from the shoot (variable root hydraulics; Kramer and Boyer, 1995; Steudle and Peterson, 1998). Transient changes of turgor in response to light showing undershoots have been also observed by Frensch and Schulze (1988) in their study on the effects of light on turgor of individual mesophyll and epidermis cells of leaves of *Tradescantia virginiana*. In the present study, when turgor pressure increased back to the original value using the root-pressure chamber, the $T_{1/2}$ recovered to the original during a light phase (Fig. 3B). Changes of $T_{1/2}$ should have reflected changes in cell *Lp* rather than changes in the elastic modulus of cells (ε, Eqn. 1), because ε remained constant during these experiments with individual cells (data not shown).

Overall, the experiments shown in Figs. 3 indicated that $T_{1/2}$ decreased by light, but there was an effect of turgor as well (see Discussion). Results of experiments such as

those shown in Fig. 3 are summarized in Fig. 4. Here, responses of $T_{1/2}$ to light of 160 µmol m^{-2} s^{-1} were compared either at constant turgor or at changing turgor. When turgor was kept constant within ±0.05 MPa, light significantly reduced $T_{1/2}$ by a factor of 2.2 within 10 min and of 2.6 within 30 min (statistics with cells of $T_{1/2}^c > 2$ s; n = 6 cells). However, in the presence of decrease in turgor bigger than 0.2 MPa, $T_{1/2}$ first reduced, but when turgor had changed, usually when reaching at the minimum turgor, there were re-increases in $T_{1/2}$ by a factor of as large as 4 compared to $T_{1/2}^c$ (n = 6-11 cells). Depending on the individual cells, re-increase of $T_{1/2}$ happened between 10 to 25 min after light was turned on. When turgor was increased back under the irradiance, $T_{1/2}$ recovered to the value as small as 75 % of $T_{1/2}^c$ (n = 4 cells).

(3) Effect of light intensity on $T_{1/2}$

When cells with half times of between 0.5 and 2 s were exposed to light, there was hardly a response in $T_{1/2}$ within 10 min. This may be due to the fact that these cells already had their maximum cell Lp (maximum activity of AQPs; see Discussion). For cells having $T_{1/2}^c$ s of larger than 2 s, illumination of leaves resulted in a decrease of $T_{1/2}$ by a factor of two to five within 10 min depending on light intensity. Results are summarized in Fig. 5. At light intensities of 100, 160, and 650 µmol m^{-2} s^{-1}, $T_{1/2}$ s decreased in 10 min to 54, 40, and 17 % of $T_{1/2}^c$, respectively (statistics with cells of $T_{1/2}^c > 2$ s; t-test; p < 0.05; n = 14, 15, 5 cells, respectively), i.e. higher light intensities induced significant increases of cell Lp. In the results presented in Fig. 5, we included those cells, where decreases in turgor were up to 0.2 MPa during 10 min of illumination. Hence, the conclusion about significant effects of light and that they increase with increasing intensity is safe, because decreases in $T_{1/2}$ would have been even bigger when keeping turgor strictly constant (see above). On the other hand, for cells having $T_{1/2}^c$ smaller than 2 s, the reduction in $T_{1/2}$ during 10 min of illumination was negligible and statistically different from other ratios at any high intensity (t-test; p < 0.05; n = 5 cells).

Figure 4. Summary of effects of illumination either at constant turgor or at changing turgor. In order to get rid of the scatter in $T_{1/2}$ between cells, relative changes in $T_{1/2}$ are given, taking the $T_{1/2}$ before illumination as the reference (control $T_{1/2}^{c}$). For statistics, cells of $T_{1/2}^{c} > 2$ s were considered. (A) At constant turgor, light of 160 μmol m^{-2} s^{-1} caused a reduction in $T_{1/2}$ by a factor of 2.5 during 10 to 30 min. (B) On the other hand, in the presence of a decrease in turgor, $T_{1/2}$ first decreased by a factor of two, however, at a low turgor it increased to the value of bigger than the reduced $T_{1/2}$ and $T_{1/2}^{c}$ by a factor of eight and four, respectively, despite irradiance. Half times recovered when turgor was increased back to the original during a light phase. Mean values $\pm$SD are given for n = 4-11 cells. Different letters on the bars indicate significant difference at p = 0.05 level.

Figure 5. Summary of effects of different light intensities on $T_{1/2}$ within 10 min of illumination. In order to get rid of the scatter in $T_{1/2}$ between cells, relative changes in $T_{1/2}$ within 10 min of illumination are given, taking the $T_{1/2}$ before illumination as the reference (control $T_{1/2}^c$). For cells with $T_{1/2}^c > 2$ s, $T_{1/2}$ values decreased with increasing light intensity (open bars). The cells that had $T_{1/2}^c < 2$ s did not show further reduction in $T_{1/2}$ by light at any intensity (hatched bar). During 10 min of illumination, decrease in turgor was less than 0.2 MPa. Mean values ±SD are given for n = 5-15 cells. Different letters on the bars indicate significant difference at p = 0.05 level.
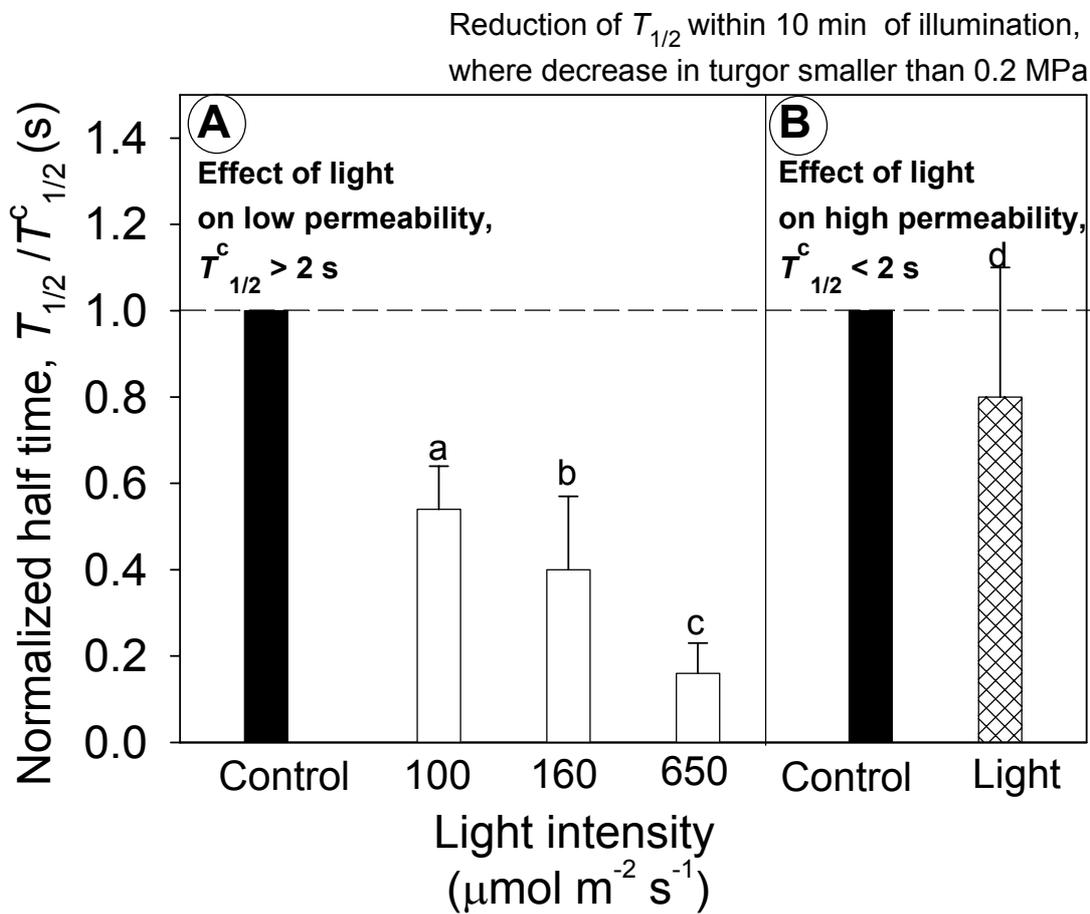
Discussion

For the first time, the data in this study show how the hydraulics of intact corn leaves change at the cell level in response to changes in light intensity (from ambient light intensity of 40 μmol m^{-2} s^{-1} to increased light intensity) and how this interferes with transpiration (turgidity). The midrib parenchyma cells used were close to major vessels in its periphery and the midrib had stomata on both the adaxial and abaxial sides. Cells were located in the vicinity of photosynthetically active cells. Hence, they may be taken as a model system for the mesophyll cells of the leaf blade, which, as yet, cannot be used because they do not allow long-term measurements, as the cells from the midrib do. In an earlier study, Frensch and Schulze (1988) used the Bayreuth pressure probe, to measure turgor and water potential of individual leaf mesophyll and epidermis cells of *Tradescantia virginiana.* They investigated how this would change during illumination and transpiration. However, these authors were not able to measure changes of half times of water exchange of cells, $T_{1/2}$, and cell *Lp* because of problems with keeping those cells on the tip of the probe for a sufficiently long time period. However, upon illumination, they found responses in turgor, which were similar to those presented in this paper.

It may be argued that there was some scatter in the responses of cells when measuring $T_{1/2}$ (*Lp*), and it took about 1 hour to get fairly constant readings to start treatments. The reason for the noise is not known. It was not due to a leakiness of cells, since cells could be measured for up to six hours at constant turgor. When turgor was kept constant at high values with the aid of the pressure chamber, stability improved and this suggested that local changes in the water status around a given cell may play a role (data not shown). One may speculate that, when changing the apoplastic water content near a cell, this should also affect local concentration of ions such as Ca^{2+} or pH, which may affect AQPs (Johansson *et al*., 1996, 1998; Tournaire-Roux *et al*., 2003; Alleva *et al*., 2006). It was clear that the noise was different from what was reported by Wan *et al*. (2004) for cortical cells of corn young roots. In root

cells, there were often transient increases in $T_{1/2}$ after puncturing, which then reduced to small values of $T_{1/2}$, which were stable for several hours. In the root, the transient changes had been referred to a mechanical gating of AQPs, namely, when big changes in water flow occurred such as during pressure relaxations at high peak values of turgor. Different from the root, the 'noise' observed in the leaf appeared to be stochastic. Most of it was circumvented by waiting for stable readings in $T_{1/2}$ before starting treatments. However, despite the noise, the results showed that changes in $T_{1/2}$ due to light and turgor were significant and effects real. Effects of light could be separated from those of turgor.

When separately measuring either the effects of light or turgor by keeping the other variable constant, it was clear that increasing light intensity reduced $T_{1/2}$ and increased *Lp*. On the other hand, reducing turgor increased $T_{1/2}$. The result suggested that, in the intact transpiring plant, both effects interact with each other. For example, high light intensity may tend to intensify the water flow across living tissue, but, as soon as the water status (turgor/water potential) declines, cell *Lp* is reduced, possibly by a closure of AQPs. This seems to be a reasonable response tending to minimize water losses and to keep cells turgid, but there may be other variables in the system, such as the symplastic or apoplastic pH or pCa, which are known to affect AQP activity (Johansson *et al.*, 1996, 1998; Tournaire-Roux *et al.*, 2003; Alleva *et al.*, 2006). It has been known that light changes the pumping of protons and Ca^{2+} (Shabala and Newman, 1999). With the set-up used in this paper, these variables could not be varied in a defined way. Excised leaves could be used to do this and to work out the role of the immediate ionic environment of protoplasts. Such experiments are currently performed. The xylem is perfused with solutions of defined composition, which contain ABA (known to stabilize AQPs; Wan *et al.*, 2004; Lee *et al.*, 2005), or certain values of pH and pCa. It is also intended to use mercuric chloride, which is known to inhibit AQPs. Provided that AQPs were inhibited by light or turgor, there should be no effects of a treatment by $HgCl_2$. Otherwise, there should be an effect. Besides the gating of AQPs, we cannot exclude at present that there are changes in expression of

AQPs in response to light as well. In walnut, this seemed to happen within 30 min (Cochard *et al.*, 2007).

At present, there is no direct proof that changes in cell *Lp* caused by turgor and light were really due to an action of AQPs as suggested at the end of the previous para. However, it is difficult to see how changes in cell *Lp* of more than one order of magnitude could be provided by, for example, changes of the water permeability of the lipid bilayer or those of other transporters (Maurel, 1997; Tyermann *et al.*, 1999). Closure of AQPs in intact plant cells, however, has shown reductions of *Lp* of as large as factors of between 4 and 20 (Henzler and Steudle, 1995, Zhang and Tyerman, 1999; Tyerman *et al.*, 1999; Tyerman *et al.*, 2002; Henzler *et al.*, 2004; Ye and Steudle, 2006). The present result that, at short $T_{1/2}$ and high *Lp*, light could not affect *Lp* anymore, may point into this direction. In this case, virtually all AQPs would have already been open prior to switching on the light.

The immediate effect of light tending to increase cell *Lp* found in this paper is in line with increases of K_{leaf} by light as found in HPFM studies (Sack *et al.*, 2002, Nardini *et al.*, 2005, Tyree *et al.*, 2005). Increases of water permeability of parenchyma cells may contribute to increases in overall K_{leaf} as already suggested by these authors. However, before concluding this, the contribution of parenchyma cells to K_{leaf} should be fully sorted out. This information is still missing. Provided the parenchyma cells were one of the major components of K_{leaf}, the overall leaf hydraulics would have differently responded to light with consideration of decrease in turgor induced by light. In corn root cells, changes in turgor pressure have been suspected to affect water permeability *via* gating of AQPs by what was called a "mechanical gating" (Wan *et al.*, 2004). The present results suggest that effects were somewhat different, i.e., there was different type of 'mechanical action' in the leaf cells in that absolute values of turgor rather than changes of turgor (and the corresponding water flows) were sensed. The decreased turgor induced by light caused an effect opposite to that of light, and this could have decreased K_{leaf}. In this case, it should be again stressed that this would be valid only when parenchyma cells play a substantial role in the leaf hydraulics. As in the present study, some caution is required

before easily concluding about effects of light on cell Lp or AQP activity from overall measurements of K_{leaf}, namely, with the issue related to turgor. It is hard to see how effects of light and turgor could be separated during overall measurements.

The recent review by Sack and Holbrook (2006) summarized data on the effects of light on K_{leaf} of 14 different herbaceous and woody species. The overall result was that K_{leaf} strongly responded to light for many species. One may argue that the response of K_{leaf} by light in corn may totally differ from that of other plants, i.e. not increasing with increasing light intensity. In response to light intensity, K_{leaf} of corn should be measured. However, these measurements would require that turgor is kept constant to avoid interference by this variable. Experimentally, this is not easy, but the problem should be solved in the future. The data on the leaf level, when available, should provide the direct linkage of hydraulics between cell and whole leaf level. Sack and Holbrook (2006) expected diurnal changes of K_{leaf} in such a way that K_{leaf} should increase in response to increasing light and temperature. However, at high rates of transpiration K_{leaf} should decline as the water potential and turgidity decreases. Using a steady state evaporation technique, Brodribb and Holbrook (2006) reported that K_{leaf} decreased in proportion to decreasing cell turgor in 16 out of the 19 species investigated. The authors suggested that hydraulic conductivity of living cells were affected by decreasing turgor, as shown here for cells of corn leaves. Responses of K_{leaf} and cell Lp to light should be only compared under the same experimental conditions including cell turgor. Otherwise, one may produce quite variable and, in part, contradictory results.

The high variability of cell Lp measured could have been originated not only by the temporal changes in cell Lp, but also by the inhomogeneity of cells in the tissue depending on their position. Water permeability of a parenchyma cell could vary between different cells in a tissue, which may be related to local effects of light, turgidity, or others (such as apoplastic concentrations of ions, see above). The present finding of a high variability of $T_{1/2}$ (Lp) is in line with earlier observations of Westgate and Steudle (1985), who reported an inhomogeneous Lp for the same tissue. According to these authors, the Lp of individual cells varied by a factor of as large as

10 depending on the position. Perhaps, cells may need to have an inhomogeneous *Lp* depending on their location in the tissue. Different from the present paper, Westgate and Steudle (1985) could not make long-term measurements. However, using excised leaves, they did show that cell $T_{1/2}$ (*Lp*) was a crucial parameter determining the propagation of changes of water potential in the tissue in response to changes of pressure in the xylem, which affects the ability of tissue to dampen rapid changes of water potential (pressure) in the xylem. In that context, however, other parameters such as elastic properties of cells and the hydraulic conductivity of the apoplast would have to be considered as well.

A variability of $T_{1/2}$ (*Lp*) of as large as a factor of ten was found by Tomos *et al*. (1981) in leaf epidermal cells of *Tradescantia virginiana*, and by Zhu and Steudle (1991) in cortical cells of young corn roots (factor of five depending on cell layer). There was some variability in turgor of tissue cells of stems of soybean (Nonami *et al*., 1987). There was also a variability of cell sizes and ε of as big as a factor of ten in leaf epidermal cells of *Tradescantia virginiana* (Tomos *et al*., 1981). Hence, there can be a substantial variability of water relation parameters when measured at a microscopic scale. This would be evened out when measuring overall parameters (Scholander bomb, psychrometer, HPFM).

In the present study, we investigated effects of relatively low intensities of light on cell *Lp* compared to those in the field. To simulate field conditions, it should be further investigated how cell *Lp* would respond to higher light intensities comparable to those in the field. At relatively high light intensities of up to 2000 μmol m^{-2} s^{-1} encountered in the field, it is curious of how living cells around the xylem will survive under high rates of transpiration (as they do). With very negative xylem pressure, cells may plasmolyze. There is convincing evidence that cells cannot sustain substantial negative turgor pressures, but up to now, there was no direct evidence by direct measurements of turgor of individual cells (Tyree, 1976; Oertli, 1986; Rhizopoulou, 1997; Thürmer *et al*., 1999). It is curious to observe that even at the light intensity, which was lower than that in the field on a sunny day, cells experienced a turgor pressure of lower than

atmospheric. It is not yet clear how plant cells survive at high light intensities, i.e. how they improve their water status. Additional experiments are required to measure cell turgor and $T_{1/2}$ (Lp) under conditions of high rates of transpiration causing substantial tensions in the xylem. There may be an interplay of variable water supply from roots, stomata, turgor, and Lp to orchestrate a water status that is favorable to the plant (Kramer and Boyer, 1995; Franks *et al*., 2007).

In conclusion, this detailed study of the hydraulics of parenchyma cells of leaves of intact plants, which are close to xylem vessels and stomata, revealed big ranges of water permeability (and $T_{1/2}$) of the cells. Despite some noise and variability in the hydraulics of cells, long-term measurements (up to six hours for an individual cell) indicated that increasing light intensity increased cell Lp. Turgor had an ameliorative effect as well. Using a root-pressure chamber, both effects could be separated from each other. Illuminating the leaves while keeping turgor constant increased cell Lp by a factor of three within 30 min at a light intensity of 160 μmol m^{-2} s^{-1}. Without keeping turgor constant, effects of light on cell Lp was compensated or even overcompensated by a decrease in turgor induced by an increase in transpiration. It is concluded that, without separating the effects of light and turgor, the results from measurements of overall leaf hydraulics (K_{leaf}) should be interpreted with caution. Although effects of light and turgor on cell Lp are probably related to a gating of AQPs, mechanism(s) of the action of light and turgor are not yet clear.

Acknowledgements

References

Alleva K, Niemietz CM, Sutka M, Maurel C, Parisi M, Tyerman SD, Amodeo G. 2006. Plasma membrane of *Beta vulgaris* storage root shows high water channel activity regulated by cytoplasmic pH and a dual range of calcium concentrations. *Journal of Experimental Botany* **57**, 609-621.

Brodribb TJ, Holbrook NM. 2004. Diurnal depression of leaf hydraulic conductance in a tropical tree species. *Plant, Cell and Environment* **27**, 820-827.

Brodribb TJ, Holbrook NM. 2006. Declining hydraulic efficiency as transpiring leaves desiccate: two types of response. *Plant, Cell and Environment* **29**, 2205-2215.

Cochard H, Nardini A, Coll L. 2004. Hydraulic architecture of leaf blades: where is the main resistance? *Plant, Cell and Environment* **27**, 1257-1267.

Cochard H, Venisse J-S, Barigah TS, Brunel N, Herbette S, Guilliot A, Tyree MT, Sakr S. 2007. Putative role of aquaporins in variable hydraulic conductance of leaves in response to light. *Plant Physiology* **143**, 122-133.

Franks PJ, Drake PL, Froend RH. 2007. Anisohydric but isohydrodynamic: seasonally constant plant water potential gradient explained by a stomatal control mechanism incorporating variable plant hydraulic conductance. *Plant, Cell and Environment* **30**, 19-30.

Frensch J, Schulze ED. 1988. The effect of humidity and light on cellular water relations and diffusion conductance of leaves of *Tradescantia virginiana* L. *Planta* **173**, 554-562.

Henzler T, Steudle E. 1995. Reversible closing of water channels in *Chara* internodes provides evidence for a composite transport model of the plasma membrane. *Journal of Experimental Botany* **46**, 199–209.

Henzler T, Waterhouse RN, Smyth AJ, Carvajal M, Cooke DT, Schäffner AR, Steudle E, Clarkson DT. 1999. Diurnal variations in hydraulic conductivity and root pressure can be correlated with the expression of putative aquaporins in the root of *Lotus japonicus*. *Planta* **210**, 50-60.

Henzler T, Ye Q, Steudle E. 2004. Oxidative gating of water channels (aquaporins) in *Chara* by hydroxyl radicals. *Plant, Cell and Environment* **27**, 1184-1195.

Javot H, Maurel C. 2002. The role of aquaporins in root water uptake. *Annals of Botany* **90**, 301-313.

Johansson I, Larsson C, Ek B, Kjellbom P. 1996. The major integral proteins of spinach leaf plasma membranes are putative aquaporins and are phoshorylated in response to Ca^{2+} and apoplastic water potential. *The Plant Cell* **8**, 1181-1191.

Johansson I, Karlsson M, Shukla VK, Chrispeels MJ, Larsson C, Kjellbom P. 1998. Water transport activity of the plasma membrane aquaporin PM28A is regulated by phosphorylation. *The Plant Cell* **10**, 451-459.

Kjellbom P, Larsson C, Johansson I, Karlsson M, Johanson U. 1999. Aquaporins and water homeostasis in plants. *Trends in Plant Science* **4**, 308-314.

Kramer PJ, Boyer JS. 1995. *Water relations of plants and soils*. San Diego, California: Academic Press.

Lee SH, Chung GC, Steudle E. 2005. Low temperature and mechanical stresses differently gate aquaporins of root cortical cells of chilling-sensitive cucumber and -resistant figleaf gourd. *Plant, Cell and Environment* **28**, 1191-1202.

Lo Gullo MA, Nardini A, Trifilo P, Salleo S. 2005. Diurnal and seasonal variations in leaf hydraulic conductance in evergreen and deciduous trees. *Tree physiology* **25**, 505-512.

Maurel C. 1997. Aquaporins and water permeability of plant membranes. *Annual Review of Plant Physiology and Plant Molecular Biology* **48**, 399-429.

Maurel C, Chrispeels MJ. 2001. Aquaporins. A molecular entry into plant water relations. *Plant Physiology* **125**, 135-138.

Moshelion M, Becker D, Biela A, Uehlein N, Hedrich R, Otto B, Levi H, Moran N, Kaldenhoff R. 2002. Plasma membrane aquaporins in the motor cells of *Samanea saman*: diurnal and circadian regulation. *The Plant Cell* **14**, 727-739.

Nardini A, Salleo S, Andri S. 2005. Circadian regulation of leaf hydraulic conductance in sunflower (*Helianthus annuus* L. cv Margot). *Plant, Cell and Environment* **28**, 750-759.

Nonami H, Boyer JS, Steudle E. 1987. Pressure probe and isopiestic psychrometer measure similar turgor. *Plant Physiology* **83**, 592-595.

Oertli JJ. 1986. The effect of cell size on cell collapse under negative turgor pressure. *Journal of Plant Physiology* **124**, 365-370.

Rhizopoulou S. 1997. Is negative turgor fallacious? *Physiologia Plantarum* **99**, 505-510.

Sack L, Holbrook NM. 2006. Leaf hydraulics. *Annual Review of Plant Biology* **57**, 361-381.

Sack L, Melcher PJ, Zwieniecki MA, Holbrook NM. 2002. The hydraulic conductance of the angiosperm leaf lamina: a comparison of three measurement methods. *Journal of Experimental Botany* **53**, 2177-2184.

Sack L, Tyree MT, Holbrook NM. 2005. Leaf hydraulic architecture correlates with regeneration irradiance in tropical rainforest trees. *New Phytologist* **167**, 403-413.

Shabala S, Newman I. 1999. Light-induced changes in hydrogen, calcium, potassium, and chloride ion fluxes and concentrations from the mesophyll and epidermal tissues of bean leaves. Understanding the ionic basis of light-induced bioelectrogenesis. *Plant Physiology* **119**, 1115-1124.

Steudle E. 1993. Pressure probe techniques: basic principles and application to studies of water and solute relations at the cell, tissue and organ level. In: Smith JAC, Griffiths H, eds. *Water deficits: plant responses from cell to community*. Oxford, UK: BIOS Scientific Publishers, 5-36.

Steudle E. 2000. Water uptake by roots: effects of water deficit. *Journal of Experimental Botany* **51**, 1531-1542.

Steudle E. 2001. The cohesion-tension mechanism and the acquisition of water by plant roots. *Annual Review of Plant Physiology and Plant Molecular Biology* **52**, 847-875.

Steudle E, Henzler T. 1995. Water channels in plants: do basic concepts of water transport change? *Journal of Experimental Botany* **46**, 1067-1076.

Steudle E, Peterson CA. 1998. How does water get through roots? *Journal of Experimental Botany* **49**, 775-788.

Thürmer F, Zhu JJ, Gierlinger N, Schneider H, Benkert R, Geßner P, Herrmann B, Bentrup F-W, Zimmermann U. 1999. Diurnal changes in xylem pressure

and mesophyll cell turgor pressure of the liana *Tetrastigma voinierianum*: the role of cell turgor in long-distance water transport. *Protoplasma* 206, 152-162.

Tomos AD, Steudle E, Zimmermann U, Schulze ED. 1981. Water relations of leaf epidermal cells of *Tradescantia virginiana*. *Plant Physiology* 68, 1135-1143.

Tournaire-Roux C, Sutka M, Javot H, Gout E, Gerbeau P, Luu DT, Bligny R, Maurel C. 2003. Cytosolic pH regulates root water transport during anoxic stress through gating of aquaporins. *Nature* 425, 393-397.

Tyerman SD, Bohnert HJ, Maurel C, Steudle E, Smith JAC. 1999. Plant aquaporins: their molecular biology, biophysics and significance for plant water relations. *Journal of Experimental Botany* **50**, 1055-1071.

Tyerman SD, Niemietz CM, Bramley H. 2002. Plant aquaporins: multifunctional water and solute channels with expanding roles. *Plant, Cell and Environment* **25**, 173-194.

Tyree MT. 1976. Negative turgor pressure in plant cells: fact or fallacy? *Canadian Journal of Botany* **54**, 2738-2746.

Tyree MT, Nardini A, Salleo S, Sack L, Omari BE. 2005. The dependence of leaf hydraulic conductance on irradiance during HPFM measurements: any role for stomatal response? *Journal of Experimental Botany* **56**, 737-744.

Wan XC, Steudle E, Hartung W. 2004. Gating of water channels (aquaporins) in cortical cells of young corn roots by mechanical stimuli (pressure pulses): effects of ABA and of $HgCl_2$. *Journal of Experimental Botany* **55**, 411-422.

Wei C, Tyree MT, Steudle E. 1999. Direct measurement of xylem pressure in leaves of intact maize plants. A test of the cohesion-tension theory taking hydraulic architecture into consideration. *Plant Physiology* **121**, 1191-1205.

Westgate ME, Steudle E. 1985. Water transport in the midrib tissue of maize leaves. *Plant Physiology* **78**, 183-191.

Ye Q, Steudle E. 2006. Oxidative gating of water channels (aquaporins) in corn roots. *Plant, Cell and Environment* **29**, 459-470.

Zhang WH, Tyerman SD. 1999. Inhibition of water channels by $HgCl_2$ in intact wheat root cells. *Plant Physiology* **120**, 849-857.

Zhu GL, Steudle E. 1991. Water transport across maize roots – simultaneous measurement of flows at the cell and root level by double pressure probe technique. *Plant Physiology* **95**, 305-315.

Zwieniecki MA, Melcher PJ, Holbrook NM. 2001. Hydrogel control of xylem hydraulic resistance in plants. *Science* **291**, 1059-1062.

5 Gating of aquaporins by light and reactive oxygen species in leaf parenchyma cells in the midrib of *Zea mays*

Yangmin X. Kim and Ernst Steudle

Department of Plant Ecology, Bayreuth University, D-95440 Bayreuth, Germany

Corresponding author: E. Steudle
E-mail: ernst.steudle@uni-bayreuth.de
Fax: +49 921 552564

Number of Figures: 7
Number of Tables: 0

Abstract

Changes of the water permeability of leaf cells were investigated in response to different light regimes (low *vs.* high). Using a cell pressure probe, parenchyma cells in the midrib tissue of corn (*Zea mays* L.) leaves have been investigated to measure hydraulic properties (half time of water exchange, $T_{1/2} \propto 1$/water permeability). A new perfusion technique was applied to excised leaves to keep turgor constant and to modify the environment around cells by perfusing solutions using a pressure chamber. In response to low light (LL) of 200 µmol m^{-2} s^{-1}, $T_{1/2}$ decreased during the perfusion of a control solution of 0.5 mM CaCl$_2$ by a factor of two. This was in line with earlier results from leaf cells of intact corn plants at a constant turgor. By contrary, high light (HL) at intensities of 800 and 1800 µmol m^{-2} s^{-1} increased $T_{1/2}$ in two third of cells by factors of 14 and 35, respectively. Effects of HL on $T_{1/2}$ were similar to those caused by H$_2$O$_2$ treatment in the presence of Fe^{2+}, which produced OH* (Fenton reaction; reversible oxidative gating of aquaporins as shown by Henzler *et al.*, 2004). Treatments of 20 mM H$_2$O$_2$ following Fe^{2+} pre-treatments increased $T_{1/2}$ by a factor of 30. Those increased $T_{1/2}$ could be partly recovered, either when perfusion solution was changed back to the control or when LL was applied. The antioxidant glutathione reversed HL effects as well. These data suggest that HL could induce reactive oxygen species (ROS) such as OH*, and they affected water relations. The results provide evidence that varying light climate adjusts water flow at cell level, i.e. water flow is maximised at a certain light intensity and then reduced again at HL. They are discussed in terms of an oxidative gating of aquaporins by ROS.

Key words: aquaporin, cell pressure probe, glutathione, hydraulic conductivity, hydrogen peroxide, light, oxidative gating, , reactive oxygen species, *Zea mays.*

Introduction

Plants experience various regimes of light intensity, which is an important issue during photosynthesis. In response to light, stomata open to fix carbon diffusing in as CO_2 through stomata, and plants lose substantial amounts of water using the same pathway. Therefore, plants developed strategies to efficiently manage the use of water in response to changes in the light regime. It has been shown that the overall hydraulic conductance of leaves is affected by light (Sack *et al.*, 2002; Lo Gullo *et al.*, 2005; Nardini *et al.*, 2005; Tyree *et al.*, 2005; Sack and Holbrook, 2006; Cochard *et al.*, 2007). In part, this could have happened either by a change of the conductance of the vascular system (Zwieniecki *et al.*, 2001) or by changes of water permeability of the living cells of xylem parenchyma or bundle sheath (cell *Lp*; Nardini *et al.*, 2005; Tyree *et al.*, 2005). The change in cell *Lp* in response to light was speculated *via* a gating of water channel activity sitting in the cell membranes (aquaporins, AQPs). However, there has been, to date, no direct evidence of a gating of AQPs by light. According to Cochard *et al.* (2007), the level of AQP transcripts increased in response to light. Kim and Steudle (2007) recently started to fill the gap by measuring changes in cell *Lp* in response to light. In leaf cells of corn, they found that turgor affected cell *Lp* besides the light. To separate effects of light from those of turgor, they kept turgor constant and found that, when light was varied at low absolute values of light intensity, AQP activity increased as light intensity increased, which was in agreement with earlier results obtained at the whole leaf level (see above).

There is increasing evidence that many environmental factors affect AQPs (Steudle, 2000; Maurel and Chrispeels, 2001; Tournaire-Roux *et al.*, 2003; Lee *et al.*, 2005). Light could be one of them. It is plausible that a gating of AQPs by light may involve an oxidative gating of AQP activity (Henzler et al. 2004; Ye and Steudle 2006). As photosynthesis produces O_2 and reduction equivalents, damages by reactive oxygen species may be anticipated by reactions involving the partial or complete reduction of O_2 and the production of reactive oxygen species (ROS such as superoxide, H_2O_2, hydroxyl radical; Foyer and Noctor, 2000; Dietz, 2008). In the *Chara* internode and

corn roots, an oxidative gating of AQPs has been demonstrated by Henzler *et al.* (2004) and Ye and Steudle (2006). These authors showed that AQPs could be closed by H_2O_2/OH^*, and that closure was reversible. According to Aroca *et al.* (2005), the treatment with 100 μM H_2O_2 decreased the root hydraulic conductance in a chilling sensitive, but not in a chilling-tolerant maize genotype. Oxidative gating may be a common response to different kinds of stresses (Pastori and Foyer, 2002; Xiong *et al.*, 2002), and it may provide appropriate adjustments in water relations (Ye and Steudle, 2006).

In the present study, the experiments of Kim and Steudle (2007) have been extended from low to high levels of light intensity to provide further insights into the mechanism(s) of a gating of cell *Lp via* changes of AQP activity. Measured cells were parenchyma cells in the midrib of corn leaves (Westgate and Steudle, 1985; Wei *et al.*, 1999). These cells are (i) located in the vicinity of photosynthetically active cells, stomata and xylem vessels and (ii) easy to puncture due to their big size. (iii) They are also suitable for long-term measurements in single cells (up to six hours), since the midrib tissues could be well fixed, and have been therefore, used as a model system by Kim and Steudle (2007). A cell pressure probe was applied to access cell *Lp*. The perfusion of excised leaves allowed to infiltrate leaf tissue *via* cut xylem vessels to adjust apoplastic concentrations and to apply H_2O_2 and the antioxidant glutathione. Most important, turgor could be kept constant by infiltration, i.e., this variable affecting AQP activity was excluded during light treatments. Different effects of light at two light regimes were investigated (low: up to 650 μmol m^{-2} s^{-1}, high: 800 and 1800 μmol m^{-2} s^{-1}). In response to low light, cell *Lp* increased. High light regimes, however, caused a decrease as did the infiltration of solutions of H_2O_2/OH^*. The data are discussed in terms of gating of AQPs by ROS.

Materials and methods

Plant material

Corn (*Zea mays* L. cv. symphony) plants were grown from caryopses in soil in a greenhouse of Bayreuth University as described in Kim and Steudle (2007). In the lab, where the experiments were performed, the ambient light intensity was around 5 µmol m^{-2} s^{-1} (20~25ºC; RH = 30~60%). Experiments were conducted on 4- to 8-week-old plants, which were 0.8 to 1.2 m tall and had about eight leaves.

The parenchyma cells used in the pressure probe experiments were located in the midrib region 100-200 mm behind the tip of leaves. Cells measured were located at a distance of 100 to 200 µm from the abaxial surface of the midrib i.e. in the same range as those used by Kim and Steudle (2007). They usually contained no chlorophyll, but they were close to photosynthetically active cells (about 50 µm away; see cross section in Fig. 1 of Kim and Steudle, 2007). Third or fourth leaves from the plants were used for experiments. Leaf blades were cut into a length of about 0.3 to 0.4 m. About 40 mm of the leaf tip was cut and removed to enhance the transport through xylem vessels by perfusion.

Experimental setup using a CPP

A Leitz manipulator (Wetzler, Germany) was used to carry a CPP (Kim and Steudle, 2007). It was fixed on a thick iron plate placed on a heavy stone table to minimize vibrations during the CPP measurements. Using magnetic bars, a cut leaf was fixed upside down on a metal sledge to securely expose the midrib for measurements of cell hydraulics. The basal cut end of the leaf was encased in a pressure chamber (Fig. 1), where it was immersed in a solution of defined composition (see below). The microcapillary attached to the CPP was filled with silicone oil (oil type AS4 from Wacker, Munich, Germany). It had a fine tip of up to the ≈ 8 µm in diameter. When midrib cells were punctured, a meniscus formed between cell sap and oil within the tip and tended to move away from the cell. Using the metal rod of the CPP, meniscus was

re-adjusted at a position close to the surface of the midrib. This restored cell sap volume close to its original value. The pressure transducer of the CPP measured turgor pressure (P), which was recorded by a computer. To investigate the hydraulic conductivity of cell membranes (Lp), hydrostatic relaxations of turgor were induced by instantaneously moving the meniscus to another position and keeping it there. To avoid effects by big pressure pulses ('energy-injection'; Wan *et al.*, 2004), peak sizes of hydrostatic relaxations were less than 0.1 MPa. The half times of hydrostatic relaxation, the time periods taken for pressure pulses to reach a half of the original peak ($T_{1/2}$s), were inversely proportional to Lp. Further details of the function of the CPP can be looked up in earlier papers (e.g. Steudle, 1993; Henzler and Steudle, 1995).

Figure 1. Experimental set-up used. A pressure chamber was used to perfuse a leaf tissue at constant turgor pressure during illumination and to provide certain ionic apoplastic environment. The chamber was provided with different solutions, which were infiltrated at a pressure of 0.1-0.2 MPa above atmospheric. When pressurizing the basal cut end of the xylem, guttation droplets appeared at the leaf margin and at the cut surface of the leaf outside of the pressure chamber. A cell pressure probe was used to measure turgor and hydraulic conductivity of a cell (cell Lp). The meniscus between cell sap and silicone oil in the probe was controlled while observing it with a stereomicroscope.

In this study, we used $T_{1/2}$ as a direct measure of changes of *Lp* to reduce the effect of error propagation when calculating *Lp* (Wan *et al.*, 2004; Lee *et al.*, 2005; Ye and Steudle, 2006). This could be accepted, as the volumetric elastic modulus of the cell (ε), which is also a parameter to determine *Lp,* did not change significantly during measurements (Kim and Steudle, 2007). To avoid variations between cells, relative changes of $T_{1/2}$ rather than absolute changes were often compared. Treatments were performed on individual cells. This required to measure hydraulic parameters of a given cell up to 4 h.

Perfusion of leaves with solutions of defined composition (defined apoplastic environment)

The apoplastic environment of cells was varied during treatments, for example, by infiltration of AQP inhibitors. In order to perfuse a leaf tissue at constant turgor pressure during illumination and to provide certain ionic apoplastic environment, the pressure chamber (see above) was provided with different solutions, which were infiltrated at a pressure of 0.1-0.2 MPa above atmospheric. When pressurizing the basal cut end of the xylem, guttation droplets appeared at the leaf margin and at the cut surface of the leaf outside of the pressure chamber. To test how long it took for the perfusion solution to move across the tissue, 70 mM H_2O_2 solution was injected in the chamber. The appearance of H_2O_2 in the other cut end and leaf margins was qualitatively tested with KI and starch solution. Droplets in the midrib of the cut end were collected and added to KI-starch solution and the presence of H_2O_2 in the droplets changed the solution into blue colour. According to the tests, the time required for solution to moved across the tissue and to modify the apoplastic solution was 5 to 20 min, depending on pressure applied to the pressure chamber and resistance in the water pathway of the leaf. During 1h perfusion at 0.2 MPa, the amount of perfusion solution that passed through the leaf tissue was of an order of magnitude which was similar to volume of the excised leaf. Assuming the apoplast was 10% of leaf volume (personal comm. with Kosala Ranathunge, University of Bonn), this was equivalent to 10 times of the volume of apoplast. The perfusion solution could be

exchanged *via* a tube going into the chamber, which could be closed by a valve, when the chamber was pressurized. This allowed to quickly exchange the apoplastic solution and to also change back to the original during measurements with an individual cell. To minimize variability between cells, effects and reversibility could be measured on individual cells.

Illumination experiments

In order to run the CPP experiments, both the microcapillary and tissue near the cell punctured had to be illuminated using an Osram halogen lamp (150-W, Xenophot HLX, Munich, Germany) through glass fiber optics (Schott, Mainz, Germany). The light intensity at the tissue level was about 50 μmol m^{-2} s^{-1}. Half times of hydrostatic relaxations, $T_{1/2}$s were continuously measured after a cell was punctured. Using the glass fiber optics, the light intensity could be increased to values of as big as 200 μmol m^{-2} s^{-1} (low light intensity; LL). Usually, effects of light treatment were measured following changes of $T_{1/2}$. To apply light intensities, which are similar to that in the field during a bright day ($\approx$ 2000 μmol m^{-2} s^{-1}; Nobel, 1999), a screen projector as used for powerpoint presentations (AstroBeamX211 with 200W UHP lamp, A+K, UK) was positioned at distances of 200 to 300 mm from the specimen. This was usually turned for 15 min to produce light intensities of between 800 and 1800 μmol m^{-2} s^{-1} at the tissue level (as regulated by the distance of the light source from the leaf surface; high light; HL). The UV content of the light source (UVA and UVB of spectrum from 290 nm to 390 nm) was measured by a UV light meter (PeakTech, Ahrensburg, Germany). It was verified that the light source contained less UV light (1-2 W m^{-2}) than the sun light measured outside on a bright day (PAR = 1900 μmol m^{-2} s^{-1}, UV = 47 W m^{-2}). Relaxations ($T_{1/2}$) were continuously measured during light and other treatments.

Perfusion solutions

As a control, leaves were perfused with a solution of 0.5 mM CaCl$_2$ solution, which resulted in a constant turgor pressure for at least 4 h in a given cell, even under conditions of high rates of transpiration as they occur at HL. Effects of H$_2$O$_2$ were measured by changing from 0.5 mM CaCl$_2$ to solutions that contained either 20 mM or

70 mM H_2O_2 besides the $CaCl_2$. In the presence of natural levels of Fe^{2+}, this should produce OH* (Fenton reaction: $H_2O_2 + Fe^{2+} = Fe^{3+} + OH^- + OH^*$). In order to enhance the level of OH*, leaves were also perfused with 0.5 mM $CaCl_2$ + 3 mM $FeSO_4$ for 1-2 h, and then perfusion solution was exchanged to 0.5 mM $CaCl_2$ + 20 mM H_2O_2 solution to increase the oxidative stress. To see the recovery from stress treatment, solutions were changed back to 0.5 mM $CaCl_2$. To demonstrate effects of the antioxidant glutathione (GSH), leaves were perfused by 3 mM GSH and 0.5 mM $CaCl_2$, and the perfusion solution was then changed back to the control. The solution containing GSH had a pH of 3.5. Other solutions had a pH of 4.8, which is similar to known apoplastic pH of leaves in different plant species (4.7 – 5.1; Felle and Hanstein, 2007).

Results

Half times of hydrostatic relaxations, $T_{1/2} \propto 1/Lp$

From the pressure relaxations, *Lp* values could be worked out, when elastic moduli (ε) were measured as well. However, in most of the cases half times of hydrostatic relaxations, $T_{1/2}$s (inversely proportional to cell *Lp*) were taken as a measure of cell *Lp* because ε did not change during treatments for a given cell (Kim and Steudle, 2007). In most of the cases, there was no transient effect of puncturing on $T_{1/2}$ (*Lp*) as observed with young corn roots (Wan *et al.*, 2004). When there was such an effect, it was waited for 10 min, which was sufficient to achieve a constant $T_{1/2}$. At the ambient light intensity of 50 µmol m^{-2} s^{-1}, $T_{1/2}$s of cells from leaves infiltrated with 0.5 mM $CaCl_2$ ranged from 0.3 to 35 s (mean = 4.8 s, SD = ±7.7 s, n = 31 cells; Fig. 2). The variability of $T_{1/2}$ was also known in the same tissue of intact corn plants (Kim and Steudle, 2007). However, more than 75% of those cells (24 out of 31 cells with 0.5 mM $CaCl_2$) had $T_{1/2}$s of less than 4 s, and one third of cells had $T_{1/2}$s between 1.0-2.0 s (12 out of 31 cells; Figs. 2 and 3A). Cells infiltrated with 0.5 mM $CaCl_2$/3 mM $FeSO_4$ had similar $T_{1/2}$s to those with 0.5 mM $CaCl_2$ (range= 0.8-17 s; mean = 3.6 s, SD = ±3.8 s, n = 24 cells; 21 out of 24 cells had $T_{1/2}$ less than 4 s; Figs. 2 and 3B). Usually

cells probed from one leaf had similar $T_{1/2}$s. For example, six cells probed from the same leaf had $T_{1/2}$s ranging from 0.9 s to 2.3 s. The big $T_{1/2}$s occasionally measured were observed in a few leaves and they were probably caused by a closure of AQPs, even in the absence inhibitors or HL. Those $T_{1/2}$s could be reduced by light treatments of up to 650 μmol m^{-2} s^{-1}, according to the earlier results of Kim and Steudle (2007).
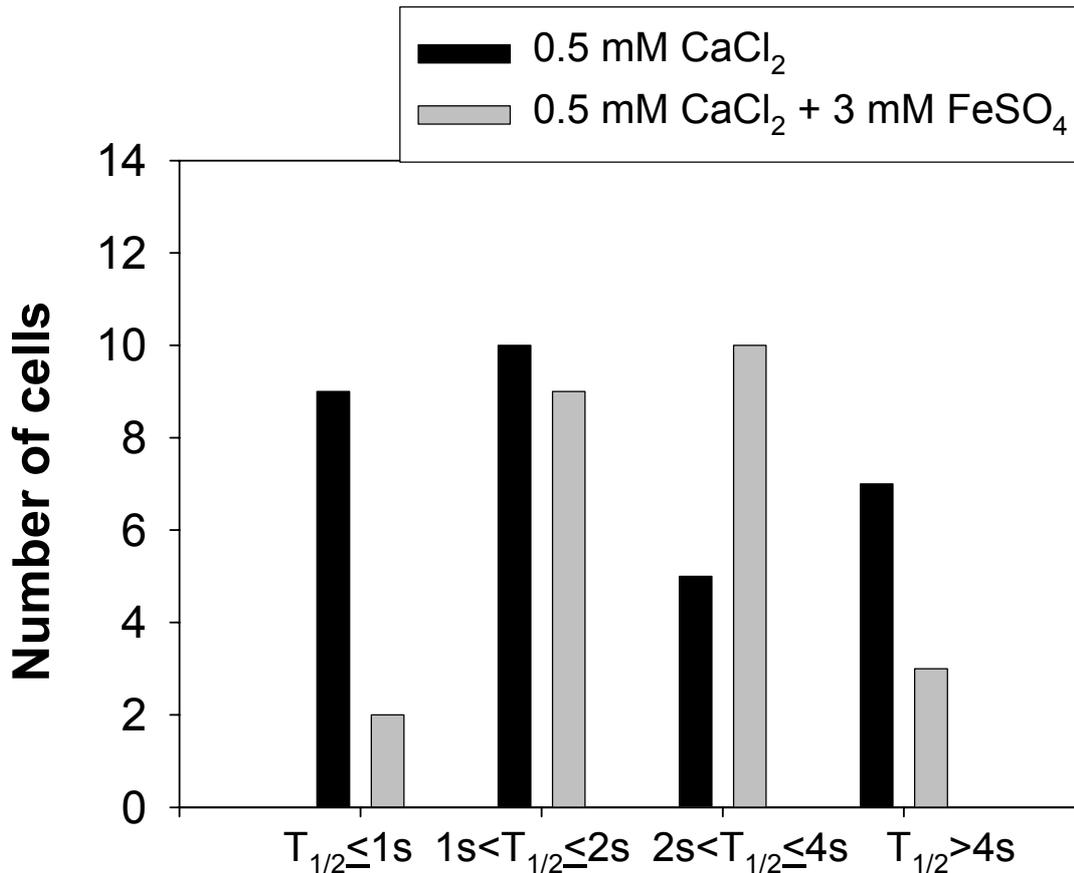

Figure 2. Frequency histogram of half time of water exchange, $T_{1/2}$ (inversely proportional to cell Lp). More than 80 % of cells from excised leaves, which were perfused either with 0.5 mM CaCl$_2$ or with 0.5 mM CaCl$_2$ + 3 mM FeSO$_4$, had $T_{1/2}$s less than 4 s. There were a few leaves showing only large $T_{1/2}$s.
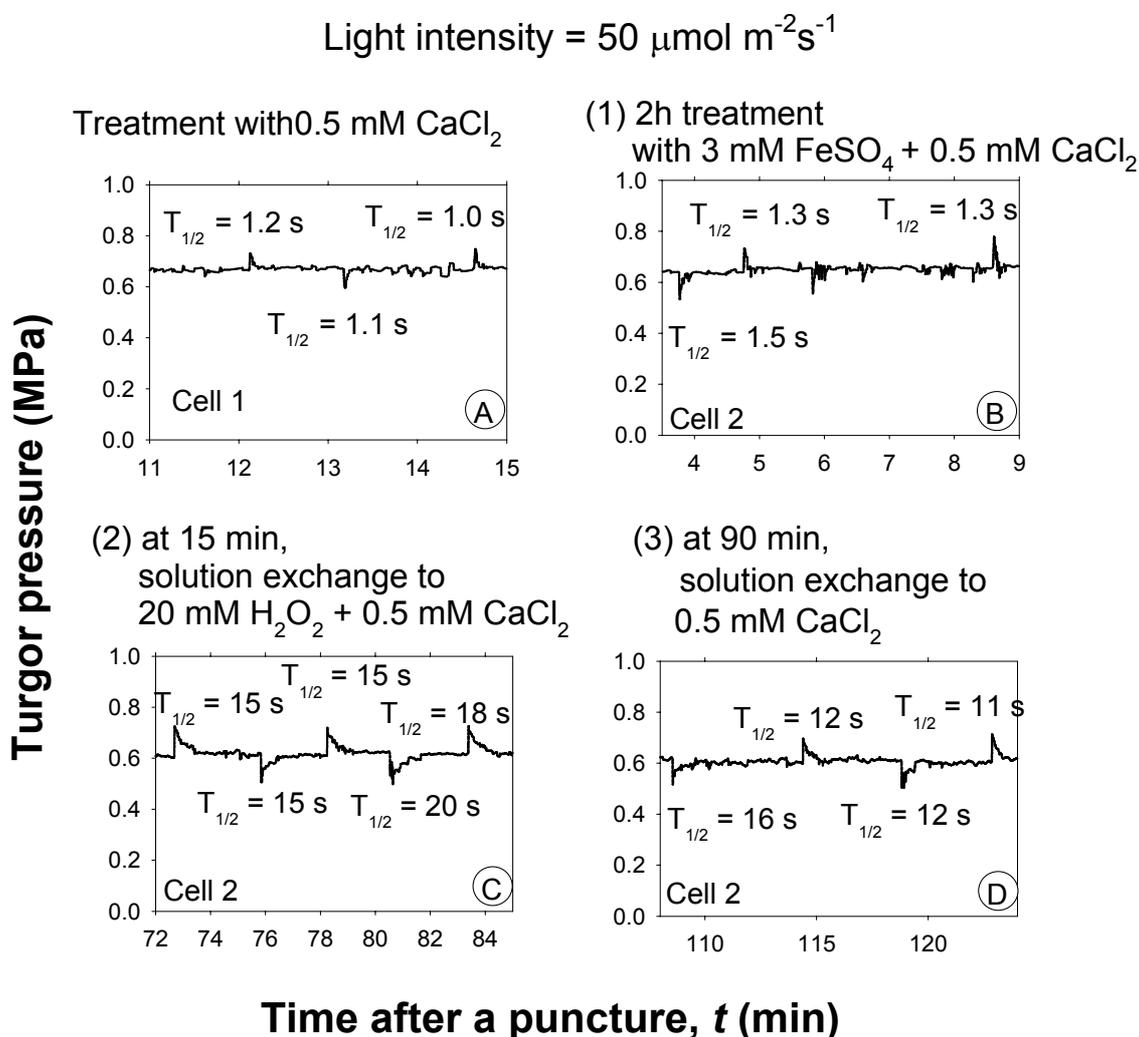
Figure 3. Representative relaxation curves to access half time of water exchange, $T_{1/2}$ (inversely proportional to cell Lp). (A) Half time of cells from excised leaves, which were perfused with 0.5 mM CaCl$_2$, typically ranged between 1.0-2.0 s. A reversible oxidative gating of AQPs was demonstrated following an individual cell in B to D. (B) Half times of cells in the presence of Fe^{2+} were similar to those in CaCl$_2$ and this was used as the control. (C) On the same cell in B, addition of 20 mM H$_2$O$_2$ produced OH* by a Fenton reaction and caused a substantial increase in $T_{1/2}$ by a factor of 27, i.e. Lp was reduced by the same factor. (D) Subsequent exchange to 0.5 mM CaCl$_2$ to remove radicals, resulted in a partial recovery of $T_{1/2}$ (Lp), i.e. the effect was reversible, at least to some extent.

Responses to OH* (Fe²⁺ & H₂O₂)

When adding 20 mM H_2O_2 to the reference solution (0.5 mM $CaCl_2$), at light intensity of 50 μmol m^{-2} s^{-1}, there was no effect on $T_{1/2}$ (4 cells tested). Most likely, this means that Fe^{2+} in apoplast was not sufficient to produce a sufficiently high level of OH* (Fenton reaction; $H_2O_2 + Fe^{2+} = Fe^{3+} + OH^- + OH^*$). However, when the concentration of H_2O_2 was raised to 70 mM, $T_{1/2}$ increased by a factor of 4. When perfusing with 3 mM $FeSO_4$ + 0.5 mM $CaCl_2$, $T_{1/2}$s were similar to those when using only 0.5 mM $CaCl_2$ (see above). There was a marked increase in $T_{1/2}$ when 20 mM H_2O_2 solutions were perfused following 2-h-treatments with Fe^{2+} (Fig. 3C).
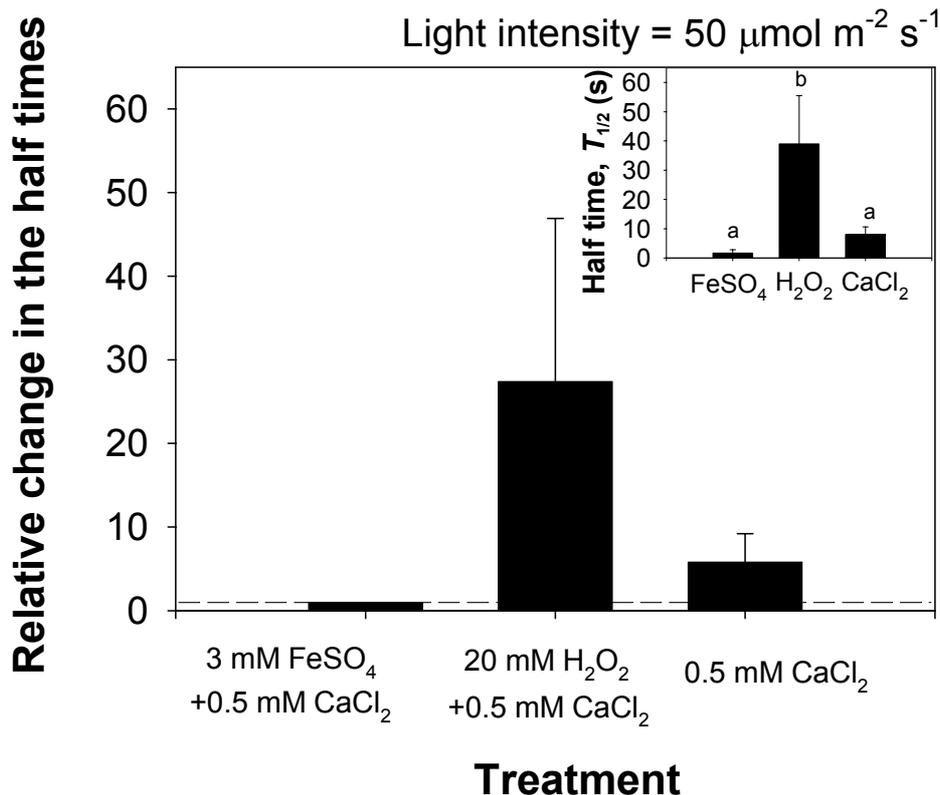

Figure 4. Summary of effects of H_2O_2/Fe^{2+} on cell *Lp*. Values are means ±SD from three independent experiments like Figs. 2B-2D. There was a significant effect of H_2O_2/Fe^{2+} (p<0.05, t-test, n=3 cells). Effects of treatments were measured following individual cells. The absolute values of $T_{1/2}$ are shown in the inset.

It can be seen from the figure that $T_{1/2}$ increased by a factor of as large as 14 probably due to the action of OH* (Fig. 3C). Changing back to 0.5 mM $CaCl_2$ again reduced $T_{1/2}$ by 50% within 30 min, to a value of 700% of the original (Fig. 3D). Recovery could be observed for only up to 30 min, because long-term measurements following oxidative responses and recovery in individual cells were demanding; however, there could have been further recovery during long-term measurements. It should be stressed that, during measurements, turgor pressure was kept constant. Similar experiments showing inhibition by H_2O_2/ Fe^{2+} treatment and partial recovery could be repeated in three different cells. Overall, $T_{1/2}$ increased by the treatment by a factor of 30, and recovered to 600% of the original value within 30 min after changing back to the control perfusion solution (Fig. 4). More data showing substantial increases in $T_{1/2}$ by H_2O_2/ $FeSO_4$ treatment are shown for other cells in Fig. 5A (see below).

Responses to low light of 200 μmol m^{-2} s^{-1}

The response to low light (200 μmol m^{-2} s^{-1}) was measured in cells, which originally had low $T_{1/2} \approx 1$ s in the $FeSO_4$/$CaCl_2$ solution, but were then inhibited to have large $T_{1/2}$ by the addition of 20 mM H_2O_2. When cells exhibited long $T_{1/2}$s in the presence of H_2O_2/ $FeSO_4$, LL of 200 μmol m^{-2} s^{-1} caused a significant reduction of $T_{1/2}$ by a factor of 7 within 30 min (Fig. 5A, n = 3 cells). In one experiment, increased $T_{1/2}$ by a factor of four caused by a treatment of 70 mM H_2O_2 could be recovered to an original value by LL of 200 μmol m^{-2} s^{-1} (data not shown). For cells, which had already a large $T_{1/2}$ of bigger than 2 s in the control solution (AQPs already closed), LL treatment reduced $T_{1/2}$ (Kim and Steudle, 2007). It can be seen from Fig. 5B that $T_{1/2}$s were reduced by a factor of 2 within 30 min (n = 4 cells). In one out of those four cells, $T_{1/2}$ levelled off into a small value within 30 min light treatment, but in the others not. Longer light treatments may further reduce $T_{1/2}$. It can be seen from these results that, although light effects were substantial, there was a considerable variability in the LL responses.
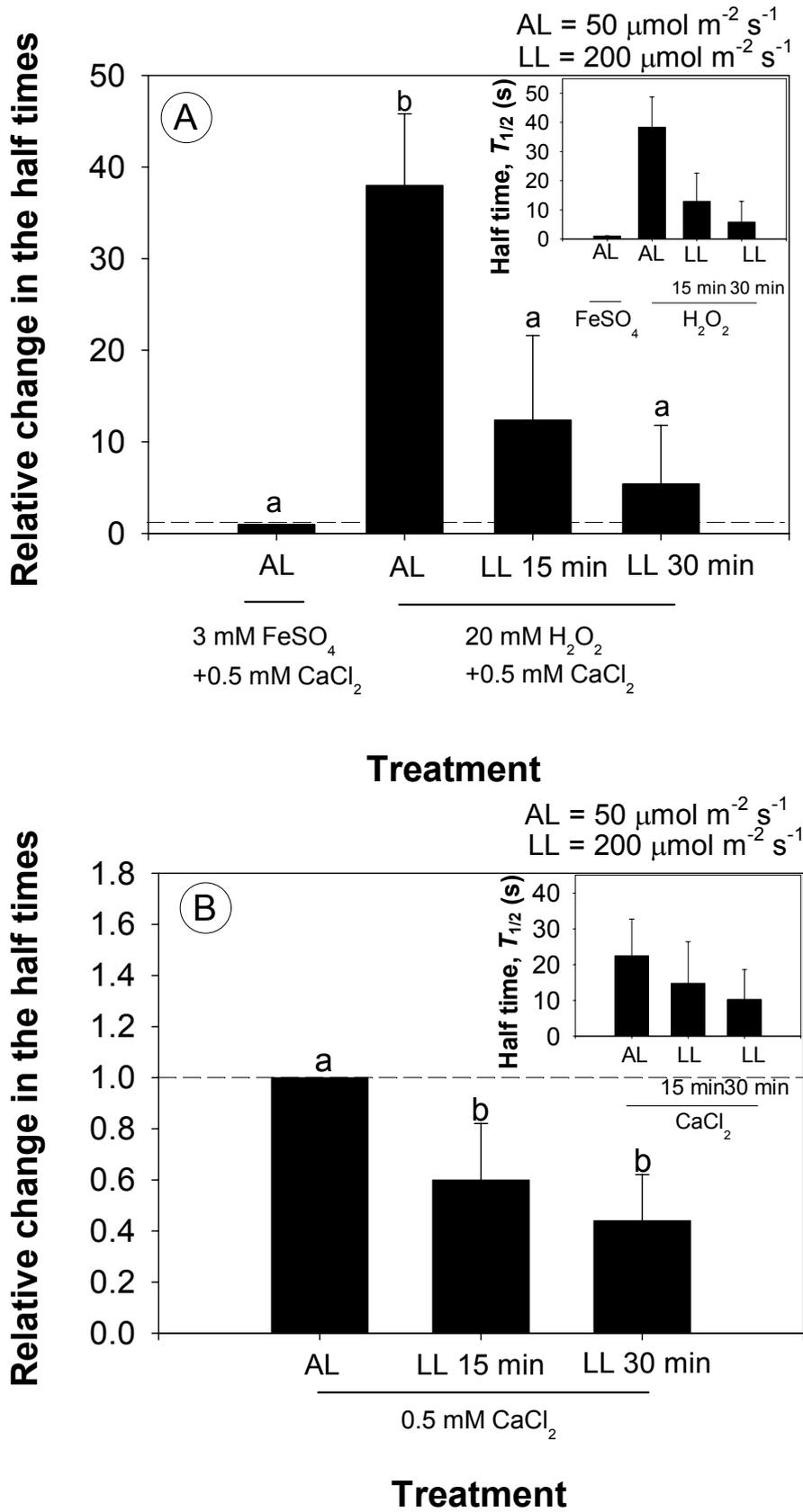
Figure 5. Low light (LL) treatment of 200 μmol m^{-2} s^{-1} reduced $T_{1/2}$, at constant turgor, as was in the

whole plant experiments of Kim and Steudle (2007). (A) Cells having $T_{1/2} < 2$ s at the ambient light

(AL) intensity of 50 $\mu mol\ m^{-2}\ s^{-1}$ were manipulated to have $T_{1/2}$ bigger than 2 s by H_2O_2/Fe^{2+} treatment as done in Fig. 3. The increased $T_{1/2}$ was reduced by 30-min LL treatment by a factor of 7 (different letters are significantly different by t-test at p<0.05, n=3 cells). (B) Cells originally having $T_{1/2} > 2$ s at AL in $CaCl_2$ solution showed a significant reduction in $T_{1/2}$ during 30-min LL by a factor of 2 (p<0.05, t-test, n=4 cells). Values are means ±SD and shown as relative changes. The absolute values of $T_{1/2}$ are shown in the inset.
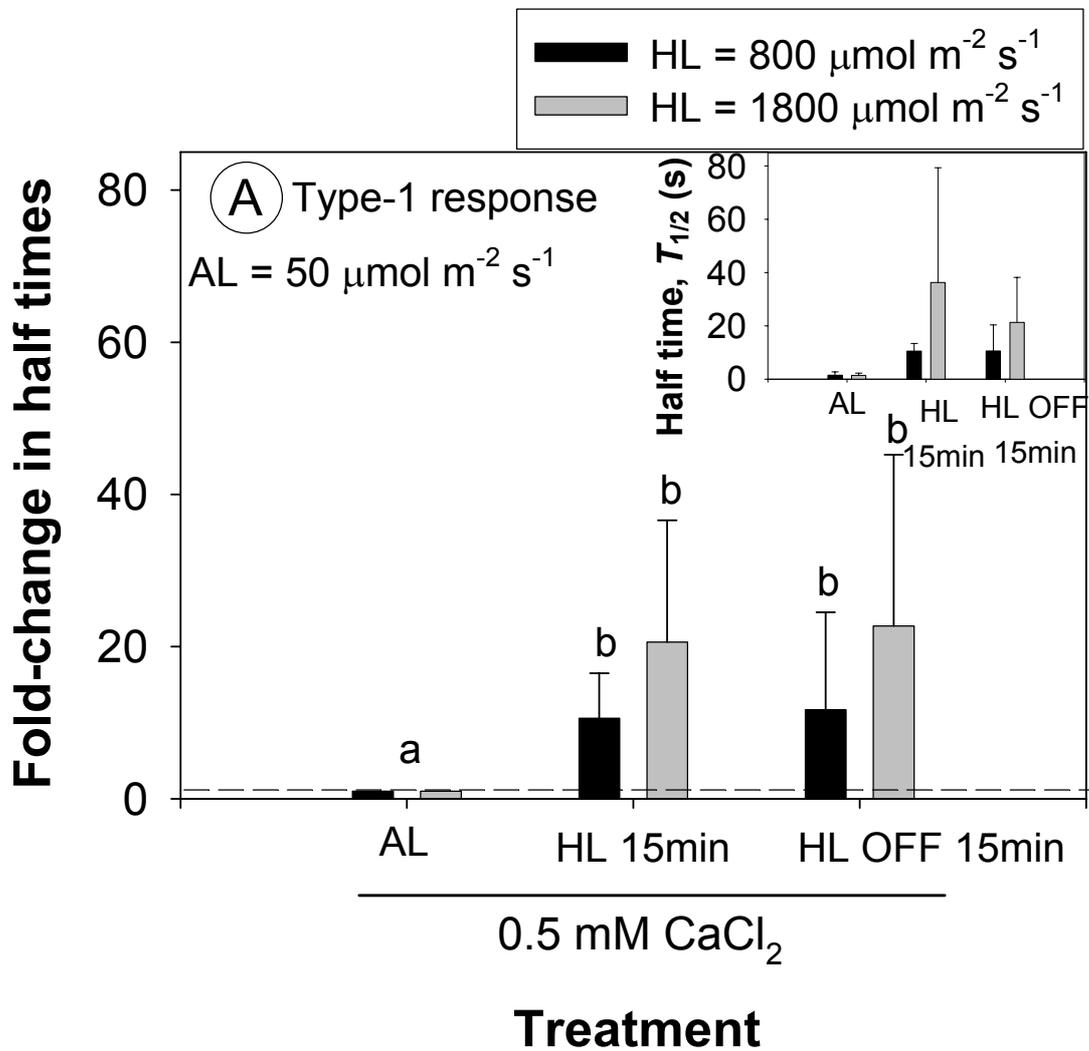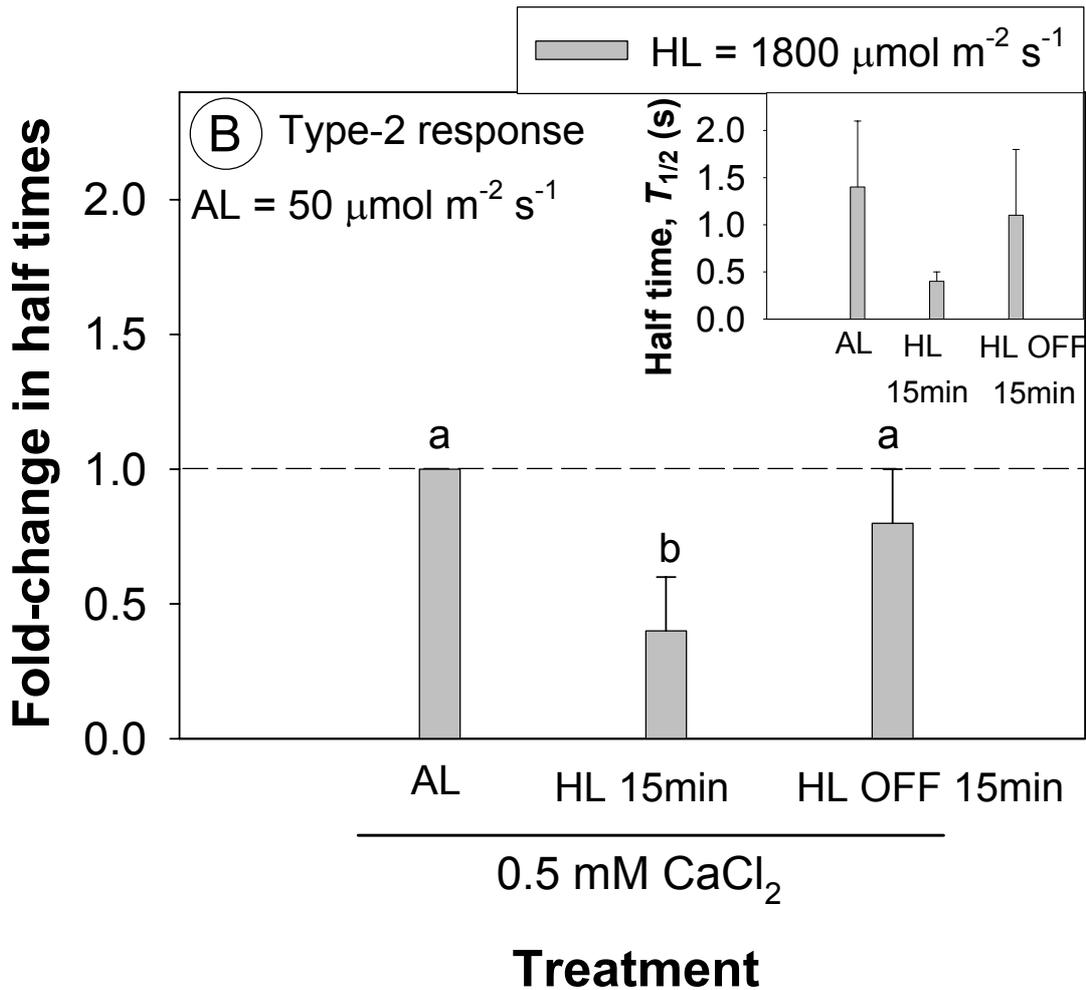
Figure 6. Two types of response to high light (HL) treatment. (A) HL of 800 μmol m^{-2} s^{-1} (black bars, n=4 cells) and 1800 μmol m^{-2} s^{-1} (grey bars, n=3 cells) increased $T_{1/2}$, at constant turgor in CaCl$_2$ solution. Increase in $T_{1/2}$ began about 10 min after HL was turned on. The largest $T_{1/2}$ s caused by HL were significantly bigger than $T_{1/2}$ s at ambient light (AL) intensity before HL treatments (p<0.05, t-test). During 15 min after light was switched off, $T_{1/2}$ s remained large, i.e. not reversible within 15 min. (B) There were cells, in which $T_{1/2}$ did not increase but decrease by HL of 1800 μmol m^{-2} s^{-1} (grey bars, n=5 cells). Values are means ±SD and shown as relative changes. The absolute values of $T_{1/2}$ are shown in the inset.
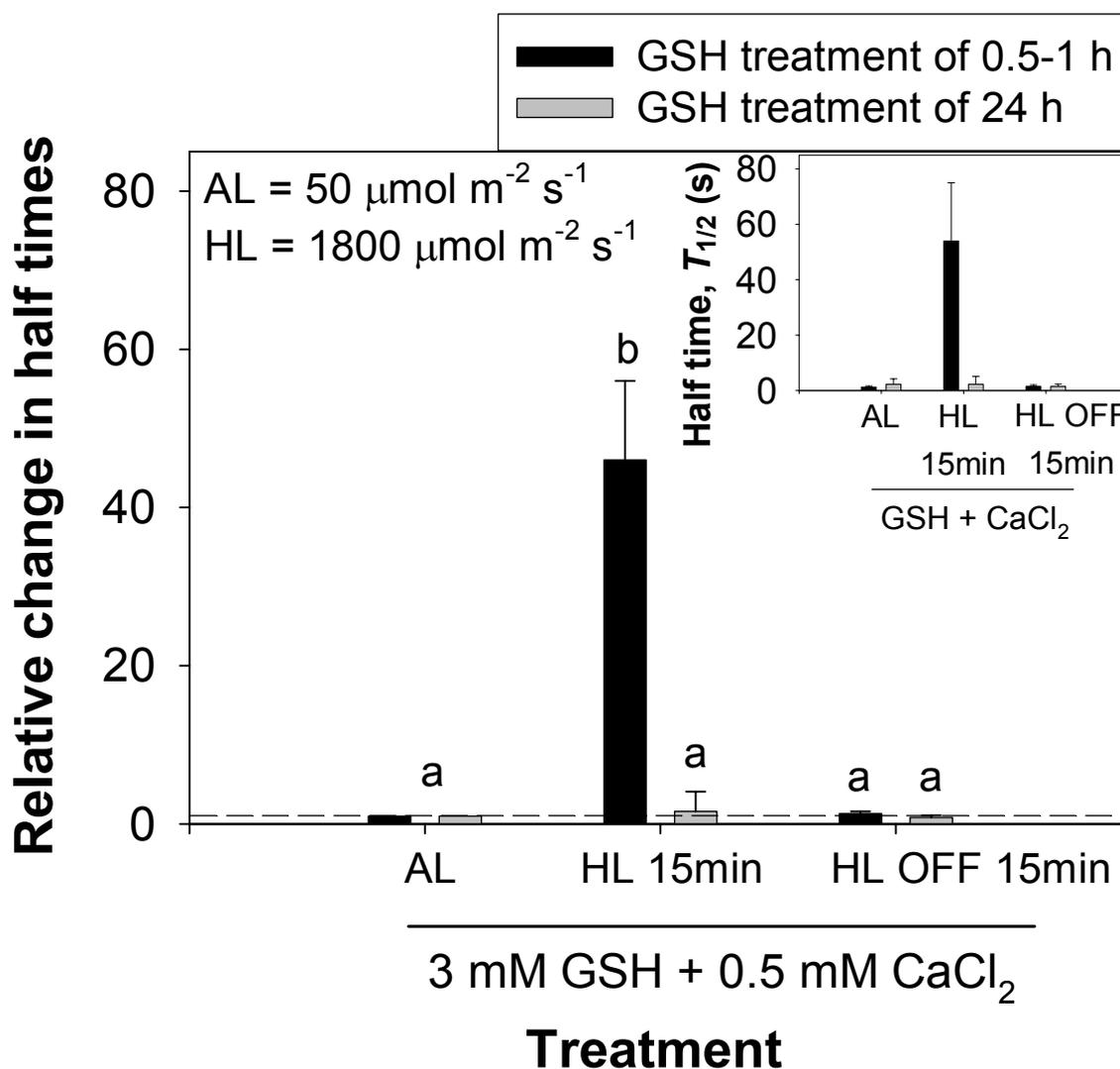
Figure 7. In the presence of the antioxidant glutathione (GSH), effects of HL treatment of 1800 μmol m^{-2} s^{-1} could be reversible. Cells pre-treated with 3 mM GSH + 0.5 mM CaCl$_2$ for 0.5-1.0 h (black bars, n=4 cells), increased $T_{1/2}$ by HL as in the absence of GSH (as in Fig. 6). In the presence of GSH, by contrast, there was a recovery within 15 min after light was switched off. Cells pre-treated by GSH for 24 h (grey bars, n=5 cells), did not increase $T_{1/2}$ by HL (p>0.05, t-test). Values are means ±SD and shown as fold-changes. The absolute values of $T_{1/2}$ are shown in the inset.

Responses to high light of 800 μmol m^{-2} s^{-1} and 1800 μmol m^{-2} s^{-1}

Although there was an overall trend of a reduction of $T_{1/2}$ following HL treatment, this was statistically not significant. As during the LL treatment, there was a substantial variability between cells. For example, high light of 800 μmol m^{-2} s^{-1} and 1800 μmol

m^{-2} s^{-1} reduced $T_{1/2}$ during the first 5 to 10 min of the 15-min period of illumination, but then $T_{1/2}$ substantially increased by factors of 14 and 35, respectively (Fig. 6A, n = 3-4 cells; Type-1 response). In total, 10 cells showed the increase in $T_{1/2}$ by HL. The 15-min treatment was chosen as the maximum treatment, which could be applied at constant turgor and stable cells. Longer HL treatments caused a continuous decrease in turgor pressure, which indicated a damage on cells. In this respect, cells punctured could have been more prone to damages in the presence of light stress than others (see Discussion). In 8 out of 10 cells, $T_{1/2}$s remained large, when light was turned off for 30 min, which was the maximum period of time measured. There were, however, cells, which were hardly affected by HL as seen in Fig. 6B (n=5 cells; Type-2 response). In those cells, there was only a reduction by 37 to 86 % within 15 min. Those five cells were from two leaves and no cells in those leaves showed Type-1 response. Maximum temperature changes on the leaf surface due to illumination of 800 µmol m^{-2} s^{-1} and 1800 µmol m^{-2} s^{-1} were 3 °C and 7 °C, respectively.

Responses to GSH

Cells pre-treated with the antioxidant GSH were exposed to 15-min period of illumination at the intensity of 1800 µmol m^{-2} s^{-1}. As seen in Fig. 7, a cell which had been perfused with 3 mM GSH + 0.5 mM $CaCl_2$ for 0.5-1.0 h, increased $T_{1/2}$ by a factor of 46 by HL, as in the absence of GSH. However, in the presence of GSH, $T_{1/2}$ recovered back to the original, within 15 min, when light was turned off (n=5 cells). This was different to the treatment in the absence of GSH. Pre-treatments by 3 mM GSH of 24 h had pronounced ameliorative effects. In contrast to short treatments, $T_{1/2}$s showed no significant increase by HL (n=4 cells). To confirm that lacks of responses were due to the presence of GSH rather than by coincidence originating from the variable responses between cells (one third of cells did not react on HL; see above), it was tested following one cell, that the $T_{1/2}$ in control solution increased in response to HL, and then the addition of GSH recovered $T_{1/2}$ to the original. On the same cell, following light treatment in presence of GSH caused only temporary increase in $T_{1/2}$,

which eventually recovered to the original value at the ambient light intensity (data not shown). In the reverse type of experiment using 3 mM GSH, there was no response in $T_{1/2}$ by 15-min HL treatment following a treatment of 3 mM GSH solution for 3 h. On the same cell, the exchange of GSH solution by the reference solution and waiting for its complete removal (about 1 h), caused a substantial increase of $T_{1/2}$ by 15-min HL treatment (data not shown). Overall, the results indicate that there was a clear ameliorative effect of GSH on cell Lp ($T_{1/2}$). Effects of HL may be related to oxidative stress in the presence of HL (see Discussion).

Discussion

The results of this paper indicate that HL intensity inhibits the AQPs in perfused leaves of corn plants. This extends earlier findings of Kim and Steudle (2007), who showed that, at constant turgor, low light intensity had an ameliorative effect on cell Lp, most likely by acting on AQPs. The treatment of the tissue with oxidants (H_2O_2 and OH* as produced by the Fenton reaction; $H_2O_2 + Fe^{2+} = Fe^{3+} + OH^- + OH^*$) had an effect similar to HL. The perfusion with a solution of the antioxidant glutathione (GSH) increased cell Lp (reduced $T_{1/2}$) in cells having long $T_{1/2}$. In the presence of HL, the presence of the antioxidant, tended to prevent the inhibition by HL. This may indicate that there was indeed an action of reactive oxygen species (ROS) on AQPs in the leaf caused by HL. Similar findings of an oxidative gating of AQPs have been found with *Chara* internodes and corn roots (Henzler *et al.*, 2004; Ye and Steudle, 2006). In *Chara*, H_2O_2 in presence of Fe^{2+} caused a reversible oxidative gating and reduced cell Lp by more than 90%. In the presence of rapidly permeating solutes, anomalous (negative) osmosis could be observed, when AQPs were closed (Henzler *et al.*, 2004). Ye and Steudle (2006) showed that in root cells, AQP activity was reduced by a factor of nine. At the whole root level, the reduction was smaller by a factor of three as expected from the composite transport model of the root. In the present study, effects of HL on cell Lp in leaves were shown for the first time suggesting that this may be related to an oxidative gating as well. It is known that,

during light stress, ROS develop in leaves by the partial reduction of oxygen or from hydrogen peroxide produced in many metabolic reactions (Foyer and Noctor, 2000).

It may be argued that the huge effects caused by HL on cell Lp (AQP activity) could be an artifact caused by the fact that cells had to be punctured to measure water relations parameters, and that these cells were more susceptible to stress. If true, effects on the 'intact' system could have been different. In principle, this may be true, but is unlikely, because cells punctured by the CPP had stable turgor for up to six hours indicating a high membrane integrity and stability. Also, punctured cells showed reversible responses during treatments (light, inhibitors, GSH), as expected. This was true, although there was a substantial variability between cells, which should have been caused by other reasons (see below). It appears that there is, at present, no alternative technique for measuring light responses at the level of individual, intact tissue cells, which is completely non-invasive.

Because a molecular analysis of AQPs was not provided, the interpretation of the present data in terms of a gating of AQPs may be questioned. In the present paper, what was directly measured was the water permeability of parenchyma cells in the midrib of cut leaves from corn plants (cell Lp). However, it would be difficult to find an alternative plausible interpretation different from the one offered. In corn, aquaporins were classified in four different groups of proteins as plasma membrane intinsic proteins (PIPs), tonoplast intrinsic proteins, Nod26-like intrinsic proteins, and small and basic intrinsic proteins (Chaumont *et al*., 2001). To date, there have been no data showing effects of light on either of these AQPs. In walnut, the transcript abundance of two AQPs (*JrPIP2,1 and JrPIP 2,2*) in response to light was correlated to the overall leaf hydraulic conductance (K_{leaf}; Cochard *et al*., 2007). The action of AQPs by light has been speculated from K_{leaf} measurements (Nardini *et al*., 2005; Tyree *et al*., 2005). Kim and Steudle (2007) started to fill the gap between the two levels by measuring changes in cell Lp in response to light. All the currently available data direct to attribute changes in cell Lp to the gating of AQPs, and the results in this paper support this interpretation, namely, by involving an oxidative gating of AQPs besides the light effect. High light decreased cell Lp most likely by closure of AQPs,

whereas LL recovered cell Lp to high value by opening of AQPs. The closure of AQPs by HL could be tightly connected to an oxidative gating by ROS produced during HL treatment (see below).

Earlier it was found that both turgor and light affect cell Lp, hence, a perfusion technique in cut leaves was applied to keep turgor constant. Kim and Steudle (2007) showed that, as transpiration increased during light treatment, turgor decreased and it resulted in a decrease of cell Lp. So, turgor had to be kept constant to separate effects of turgor from those of light. The perfusion technique used in the present paper, allowed this. Furthermore, leaves could be perfused with solutions of defined composition. For example, when using the perfusion technique, we could perfuse with H_2O_2, or with the antioxidant GSH. In the future, this technique could be used further to test other solutes such as heavy metals or solutions with different pH or pCa. It is unlikely that the perfusion of leaf tissue with solutions saturated with oxygen could have caused a deprivation of oxygen and carbon dioxide to cells, but this point needs to be clarified in further experiments.

The light intensities used in this study, were up to 1800 μmol m^{-2} s^{-1}, which is comparable to the outside on a bright day ($\approx$ 2000 μmol m^{-2} s^{-1}; Nobel, 1999). It is known that, HL produces ROS. Reactive oxygen species are unstable partly reduced oxygen species, produced as by-products of photosynthesis (singlet oxygen, H_2O_2, hydroxyl radical, superoxide; Foyer and Noctor, 2000; Jiang and Zhang, 2001). In response to a light intensity of 600 μmol m^{-2} s^{-1}, the generation of ROS could be visualized with digital imaging in *Arabidopsis* (Fryer *et al*., 2002). Reactive oxygen species are known to cause oxidative damage such as lipid peroxidation, denaturation of proteins, and DNA mutation (Jiang and Zhang, 2001). Plants have protective mechanisms to get rid of stresses caused by ROS by an adjustment of antioxidants such as ascorbate (ASC) or reduced glutathione (GSH). In the present paper, HL treatment resulted in a decrease of cell Lp, which was similar to that obtained by exogenous H_2O_2 (Fe^{2+}) applied by perfusion. This supports the idea of an action of ROS during HL. In addition, effects of HL were greater, when Fe^{2+} level in the tissue was elevated. Further support of an action of ROS was derived from the fact that the

perfusion of the tissue with the antioxidant GSH protected AQPs from inhibition, probably by reducing ROS. Although the amounts of GSH, which reached the inside of the cells, were probably small (Gukasyan *et al.*, 2002), the intracellular ratios of GSH_{red}/GSH_{ox}, which determine the redox potential, could have been high and sufficient to reduce ROS. From the results of Henzler *et al.* (2004) on *Chara* internodes, it is known that ROS (and namely on OH*) react on AQPs, even when ROS are present in a very low concentration. Overall, this circumstantial evidence suggested that the response of cell *Lp* to HL was caused by ROS.

Available data on overall water transport in leaves in response to light (K_{leaf}; see Introduction) suggest a trend that light is increasing K_{leaf}. Light intensities used in those studies ranged from 400 to 1400 μmol m^{-2} s^{-1} for different herbaceous and woody species (Sack *et al.*, 2002: 1200 μmol m^{-2} s^{-1}; Nardini *et al.*, 2005: 400 μmol m^{-2} s^{-1}; Tyree *et al.*, 2005: 1000-1200 μmol m^{-2} s^{-1}; Cochard *et al.*, 2007: 1400 μmol m^{-2} s^{-1}). At a first sight, this seems to contradict the present findings (decrease in cell *Lp* at HL of 800 and 1800 μmol m^{-2} s^{-1}). However, this may not be true because (i) there is an increase at lower light intensity (Fig. 5A; Kim and Steudle, 2007). It may be that there is a maximum of cell *Lp* in response to light intensity, which may be species dependent. This has to be worked out in future studies. (ii) K_{leaf} may incorporate effects other than those related to membranes (Zwieniecki *et al.*, 2001; Tyree *et al.*, 2005). (iii) So far, increases of K_{leaf} have been demonstrated using the 'high pressure flow meter' (HPFM), where high pressures were applied during infiltration, which, in part, was different to the present measurements (Sack *et al.*, 2002: 0.5-0.6 MPa; Nardini *et al.*, 2005: 0.15 MPa; Tyree *et al.*, 2005: 0.3-0.5 MPa; Cochard *et al.*, 2007: 0.2 MPa). Using figleaf gourd, Lee *et al.* (2008) measured midrib cell *Lp* in response to light intensity of 300 μmol m^{-2} s^{-1}. Those authors observed decrease in *Lp*. However, they did not control turgor, which should have decreased as transpiration increased by light.

There was a big variability in response to light between cells. Light effects may be different not only for different species but also for tissues. For example, in *Arabidopsis* singlet oxygen and superoxide production were primarily located in

mesophyll tissue whereas hydrogen peroxide accumulation was localized in the vascular tissues (Fryer *et al.*, 2002). Maize leaf cells are known to have differential intercellular partitioning of GSH metabolism (Noctor *et al.*, 2002). Glutathione reductase was localized only in leaf mesophyll cells but other antioxidant enzymes could be restricted to bundle sheath cells. In the present data, there was also some variability in response to HL in that one third of cells did not show stress response to HL. Although the former possibility cannot be neglected, there is an indication that this variability in response to HL could have originated from differences of individual leaves. All the five cells measured from two leaves showed no stress response. Those leaves could have been more resistant for HL. Problems related to variability of cells, were in part solved by measuring the effects of treatments in individual cells, which required to keep measurements at least for 1-4 h. Further investigations on the response of different types of cells to light (oxidative) stress are required. Although there have been attempts to work out the contribution of vessels and of non-vascular tissue in the overall measurements, it is still necessary to work out, in greater detail, the main hydraulic resistances in leaf water transport and how they depend on light intensity (Cochard *et al.*, 2004; Nardini *et al.*, 2005; Sack *et al.*, 2005).

Although the exact mechanism(s) of how ROS react with AQPs are not yet known, it has been shown that AQPs reversibly close in the presence of ROS (Henzler *et al.*, 2004; Ye and Steudle, 2006). Reactive oxygen species could be present at different amounts at different light levels. At low light intensity, the level of ROS could be low and ROS could be reduced by the antioxidants present such as ASC or GSH. However, regardless of the precise mechanisms of the action of ROS, the data indicate that there are interactions between light and water relations, which should be of key importance during photosynthesis. To maximize photosynthesis, enough water, carbon dioxide, and light should be gained. The open/closed state of stomata is regulated not only by light but also by the water status of leaves. Stomata could be only kept open, when there is enough water uptake. Plants need to manage the resources to maximize productivity. As the present results show, the management of water resources may be a complex process dealing with many factors required to maximize productivity, which requires an interaction between light intensity and water flow. The present results

indicate that LL may promote water flow, but that, at HL, water flows are downregulated using ROS as messengers, which may be a common 'alarm' signalling system to provide defences against harmful environmental challenges (Pastori and Foyer, 2002).

In conclusion, the study presents first evidence of an inhibition of cell *Lp* by HL, which was most likely caused by an action of ROS on AQPs. High light responses of parenchyma cells in the midrib of the maize leaf were similar to those caused by $H_2O_2/OH*$ treatment. On the other hand, the antioxidant GSH had an ameliorative effect. Different from HL, AQP activity increased at LL intensity, which was in agreement with earlier results from leaves of intact plants. There should be an optimal light intensity to maximize water flow across leaf cells, but enhanced water flow could be inhibited at a certain light intensity. One may speculate that, by acting on the redox status of leaves, the light climate directly interacts with the water status of plants in a way which is different from that *via* stomata. It involves an action on the leaves' water supply by triggering cell *Lp* (AQP activity).

Acknowledgements

References

Aroca R, Amodeo G, Fernandez-Illescas S, Herman EM, Chaumont F, Chrispeels MJ. 2005. The role of Aquaporins and membrane damage in chilling and

hydrogen peroxide induced changes in the hydraulic conductance of maize roots. *Plant Physiology* **137**, 341-353.

Chaumont F, Barrieu F, Wojcik E, Chrispeels MJ, Jung R. 2001. Aquaporins constitute a large and highly divergent protein family in maize. *Plant Physiology* **125**, 1206–1215.

Cochard H, Nardini A, Coll L. 2004. Hydraulic architecture of leaf blades: where is the main resistance? *Plant, Cell and Environment* **27**, 1257-1267.

Cochard H, Venisse J-S, Barigah TS, Brunel N, Herbette S, Guilliot A, Tyree MT, Sakr S. 2007. Putative role of aquaporins in variable hydraulic conductance of leaves in response to light. *Plant Physiology* **143**, 122-133.

Dietz KJ. 2008. Redox signal integration: from stimulus to networks and genes. *Physiologia Plantarum* **133**, 459-468.

Felle HH, Hanstein S. 2007. Probing apoplastic ion relations in *Vicia Faba* as influenced by nutrition and gas exchange. In: Sattelmacher B, Horst WJ, eds. *The apoplast of higher plants: compartment of storage, transport and reactions*. Dordrecht, the Netherlands: Springer, 295-306.

Foyer CH, Noctor G. 2000. Tansley Review No. 112 Oxygen processing in photosynthesis: regulation and signalling. *New Phytologist* **146**, 359–388.

Fryer MJ, Oxborough K, Mullineaux PM, Baker NR. 2002. Imaging of photo-oxidative stress responses in leaves. *Journal of Experimental Botany* **53**, 1249-1254.

Gukasyan, HJ, Lee, VHL, Kim, KJ, Kannan R. 2002. Net glutathione secretion across primary cultured rabbit conjunctival epithelial cell layers. *Investigative Ophthalmology & Visual Science* **43**, 1154-1161.

Henzler T, Steudle E. 1995. Reversible closing of water channels in *Chara* internodes provides evidence for a composite transport model of the plasma membrane. *Journal of Experimental Botany* **46**, 199–209.

Henzler T, Ye Q, Steudle E. 2004. Oxidative gating of water channels (aquaporins) in *Chara* by hydroxyl radicals. *Plant, Cell and Environment* **27**, 1184-1195.

Jiang MY, Zhang JH. 2001. Effect of abscisic acid on active oxygen species, antioxidative defence system and oxidative damage in leaves of maize seedlings. *Plant and Cell Physiology* **42**, 1265-1273.

Kim YX, Steudle E. 2007. Light and turgor affect the water permeability (aquaporins) of parenchyma cells in the midrib of leaves of *Zea mays*. *Journal of Experimental Botany* **58**, 4119-4129.

Lee SH, Chung GC, Steudle E. 2005. Low temperature and mechanical stresses differently gate aquaporins of root cortical cells of chilling-sensitive cucumber and -resistant figleaf gourd. *Plant, Cell and Environment* **28**, 1191-1202.

Lee SH, Zwiazek JJ, Chung GC. 2008. Light-induced transpiration alters cell water relations in figleaf gourd (*Cucurbita ficifolia*) seedlings exposed to low root temperatures. *Physiologia Plantarum* **133**, 354-362.

Lo Gullo MA, Nardini A, Trifilo P, Salleo S. 2005. Diurnal and seasonal variations in leaf hydraulic conductance in evergreen and deciduous trees. *Tree physiology* **25**, 505-512.

Maurel C, Chrispeels MJ. 2001. Aquaporins. A molecular entry into plant water relations. *Plant Physiology* **125**, 135-138.

Nardini A, Salleo S, Andri S. 2005. Circadian regulation of leaf hydraulic conductance in sunflower (*Helianthus annuus* L. cv Margot). *Plant, Cell and Environment* **28**, 750-759.

Nobel PS. 1999. *Physicochemical and environmental plant physiology*. San Diego, USA: Academic Press.

Noctor G, Gomez L, Vanacker H, Foyer CH. 2002. Interactions between biosynthesis, compartmentation and transport in the control of glutathione homeostasis and signalling. *Journal of Experimental Botany* **53**, 1283-1304.

Pastori G, Foyer CH. 2002. Common components, networks, and pathways of cross-tolerance to stress: the central role of "redox" and abscissic acid mediated controls. *Plant Physiology* **129**, 460–468.

Sack L, Holbrook NM. 2006. Leaf hydraulics. *Annual Review of Plant Biology* **57**, 361-381.

Sack L, Melcher PJ, Zwieniecki MA, Holbrook NM. 2002. The hydraulic conductance of the angiosperm leaf lamina: a comparison of three measurement methods. *Journal of Experimental Botany* **53**, 2177-2184.

Sack L, Tyree MT, Holbrook NM. 2005. Leaf hydraulic architecture correlates with regeneration irradiance in tropical rainforest trees. *New Phytologist* **167**, 403-413.

Steudle E. 1993. Pressure probe techniques: basic principles and application to studies of water and solute relations at the cell, tissue and organ level. In: Smith JAC, Griffiths H, eds. *Water deficits: plant responses from cell to community*. Oxford, UK: BIOS Scientific Publishers, 5-36.

Steudle E. 2000. Water uptake by roots: effects of water deficit. *Journal of Experimental Botany* **51**, 1531-1542.

Tournaire-Roux C, Sutka M, Javot H, Gout E, Gerbeau P, Luu DT, Bligny R, Maurel C. 2003. Cytosolic pH regulates root water transport during anoxic stress through gating of aquaporins. *Nature* **425**, 393-397.

Tyree MT, Nardini A, Salleo S, Sack L, Omari BE. 2005. The dependence of leaf hydraulic conductance on irradiance during HPFM measurements: any role for stomatal response? *Journal of Experimental Botany* **56**, 737-744.

Wan XC, Steudle E, Hartung W. 2004. Gating of water channels (aquaporins) in cortical cells of young corn roots by mechanical stimuli (pressure pulses): effects of ABA and of $HgCl_2$. *Journal of Experimental Botany* **55**, 411-422.

Wei C, Tyree MT, Steudle E. 1999. Direct measurement of xylem pressure in leaves of intact maize plants. A test of the cohesion-tension theory taking hydraulic architecture into consideration. *Plant Physiology* **121**, 1191-1205.

Westgate ME, Steudle E. 1985. Water transport in the midrib tissue of maize leaves. *Plant Physiology* **78**, 183-191.

Xiong LM, Schumaker KS, Zhu JK. 2002. Cell signaling during cold, drought and salt stress. *Plant Cell* **14 (suppl.)**, S165-S183.

Ye Q, Steudle E. 2006. Oxidative gating of water channels (aquaporins) in corn roots. *Plant, Cell and Environment* **29**, 459-470.

Zwieniecki MA, Melcher PJ, Holbrook NM. 2001. Hydrogel control of xylem hydraulic resistance in plants. *Science* **291**, 1059-1062.

6   Summary

The dissertation focuses (i) on an analysis of effects of unstirred layers (USLs) during measurements of water permeability (hydraulic conductivity) at the level of single cells, during measurements with the cell pressure probe (CPP) and (ii) on the use of the latter technique to investigate changes in water permeability of leaf cells in response to light. Internodes of the giant green alga *Chara corallina* and parenchyma cells of corn leaves were used in the studies. Besides the water, the CPP has been employed to study solute flows across cell membranes. This allowed evaluating the role of different types of USLs. In response to claims, recently raised by Tyree *et al.* (2005) that USLs play a significant or even dominating role in measurements of transport coefficients with the cell pressure probe, a rigorous re-examination of effects of USLs with *Chara* internodes has been performed indicating a minor role of USLs. For the first time, responses of cell water relations to light have been worked in some detail. Light effects have been separated from those of turgor in intact tissue cells by compensating for transpiration. At low light (LL) intensity (100 to 650 μmol m^{-2} s^{-1}), hydraulic conductivity of a cell (cell *Lp*) increased with increasing light intensity by a factor of 2 to 6 in 10 min. However, at high light (HL) intensities of 800 and 1800 μmol m^{-2} s^{-1}, there was a decline of cell *Lp* with increasing light intensity at constant cell turgor by factors of 14 and 35, respectively. The effects of LL refer to literature data of overall measurements of the leaf conductances (K_{leaf}). Decreases of K_{leaf} at HL have not yet been separated for effects of turgor or light intensity, respectively (as done here). The responses to HL were most likely caused by an oxidative gating of water channels (aquaporins; AQPs), as indicated by the fact that (i) application of reactive oxygen species (ROS) resulted in responses similar to those of HL and (ii) HL effects could be reversed in the presence of the antioxidant glutathione. For the first time, the data indicate an interaction between water relations and light intensity/photosynthesis, which is most likely related to changes in the redox status of leaves.

Unstirred layers (USLs)

At any transport of water and solutes across membranes or other osmotic barriers, USLs tend to modify the measured permeability (hydraulic conductivity, solute permeability). This should be taken into account, when interpreting transport data. Namely, in a transpiring plant, water flow densities could be substantial tending to modify local concentrations such as at membrane surfaces. There are two types of USLs. One is called 'sweep-away effect' referring to the action of a water flow. The other is termed 'gradient-dissipation effect', which relates the diffusional solute supply from the bulk solution to the membrane resulting in a smaller concentration gradient across the membrane than that thought, when assuming the concentration difference between the solutions separated by the membrane or barrier. As a consequence, transport parameters such as the hydraulic conductivity (Lp), the solute permeability (P_s), and the reflection (σ_s) coefficient are underestimated. During experiments with giant internodes of green algae *Chara corallina*, a quantitative re-examination indicated a minor role of USLs for the measurement of membrane transport coefficients for water and solutes with the CPP. The results show that the hydraulic conductivity measured in hydrostatic pressure-relaxations (Lp_h) was not significantly affected by 'sweep-away effects', even when peak sizes of pressure pulses ($\pm \Delta P$) were increased by one order of magnitude above normal. The osmotic hydraulic conductivity (Lp_o) increased with increasing the external stirring rate of the medium (v_{med}). The Lp_o became saturated at $v_{med} = 0.20 - 0.30$ m·s^{-1} and reached a value close to Lp_h, which was proved to be rather free of USLs effects. Substantially smaller values of v_{med} were required to saturate P_s and σ_s ($v_{med} \approx 0.10$ m·s^{-1}). During osmotic experiments, the cell membrane of *Chara* internodes acted as a rate-limiting resistance usually allowing sufficient time for an internal mixing of solutes by diffusion. Even for the most rapidly permeating solute acetone (used as a test solute), USLs should have resulted in an underestimation of P_s and σ_s by less than 30 %. For the less permeating solute dimethylformamide (DMF), it reduces to 15 %. Estimations of thicknesses of external and internal USLs indicated that real values of USLs are 30 and 50 µm, respectively, in the presence of the most rapidly permeating solutes (acetone or heavy water), provided that there was a vigorous external stirring.

Internal unstirred layers

Different from external USLs, internal USLs could not be manipulated by stirring, and it was more difficult to evaluate the role of internal USLs for the measurement of transport coefficients. A new stop-flow technique (SFT) was employed to quantify the impact of internal USLs on the measurement of the solute permeability coefficient (P_s) across the plasma membrane of *Chara*. During permeation experiments with permeating solutes, the solute concentration inside the cell was estimated and the external medium was adjusted in order to stop the solute transport across the membrane, after which responses in turgor were measured. This allowed estimation of the solute concentration right at the inner surface of the membrane. The SF experiments were also simulated with a computer. Both the SF experiments and the simulations provided quantitative data about concentration gradients in the cell and the contribution of internal USLs to overall measured values of P_s (P_s^{meas}). The SF experimental results agreed with SF simulations, when assuming that solutes diffused into a completely stagnant cell interior, however, this is the pessimistic assumption due to a protoplasmic streaming. The effects of internal USLs on the underestimation of membrane P_s declined inasmuch as P_s decreased. They were no bigger than 37% in the presence of the most rapidly permeating solute acetone ($P_s^{meas} = 4.2 \times 10^{-6}$ m s^{-1}), and 14% for the less rapidly permeating DMF ($P_s^{meas} = 1.6 \times 10^{-6}$ m s^{-1}). Even in the case of extremely rapidly permeating solutes such as isotopic water, an upper limit for the underestimation of P_s due to internal USLs was similar to that for acetone. This study with detailed quantitative data supports earlier estimations of the role of USLs in the literature on cell water relations. It throws some doubt on recent claims by Tyree *et al.* (2005) of a dominating role of USLs in *Chara* experiments using the CPP, which were based on wrong assumption and physical flaws.

Responses of cell *Lp* to LL (100 to 650 µmol m^{-2} s^{-1}) and to cell turgor

There is evidence that the overall hydraulic conductance of leaves (K_{leaf}) is substantially increased in the presence of light. The increase in K_{leaf} was suspected to occur most likely due to changes in the activity of AQPs, which, in turn, affected cell hydraulic conductivity (cell *Lp*). However, there have been as yet no direct

measurements of change either in cell Lp or in a gating of AQPs by light. The present thesis intended to fill the gap between overall data (K_{leaf}) and the molecular (AQP) level. In response to low light (LL) ranging from 100 to 650 μmol m^{-2} s^{-1}, water relation parameters of individual cells (turgor and cell Lp) were measured using a CPP. Used cells were parenchyma sitting in the midrib of both in leaves of intact corn plants and excised leaves. Parenchyma cells were used as model cells for the leaf mesophyll, because they are close to photosynthetically active cells and stomata. The hydraulics of those cells revealed a big variability in cell Lp. Despite some noise and variability in the hydraulics of cells, long-term measurements (up to six hours for an individual cell) indicated that increasing light intensity increased cell Lp. Increase in turgor had an ameliorative effect as well. Using a pressure chamber, both effects could be separated from each other. Illuminating the leaves, while keeping turgor constant, cell Lp increased by a factor of three within 30 min at a light intensity of 160 μmol m^{-2} s^{-1}. Without keeping turgor constant, effects of LL on cell Lp was compensated or even overcompensated by a decrease in turgor induced by an increase in transpiration. Effects of light and turgor on cell Lp may be due to a gating of AQPs.

Responses of cell Lp to HL (800 and 1800 μmol m^{-2} s^{-1}) and its relation to oxidative gating of AQPs

In response to high light (HL), changes in cell Lp were in the opposite direction indicating a closure of AQPs as light intended become stressful. The hypothesis that HL triggers an oxidative gating of AQPs was tested. The HL responses were similar to those by perfusing the leaf tissue with solutions containing H_2O_2 which should create OH* in the presence of Fe^{2+} (Fenton reaction), which is known to cause a closure of AQPs. The perfusion of leaves with 20 mM H_2O_2 caused decreases of cell Lp by a factor of 30, when leaves were pre-treated with 3mM $FeSO_4$. In part, the effects were reversible in the control perfusion solution. High light intensities of 800 and 1800 μmol m^{-2} s^{-1} decreased cell Lp by factors of as large as 14 and 35 in two third of the cells investigated, as H_2O_2/OH* treatments did. On the other hand, the perfusion of leaves with 3mM of the antioxidant glutathione had an ameliorative effect on cell Lp, which supported the hypothesis of an oxidative gating of water pores. Although there was a variability between cells in absolute values of Lp and in the stress response, the

data suggest a trigger or even a regulation of cell water relations by light *via* reactive oxygen species (ROS), which may act as signalling agents. The study suggests that there should be an optimal light intensity to maximize water flow across leaf cells. Further investigations have to provide more insight into the precise mechanism(s) of the gating of AQPs by ROS and how this works in the intact system under field conditions, where, different from the experimental approach, the water status (water potential, turgor) should be subject to change as well as the light climate is changing. Under field conditions, the effect of cell turgor on the open/closed state of AQPs has to be considered besides the light. In other words, when turgidity is low and plants suffer from water shortage, AQP activity is down regulated (and stomata close) to reduce water losses from leaf cells. On the other hand, when there is sufficient water, an increase of the overall leaf hydraulic conductance may allow the plant to keep stomata open for longer periods of time, which may be advantageous in terms of productivity.

7 Zusammenfassung

Die Dissertation konzentriert sich (i) auf die Analyse des Einflusses von ungerührten Schichten (Unstirred layers; USLs) auf Messungen der Wasserpermeabilität (hydraulischen Leitfähigkeit) auf der Ebene einzelner Zellen wie etwa bei Untersuchungen mit der Zelldruckmesssonde (CPP), und (ii) auf die Anwendung der CPP bei Untersuchungen zur Lichtabhängigkeit der Wasserpermeabilität von Blattzellen. Die Untersuchungen wurden an Internodialzellen von *Chara corallina* und an Parenchymzellen von Maisblättern durchgeführt. Neben den Messungen der Wasserpermeabilität wurde die CPP auch zu Messungen der Teilchenpermeabilität herangezogen. Dies erlaubte es, den Einfluss verschiedener Typen von ungerührten Schichten zu quantifizieren. Von Tyree *et al.* (2005) ist die CPP jüngst kritisiert worden, da bei dieser Technik USLs eine bedeutende oder sogar dominierende Rolle spielen. Deshalb wurde eine gründliche Nachprüfung des Einflusses von USLs mit *Chara*-Internodien durchgeführt, welche eine geringe Rolle von USLs ergab. Zum ersten Mal wurde mithilfe der CPP der Einfluss des Lichtes auf den Wasserhaushalt von Blattzellen untersucht, wobei dieser Einfluss von der Turgorabhängigkeit der Wasserpermeabilität separiert werden musste. Im Bereich niedriger Lichtintensitäten (Low light, LL; 100 bis 650 μmol m^{-2} s^{-1}) ergab sich innerhalb von 10 min mit steigender Intensität ein Anstieg der Wasserleitfähigkeit der Zellen um einen Faktor von 2 bis 6. Im Bereich hoher Lichtintensitäten (High light, HL; 800 und 1800 μmol m^{-2} s^{-1}) war dagegen bei konstantem Turgor eine Abnahme um einen Faktor von 14 bzw. 35 zu verzeichnen. Die Befunde im LL-Bereich entsprechen denen von Messungen an ganzen Blättern (K_{leaf}), wobei bei den Messungen von K_{leaf} mit Overall-Techniken bisher die Einflüsse der Blattturgeszenz nicht, wie in dieser Arbeit, von denen eines direkten Einflusses des Lichtes abgetrennt werden konnten. Die Ergebnisse legen nahe, dass die Antwort auf HL auf ein oxidatives 'Gating' von Wasserkanälen (Aquaporinen; AQPs) zurückzuführen ist, da (i) die Applikation reaktiver Sauerstoffspezies ähnliche Effekte ergab und (ii) der Einfluss hoher Lichtintensität in Gegenwart des Antioxidants Glutathion unterdrückt werden konnte. Die Ergebnisse weisen zum ersten Mal auf Wechselwirkungen zwischen dem

Wasserhaushalt und der Lichtintensität/Photosynthese hin, die höchstwahrscheinlich über den Redox-Zustand der Blätter gesteuert werden.

Ungerührte Schichten

Beim Transport von Wasser und darin gelösten Stoffen durch Membranen oder andere osmotische Barrieren werden die erwarteten Flüsse durch Effekte von USLs modifiziert, so dass bei Messungen auch die hydraulische Leitfähigkeit und Teilchenpermeabilität modifiziert werden. Dies ist darauf zurückzuführen, dass durch die Flüsse die aktuellen Konzentrationen an den Membranoberflächen modifiziert werden. In transpirierenden Pflanzen können die Wasserflüsse erheblich sein und die lokalen Konzentrationen deutlich ändern. Es gibt zwei verschiedene Typen von USLs. Zum einen gibt es den „Sweep-away-Effekt", der sich auf die Wirkung von Wasserflüssen beim Durchtritt durch Barrieren bezieht. Der andere Typ wird als „Gradient-dissipation-Effekt" bezeichnet. Er bezieht sich auf den Nachtransport von diffundierenden Substanzen aus der Lösung, wenn diese rasch durch die Membran treten. Der „Gradient-dissipation-Effekt" bewirkt, dass die tatsächliche Konzentrationsdifferenz über der Membran kleiner ist als die Konzentrationsdifferenz zwischen den Lösungen auf beiden Seiten der Membran. Als Konsequenz aus den USLs ergibt sich eine Unterschätzung der gemessenen Transportparameter gegenüber den tatsächlichen (hydraulische Leitfähigkeit, Lp, Teilchenpermeabilität, P_s, und Reflexionskoeffizient, σ_s). Bei den Untersuchungen an den Internodialzellen von *Chara* mithilfe der CPP konnte quantitativ gezeigt werden, dass die Bedeutung der USLs relativ gering ist. Die hydrostatische hydraulische Leitfähigkeit, Lp_h, wurde durch den „Sweep-away-Effekt" nicht signifikant erniedrigt, auch wenn die treibende Kraft für den Wasserfluss ($\pm\Delta P$) um eine Größenordnung erhöht wurde. Die osmotische hydraulische Leitfähigkeit (Lp_o) erhöht sich mit steigender Geschwindigkeit, mit der das Medium gerührt wurde (v_{med}). Lp_o wurde bei $v_{med} = 0{,}20$ – $0{,}30$ m·s^{-1} gesättigt und erreichte fast den Wert für Lp_h, welcher mithilfe von hydraulischen Druckimpulsen bestimmt wurde und sich als unabhängig von USLs zeigte. Wesentlich kleinere Werte von v_{med} waren erforderlich, um P_s und σ_s ($v_{med} \approx 0{,}10$ m·s^{-1}) zu sättigen. In den osmotischen Experimenten erwiesen sich die Zellmembran der *Chara*-Internodien als limitierender Widerstand, was in der Regel

eine ausreichende Zeit für ein Mischen der gelösten Substanzen innerhalb der Zelle gewährleistet. Sogar für sehr schnell permeierende Stoffe wie schweres Wasser (HDO) oder Aceton sollten P_s und σ_s um lediglich 30% unterschätzt worden sein. Für langsamer permeierende Stoffe wie Dimethylformamid (DMF) sollten P_s und σ_s um lediglich 15% unterschätzt worden sein. In der Arbeit wurden die Dicken der äußeren und inneren USLs mit 30 bzw. 50 µm abgeschätzt, wenn das Außenmedium kräftig gerührt wird.

Innere Ungerührte Schichten

Anders als bei den äußern USLs konnten innere USLs nicht durch Rühren manipuliert werden, und es war schwieriger, die Rolle von inneren USLs für die Messung von Transportkoeffizienten abzuschätzen. Deshalb wurde eine neue „Stop-Flow Technik" (SFT) verwendet, um den Einfluss von inneren USLs auf die Messung der Stoffpermeabilität (P_s) durch die Plasmamembran von *Chara* zu quantifizieren. Während der Experimente mit den permeierenden Stoffen wurde die Stoffkonzentration innerhalb der Zelle zunächst abgeschätzt und die Konzentration im Außenmedium daran angepasst, um so den Stofftransport durch die Membran zu stoppen. Anschließend wurden die Reaktionen in Turgor-Druck der Zelle gemessen. Dies ermöglichte eine Abschätzung der Stoffkonzentration direkt an der Innenseite der Zellmembran. Die SF-Experimente wurden auch in einem Computerexperiment simuliert. Sowohl die SF-Experimente als auch deren Simulationen ergaben quantitative Daten über die Konzentrationsgradienten in der Zelle und den Beitrag von internen USLs zu den gesamten Messwerten von P_s (P_s^{meas}). Die experimentellen Ergebnisse mit SF stimmten mit SF-Simulationen überein, wobei angenommen wurde, dass die Stoffe in ein völlig ungerührtes Zellinneres diffundierten, was wegen des Vorhandenseins einer Protoplasmaströmung eine pessimistische Annahme darstellt. Die Effekte von inneren USLs auf die Unterschätzung der Membran-P_s sanken in dem Maße, wie sich Absolutwerte von P_s verringerten. Sie waren nicht größer als 37 % in Anwesenheit des sehr schnell permeierenden Aceton ($P_s^{meas} = 4,2 \times 10^{-6}$ m s^{-1}) und 14 % für das weniger schnell permeierende DMF ($P_s^{meas} = 1,6 \times 10^{-6}$ m s^{-1}). Sogar im Fall des extrem rasch permeierenden schweren Wassers war die obere Grenze für die

Unterschätzung von P_s ähnlich der für Aceton. Die in dieser Arbeit erhobenen detaillierten quantitativen Daten stützen frühere Abschätzungen der Rolle von USLs in der Literatur. Es konnte gezeigt werden, dass die Thesen von Tyree *et al.* (2005) über eine dominierende Rolle von USLs in *Chara*-Experimenten mit der CPP auf falschen Annahmen und physikalischen Fehlern beruhen.

Änderung im Zell-*Lp* durch niedrige Lichtintensitäten (100 bis 650 µmol m⁻² s⁻¹) und durch den Turgor

Es gibt Hinweise, dass die hydraulische Leitfähigkeit von Blättern (K_{leaf}) durch das Licht wesentlich beeinflusst wird. Es wurde vermutet, dass die Zunahme in K_{leaf} auf Änderungen in der Aktivität von AQPs zurückgeht, welche die hydraulische Leitfähigkeit auf der Zellebene steuern (Zell-*Lp*). Jedoch hat es bis jetzt direkte Messungen der Änderung weder im Zell-*Lp* noch in einem Gating von AQPs durch das Licht gegeben. Es war erforderlich, die Lücke zwischen Änderungen in K_{leaf} und solchen auf der molekularen Ebene (AQPs) zu schließen. Als Reaktion auf das Licht im Intensitätsbereich von 100 bis 650 µmol m⁻² s⁻¹ wurden unter Verwendung der CPP Wassertransportparameter von individuellen Zellen gemessen (Turgor und Zell-*Lp*). Die verwendeten Zellen waren Parenchymzellen aus der Hauptblattader von Blättern intakter Maispflanzen, aber auch abgeschnittener Blätter. Die Parenchymzellen wurden als Musterzellen für das Blattmesophyll verwendet. Sie befinden sich in der Nähe von photosynthetisch aktiven Zellen und von Stomata. Die Zellen zeigten ein große Variabilität im Zell-*Lp*. Ungeachtet einiger Abweichungen und der hohen Variabilität in der Hydraulik der Zellen zeigten Langzeitmessungen (bis zu sechs Stunden für eine individuelle Zelle), dass die Erhöhung der Lichtintensität das Zell-*Lp* vergrößerte. Eine Erhöhung des Zellturgors hatte ebenfalls eine positive Wirkung. Durch Verwendung eines Wurzeldrucktopfes konnten beide Effekte voneinander getrennt werden. Die Beleuchtung der Blätter mit einer Lichtintensität von 160 µmol m⁻² s⁻¹ erhöhte das Zell-*Lp* bei konstantem Turgor innerhalb von 30 Minuten um den Faktor drei. Wurde der Turgor nicht konstant gehalten, wurden die Effekte des Lichtes auf die Zell-*Lp* kompensiert oder sogar durch eine Abnahme im Turgor, veranlasst durch eine Zunahme in der Transpiration, überkompensiert. Die Effekte des Lichtes und des Turgors auf die Zell-*Lp* könnten mit einem Gating von AQPs verbunden sein.

Änderung im Zell-*Lp* durch hohe Lichtintensitäten (800 und 1800 µmol m^{-2} s^{-1}) und seine Beziehung zu einem oxidativem Gating von AQPs

Bei hoher Lichtintensität (HL) traten Effekte in entgegengesetzter Richtung auf, was auf einen Verschluss der AQPs unter diesen Bedingungen hindeutet (Lichtstress). Es wurde die Hypothese geprüft, ob ein oxidatives Gating der AQPs hierbei eine Rolle spielt. Dazu wurden die Blätter mit H_2O_2-Lösungen perfundiert, was in Gegenwart von Fe^{2+} zur Bildung von OH*-Radikalen führen sollte (Fenton-Reaktion). Von letzteren ist bekannt, dass sie ein Schließen von AQPs bewirken. Die Perfusion mit 20 mM H_2O_2 bewirkte Abnahmen im Zell-*Lp* um einen Faktor 30, wenn die Blätter zuvor mit 3 mM $FeSO_4$ behandelt worden waren. Teilweise waren die Effekte reversibel. HL-Effekte von 800 und 1800 µmol m^{-2} s^{-1} erniedrigten das Zell-*Lp* um einen Faktor 14 bzw. 35 in zwei Dritteln der Zellen. Die Vorbehandlung der Blätter mit 3 mM Glutathion unterdrückte den Effekt von HL, was die Hypothese eines oxidativen Gating der Wasserkanäle stützt. Obwohl es eine Variabilität der Zellen im Absolutwert von *Lp* und in der Stressantwort gab, legen die Daten eine Steuerung des Zellwasserhaushaltes durch das Licht nahe, die durch reaktive Sauerstoffspezies vermittelt wird. Die Studie deutet auch auf ein Optimum in der Lichtintensität hin, bei dem die Wasserflüsse (das Zell-*Lp*) maximal sind. Weitere Untersuchungen müssen tiefere Einblicke in die detaillierten Mechanismen des Licht-Gating der AQPs über reaktive Suaerstoffspezies geben und wie sich dies in der intakten Pflanze unter Feldbedingungen abspielt. Im Gegensatz zu den hier geschilderten Untersuchungen ändert sich im Feldversuch neben der Lichtintensität auch der Wasserstatus der Pflanze (Wasserpotential, Turgeszenz) je nach den Bedingungen mehr oder weniger stark. Bei geringer Turgeszenz und Wasserknappheit sollten die AQPs herunterreguliert sein (und die Stomata geschlossen), um Wasserverluste über das Blatt zu minimieren. Andererseits sollte bei ausreichendem Wasserangebot die hydraulische Leitfähigkeit des Blattes erhöht werden, um die Stomata länger offen zu halten, was wiederum die Produktivität erhöht.

8 Erklärung

Hiermit erkläre ich, dass ich die Arbeit selbständig verfasst und keine anderen als die von mir angegeben Quellen und Hilfsmittel benutzt habe.

Ferner erkläre ich, dass ich anderweitig mit oder ohne Erfolg nicht versucht habe, diese Dissertation einzureichen. Ich habe keine gleichartige Doktorprüfung an einer anderen Hochschule endgültig nicht bestanden.

Bayreuth, den 16. Juli 2008

(Yangmin Kim)